THE KINEMATICS AND VIBRATION OF PLANAR LINKAGE MECHANISMS

Abstract

This thesis reports an investigation into three problems encountered in the design of linkage mechanisms, namely kinematic synthesis, balancing of inertia forces and vibration analysis.

A general method of synthesizing planar linkages with pin and sliding joints using an optimization approach has been investigated. A concise but easily interpreted technique for prescribing the topology of linkages formed by connecting pairs of links together has been developed. The displacement analysis of a linkage is achieved using a direct method which is considerably faster than alternative techniques. A non-linear optimization algorithm has been modified to cater for non-linear constraints such as transmission angle. These techniques have been incorporated into a computer program.

Two case studies of using the program are given. The first is the synthesis of a six-bar linkage for a motorcycle rear suspension such that a constant centre distance is maintained between the chain-wheels as the suspension deflects. The second concerns the modification of two linkages, containing eight and ten links respectively, to give an improved knitting action for a warp-knitting machine.

Operating linkages at high speeds can result in rapidly varying forces acting on the frame due to the mass of the moving links. A procedure to determine suitable counterweights to balance these forces has been developed. Since adding the counterweights may double the total mass of the linkage, the links should have minimum mass.

If the mass of a link is reduced too far, the link may vibrate and so detrimentally affect the performance of the linkage. Accordingly the final part reports an investigation into the forced vibration, assuming stability, of a uniform, pin-jointed, binary link. The equations of motion are derived and stability boundaries determined. The theoretical predictions are compared with experimental results from the coupler of a four-bar linkage.

K. Oldham.

UNIVERSITY OF NEWCASTLE UPON TYNE

THE KINEMATICS AND VIBRATION OF PLANAR LINKAGE MECHANISMS.

by

K. OLDHAM, M.A.,C.Eng.,M.I.Mech.E., A.T.I.

A Thesis submitted for the Degree of Doctor of Philosophy in the Faculty of Applied Science, University of Newcastle upon Tyne.

November 1977

'All design is a compromise between divergent requirements - safety and cost, mobility and strength, speed and reliability, and so forth. It requires a touch of artistic genius to get the balance right. This is the function of the design engineer, whether he is producing a bridge, a motor car, a radar station, a military aircraft, or a safety razor'.

Lord Hailsham, 'The Door wherein I Went', Collins, 1975, p.184.

PREFACE

The work reported in this thesis was carried out under three Science Research Council grants and a Department of Industry contract. The original intention was to devote it to an investigation into vibrations in planar linkage mechanisms. However, the Science Research Council visiting panel felt that the needs of industry should be ascertained to ensure industrial relevance. As a result, three problems encountered in the design of planar linkage mechanisms have been investigated, namely kinematic synthesis, balancing of inertia forces and vibration analysis.

The kinematic synthesis of planar linkages containing pin and sliding joints using an optimization approach has been investigated. A concise but easily interpreted technique has been developed for prescribing the topology of linkages formed by connecting pairs of links together. The displacement analysis of a linkage is achieved using a direct method which is considerably faster than alternative techniques. A non-linear optimization algorithm has been modified to cater for non-linear constraints such as transmission angle and loop closure. These techniques have been incorporated into a computer program.

Two case studies of using the program are given. The first is the synthesis of a six-bar linkage for a motorcycle rear suspension. The linkage maintains a constant centre distance between the chainwheels as the suspension deflects. The second concerns the modification of two linkages, containing eight and ten links respectively, to give an improved knitting action for a warp-knitting machine. The discussion following these case studies differs from the usual form in that it compares different techniques and methods rather than theory and experiment.

Operating linkages at high speeds can result in rapidly varying forces acting on the frame due to the mass of the moving links. Accordingly the second part contains the theory and a procedure to determine suitable counterweights to balance these forces. Since adding the

CONTENTS

FIGURES

1. GENERAL INTRODUCTION

1.1 APPLICATIONS OF LINKAGE MECHANISMS

Linkage mechanisms have a long history. For example, a crank-rocker linkage is illustrated in a compendium of agriculture and rural engineering dated 1313 AD (See Nolle {1.1} *). Linkage mechanisms are in widespread use today, both in the home and in industry. Examples range in complexity from slider-crank mechanisms used in conventional umbrellas and a cream-making attachment for a domestic food-mixer to an eleven-bar linkage used in shoe machinery {1.2a} and a fourteen-bar circuit-breaker mechanism {1.3}.

Linkage mechanisms are indispensable where an operation depends on the relative motion between two or more machine elements undergoing simultaneous but different movements at high speed. For example, Kestell {1.2b} describes a machine for stitching a sole to the welt of a shoe at a rate of 1000 stitches/min. In this machine, the combined movements of several elements, e.g. the awl, needle and looper, are required to form a stitch, so linkage mechanisms are used to control them. The awl and needle mechanisms are crank-driven whereas the looper mechanism is cam-driven.

Cams and followers are sometimes regarded as alternatives to linkages,e.g. Eder {1.4} , but there are circumstances, where cams are used, that require a linkage as well. In such cases, one or more of the following conditions applies :

a) there is insufficient space to accommodate the cam close to where the output motion is required, e.g. the valve-gear for an internal combustion engine,

b) the output motion is adjustable e.g. Kestell {1.2c} illustrates a cam-driven, thread-

* References will be found in Appendix A.

measure mechanism in which the length of thread paid out depends on the thickness of the work being stitched,

c) the amplitude of the output motion is different from that of the cam follower; the output amplitude may be larger, as in the case of a draw mechanism for a weft-knitting machine (one version of which is given by Wignall {1.5}) in which the output amplitude is adjustable and may be a maximum of 42 in. compared with a cam throw of 9 in., or smaller, as in a copying machine where a negative magnification, to reduce errors, is obtained using a pantograph mechanism,

d) two cams are used to generate a two-dimensional output motion, the linkage being required to combine the motions, e.g. Bloom {1.6} and Wray et al. {1.7} where one component of the output is adjustable to provide different spacings of the loops in a looped pile fabric machine,

e) a positive drive is required from a single cam profile using swinging followers e.g. Jackowski and Dubil {1.8} , an early example of its use is illustrated by Willkomm {1.9}.

There is a continual demand made on industrial designers for machines that will run faster and yet be simpler to manufacture. If cams are used at higher speeds, greater attention must be paid to producing a profile that gives the desired dynamic performance as this is significantly affected by local profile errors. In addition, if a spring-loaded follower is used, high spring forces will be necessary to maintain contact and these forces will cause high contact stresses and possible surface failure. A closed-track cam with a single roller follower suffers from impact and skidding, causing noise and wear, when the roller changes from one side of the track to the other. To overcome these

problems, a form-closed, double roller system is commonly used (see Rothbart {1.10}. However, such a system must be produced very accurately (which is expensive), otherwise interference will result causing large contact stresses at the high spots or backlash will occur at the low spots with the possibility of impact. Having paid attention to the cam law and used two pairs of conjugate cams (cam and countercam), Tovey and Arnold {1.11} found that they were able to double the speed of their loom by replacing the cam-driven mechanisms by a six-bar linkage and a four-bar linkage. In view of these factors, the trend is likely to be away from cam-driven mechanisms towards crank-driven linkages.

1.2 SURVEY OF DESIGN FACTORS

The first stage in designing a linkage mechanism is to determine the link lengths that give the required motion or force transformation between the input and output. Design aids are available for both slider-crank mechanisms and four-bar linkages. Examples include those published by VDI {1.12}, which cover both planar and spatial linkages, the atlas by Hain {1.13}, the design memorandum prepared by ESDU {1.14} and the atlas of four-bar linkage curves by Hrones and Nelson {1.15}. However, slider-crank mechanisms and four-bar linkages are limited in the output motion that they can produce. For instance, a four-bar linkage with a constant speed input crank cannot produce a dwell, so use must be made of more links, e.g. a six-bar linkage, and/or gears, as, for example, by Yokoyama {1.16}. As a result, there will be an increasing requirement for a design aid that will help the machine designer to synthesize a wide variety of linkage mechanisms without having to learn a multiplicity of techniques, such as those given by Hain {1.17}.

Material	Density t/m^3	Specific Modulus MJ/kg	Specific Strength kJ/kg
Cast iron - BS 1452, grade 17	7.25	16	40
SG iron, annealed BS 2789, type SNG 27/12	7.1	24	60
Mild steel	7.8	26.5	50
Low alloy steel	7.8	26.5	125
Aluminium casting	2.7	25.8	80
Magnesium casting, heat-treated	1.8	25	110
Titanium alloy, DTD 5173	4.5	25	200
Carbon fibre reinforced plastic, unidirectional, 50% high modulus polyacrylonitrile based	1.5	115	550

Table 1.1. Representative Values of Specific Modulus and Strength of Various Materials.

measures of the stiffness-weight and strength-weight ratios respectively. Cast iron is easy to machine and has good damping properties. Aluminium alloy links should form flat laminae {1.11} but the low density means that thicker sections can be used for a given mass. Titanium has been used for the guide-bars of a warp-knitting machine but has now been replaced by 'Grafil', a carbon fibre reinforced plastic (CFRP) {1.23}. Partly as a result of this change, the machine speed was increased by 10%. A 50% improvement in the speed of a narrow-fabric loom was obtained by using CFRP instead of steel for the heddle frames {1.21}. Although CFRP offers the twin advantage of high specific modulus and strength, close co-operation between the manufacturer and the machine designer is required to obtain the best results since the directional properties of the material depend on the lay of the carbon fibres.

If the stiffness of the links is too low, the linkage may start to resonate at various speeds resulting in material fatigue with possibly an incorrect output motion and noise radiation from other parts of the machine. If the mechanism is driven by a cam running at constant speed, it is possible to design the cam profile to take into account the effect of mechanism flexibility on the output motion. Dudley {1.24} proposed the use of polynomial curves and Kanzaki and Itao {1.25} have investigated the use of such cams for positioning the typehead in high-speed teleprinters. However, this approach is not applicable to a crank-driven linkage, so, in this case, the designer will want to know how light the links can be to avoid these problems within the envisaged speed range.

The output motion can also be affected by clearance at the joints. For example, in a plain revolute joint, the pin may move from one side of the bush to the other

side across the clearance gap. Under high speed conditions, this change can take place rapidly causing impact, noise and wear when the pin reaches the other side. Earles and Wu {1.26} have developed an empirical formula to predict when contact between the pin and the bush will be lost. The expression includes the rate of change of direction and the magnitude of the applied load calculated under no clearance conditions. Fawcett {1.27} has considered how the tendency to lose contact can be overcome (rather than the alternative approach of attempting to predict what happens once contact has been lost). Sometimes clearance, in addition to that required for lubrication, is necessary and the effects have to be endured. For example, in a shunting engine, parallelogram linkages are used in parallel to transmit the drive to the wheels. There must be sufficient clearance in the joints to allow for any errors in the link lengths so that the linkages can pass through the in-line positions.

Friction at the joints depends on the type of joint, the materials and the lubrication. Kraniauskas and Maunder {1.28} have carried out tests on dry, revolute, PTFE-based bearings of the Glacier DU type which are used extensively in switchgear mechanisms. They found that the coefficient of friction lay between 0.04 and 0.20. It increased with increasing speed until the bearing temperature rose to around 25^{o}C above which the coefficient of friction fell. It also fell markedly as the load was increased. Experimental tests by other workers are also referred to. Tovey and Arnold {1.11} initially used oil splash lubrication but later used a circulatory oil system to reduce the temperature of their SG iron bushes.

Once it has been designed, the mechanism must be manufactured and assembled. The cost of producing the components depends on the tightness of the tolerances and the cost of assembly depends on the method used

which, again, is affected by the tolerances on the link dimensions. There are five assembly methods from which to choose :

a) random assembly with total interchangeability
   - this may require tight tolerances on the link dimensions,

b) random assembly with limited interchangeability based on probability theory
   - it is assumed that the variations in each component due to manufacturing errors are independent; as a result there is only a small probability that the maximum variation will occur simultaneously on several links and that the effects of all of the variations will be additive,

c) random assembly with a compensating member
   - the mechanism is assembled without the compensating member which is then machined to suit the combined variations in the other links,

d) random assembly with an adjustable link
   - this is similar to (c) except that the link may be re-adjusted incorrectly at any time,

e) selective assembly
   - for this to be feasible, there must be a sufficient number of each component from which to select and the number of components in each assembly should be small so that their interaction can be determined.

Thus the choice of the tolerances is an important decision and, to make the correct choice, the designer must know the sensitivity of the output motion from the mechanism to variations in the link lengths. It is desirable that the method for determining this shall be the same as that used originally for selecting the link lengths.

Further development of design methods is both possible and desirable. Contacts with industry have shown that machine designers would appreciate assistance with the determination of the link lengths and the anticipation of linkage vibration. Reflecting these requirements, the thesis is divided into three parts entitled Kinematic Synthesis, Force Balancing and Vibration Analysis respectively.

Summary

After noting some applications of linkage mechanisms, the conditions where linkages are necessary are listed. Their relationship with, and their advantages over, cam-driven mechanisms are then considered. This is followed by a survey of factors to be taken into account in the design of linkage mechanisms. These factors include material selection, force balancing and vibration in addition to clearance and friction at the joints. As well as determining the nominal dimensions of the links, the designer must decide on suitable tolerances for manufacture and assembly. In conclusion, the need for further work in kinematic synthesis, force balancing and vibration is emphasized.

2. SCOPE

2.1 REQUIREMENT

Reuleaux {2.1} defined kinematic synthesis as 'the determination of the pairs, chains or mechanisms necessary to produce a given constrained motion'. Constrained motion means that the mechanism forms exactly the same configuration each time the input assumes the same position. This implies that the elements of the mechanism are rigid, i.e. the dimensions are independent of any forces, and that there is no backlash or clearance at the connections between the elements.

Few machine designers spend all their time designing linkage mechanisms. For many, it is an occasional occupation, so there is a need for a method of kinematic synthesis that applies to all of the linkage mechanisms in general use or likely to be so in the future.

Such a method could be either automatic or interactive. Given a specification, a fully automatic method would select the type of mechanism (e.g. planar, spherical or spatial), the number and types of joints and the number and lengths of the links without further reference to the designer. A method of this type would relegate the designer to a passive role. On the other hand, a suitable interactive method would make full use of the creative skill and experience of the designer whilst relieving him of the search for an appropriate method and the tedium of any repetitive graphical constructions or numerical calculations. An interactive method, perhaps including some automatic procedures, is therefore to be preferred.

In addition to being general and interactive, any method should be systematic and it should be possible to use the same method to determine the sensitivity of the linkage to manufacturing tolerances.

2.2 REVIEW OF CURRENT METHODS

Many methods, both graphical and analytical, have been developed for kinematic synthesis. Nolle {2.2} and Thompson {2.3} have recently reviewed those for

synthesizing linkages to generate coupler curves. They can be divided into two groups depending on the relationship between the number of points used to define the desired motion and the number of unknown parameters, such as link lengths, in the mechanism. Precision point methods depend on the number of points being less than or equal to the number of parameters. The resulting mechanism will produce the desired motion exactly at those points but there is no control over intermediate positions. Optimization methods are used where the number of points is greater than the number of parameters. In this case, there is no guarantee that the resulting mechanism will pass through any of the specified points exactly but there is more control over the general shape of the motion curve. Thompson {2.3} concludes that this is the best type for kinematic synthesis. Kestell {2.4} also followed this approach, using graphical methods, by 'plotting the trend'. Of the graphical and analytical methods, only the analytical ones offer the promise of general application, but, to obtain the full benefit for linkages with more than a few links, they require the use of a computer. There have been three attempts to develop computer-based methods applicable to virtually all planar linkages.

The first, called KOGEOP (KOppel-GEtriebe-OPtimierung), has been developed by Dresig et al {2.5 - 2.7} for both kinematic synthesis and dynamic optimization using a BESM-6 computer. No indication of the size of the program (I reserve this spelling for computer programs) is given, but it must be considerable since the user has the choice of eight optimization routines.

The second, called KINSYN, has been developed by Kaufman {2.8, 2.9}. The original version used a precision point approach and relied on the user being familiar with Burmester theory. It was designed for an

IBM 1130 computer with 8K words of core storage and a storage tube display. Later it grew until, by 1973, it consisted of well over 15,000 cards of Fortran and Assembler language code. Since this is difficult to manage, a new version is being developed to make use of a computer system with a refresh-type graphical display (which is considerably more expensive than a storage tube display).

The most ambitious attempt is that by Bona et al {2.10}. This consists of a suite of 27 programs (one of which is based on KINSYN). The scope is considerable, including, in addition to linkage synthesis and analysis, cam and gear design, stress and tolerance analysis, automatic drafting and preparation of NC tapes. The intention was also to include a mechanism data bank but, although this is considered to be feasible, it has been discontinued because of lack of storage space and limited availability of suitable computer terminals. The package uses an IBM 1130 computer with 32K words of core storage and one million words of disc storage with an IBM 2250 refresh-type graphic display.

These attempts, which cater for only planar linkages, all require a large amount of computer storage and two use refresh-type graphic displays. This combination of facilities is not generally available to machine designers in this country.

The use of analogue, rather than digital, computers has also been advocated for the kinematic synthesis of planar linkages. Keller {2.11} used an analogue computer to simulate a slider-crank mechanism and a four-bar linkage. Brat and Vaclavik {2.12} synthesized a four-bar linkage for a crane and Rees Jones {2.13} synthesized a six-bar linkage for a power press. There are two main advantages. The first is speed of computation. Secondly, the user can control the linkage parameters directly and so determine the effect

of changes quickly. There are also two main disadvantages. The first lies in gaining access to a computer of adequate size. Secondly, unless it is frequently used for the synthesis of linkages of the required type, it must be specially patched. This requires an understanding of the operation of the computer so that the desired results are obtained without overloading the amplifiers. Also the accuracy of computation is limited. Thus, while the analogue computer can play a useful role in kinematic synthesis, its application is severely limited by its disadvantages.

However, only computer-based methods offer the prospect of a technique that is generally applicable but, to be fully effective, they should be used directly by the designer, since he alone knows the full specification, both implicit as well as explicit. Thus there is a need for a smaller package for a digital computer which does not require so much storage or expensive, special purpose peripheral equipment. Preferably the package should be portable i.e. easily transferable from one model of computer to another. Such a package will almost certainly cater for a more limited (but hopefully still wide) range of linkages.

2.3 CHOICE OF APPROACH

At this stage, it is useful to consider the role that such a computer program could play in kinematic synthesis. Hartenberg and Denavit {2.14} divide kinematic synthesis into three phases - type synthesis, number synthesis and dimensional synthesis.

Type synthesis is the choice of the types of machine elements, such as links, gears, cams and belts, that will constitute the mechanism. In this thesis, attention will be confined to mechanisms consisting only of links since design methods for cams, gears etc. are well established.

Number synthesis is concerned with the choice between mechanisms of the same constructional type. Since it forms a convenient approach to identifying a suitable group of mechanisms, it is used for this purpose in the next chapter. The selection of an appropriate mechanism from the group is left to the discretion of the designer since number synthesis, whilst identifying the different possibilities, at present provides little guidance in this respect.

The determination of the sizes of the elements in the chosen mechanism is the province of dimensional synthesis. If the computer program is based on an optimization approach, then the designer must not only decide on the type of mechanism, but also provide an estimate of its dimensions. The program would then refine this estimate to give a mechanism that would produce a more accurate approximation to the desired motion. This approach fulfils the requirement that the designer shall be able to make full use of his creative skill and experience since he can use any methods, with which he is familiar, to obtain the initial estimate. Such methods include the construction of cardboard models (see Reference {2.14}) 'to get the feel', graphical methods of all types, precision point analytical techniques and the use of analogue computers. Alternatively, the designer can use an existing mechanism as the starting point.

In order to fulfil this refining function, any general kinematic synthesis program of this type must :

a) enable the designer to choose an appropriate mechanism and inform the computer of his choice - this may involve the designer in specifying the structure (or topology) of the selected mechanism,

b) automatically set up the equations necessary to analyse that mechanism and so determine the difference between the desired motion and the actual motion,

c) automatically change the link dimensions to provide an improved output motion, i.e. contain a suitable optimization routine, whilst allowing the designer to keep some dimensions fixed in case he wants to make use of existing standard components.

In addition, it should be possible to use the same program to determine the effect of manufacturing tolerances.

The next chapter is therefore concerned with identifying a set of mechanisms that form an easily recognizable, coherent group which is of wide application. This is followed by three chapters concerned with topology, analysis and optimization since, to a certain extent, these three aspects are independent.

Summary

This chapter starts with a definition of kinematic synthesis. Since most machine designers synthesize linkage mechanisms only occasionally, they would prefer a general method of kinematic synthesis that caters for all of the linkages that they are likely to use. The desirability of the designer being involved in the synthesis is noted and it is concluded that an optimization method gives more scope for this than a precision point method. Such a method requires the use of a computer and the relative advantages of a digital computer over an analogue computer for this purpose are given. The computer programs in the literature are either specific to particular linkages or very general and hence large and unwieldy. The conclusion is that there is a need for a program between these extremes and the desirable features of such a program are given.

3. SELECTION

3.1 TERMINOLOGY AND CONVENTIONS

This section contains definitions of the various terms and details of the conventions used. In general, only the skeleton of a linkage is drawn.

An arc is a straight line connecting one joint to another in the same link. A link with j joints has j(j-1)/2 possible arcs, e.g. a binary link has one arc and a ternary link has three.

A loop is a closed kinematic chain formed by a number of rigid links connected by joints that permit relative motion between the links they connect. This convention differs from that usually adopted in graph theory where loops formed by arcs within a single link are also valid.

A set of independent loops in a linkage, as defined by Paul {3.1}, is determined by the following procedure. Wherever a loop exists, cut a link in that loop close to one of its joints that is also in the loop so that the joint is severed from the link thereby opening the loop and, maybe, others. When no loops remain, the reconnection of any one of the cut links to the corresponding joint will result in the formation of only one loop. The loop so formed is an independent loop. The set of loops formed by reconnecting each cut link individually constitutes the required set. Different sets of independent loops are formed by cutting different sets of links, but the number of loops is constant for a given linkage. The unclosed but connected chains that result when all of the cut arcs are removed are called spanning trees. Each set of arcs severed by a cut constitutes a chord, Deo {3.2}.

The axis of sliding associated with a prismatic (or sliding) joint may be taken as passing through another joint in one of the two links connected by the prismatic joint. That link is regarded as the sliding link with

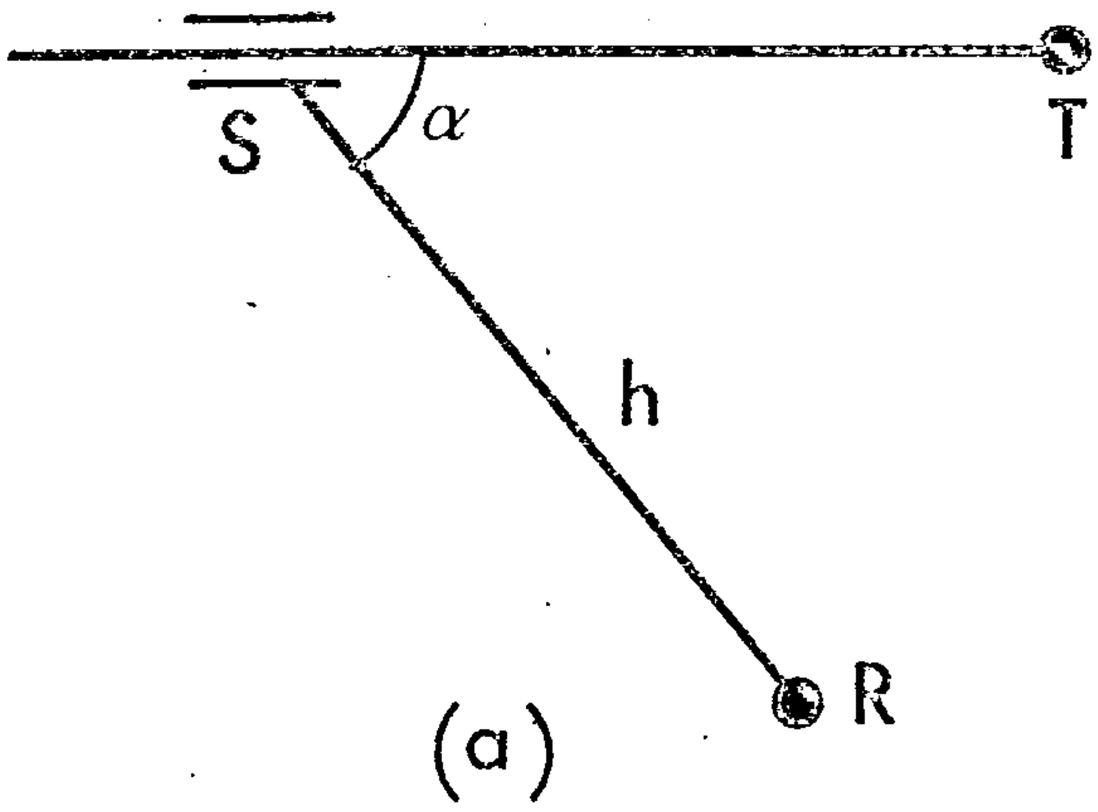

(a)

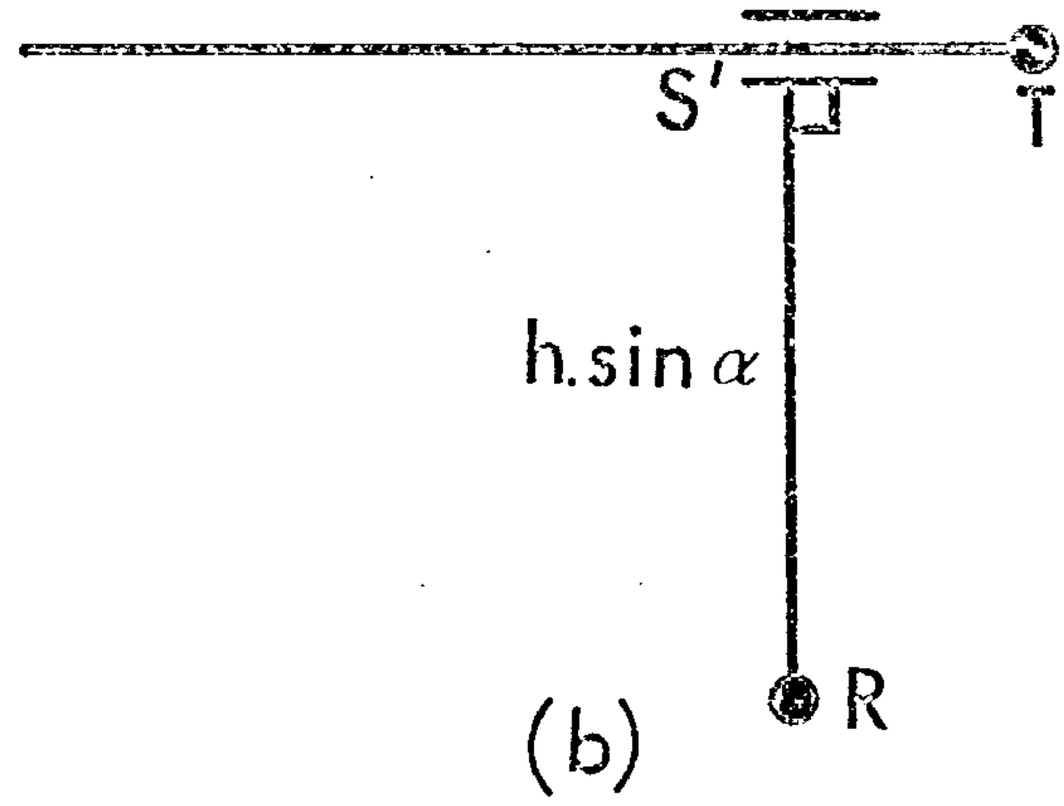

(b)

EQUIVALENT GUIDE LINK RS'

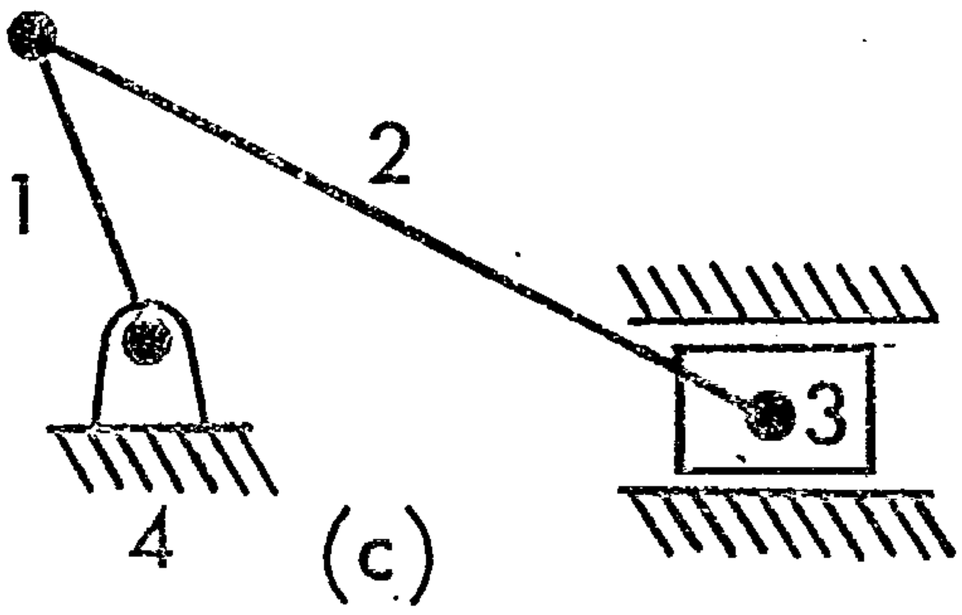

(c)

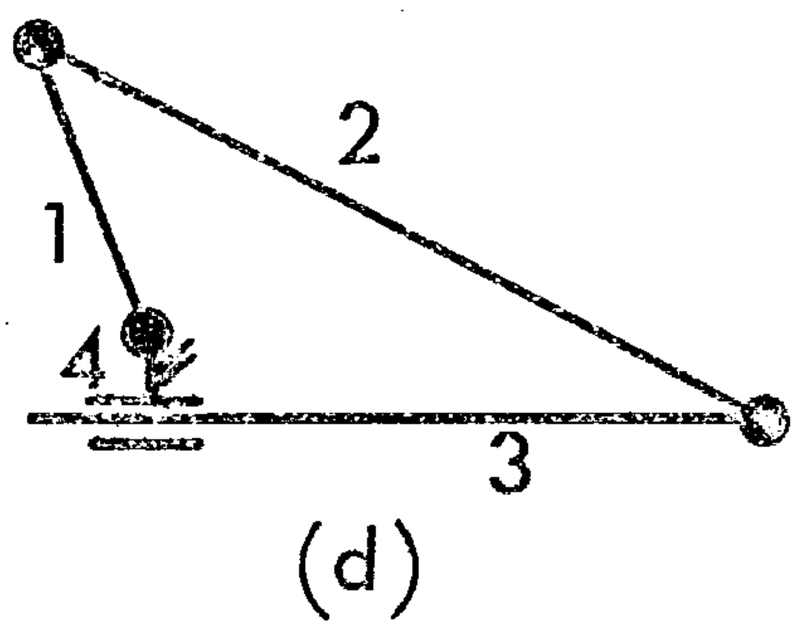

(d)

OFFSET SLIDER CRANK

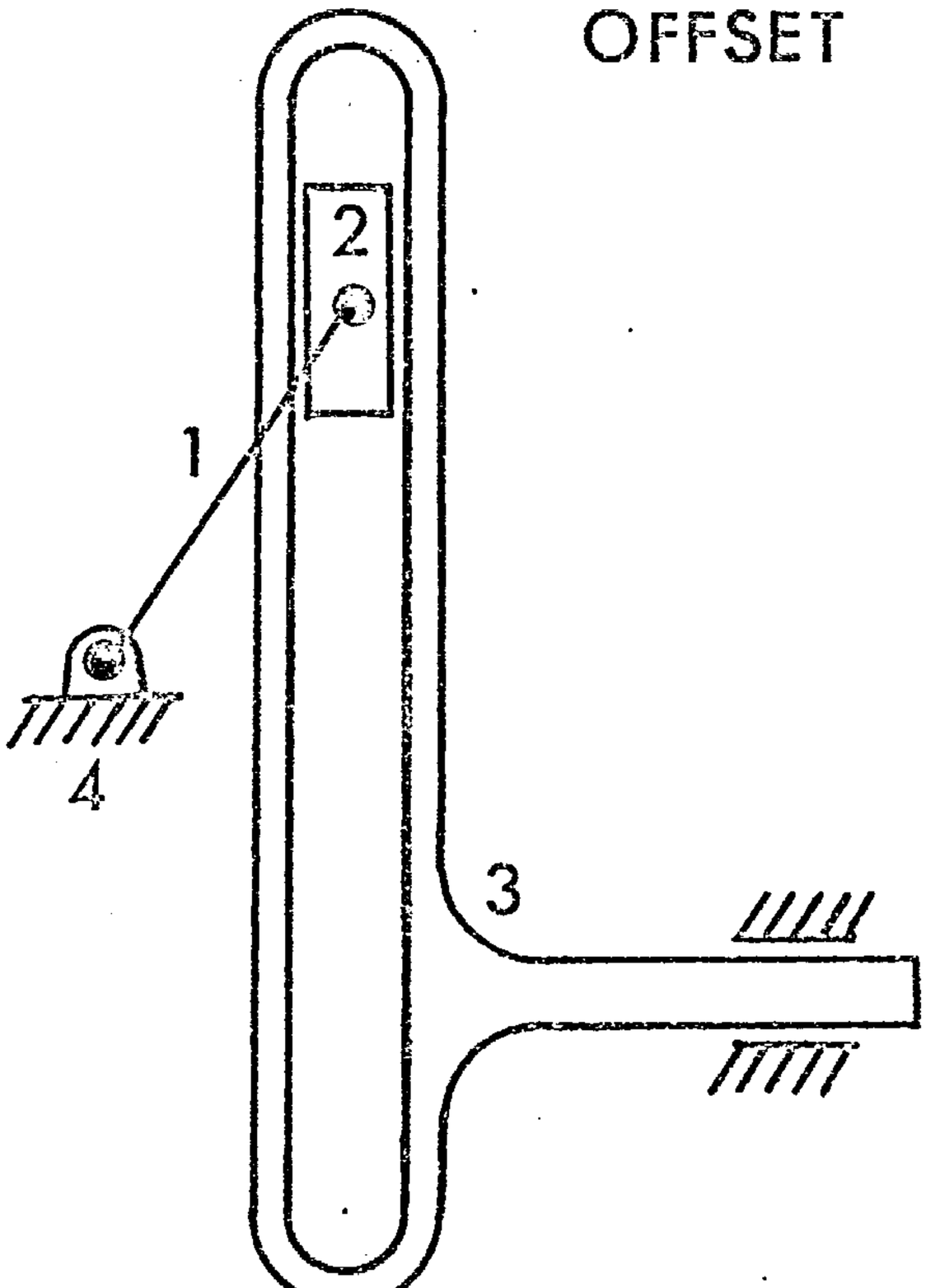

(e)

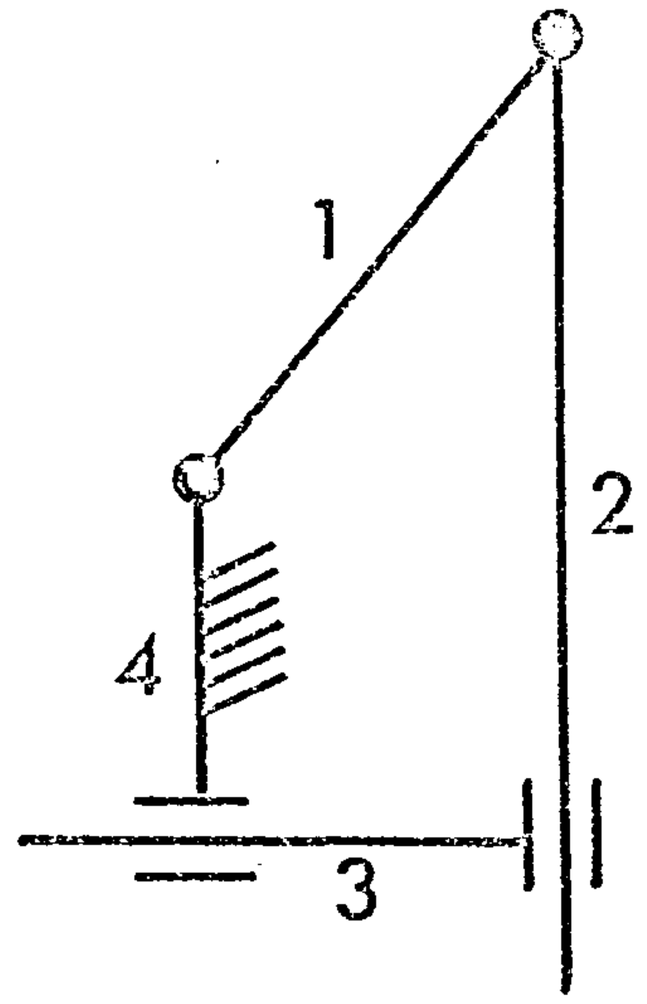

(f)

SCOTCH YOKE MECHANISM

FIGURE 3.1. PRISMATIC JOINTS

the other link acting as the guide link. A guide link is taken as being perpendicular to the associated sliding link, a convention that is retained even when the guide link has zero length. Thus, for example, in Figure 3.1a if a link RS of length h carries at its end S a guide through which passes a sliding link ST at a constant angle RST equal to α, a kinematically equivalent arrangement, Figure 3.1b, is adopted in which link RS is replaced by link RS' of length $(h\sin\alpha)$ disposed at right angles to ST. The length of the sliding link is then regarded as S'T.

If there is a revolute (or turning) joint coincident with a prismatic joint to allow relative rotation as well as sliding, the two joints are separated by a link which may be of zero length. The resulting arrangement must have the same kinematic characteristics as the original. Thus the offset slider-crank mechanism shown in Figure 3.1c is redrawn as shown in Figure 3.1d. Similarly, the scotch yoke mechanism shown in Figure 3.1e becomes Figure 3.1f in which the sliding link 3 (the yoke) acts as the guide link for the other sliding link, 2.

Different combinations of revolute and prismatic joints may be used in a linkage as long as the following conditions are observed (Grübler {3.3}) :

a) No loop in the linkage may have less than two revolute joints,

b) Binary links with only prismatic joint elements may not be connected directly together.

c) No link may contain only prismatic joints whose directions of motion are parallel to each other.

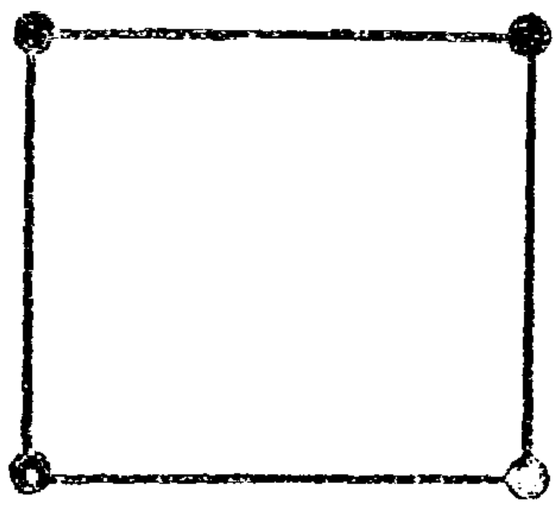

(a) All revolute joints

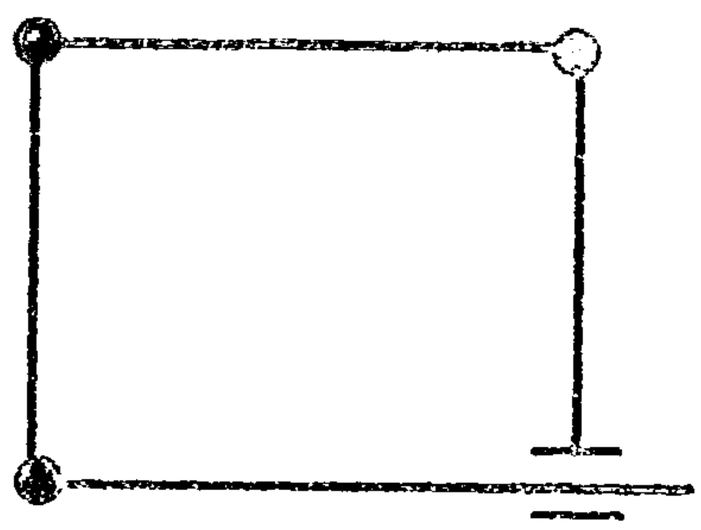

(b) One prismatic joint

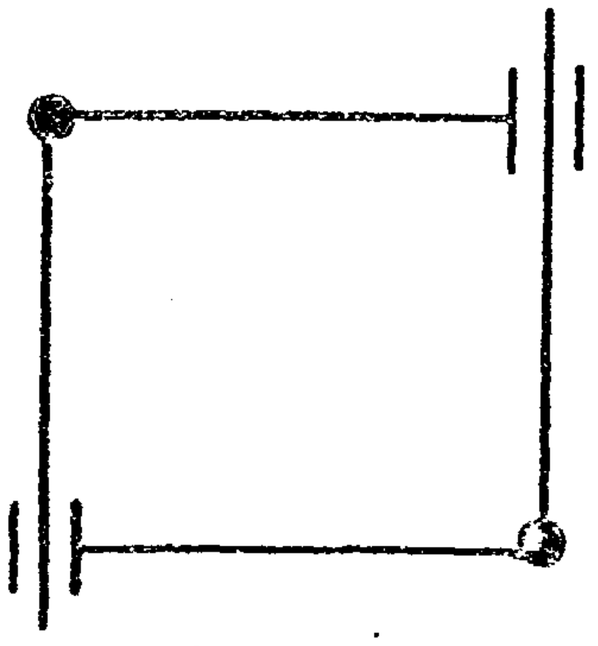

(c) Alternate prismatic joints

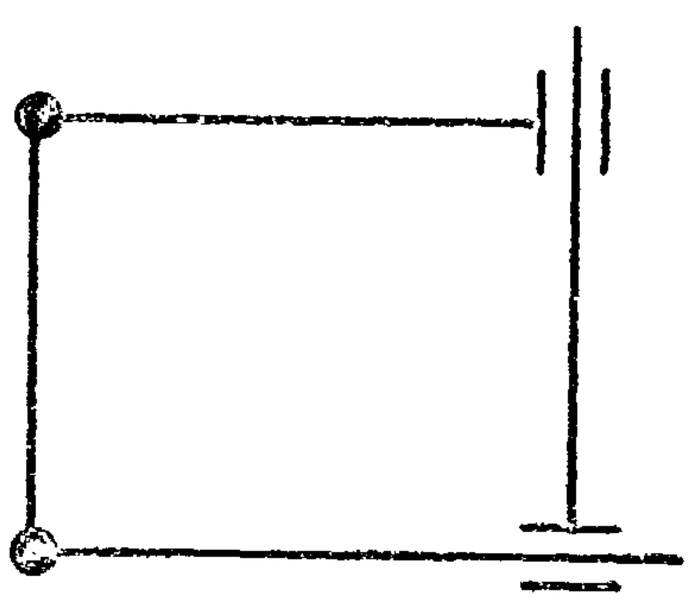

(d) Adjacent prismatic joints

FIGURE 3.2. FOUR-BAR CHAINS WITH ONE DEGREE OF FREEDOM

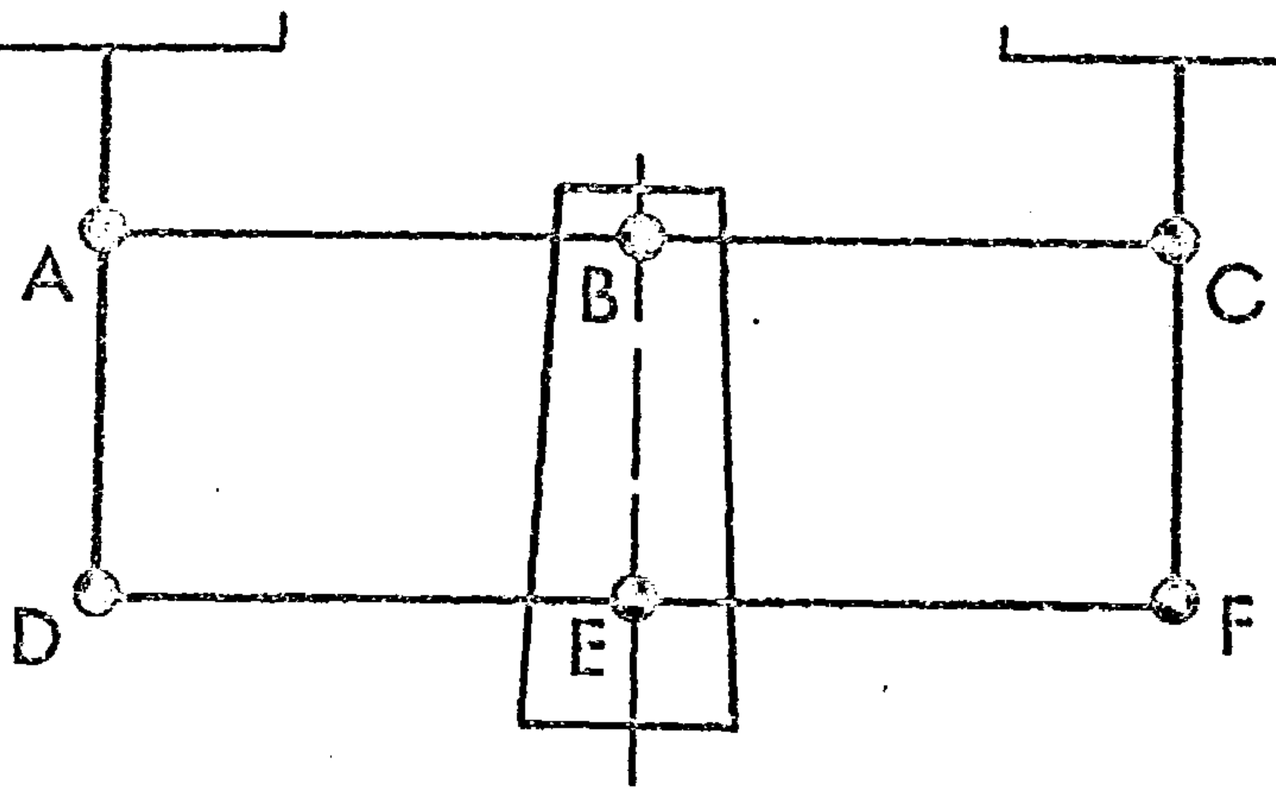

FIGURE 3.3. ROBERVAL SCALE

Thus, for example, a loop of four links may take the four forms shown in Figure 3.2. When one of the links is fixed, i.e. is chosen as the frame link, these become, respectively :

a) a four-bar linkage,
b) different inversions of the slider-crank mechanism,
c) Rapson's slide,
d) scotch yoke mechanism, Oldham's coupling and elliptic trammel.

3.2 DEGREES OF FREEDOM

With linkage mechanisms, the designer is free to choose the number of links and joints subject to the resulting assembly being a mechanism with the required degrees of freedom (equal to the number of inputs necessary for constrained motion) and not a structure. Many investigators have proposed equations to determine the degree of freedom of a mechanism. Some recent work may be found in References {3.4-3.7}. The main difficulty lies in finding an equation which holds for mechanisms with mixed mobility, i.e. having both planar and spatial loops, and metric restrictions (i.e. special relationships between link lengths or angles).

Following Freudenstein and Alizade {3.7}, the degree of freedom of any mechanism is the difference between the number of independent, scalar, displacement variables and the number of independent, scalar, zero-order differential constraint equations. For a linkage mechanism, it is convenient to take the displacement variables as those associated with the relative motion between paired links. The appropriate constraint equations are then the equations of loop closure of the independent loops formed by the links.

The degree of freedom of any linkage mechanism in any position is then given by :

$$F = \sum_{i=1}^{M} m_i - \sum_{i=1}^{L} \lambda_i \qquad (3.1)$$

where F = degree of freedom of the mechanism,

m_i = i-th independent, scalar, displacement variable of the mechanism (associated with the relative displacements at a joint),

M = total number of independent, scalar, displacement variables,

L = number of independent loops in the mechanism,

λ_i = number of independent, scalar, loop-closure equations associated with the i-th independent loop.

The number of independent loops is given by (Deo {3.2}):

$$L = k+j-\ell \qquad (3.2)$$

where k = number of spanning trees formed when a set of independent loops is determined by the procedure given in Section 3.1; for a linkage mechanism, k equals one,

j = number of joints in the mechanism, a joint connecting n links being counted as (n-1) joints,

ℓ = number of links in the mechanism.

Equation (3.1) may be difficult to apply in particular cases where metric conditions apply. For example, Figure 3.3 shows a Roberval Scale in which the two congruent ternary links, ABC and DEF, are connected by three equal binary links, AD, BE and CF. From equation (3.2), there are two independent loops, namely any two selected from ABEDA, BCFEB and ACFDA. The displacement variables consist of eight angles, of which only two are different because of the parallelogram construction.

Hence,

$$\sum_{i=1}^{M} m_i = 2 \qquad (3.3)$$

There is one condition, which is both necessary and sufficient, to ensure loop closure, namely that the sum of these two angles shall be two right angles, so

$$\sum_{i=1}^{L} \lambda_i = 1 \qquad (3.4)$$

The other loop-closure equations reduce to identities because of the special proportions and so disappear. Substituting equations (3.3) and (3.4) into equation (3.1) gives one degree of freedom.

Metric conditions are necessary in an overclosed linkage if certain of the links are not to form a structure. Further discussion of this may be found in References {3.6, 3.8 to 3.10}. For the remainder of this section, attention is restricted to cases where there are no metric conditions. This is not unduly restrictive since, in general, a designer will not use metric conditions to provide an extra degree of freedom because manufacturing tolerances and elasticity effects may well nullify those conditions. The acceptable exception to this exclusion occurs in planar linkages containing only revolute and prismatic joints. In such linkages, the axes of the revolute joints must be parallel and the axes of sliding of the prismatic joints must lie in the plane of the linkage. Alternatively, the clearance at the joints must be sufficient to accommodate any misalignment. (For further discussion of this see Davies and Umphrey {3.11}). This condition is widely used since it is easily obtained.

In the absence of metric conditions other than that noted above, the loop-closure equations essentially express the closure around a polygon of the relative motion of adjacent rigid bodies. They result from the algebraic sum of the projections of the links forming a loop on a set of fixed Cartesian axes being zero and

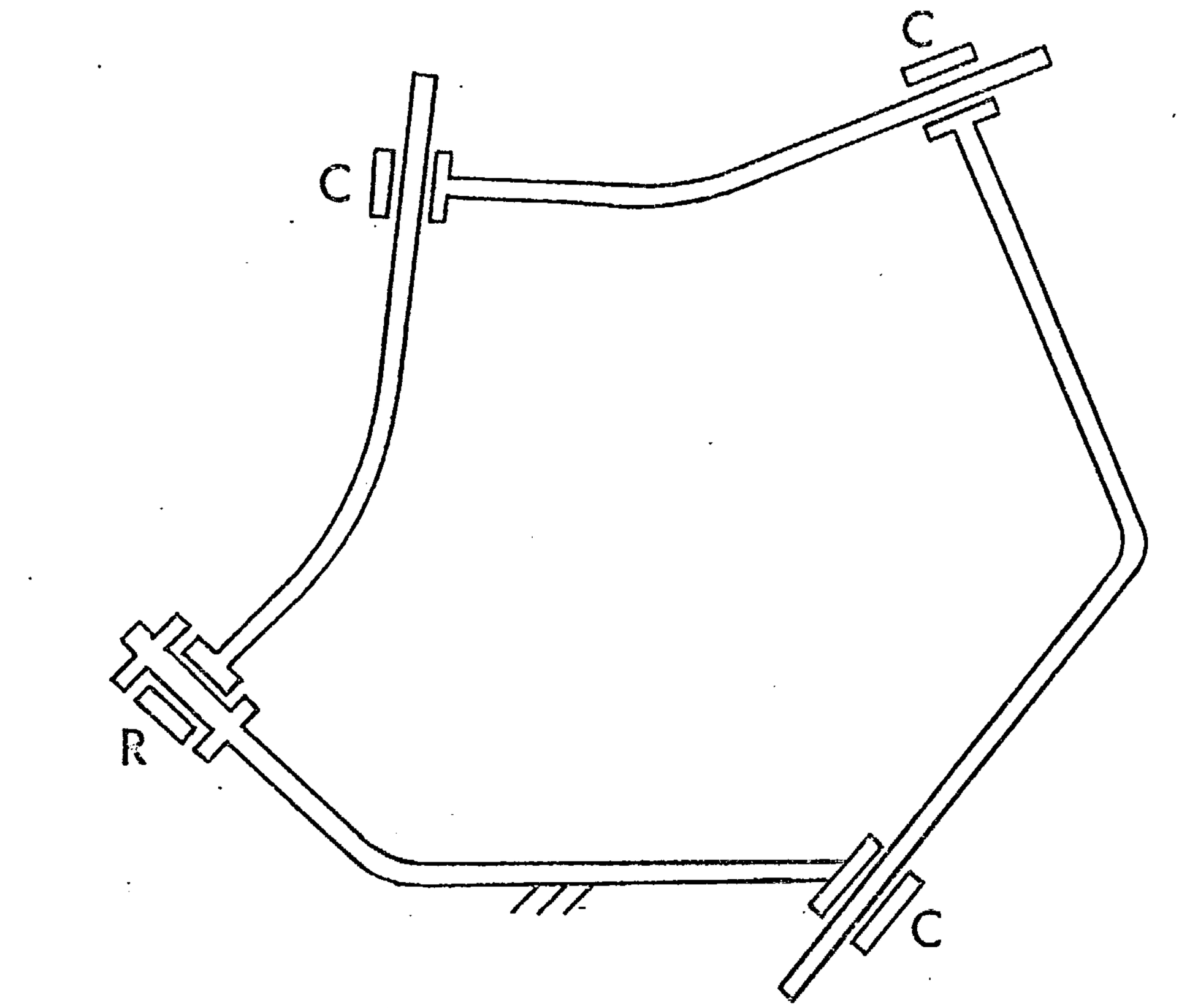

FIGURE 3.4. SPATIAL RCCC MECHANISM

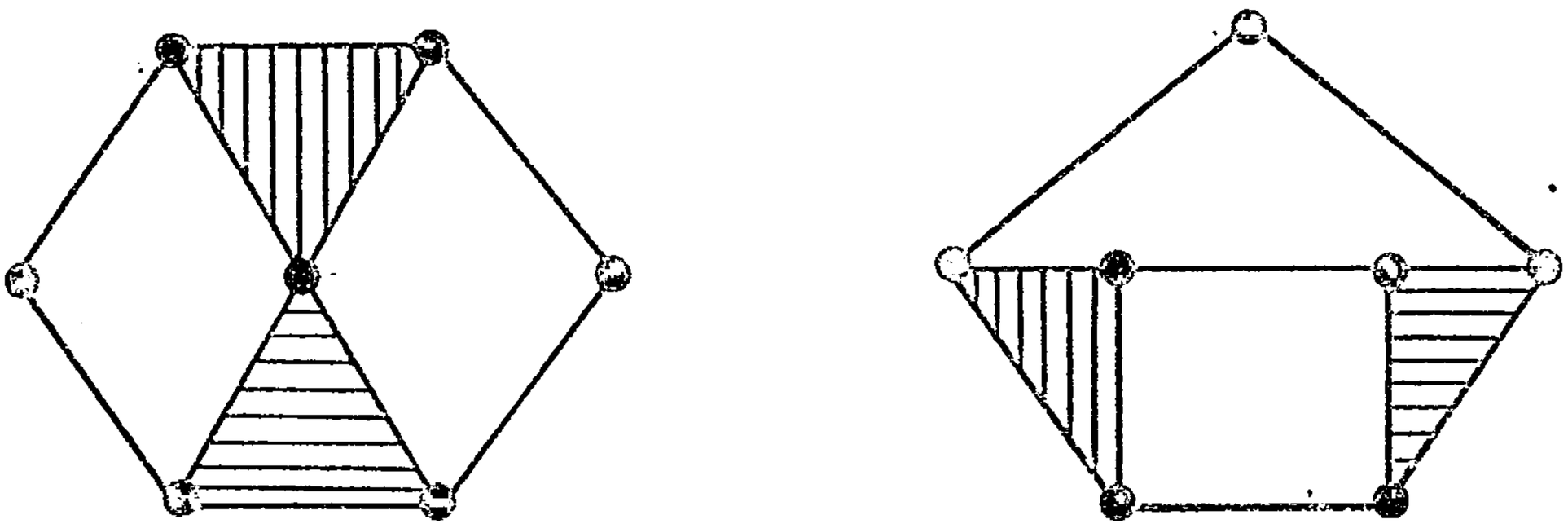

(a) Watt (b) Stephenson

FIGURE 3.5. SIX-BAR CHAINS WITH ONE DEGREE OF FREEDOM

also from the angle turned through, while traversing the projection of the loop on the Cartesian co-ordinate planes, being 360 degrees. The mobility number, λ, then equals the degree of freedom of the space in which the loop operates and so is six for a spatial loop and three for a planar loop. If the number of independent, scalar, loop-closure equations is identical in each independent loop, i.e. the mechanism does not have mixed mobility, we may write :

$$\lambda = \lambda_i \quad (i = 1,2,3,....L) \tag{3.5}$$

In addition, each displacement variable, m_i, is associated with one of the degrees of freedom of the relative motion at a joint. Hence :

$$\sum_{i=1}^{M} m_i = \sum_{i=1}^{j} f_i \tag{3.6}$$

where f_i = degree of freedom of relative motion permitted at the i-th joint

Note that to provide any constraint, f_i cannot be greater than, or equal to, λ. Combining equations (3.1, 3.5 and 3.6), we have :

$$F = \sum_{i=1}^{j} f_i - \lambda L \tag{3.7}$$

As an example, Figure 3.4 shows a spatial four-bar linkage with one revolute joint, for which f_i equals one, and three cylindrical joints, for which f_i equals two. There are seven scalar displacement co-ordinates corresponding to four angles and three sliding displacements. There is one spatial loop with a mobility number of six. Thus, from equation (3.7), the linkage has one degree of freedom. Under certain conditions, one of the cylindrical joints may be replaced by a revolute joint. This gives either a spatial scotch yoke mechanism, in which the two

cylindrical joints are adjacent, or a three-dimensional slider-crank mechanism in which the revolute and cylindrical joints alternate. The latter mechanism was used in Robertson's steam-engine, Reuleaux {3.12}. The two forms are clearly illustrated in Reference {3.9a}.

Using equation (3.2), equation (3.7) may be written in the form :

$$F = \lambda(\ell-1) - \sum_{i=1}^{\lambda} i.p_i \qquad (3.8)$$

where p_i = number of joints of class i - class i joints are those with degree of freedom $(\lambda-i)$.

This terminology corresponds to East European practice (see, for example, Morecki {3.13}). Equations (3.7) and (3.8) are equivalent to the Kutzbach Criterion or the Structural Formula of Artobolevskii and Dobrovolskii for spatial mechanisms and the Chebyshev and Grubler Criteria for planar mechanisms. Freudenstein and Alizade {3.7} also list a selection of other degree-of-freedom equations which have been proposed during the last hundred years.

3.3 KINEMATIC CHAINS AND PLANAR LINKAGES

The great majority of linkage mechanisms in use in industry are planar linkages with a single degree of freedom. In the absence of cams, gears and belts, the joints in these linkages will be lower kinematic pairs with one degree of freedom, i.e. revolute and prismatic joints. For such linkages, equation (3.8) becomes :

$$1 = 3(\ell-1) - 2p \qquad (3.9)$$

where p = number of prismatic and simple revolute joints, i.e. a revolute joint connecting n links is counted as $(n-1)$ joints.

In defining the kinematic chain associated with a linkage, no distinction is made between the different types of lower kinematic pairs. Thus the four versions of a loop of four links shown in Figure 3.2 are counted as one chain. There is a finite number of distinct (non-isomorphic) kinematic chains that satisfy equation (3.9). The numbers of such chains with up to twelve links are given in Table 3.1.

Table 3.1 Kinematic Chains with One Degree of Freedom

Number of links, ℓ	Number of joints, j	Number of chains
4	4	1
6	7	2
8	10	16
10	13	230
12	16	6855

The four-bar chain is shown in Figure 3.2a and the two six-bar chains - Watt and Stephenson - are shown in Figure 3.5. The 16 eight-bar chains have been known for at least sixty years, but the number was finally confirmed by Crossley {3.14}. In 1917, Klein {3.15} stated that there are 228 ten-link chains, but Davies and Crossley {3.16} showed that the correct number is 230 and these are depicted by Woo {3.17}. Klein {3.15} estimated that there are about 4000 twelve-link chains but Kiper and Schian {3.18} have shown that there are 6855. The problem of recognizing whether chains are equivalent has been discussed recently by Uicker and Raicu {3.19}.

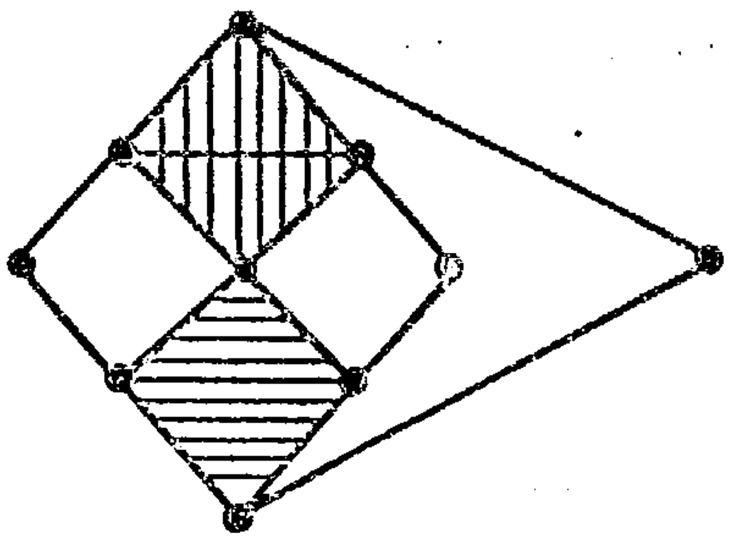

(a)

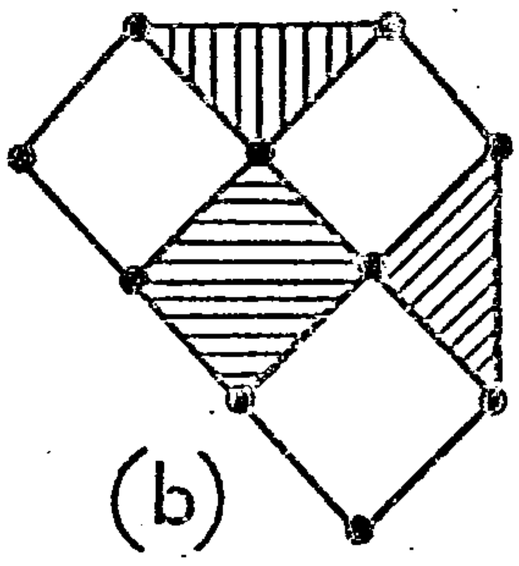

(b)

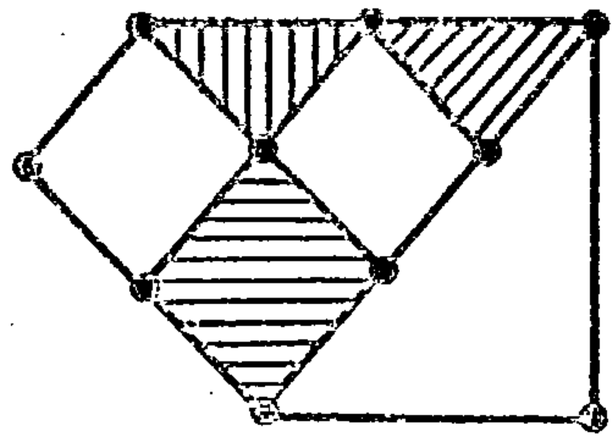

(c)

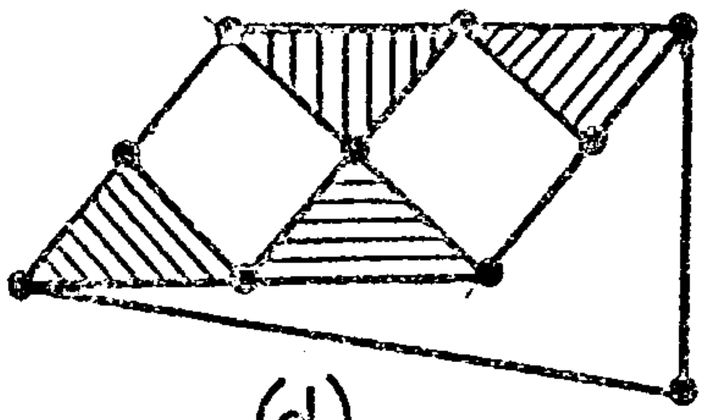

(d)

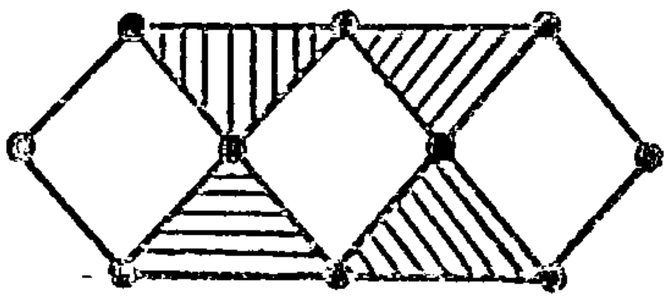

(e)

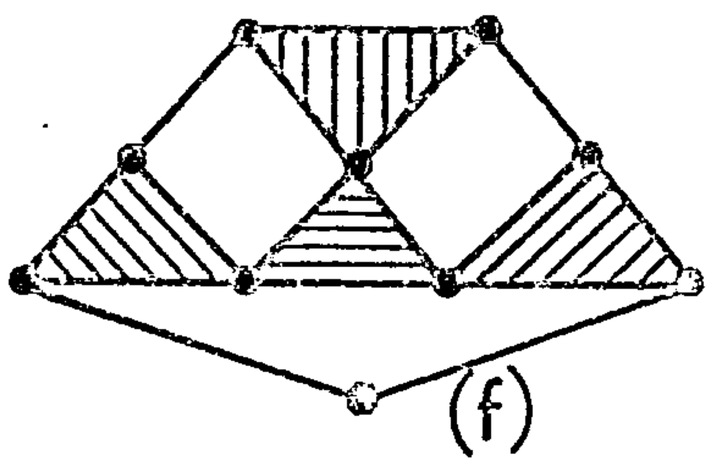

(f)

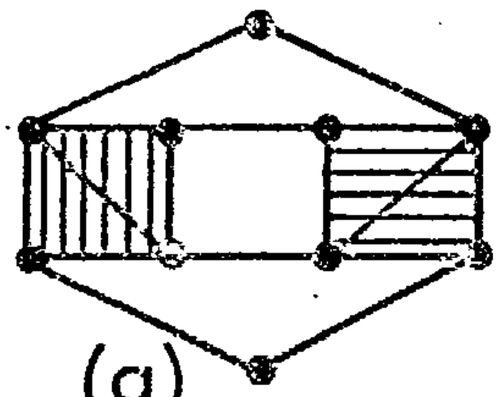

(g)

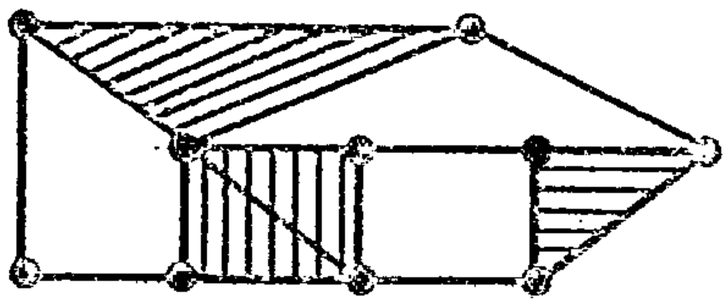

(h)

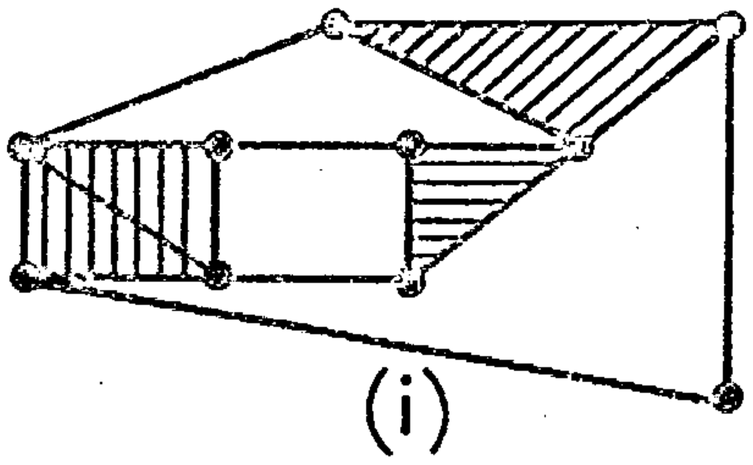

(i)

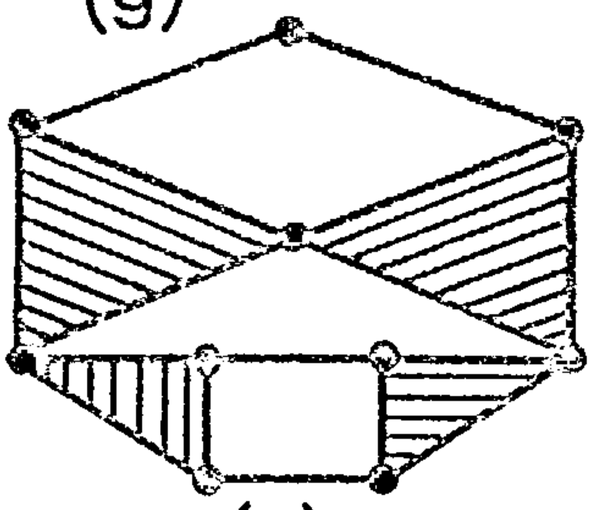

(j)

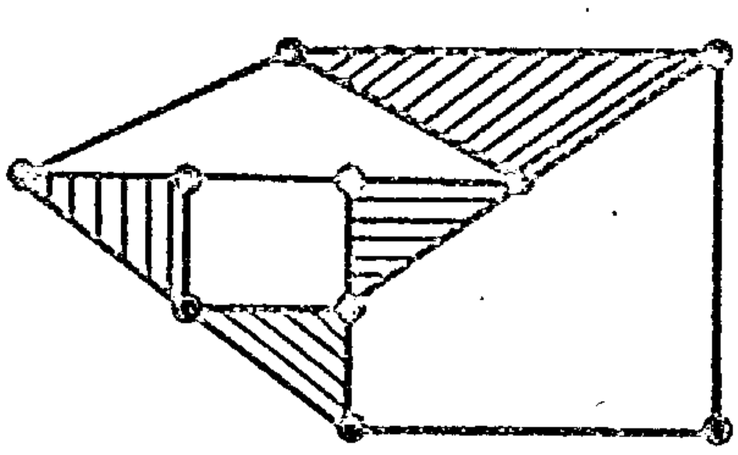

(k)

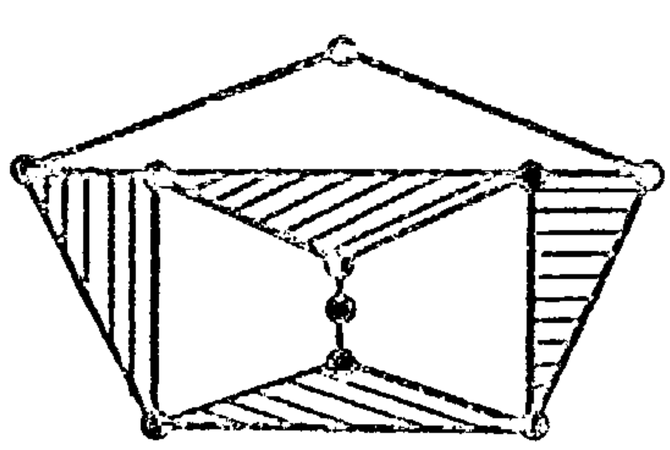

(l)

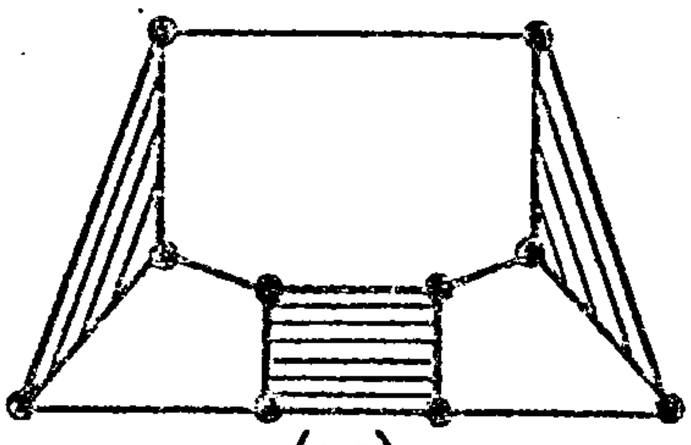

(m)

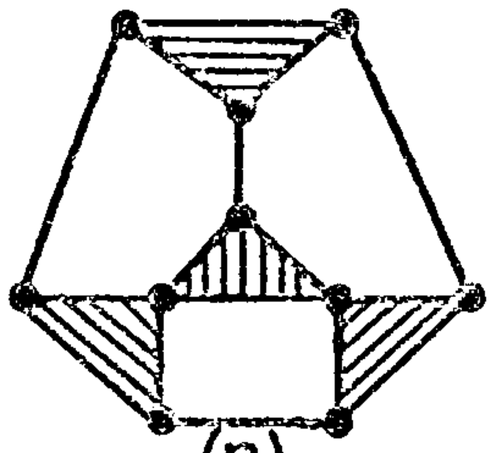

(n)

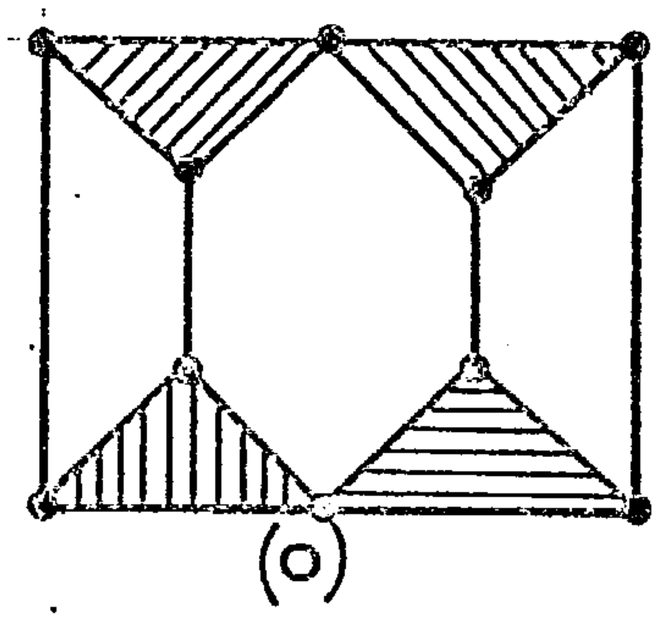

(o)

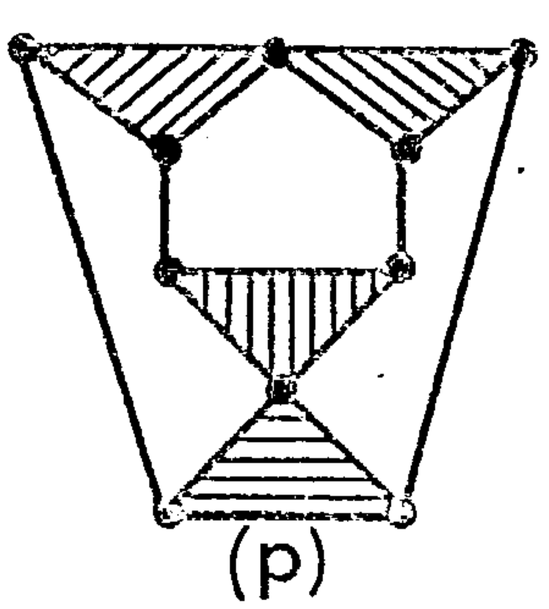

(p)

FIGURE 3·6 EIGHT-BAR CHAINS WITH ONE DEGREE OF FREEDOM

The 16 eight-bar chains are shown in Figure 3.6. The first six (a-f) may be formed by attaching a dyad, i.e. a pair of binary links, to the Watt six-bar chain and the second six (g-ℓ) similarly from the Stephenson six-bar chain shown in Figure 3.5. In turn, the six-bar chains may be formed by attaching a dyad to the four-bar chain in Figure 3.2a. Following Klein {3.15}, we may call these 'peelable dyads' since peeling one from any of the twelve chains would leave a connected chain with one degree of freedom. No dyads can be removed from the remaining four chains, Figure 3.6 m-p, without altering the degree of freedom. This suggests that these latter chains should possess characteristics which are unobtainable with the other chains. This is particularly true of chain (p) which does not contain a four-bar loop.

A linkage is formed from a kinematic chain by anchoring one link to form the frame link. For a single degree-of-freedom linkage, one input must be applied to produce constrained motion. This input will act between a pair of links and is associated with the joint connecting those links. Following Davies {3.20} , this joint is termed an 'actuator pair'. If the actuator pair connects the frame link to another link, that link is termed the 'input link'.

The linkage can be divided into an active unit, that contains the actuator pair and the associated links, and one or more passive units (see Verho {3.21}). If the frame link is included in the active unit, that unit is regarded as the basic unit of the linkage. The basic unit is expanded in one or more stages until it forms the linkage. Each stage consists of the addition of a passive unit to the (expanded) basic unit. At each stage in the expansion, the assembly must have the same number of degrees of freedom as the original basic unit.

As defined above, each passive unit forms an Assur group. This is a chain of links, connected by lower

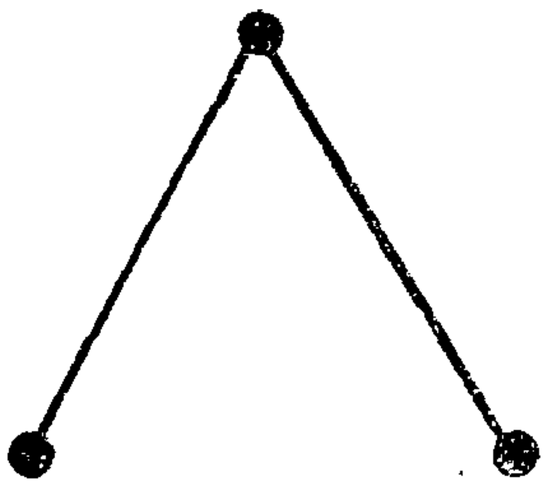

(a) Binary group

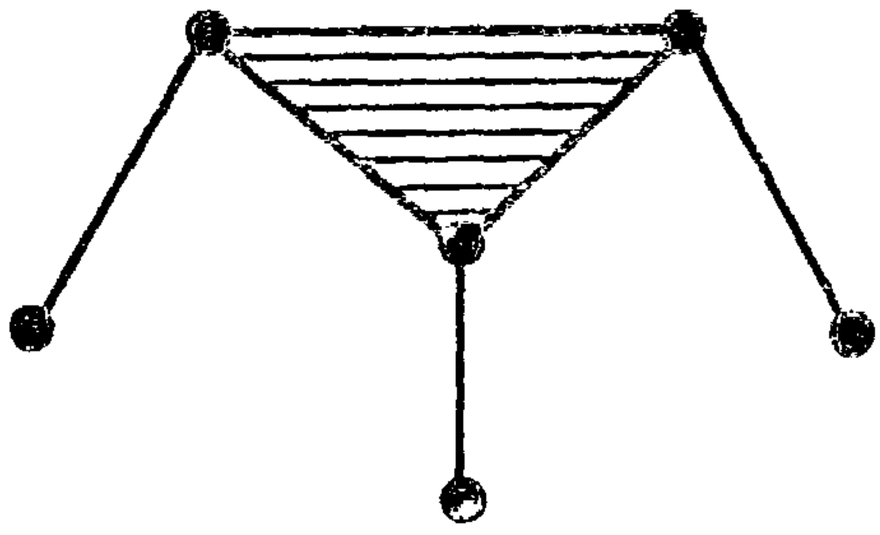

(b) Ternary group

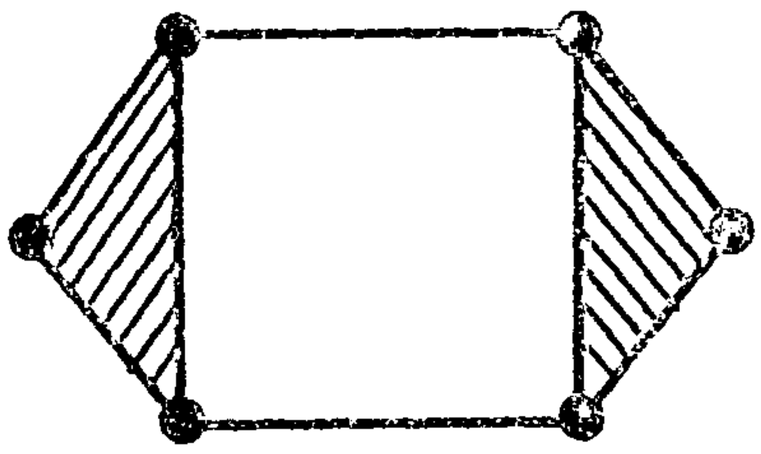

(c) Quadrilateral group

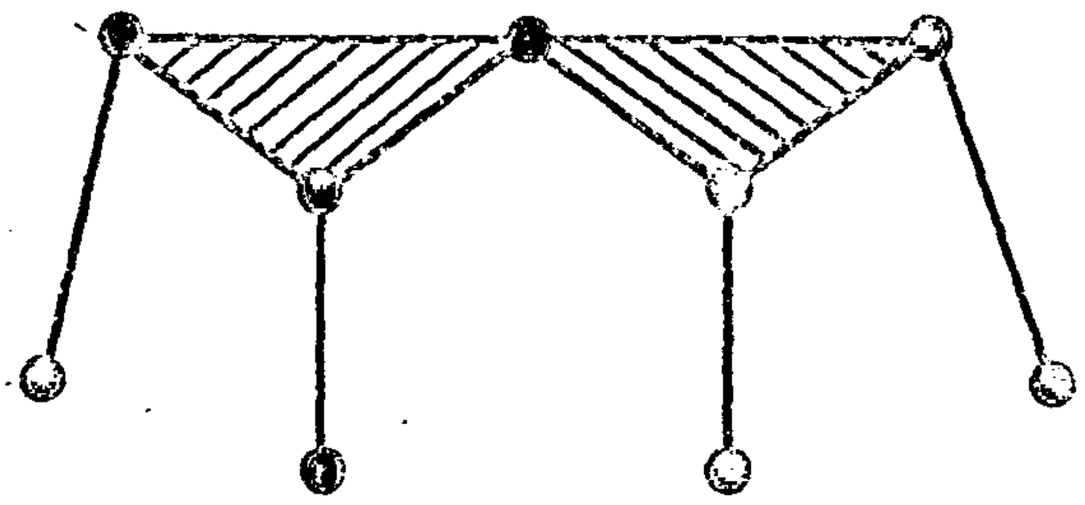

(d) Biternary group

FIGURE 3.7. ASSUR GROUPS

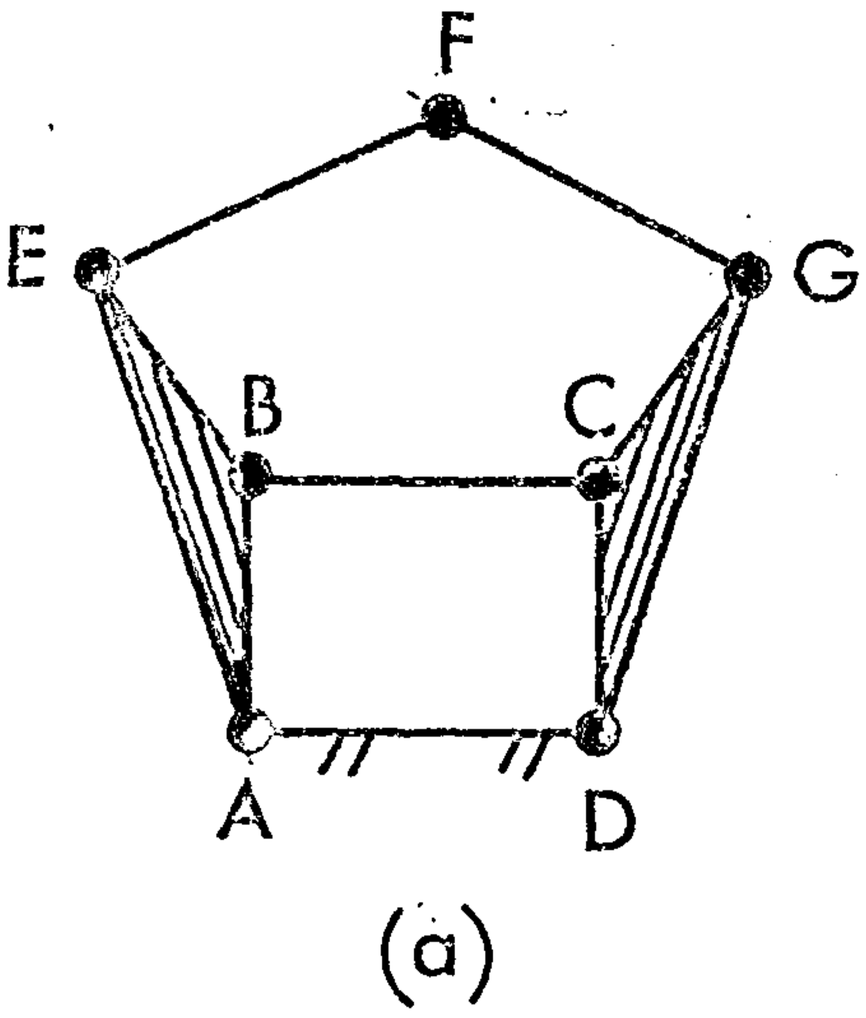

(a)

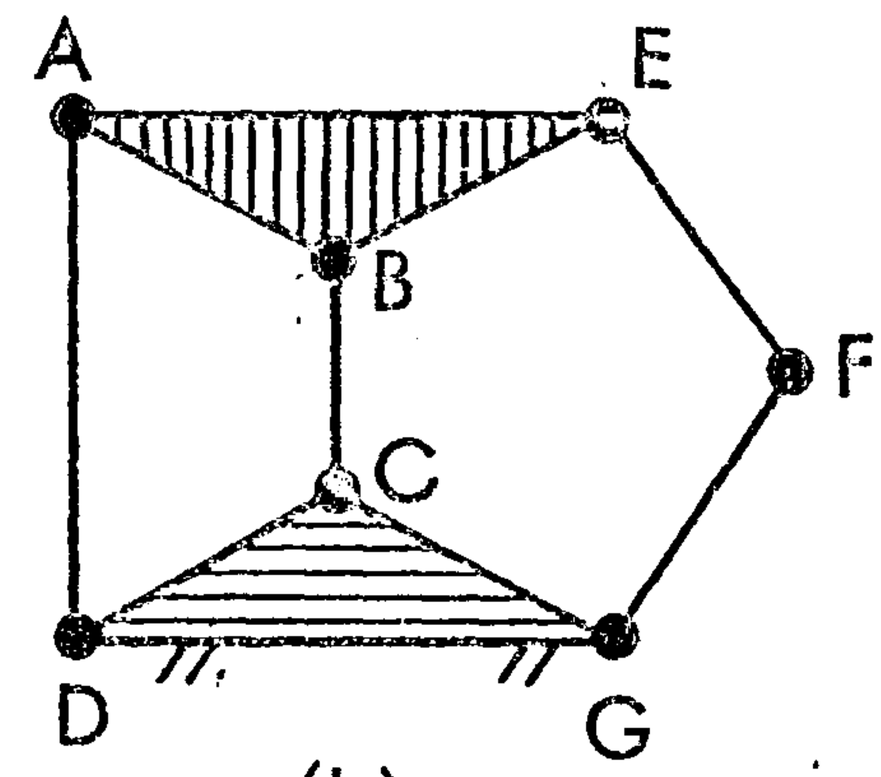

(b)

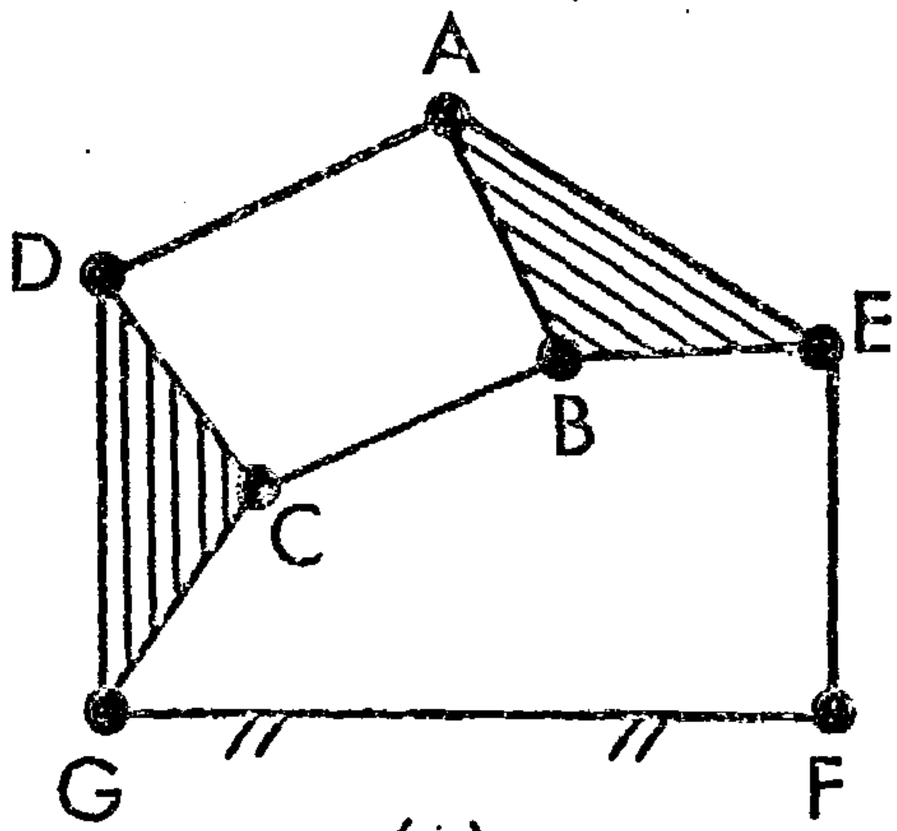

(c)

FIGURE 3.8. STEPHENSON SIX-BAR LINKAGES

kinematic pairs, that would have zero degrees of freedom if all the 'free' joints were connected to the frame (see Brat and Lederer {3.22}). Hence, for such a group,

$$0 = 3\ell - 2p \qquad (3.10)$$

where ℓ = number of links in the group,

p = number of simple joints (see equation 3.9) including the 'free' joints, i.e. those that are used to connect the group to the (expanded) basic unit.

Four Assur groups are shown in Figure 3.7 and a further 181 are given by Manolescu et al. {3.23}. Thus the 'peelable dyads' referred to above correspond to a binary Assur group, Figure 3.7a.

A four-bar linkage consists of a basic unit and a binary group and a Watt six-bar linkage is formed from a basic unit and two binary Assur groups. The three possible inversions of a Stephenson six-bar linkage are shown in Figure 3.8. The construction of each of these depends on the input link as shown in Table 3.2.

Table 3.2. Construction of Stephenson Six-Bar Linkages using Assur Groups.

Case, Figure 3.8	Frame Link	Input Link	Assur Groups in addition to the Basic Unit	Type Figure, 3.7
(a)	AD	ABE or DCG	2 binary	(a)
(b)	DCG	AD or BC FG	2 binary 1 ternary	(a) (b)
(c)	FG	DCG EF	1 ternary 1 quadrilateral	(b) (c)

Verho {3.21} shows that, if the actuator pair can connect any pair of adjacent links, one of which is not necessarily the frame link, there are eleven Watt's and fourteen Stephenson's six-bar linkages which are topologically distinct. Returning to Figure 3.6, the eight-bar chains (m) and (n) can be assembled from a four-bar chain and a ternary Assur group whilst chains (o) and (p) consist of a basic unit and a biternary Assur group, Figure 3.7d.

To summarize, the number of distinct planar kinematic chains with 12 links or less and one degree of freedom has been identified. A coherent subset of planar kinematic chains with one degree of freedom is formed by those consisting of a four-bar chain with additional peelable dyads. If this selection is insufficient, it can be extended by including other Assur groups besides the binary group. A wide variety of linkages may be constructed from these by using revolute and prismatic joints subject to certain conditions and by fixing different members of the chain. Suitable methods for prescribing the topology of such linkages will be considered in the next chapter.

Summary

In this chapter, an easily recognized group of linkage mechanisms is selected. Firstly equations are given to determine the number of degrees of freedom of a linkage. Attention is then restricted to planar linkages with one degree of freedom. Finally those linkages that can be assembled by connecting pairs of links are selected. This group includes most of the linkages used in industry and the advantages of this choice are given in later chapters. Catering for additional, but different, Assur groups would give discrete increases in the selection. Several conventions and terms are defined. The procedure for determining a set of independent loops has been developed by the author from that used in graph theory. The co-ordination of this material from widely scattered sources provides a framework for the chapters that follow.

4. TOPOLOGY

4.1 SPECIFICATION

Any optimization algorithm must be supplied with a set of values from which to start searching and one used for the kinematic synthesis of linkage mechanisms is no exception. If the algorithm is part of a computer program that caters for a variety of linkages, then the program must not only be supplied with an initial set of dimensions but also be informed of the topology (or structure) of the associated linkage. The topological information will consist of the number and types of the links, the number and types of the joints, the manner in which they are connected, which is the input link and which the frame.

This information can be provided either in full or by using a code. Whichever method is used, it must be unambiguous. If provision is made for only a limited set of linkages, it is preferable that the method should reflect this. A balance must be struck between conciseness, redundancy and intelligibility. The inclusion of suitable redundant information provides an opportunity for checking the consistency of the data whilst there should be fewer errors in the data if it is concise and easily understood.

4.2 SURVEY

One method of developing a code would be to draw all the possible linkages and assign a unique code to each. However, the problems of obtaining a complete set and then retrieving a particular linkage from it make this impractical. For example, there are 71 basically different inversions of the 16 distinct eight-bar chains (Hain {4.1a}) and a greater number of linkages can be formed from these using different combinations of revolute and prismatic joints. The number of linkages

that can be formed from the 230 distinct ten-bar chains and those with even more links is correspondingly larger.

Molian {4.2} has proposed a twelve-digit code for information retrieval purposes. This code includes the number and types of the links and the number of each type of joint. However, this code is not suitable for the present purposes as it gives no indication of which link is connected to which or of which are the frame and input links. To do this requires some method of identifying individual links.

Dresig and Pausch {4.3} number the links in an arbitrary manner apart from the frame and the input link which are numbered 1 and 2 respectively. The connections between the links are prescribed in the connection matrix C which is an ℓ by ℓ matrix for a linkage with ℓ links. The elements of C are given by :

c_{ik} = 1 if there is a joint that connects links i and k and is fixed in link i, i.e. is a revolute joint or link i is a sliding link associated with a prismatic joint (as defined in Section 3.1),

= -1 if there is a joint that connects links i and k and moves in a straight line in link i, i.e. link i is a guide link associated with a prismatic joint,

= 0 if there is no joint connecting links i and k.

A set of independent loops within the linkage can be determined from the connection matrix using an algorithm developed by Taubald {4.4} . The set of loops is not unique as it depends on the order in which the links are numbered.

The connection matrix contains a large amount of redundant information since, if all the joints are simple, the number of zero elements, from equation (3.7), is $(\ell^2 - 3\ell + 4)$ which represents at least half the matrix.

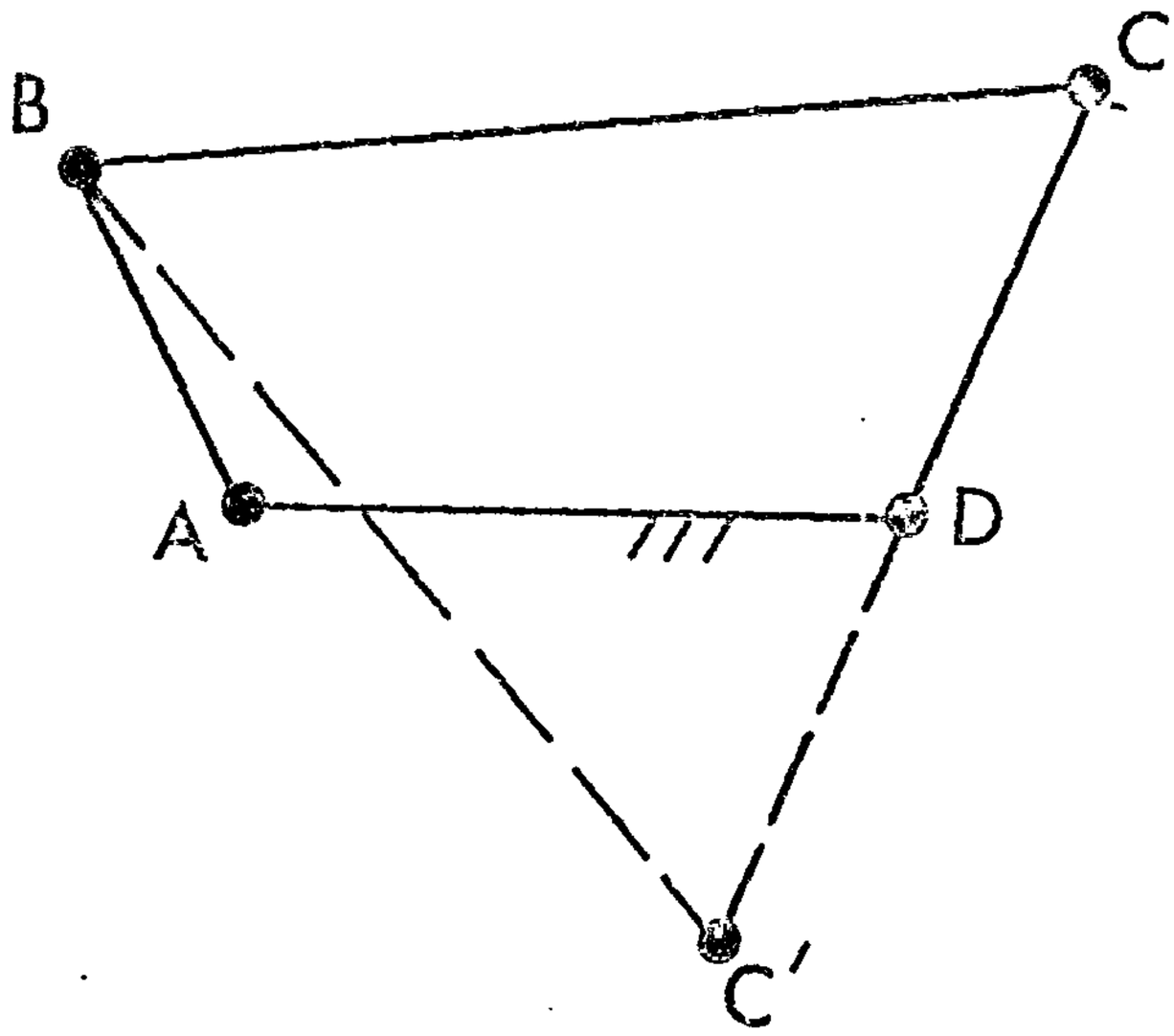

a) Four-bar Linkage

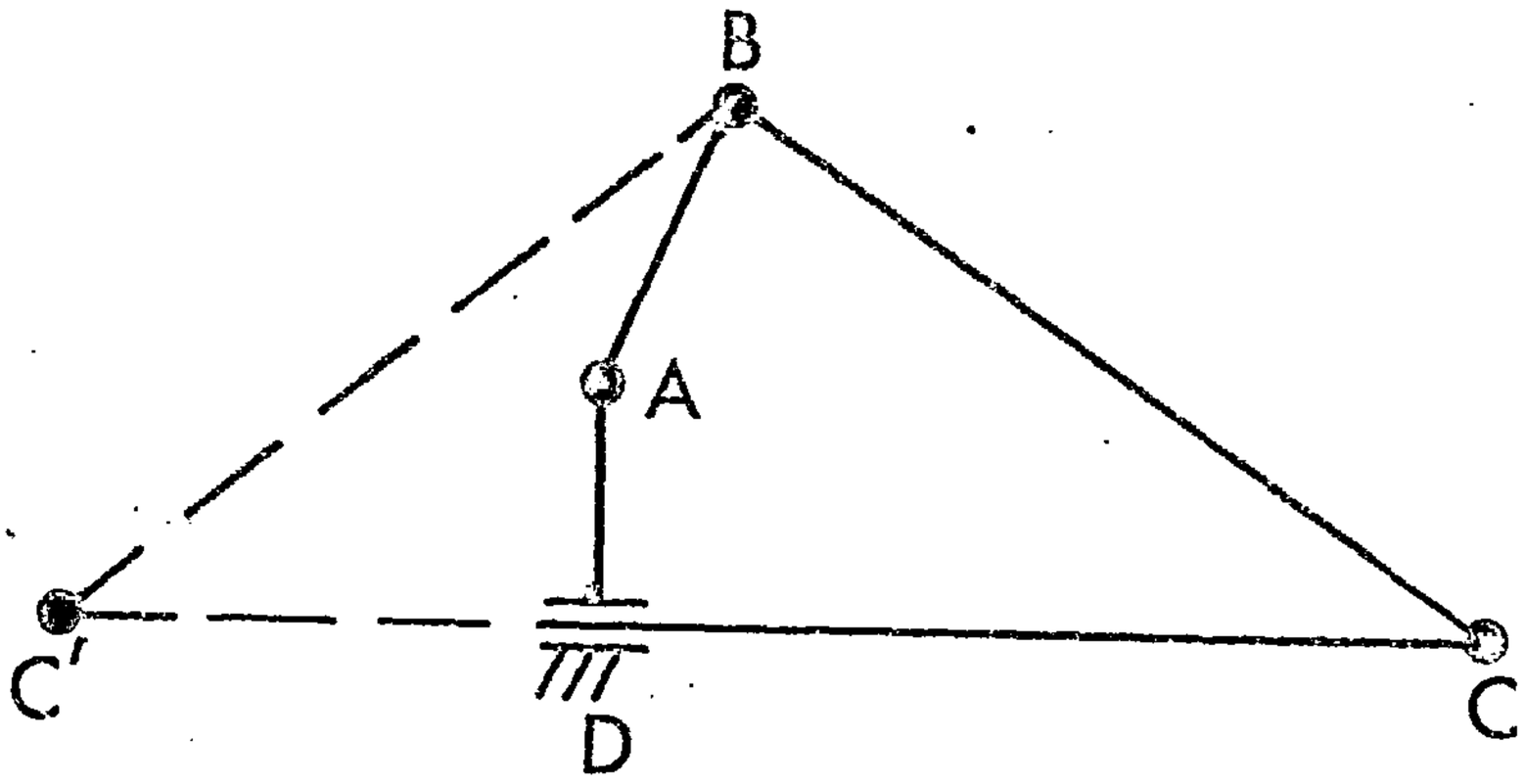

b) Crank-slider Mechanism

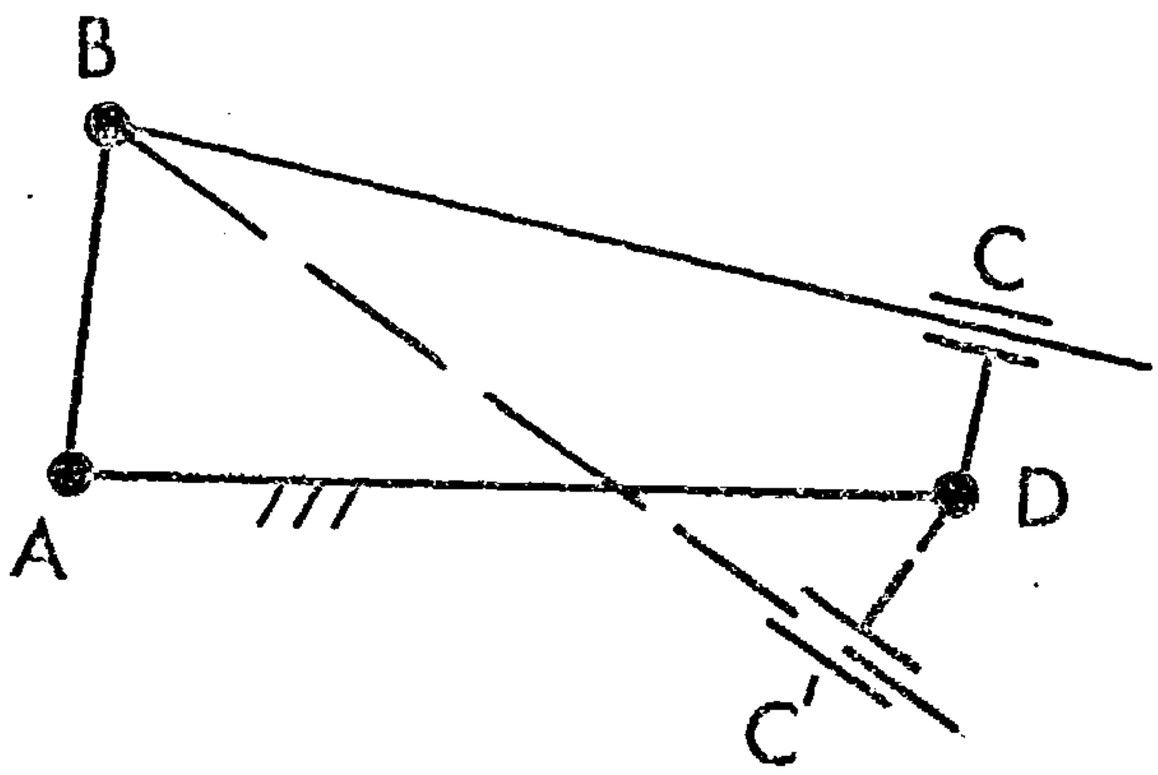

c) Oscillating Slider-crank Mechanism

FIGURE 4·1 ALTERNATIVE CLOSURES FOR FOUR-LINK MECHANISMS

Chace and Angell {4.5} and Sheth and Uicker {4.6} avoid this by, in effect, only prescribing the non-zero elements. A keyword, such as ROTATION or TRANSLATION, is used to indicate the type of joint. Either two numbers indirectly denote the links connected by that joint or two names are used. From this information, Smith et alia {4.7} set up a part-contact network and then use an algorithm developed by Branin {4.8} to determine a set of independent loops. The associated spanning tree (defined in Section 3.1) includes the frame link and the chords are chosen to minimize the number of links in each loop. Sheth and Uicker {4.6} use an algorithm by Hu {4.9} to recognize a suitable set of independent loops.

Kraniauskas {4.10} and Rooney {4.11} used a 'building block' approach to specify the topology. Kraniauskas found that four-bar linkages connected by frame-pivoted ternary links were too restrictive and that dyads offered a more versatile approach. Rooney used binary Assur groups, identifying them by a code number. Other users found this concept difficult to apply, so Rooney {4.12} now numbers the joints and then uses two of these numbers to denote the link that connects them. Using this information, he derives a constraint incidence matrix in which the columns correspond to joints and the rows to links. From this matrix, he determines a strategy for analysing the linkage corresponding to the sequence of drawing the linkage graphically.

As described above, the methods do not distinguish between the alternative ways of closing a loop since these are topologically equivalent. However, it is convenient to consider this aspect at this juncture. Figure 4.1 shows the alternative closures for four-link mechanisms. The method for prescribing the appropriate closure is usually related to the method of analysis. Where the analysis involves an iterative method, even if only for the initial position, it is appropriate for the user to supply approximate values for either the co-ordinates of the joints or the angular positions of the links and the lengths of the sliding links from

which the iteration can start. This approach is adopted in References {4.5, 4.6, 4.10 and 4.12}. Rooney {4.11} uses a non-iterative method for analysis and a code for the closure, so avoiding the necessity for approximate values.

The methods fall into two groups - those in which the links are prescribed in an arbitrary sequence, References {4.3, 4.5, 4.6, 4.12 and 4.13}, and those in which the sequence is ordered, References {4.10 and 4.11}. Where the sequence is arbitrary, redundant information, usually in the form of keywords such as those in References {4.5, 4.6, 4.12 and 4.13}, is used to make the data intelligible. The repetitive use of keywords is tedious and the data becomes verbose because the redundant information is useless for checking the data. If the keywords are shortened to the initial letter, say, the intelligibility is lost. Even with an ordered sequence of links, the intelligibility of the data can be low if the data associated with each link is prescribed in an arbitrary manner. For example, the amount and ordering of the data required for a'building block' used by Rooney {4.11} depends on the particular unit and this results in a set of data which is hard to interpret.

In contrast, the connection matrix used by Dresig and Pausch {4.3} is easy to interpret but at least half of the data is redundant. Thus there is a need for a method which uses a systematic arrangement of data, comparable to the connection matrix, with an ordered sequence of links to reduce the necessity for redundant information. Furthermore, if a non-iterative method of analysis is applicable to the range of linkages for which the method caters, there will be no need to supply approximate values to define loop closure.

4.3 LOOPS

In the remainder of this chapter, consideration is confined to linkages formed by the addition of one or more 'peelable dyads' to a basic unit consisting of a frame link with a single input link pivoted to it. The addition of each dyad results in the formation of a new independent loop. This enables us to prescribe the topology and loop closure of the linkage in two arrays in which the rows correspond to a set of independent loops and the columns to the arcs contained within each loop. The actuator pair, i.e. the input link pivot, is common to all of the loops and forms the start of each loop. The last arc in each loop is associated with the frame link. In addition to the restrictions on the use of prismatic joints given in Section 3.1, the requirements are that each loop must contain :

a) at least four arcs, one of which may be of zero length if the loop contains a prismatic joint,

b) at least one frame arc, one joint of which is the input link pivot,

c) at least two revolute joints,

d) only two undetermined arcs which are connected together to form an undetermined dyad as described below.

For a planar linkage with a single degree of freedom, the number of loops, L, satisfying these requirements, from equations (3.2) and (3.9), is given by :

$$L = (\ell-2)/2 \qquad (4.1)$$

where ℓ = number of links in the mechanism. The loops are identified in an ordered sequence such that

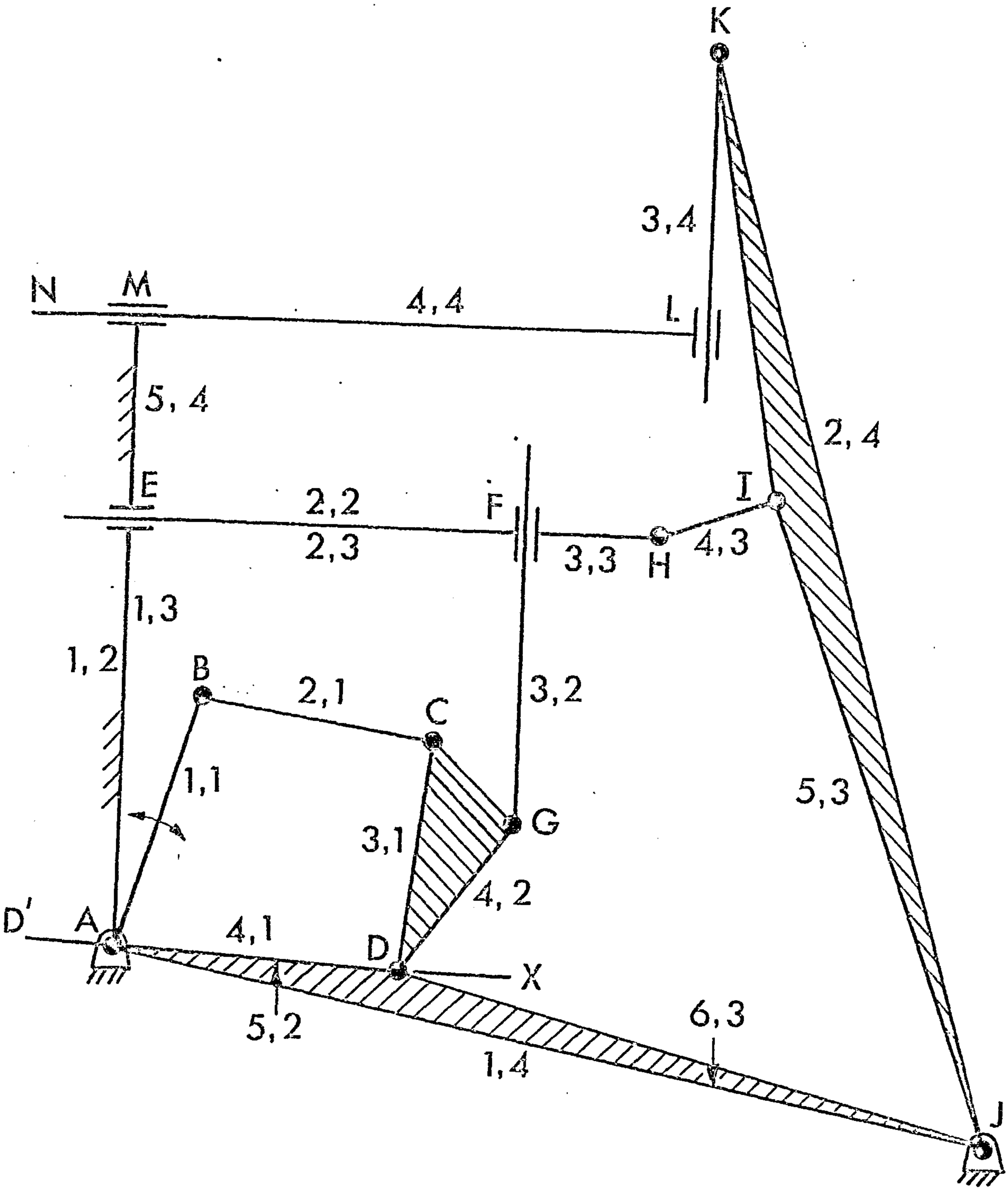

FIGURE 4·2 TEXTILE TEN-BAR LINKAGE

the solution of one loop provides the necessary input information for the next. This sequence corresponds to that which a designer would use if he were drawing the linkage graphically.

The procedure can be illustrated by reference to Figure 4.2. This shows a ten-bar linkage which is based on the draw mechanism used in a straight-bar, fully-fashioned outerwear knitting machine. The linkage is cam-driven, the roller follower being mounted on the input link AB. On the machine, the length of the link DG can be varied to adjust the amplitude of the displacement of the output N according to the width of fabric being knitted. In this linkage, since it has one degree of freedom and ten links, the number of loops, from equation (4.1), is four. In loop ABCDA, we start with the frame arc DA and the input arc AB whose positions are prescribed. These are determined arcs. The remaining arcs BC and CD constitute an undetermined dyad whose positions can be found by simple analysis. Proceeding to loop AEFGDA, we solve for the corresponding undetermined dyad EF and FG. This allows us to solve for HI and IJ in loop AEFHIJA, and finally for KL and LM in loop AJKLMA.

Cutting arcs BC, FG, HI and KL, which are those arcs in the undetermined dyads that do not form part of a later loop, results in an unclosed but connected chain. This chain, consisting of the frame link, ADJEM, the input link, AB, and links CDG, EFH, IJK and LMN, is a spanning tree for the linkage. Since the cut arcs are associated with binary links, cutting them is equivalent to removing the links from the linkage. When any one is replaced, only one loop is formed and so they are chords. The loops so formed, namely ABCDA, AEFGDA, AEFHIJA and AJKLMA, therefore constitute a complete set of independent loops which also satisfies the conditions given above.

Group (i) Three Revolute Joints

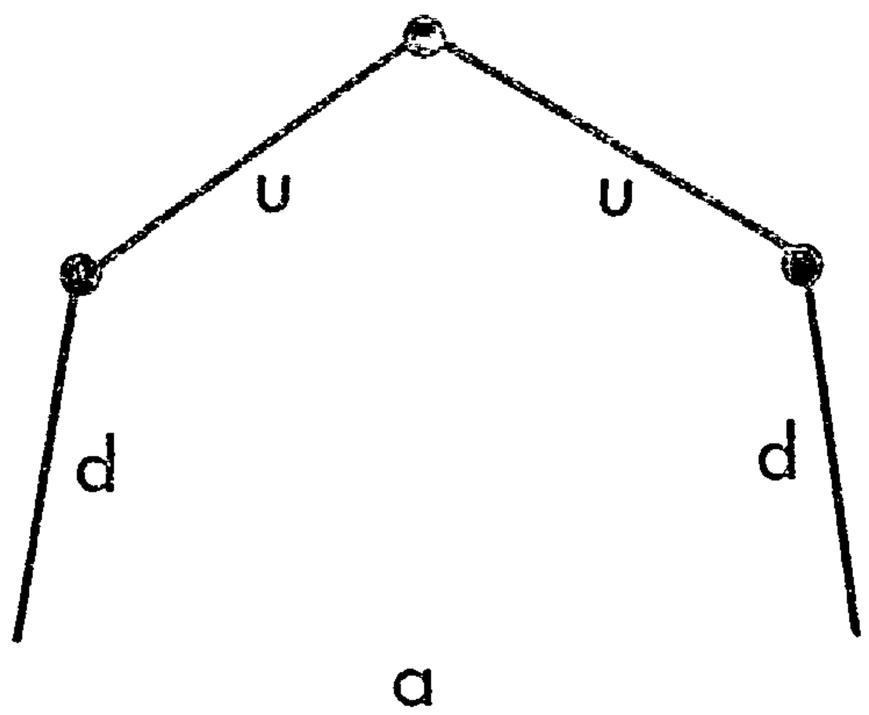

a

Group (ii) Two Revolute Joints, One Prismatic Joint

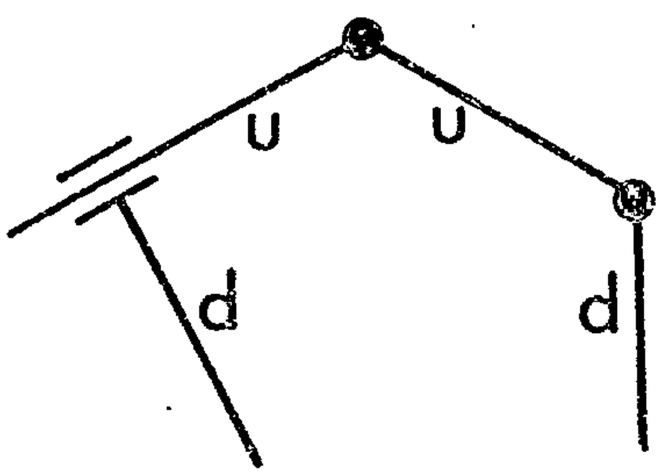

a

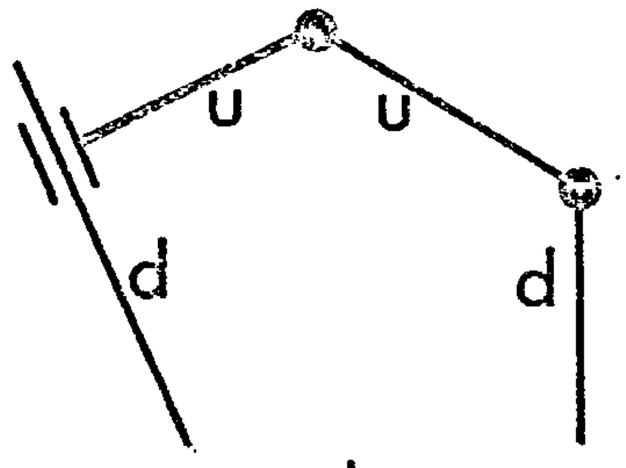

b

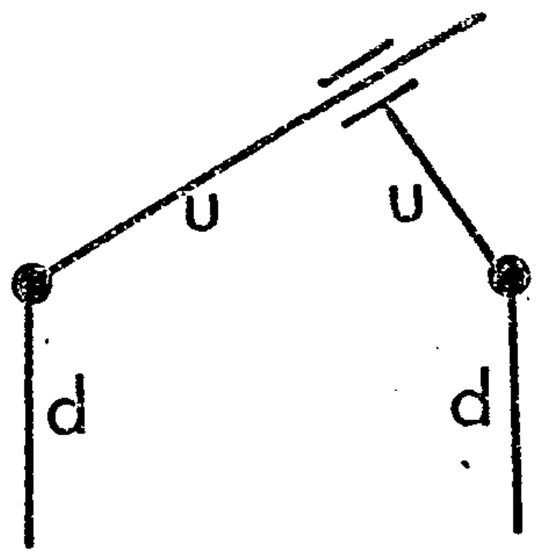

c

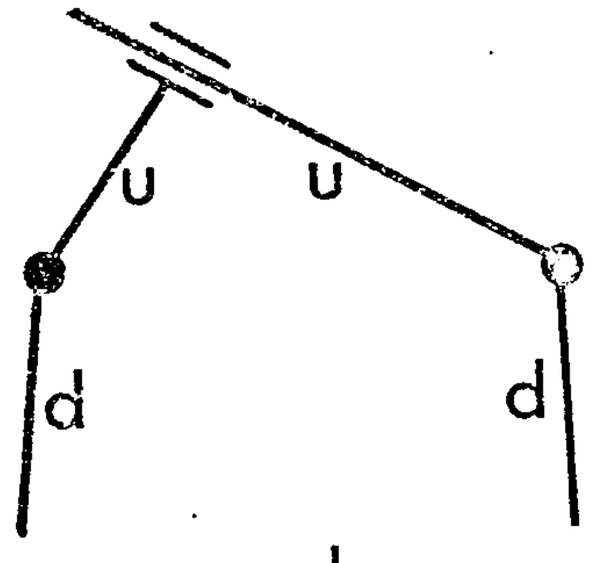

d

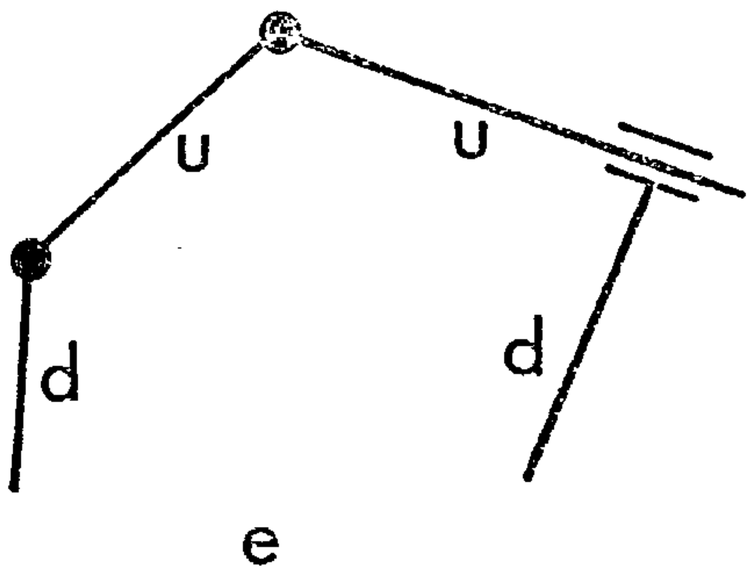

e

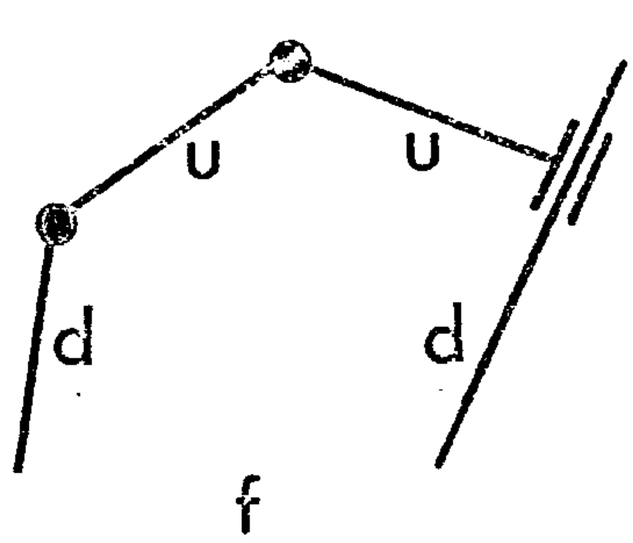

f

d = determined arc
u = undetermined arc

FIGURE 4·3 UNDETERMINED DYADS

Group (iii) One Revolute Joint, Two Prismatic Joints

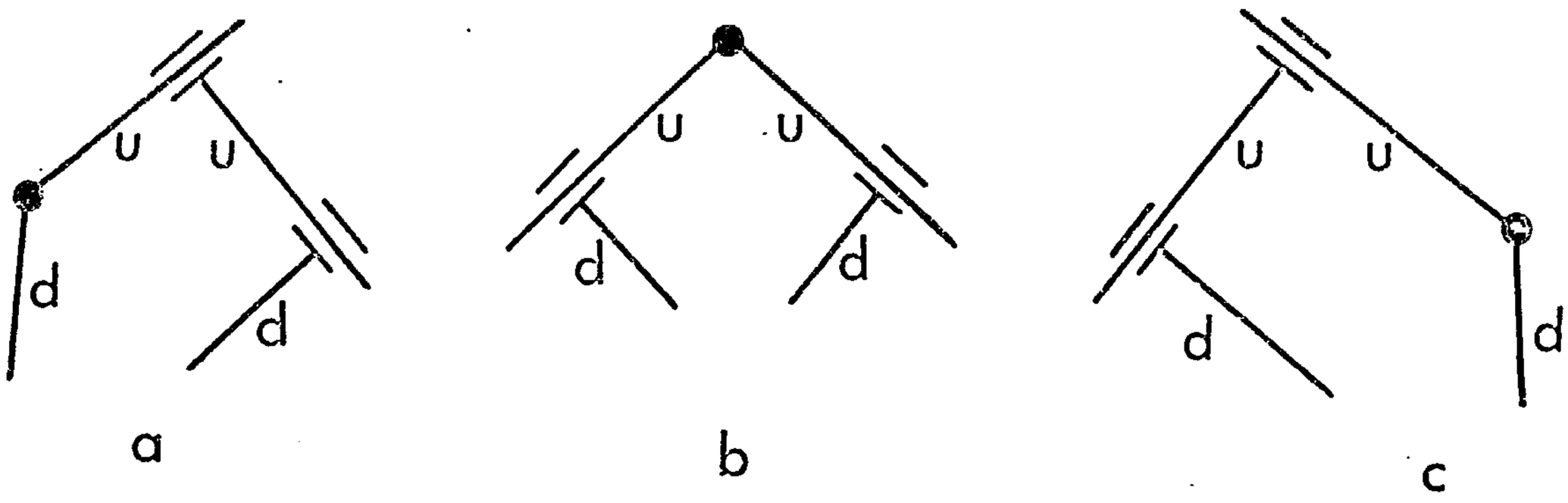

FIGURE 4·3 Continued

Group (iv) Three Prismatic Joints

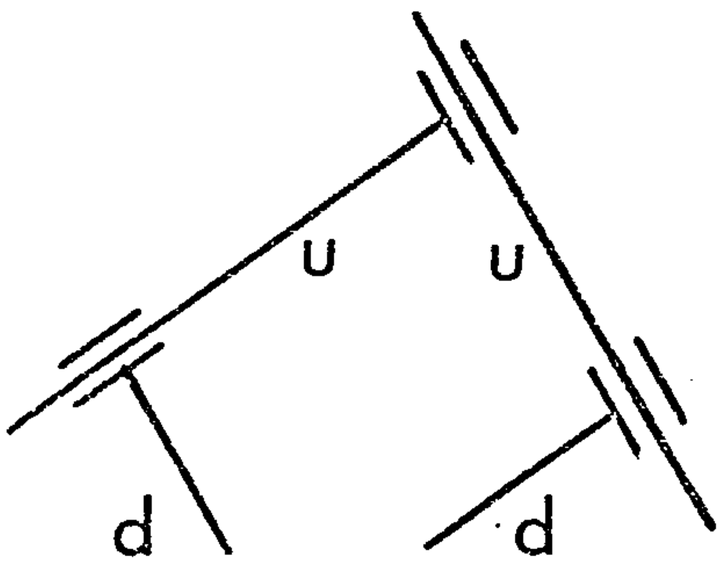

a

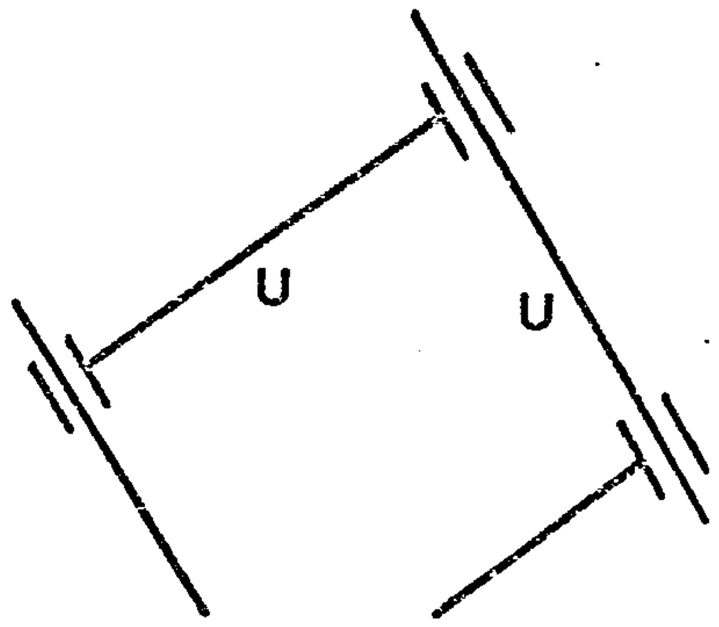

b

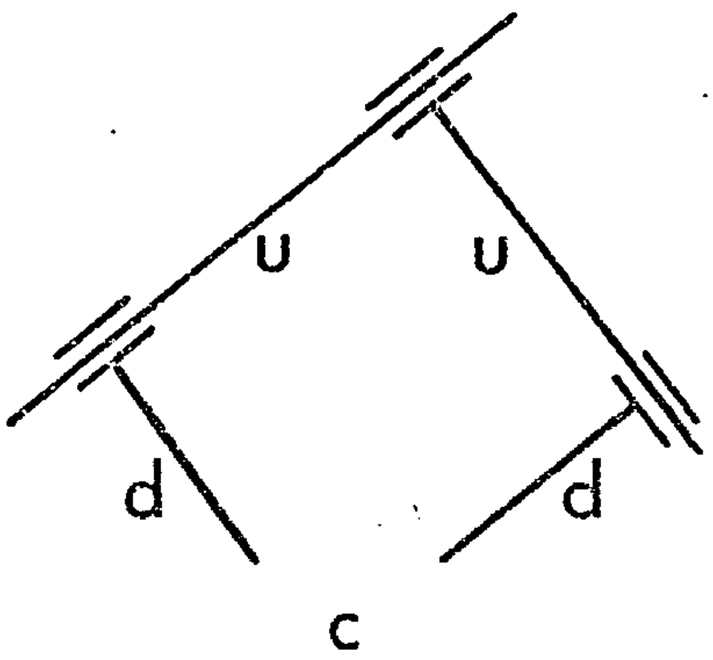

c

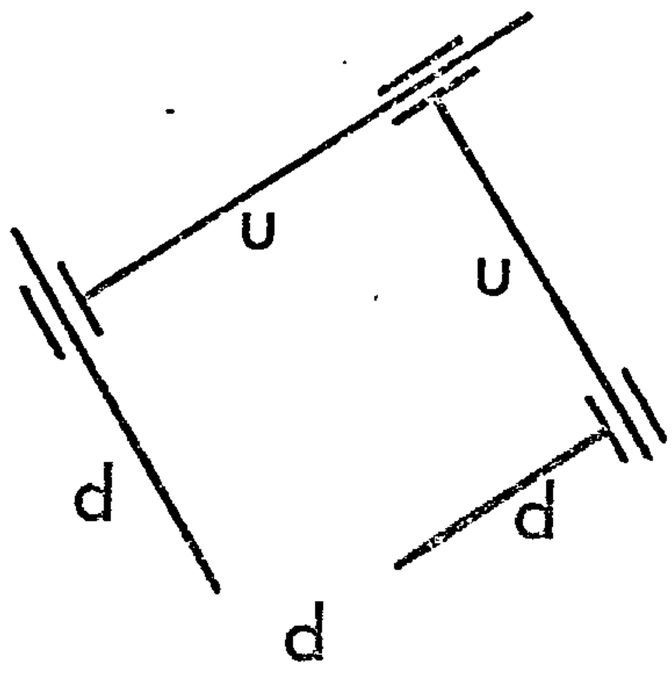

d

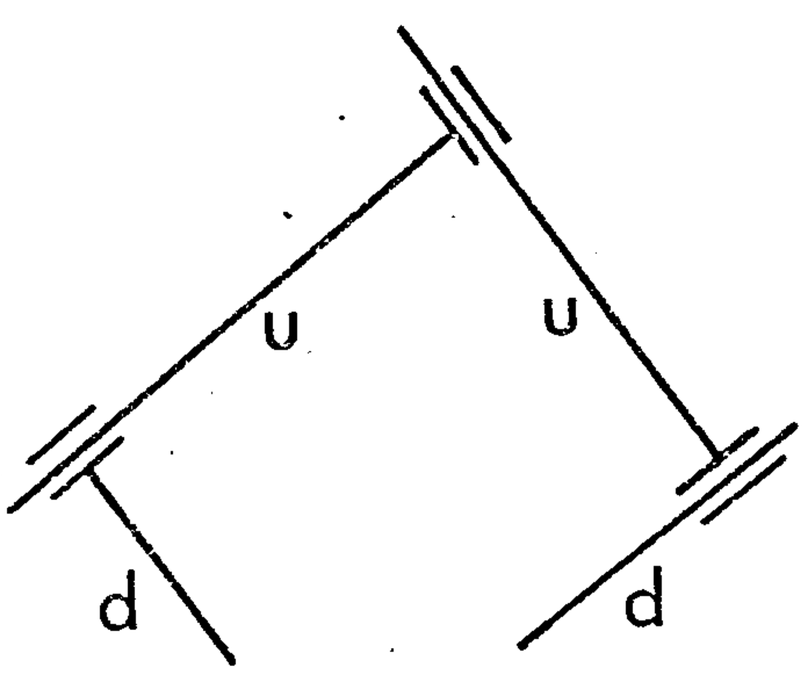

e

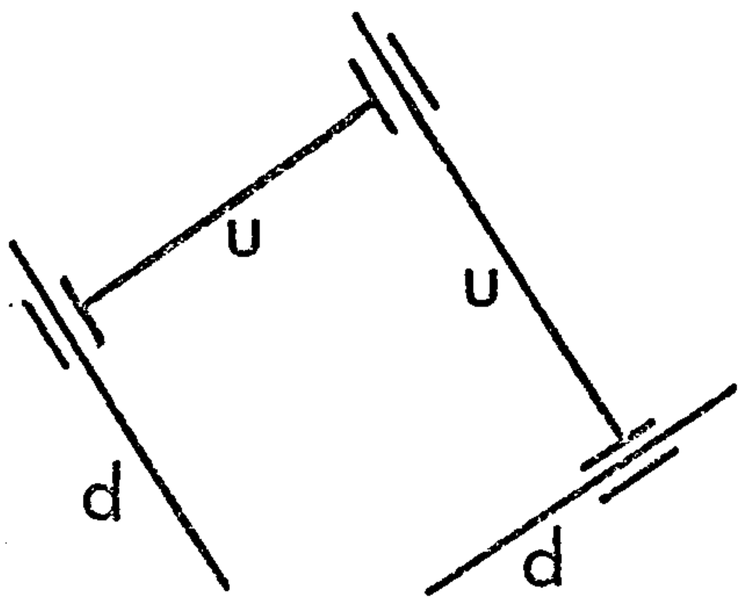

f

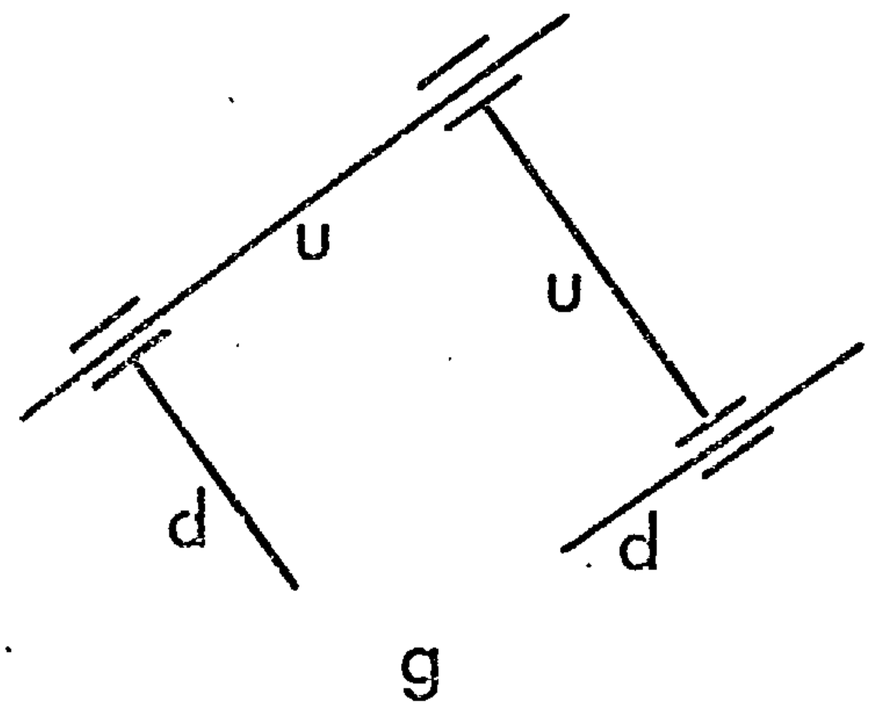

g

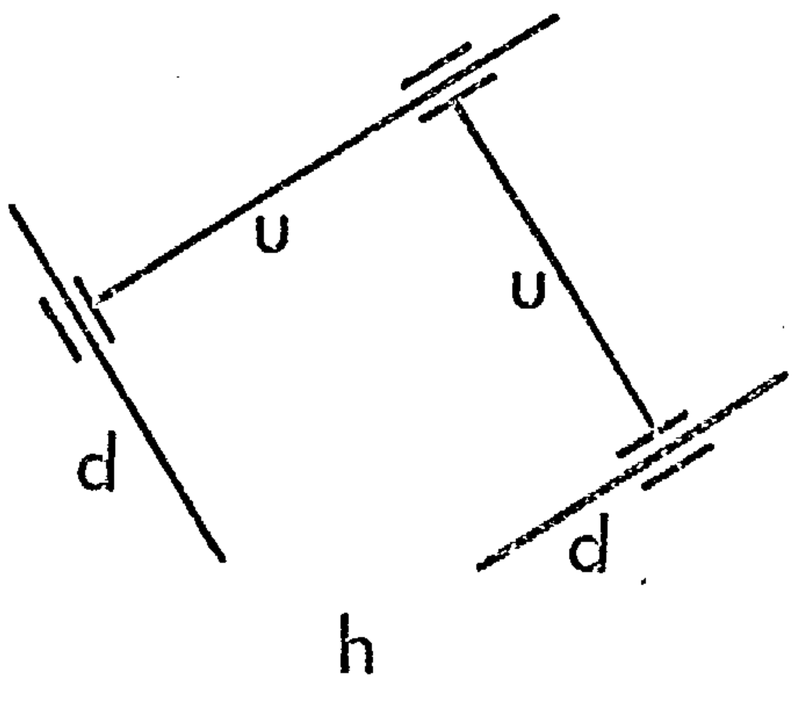

h

FIGURE 4·3 Concluded

Group (i)

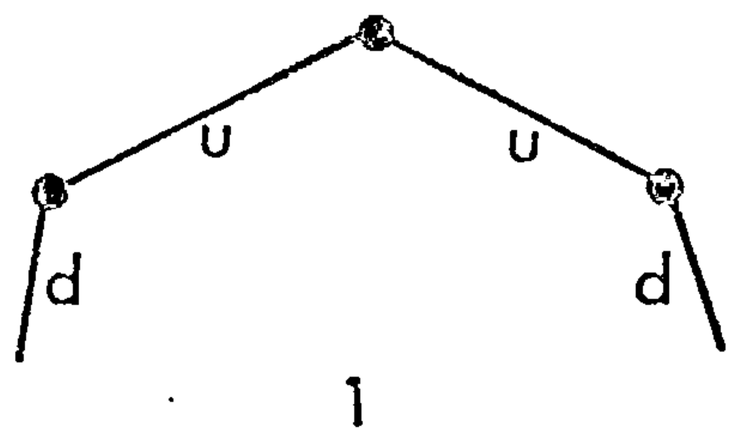

1

Type (a)

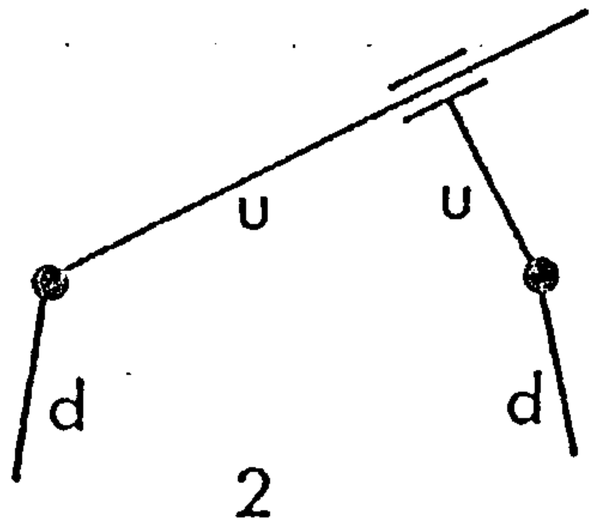

2

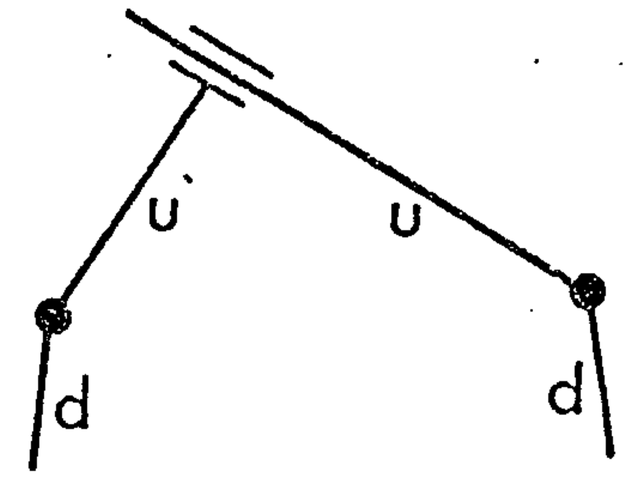

3

Group (ii)

Type (b)

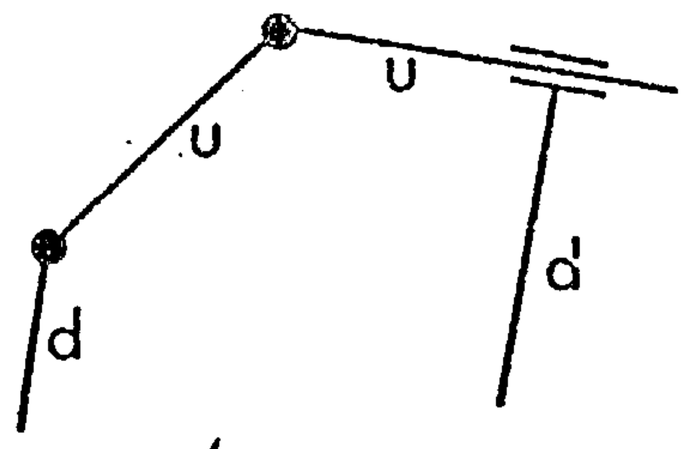

4

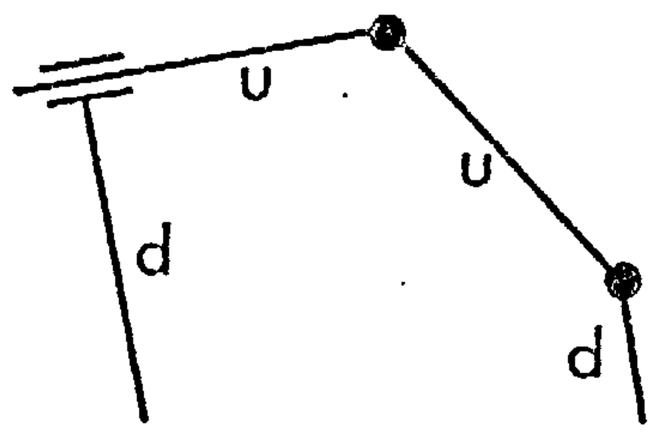

5

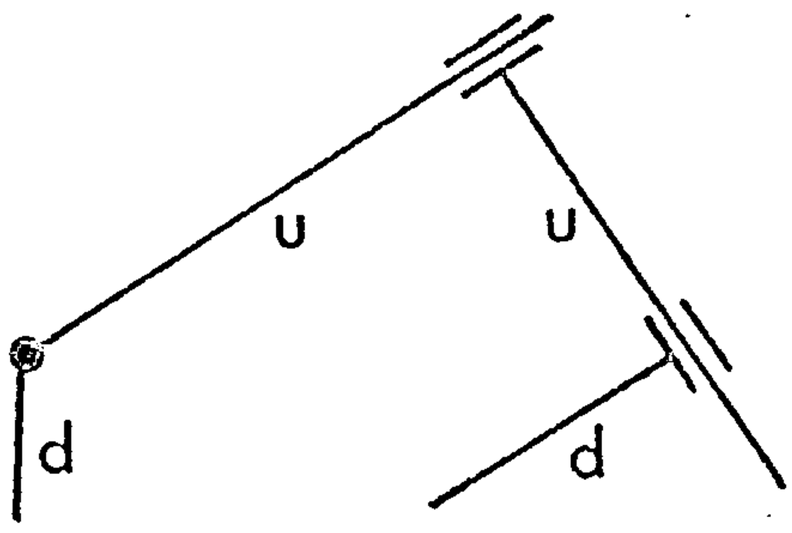

6

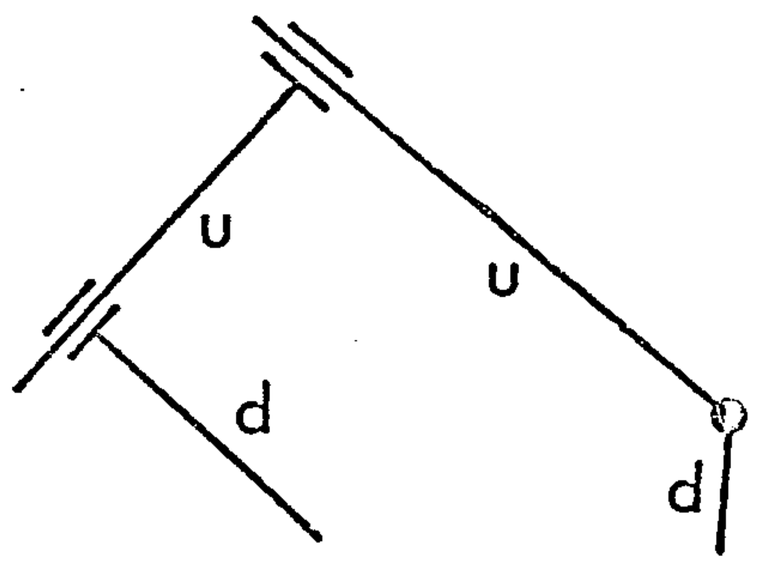

7

Group (iii)

d = determined arc
u = undetermined arc

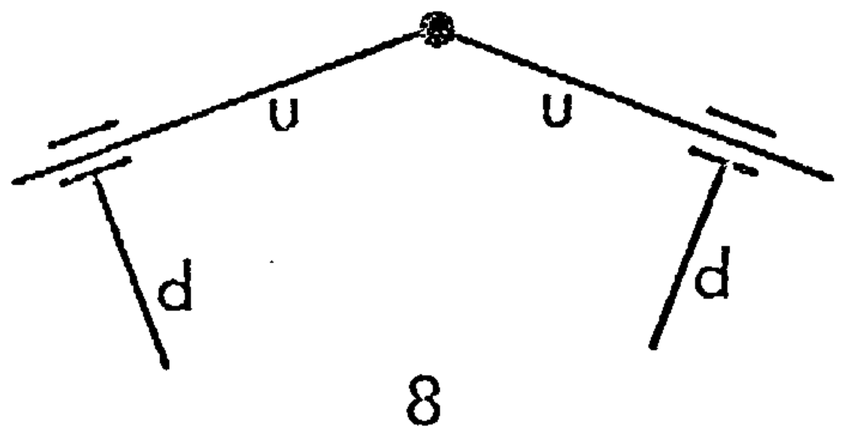

8

FIGURE 4·4 VALID UNDETERMINED DYADS

4.4 UNDETERMINED DYADS

The nature of the undetermined dyad determines the form of solution appropriate to any given case. Every dyad possesses three joints, each of which may be revolute or prismatic. If a distinction is drawn between a prismatic joint in which (i) the guide precedes the sliding link in the chain order of the loop, and (ii) the reverse applies, there will be 3 x 3 x 3 = 27 possible combinations of joints in the dyad. These are shown in Figure 4.3 in four groups according to the number of revolute and prismatic joints. Group (i), which has a single member, has three revolute joints; the six members of group (ii) each have two revolute joints and one prismatic joint; the twelve members of group (iii) each have one revolute and two prismatic joints whilst the eight members of group (iv) each have three prismatic joints. However, many of these are invalid. A sliding link and its guide link must both appear in the same loop if either is undetermined. In order to determine the length of the sliding link, the guide link must be taken into account and, in the process, its angular position will become determined if it were not already so. Thus a guide link cannot be undetermined if the corresponding sliding link is determined. This invalidates members b and f of group (ii), members e,g,h,i,j,k, and ℓ of group (iii) and members b,d,e,f,g and h of group (iv). Restriction (c) in Section 3.1 is violated by members d,f,g and i of group (iii) and members a,b,c,f,g and h of group (iv). Finally, all the members of group (iv) violate restriction (b) in Section 3.1.

The acceptable combinations for present purposes number eight, which are summarized in Figure 4.4. The sole member of group (i) - dyad 1 - appears in loops ABCDA and AEFHIJA in Figure 4.2. The first member

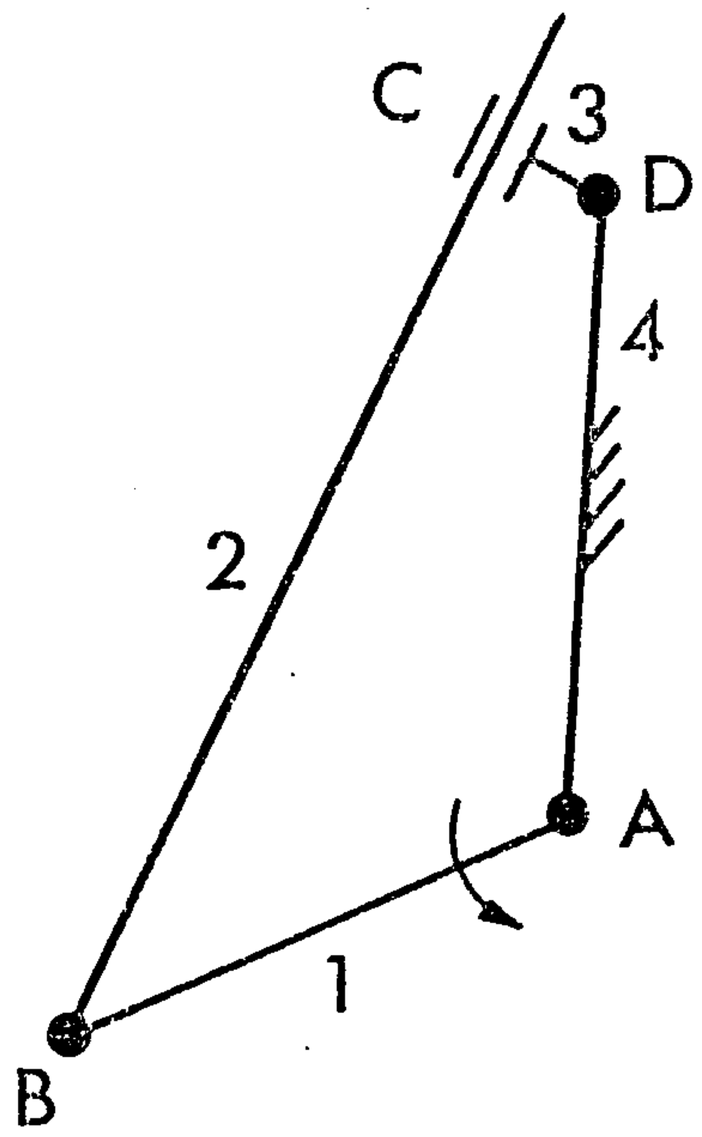

FIGURE 4·5 OSCILLATING SLIDER-CRANK MECHANISM

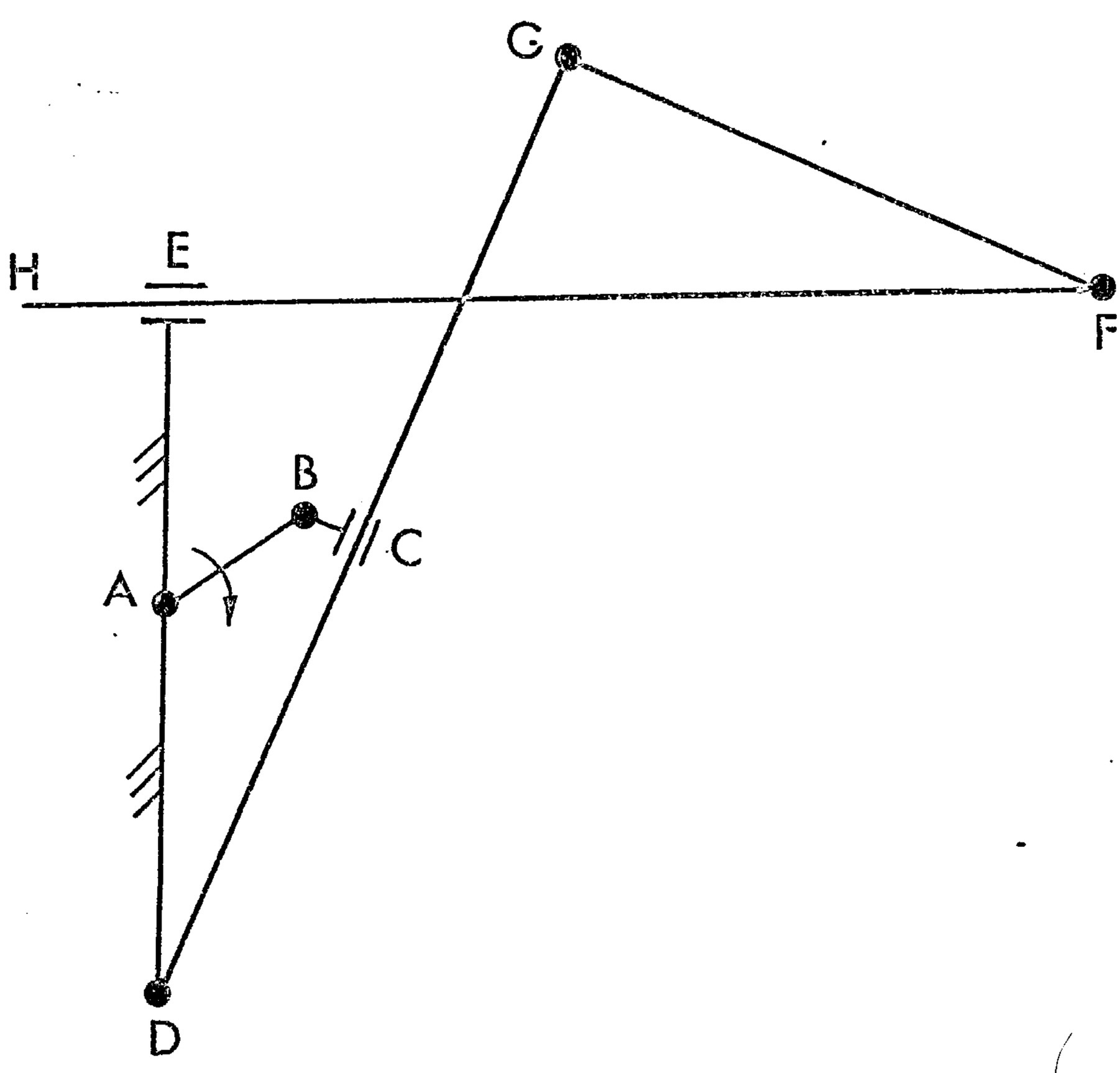

FIGURE 4·6 QUICK-RETURN MECHANISM

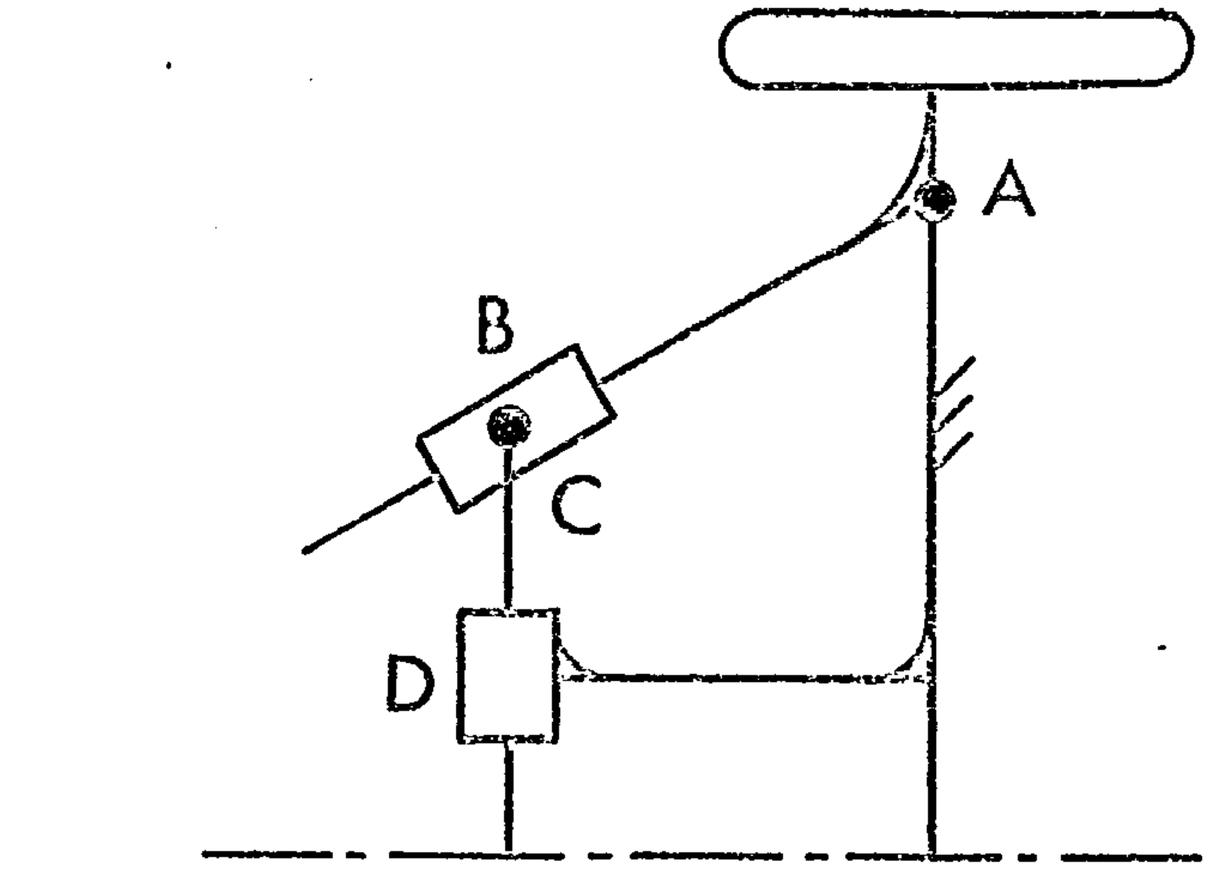

a) Davis automobile steering gear

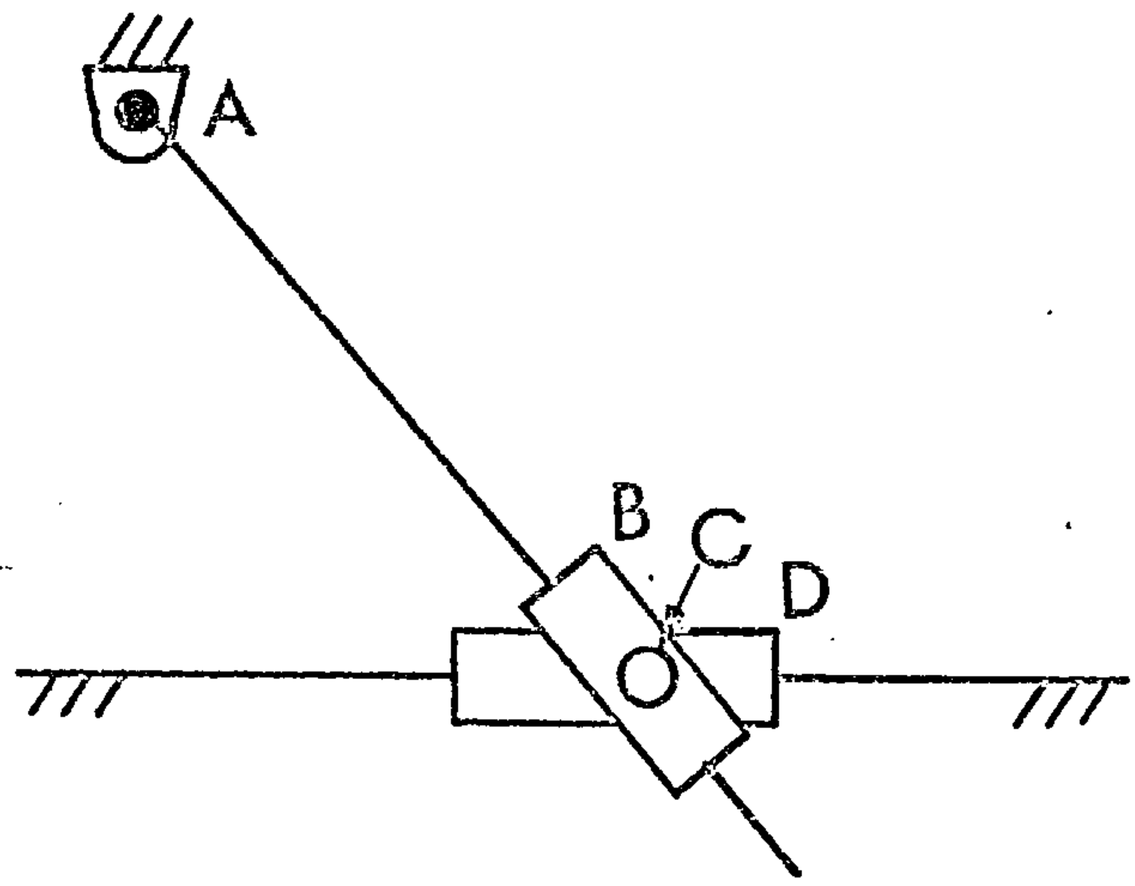

b) Rapson slide mechanism

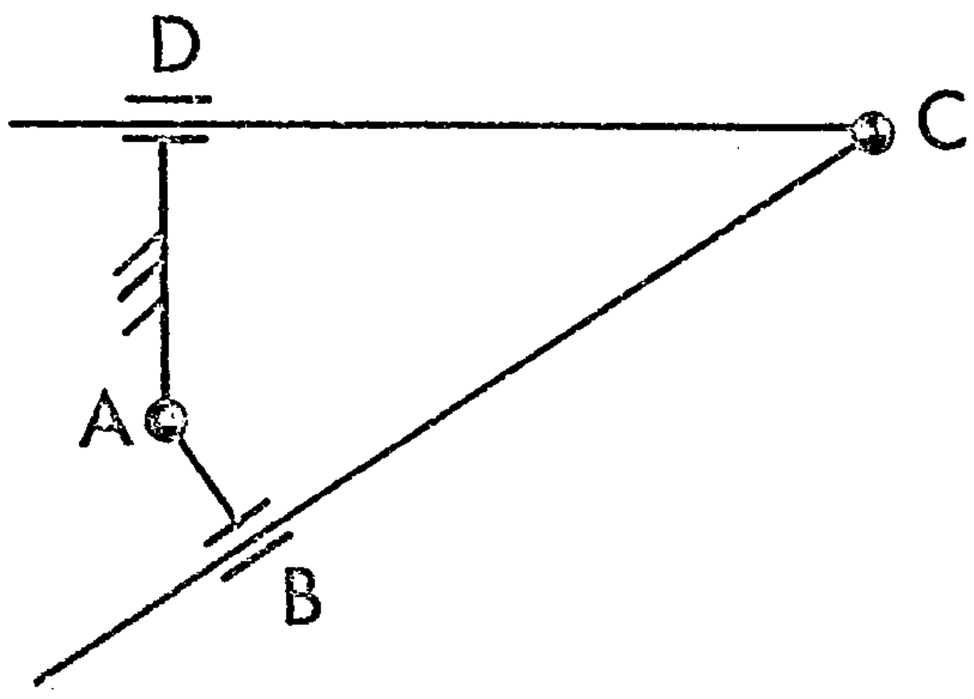

c) Kinematically equivalent linkage

FIGURE 4·7 EQUIVALENT LINKAGES

of group (iia) - dyad 2 - occurs in the inversion of the slider-crank mechanism shown in Figure 4.5. This inversion has been given a variety of names such as oscillating slider-crank mechanism (Rosenauer and Willis {4.14}), crosshead mechanism (Hain {4.1b}) and trunnion engine (Hannah and Stephens {4.15}). Hain {4.1c} lists examples of its applications. The second member of group (iia) - dyad 3 - is found in loop ABCDA of the quick-return mechanism shown in Figure 4.6 which is used in some shaper machines. The first member of group (iib) - dyad 4 - occurs in the slider-crank mechanism in Figure 4.1(b) and the second member - dyad 5 - in loop AEFGDA of Figure 4.6. The first two members of group (iii) - dyads 6 and 7 - appear in loops AJKLMA and AEFGDA respectively of Figure 4.2. The final member of group (iii) - dyad 8 - is found in two kinematically equivalent mechanisms (Hartenberg and Denavit {4.16}), the Davis automobile steering gear, Figure 4.7 (a), and Rapson's slide, Figure 4.7 (b). The latter mechanism is used in the steering gear of most modern ships, in which case AB is the tiller attached to the rudder stock pivoted at A, BCD is the swivel block and D is actuated by a hydraulic cylinder. Since the moving guide links are of zero length, both linkages may be represented as shown in Figure 4.7 (c).

4.5 ARCS AND ARRAYS

Individual arcs within a loop are identified by a standard convention whereby the input link pivot is taken as the start of each loop. In the first loop, arc 1 is always the input link. In the other loops, the first arc may be associated with either the input link or the frame link. In all loops, the last arc is associated with the frame link. The remaining arcs are numbered consecutively around the loop. If

the loop contains a sliding link and its guide, they are given different numbers. For example, in Figure 4.2, each arc has been labelled with a pair of numbers - the first being the arc number and the second the loop number. In the second loop, AEFGDA, the first arc, AE, is associated with the frame link, AEMDJ, and forms the guide link for the second arc, EF, which is associated with the sliding link EFH. This, in turn, acts as the guide link for the third arc, FG, which is also a sliding link. The fourth arc, GD, is associated with the rocker link, CDG, and the last arc, DA, is also associated with the frame link.

Two or more arcs in different loops are regarded as common and are specified accordingly if they are associated with the same link and so remain at a fixed angle relative to each other during the motion. Common arcs will be found in binary links that form part of more than one loop, ternary links and frame links. Examples in Figure 4.2 are CD and GD, EF and FH, IJ and JK and the frame arcs AD, AE, AJ and AM.

Details of the two arrays that contain the topological and loop closure information are given in Appendix B2. The arrays are obtained systematically. Each row corresponds to an independent loop and these are prescribed in an ordered sequence. Similarly, the columns are associated with the arcs, which are also prescribed in an ordered sequence, in each loop. Positive and negative signs are used to denote the appropriate manner of closing each loop. Interpretation of the arrays is therefore straightforward and intelligibility is aided by using a keyword to identify each array. The arrays offer a wide range of application and are concise provided that the general strategy involved in the definition of the loops is deployed to the maximum advantage. As an example, the arrays for the linkage

in Figure 4.2 contain a total of 48 elements compared with 100 elements for the corresponding connection matrix which does not contain any loop closure information. The arrays thus contain the required information in a concise and intelligible form without an undue amount of redundant information.

Summary

After a survey of methods that have been proposed for prescribing the topology, i.e. structure, of planar linkage mechanisms, it is concluded that any such methods should possess certain features. These are :

(a) there should be a systematic arrangement of data so that it is more intelligible,

(b) the links should be considered in an ordered sequence to reduce the need for redundant information,

(c) the specification of the desired configuration of the linkage by supplying the initial angular positions of the links and the lengths of the sliding links should be avoided to make the data more concise and to reduce data preparation.

The valid undetermined pairs of links, i.e. dyads, that can occur when account is taken of both revolute and prismatic joints are identified. A new method for prescribing the topology of linkages containing such dyads is then developed. The systematic arrangement of data is obtained by using an ordered sequence of independent loops and 'sides' of links, i.e. arcs, within each loop. Since there are only two possible closures for each dyad, a sign convention is used to prescribe the appropriate one.

5. KINEMATICS

5.1 APPROACH

Once the user has prescribed the topology and link dimensions of a linkage, the computer should set up and solve an appropriate set of kinematic equations automatically. The method of solution should be rapid, particularly if it forms part of an optimization process. What constitutes an appropriate set of equations depends on the object of that process. In this thesis it is assumed that the requirement is for a linkage that will produce a prescribed output motion. This motion can be specified in terms of a set of positions of a link or a point on that link corresponding to a set of positions of the input link (see Appendix B3). Thus we are concerned only with obtaining and solving a set of equations for the required displacements.

The variables in the equations can be Cartesian co-ordinates, variable link angles and lengths or a mixture of these. Cartesian co-ordinates of joints are used in References {5.1 - 5.3} whereas variable link angles and lengths are preferred in References {5.4 - 5.6} and a mixture is used in Reference {5.7}.

The displacement equations relating the Cartesian co-ordinates of joints are each associated with a link. For two joints connected by a fixed length link, the condition is that the distance between the joints remains constant, i.e.

$$(x_i - x_j)^2 + (y_i - y_j)^2 - \ell_{ij}^2 = 0 \qquad (5.1)$$

where i,j denote the two joints and ℓ_{ij} is the length of the link connecting them. For a prismatic joint the condition is that the joint must lie on the sliding axis, i.e.

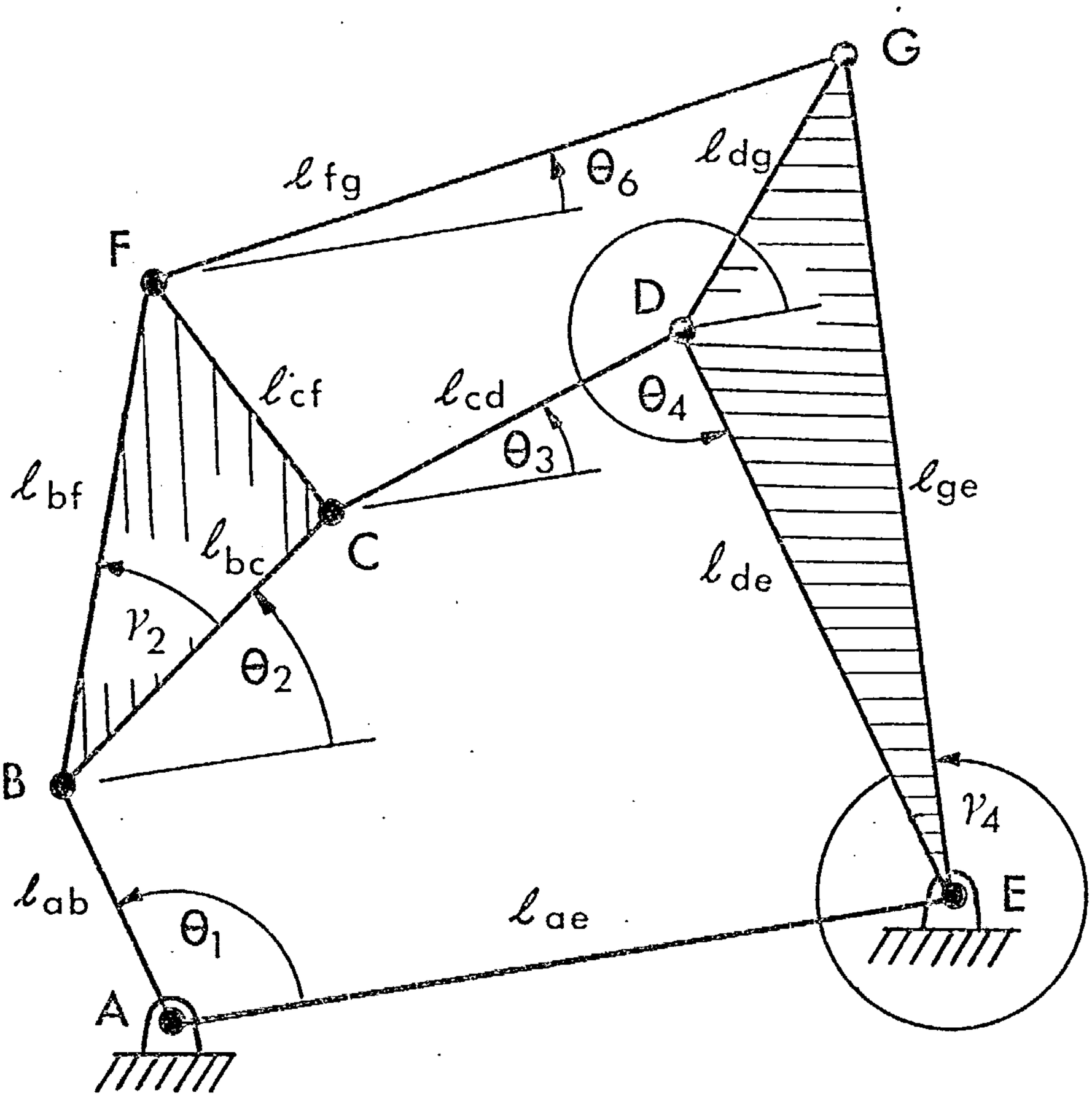

FIGURE 5·1 SIX BAR LINKAGE

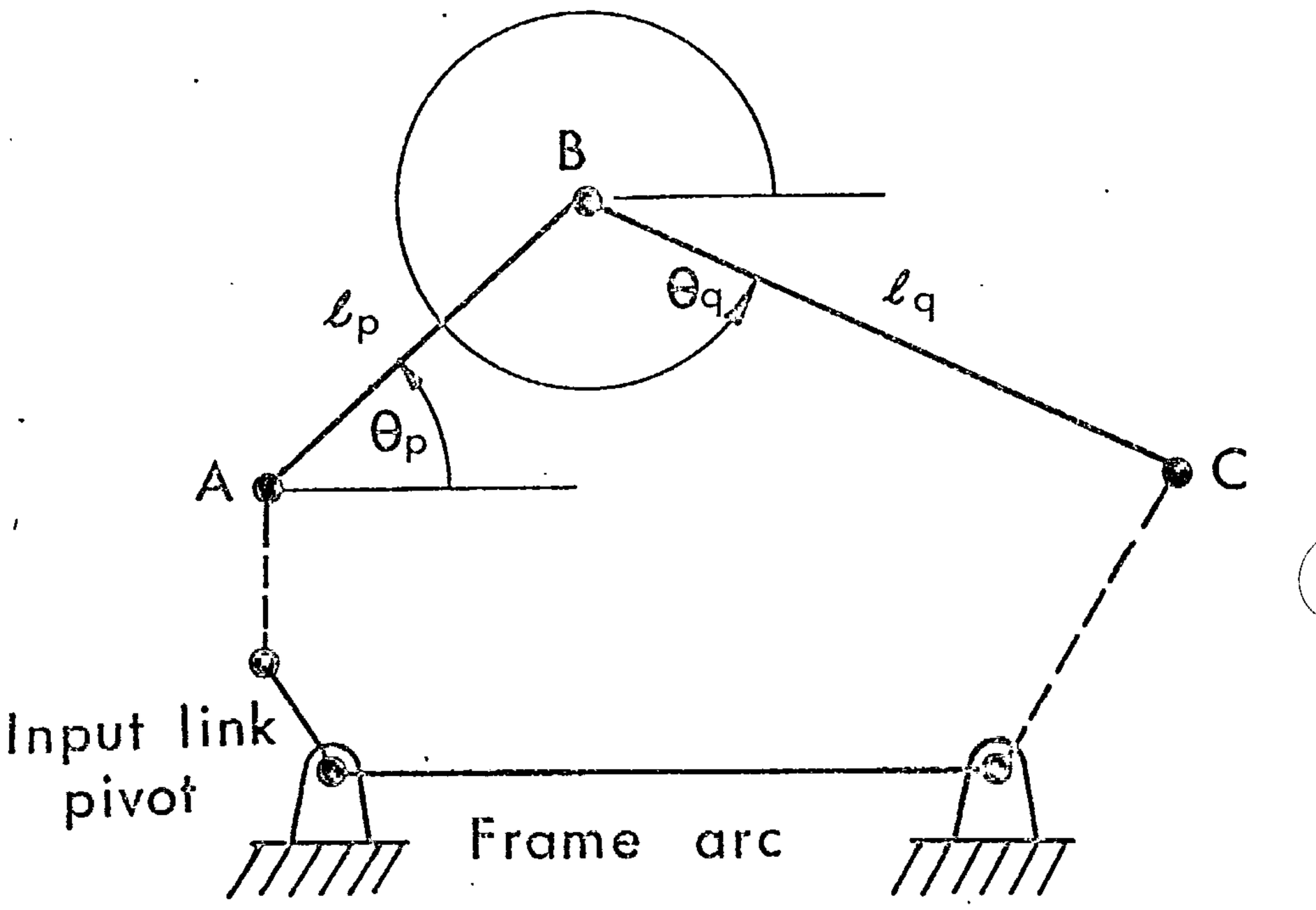

FIGURE 5·2 GENERAL UNDETERMINED DYAD

$$(x_k - x_j)(y_i - y_j) - (y_k - y_j)(x_i - x_j) = 0 \qquad (5.2)$$

where i,j denote two points that are both on the sliding axis and fixed in the guide link and k denotes the prismatic joint.

The displacement equations relating the variable link angles and lengths are each associated with an independent loop. They take the form

$$\sum_{i=1}^{n} \ell_i \cos\theta_i = 0$$

$$\sum_{i=1}^{n} \ell_i \sin\theta_i = 0 \qquad (5.3)$$

where n = number of arcs in the loop,

ℓ_i = length of arc i,

θ_i = angular position of arc i.

If the angular position of each arc is measured with respect to a fixed datum, these two equations are sufficient for a loop. If, however, it is measured with respect to the adjoining link, e.g. Molian {5.4} uses the exterior angles of the loop, an additional equation of the form

$$\sum_{i=1}^{n} \theta_i = 2\pi \text{ radians} \qquad (5.4)$$

is necessary.

For example, consider the inversion of the Stephenson six-bar linkage shown in Figure 5.1. As noted in Chapter 3, this inversion consists of a basic unit and a quadrilateral Assur group if AE is the frame link and AB is the input link. If A is

regarded as the origin, the co-ordinates of B and E will be determined for a prescribed value of the input angle, θ_1. Using the joint co-ordinates as variables gives eight equations, namely

$$(x_i-x_j)^2 + (y_i-y_j)^2 - \ell_{ij}^2 = 0 \qquad (5.5)$$

where i = b, c, d, b, f, g, f, d.
j = c, d, e, f, g, e, c, g.

with the co-ordinates of joints C, D, F and G as undetermined variables, ℓ_{ij} being the link lengths.

Since the linkage has one degree of freedom and six links, from equation (4.1) there are two independent loops. Using the method of prescribing the topology developed in Chapter 4, these are ABCDEA and ABFGEA. The associated spanning tree consists of the frame link, AE, and links AB, BCF and DEG since no loops remain if links CD and FG are cut. If the loops concerned comprise a complete set of independent loops for the linkage (as in this case), then the associated loop equations will constitute a complete set of independent equations for the linkage. Thus the following four equations form a complete set for this linkage. We have

$$\ell_{ab}\cos\theta_1+\ell_{bc}\cos\theta_2+\ell_{cd}\cos\theta_3+\ell_{de}\cos\theta_4-\ell_{ae} = 0$$

$$\ell_{ab}\sin\theta_1+\ell_{bc}\sin\theta_2+\ell_{cd}\sin\theta_3+\ell_{de}\sin\theta_4 = 0$$

$$\ell_{ab}\cos\theta_1+\ell_{bf}\cos(\theta_2+\gamma_2)+\ell_{fg}\cos\theta_6$$
$$+\ell_{ge}\cos(\theta_4+\gamma_4)-\ell_{ae} = 0$$

$$\ell_{ab}\sin\theta_1+\ell_{bf}\sin(\theta_2+\gamma_2)+\ell_{fg}\sin\theta_6$$
$$+\ell_{ge}\sin(\theta_4+\gamma_4) = 0 \qquad (5.6)$$

with the angular positions of links BCF, CD, FG and DEG as undetermined variables, all angular

positions being measured with respect to the frame arc. Thus using joint co-ordinates as variables may result in more equations than when link angles and lengths are used as variables.

The displacement equations form a set of simultaneous nonlinear equations in u unknowns where u is at least twice the number of independent loops involved. They may be represented by

$$f_i(\bar{v}) = 0 \qquad i = 1,2,\ldots,u \tag{5.7}$$

where $\bar{v}$ = vector of variables, v_1, v_2 etc. This set of equations may be solved in a variety of ways such as iteration, minimization and integration.

Iterative methods are commonly used. The iterations start from a user-supplied estimate of the variables and thereafter the results from one position of the input link are used as the estimate for the next position. The Newton-Raphson method is used in References {5.1 - 5.5}. The correction terms for each iteration are calculated on the basis of Taylor's theorem. We have

$$f_i(\bar{v}) = f_i(\bar{v}_o + \delta\bar{v}) \simeq f_i(\bar{v}_o) + \delta v_k \left[\frac{\partial f_i}{\partial v_k} \right]_o \quad i,k=1,2\ldots,u \tag{5.8}$$

where the zero subscript indicates values associated with the current estimate and $\delta\bar{v}$ is the vector of correction terms. From equations (5.7) and (5.8)

$$\left[\frac{\partial f_i}{\partial v_k} \right]_o \cdot \delta v_k = -f_i(\bar{v}_o) \tag{5.9}$$

from which the correction terms may be calculated. The matrix of terms $[\partial f_i/\partial v_k]_o$ is an approximation

to the Jacobian of f. The method (and all like it) may diverge and hence fail if this matrix becomes (nearly) singular. Van der Werff {5.7} proposes that the third term in the Taylor series should be used but the improvement in the correction terms may be offset by the increase in computation per iteration. Bus {5.8} has recently compared nine Algol 60 programs and six Fortran programs for solving simultaneous nonlinear equations. He used fifteen test problems and concluded that, of the Fortran programs, that by Brown {5.9} is best for fifteen or less undetermined variables whereas that by Powell {5.10} is often better for a larger number of variables.

Rooney and Rees Jones {5.11} noted that, if variables are eliminated from the displacement equations, extraneous roots may be obtained and singularities may be introduced that are not present in the original equations. Accordingly they regard all variables as interdependent. The equations then define a curve in n-dimensional Euclidean space. Fletcher's minimization algorithm {5.12} is used to find a starting point on the curve and then to move along the curve. One problem with this approach is that there is no indication of how many steps along the curve correspond to a prescribed movement of any link. Crossley and Seshachar {5.5} compared the cyclic stepping method and the method of steepest descent, as representative minimization techniques, with the Newton-Raphson method. For a twelve-bar linkage, the relative solution times were 310, 16 and 8.3 seconds respectively.

Paul and Krajcinovic {5.6} proposed that the velocity equations, obtained by differentiating the displacement equations, should be integrated numerically using the Adams-Moulton predictor-corrector method with automatic interval refining.

The displacement equations can be used as a check on the accuracy. One advantage of the velocity equations is that they are linear in the velocities. However, whereas the DRAM program previously analysed both dynamic and kinematic problems using an Adams-Moulton routine with a Newton-Raphson routine for the initial conditions {5.13}, it has recently been altered so that this approach is used only for dynamic problems. For kinematic problems, the Newton-Raphson routine is now used alone.

The solution times for many iterative methods are proportional to the cube of the number of undetermined variables. Therefore it is advantageous to solve the equations sequentially rather than simultaneously if this is possible. Crossley and Seshachar {5.5} developed a method for determining the variables associated with individual Assur groups. They noted that only half of the variables for any one group had to be determined simultaneously. Thus only one variable has to be determined at any one time for the dyad Assur group since this has two associated undetermined variables e.g. the angular positions of the two links or the Cartesian co-ordinates of the joint connecting them. Consequently, by restricting the range of linkages to those consisting of a basic unit and additional (peelable) dyads, the direct method given in the next Section can be used to determine the variables instead of an indirect method such as those considered above.

5.2 THEORY

The method given in this section is based on the use of loop equations with the varying link angles and lengths as variables. The angular position, θ, of each arc is defined relative to the last (frame) arc in its loop as follows. In the linkage shown in

Group (i)

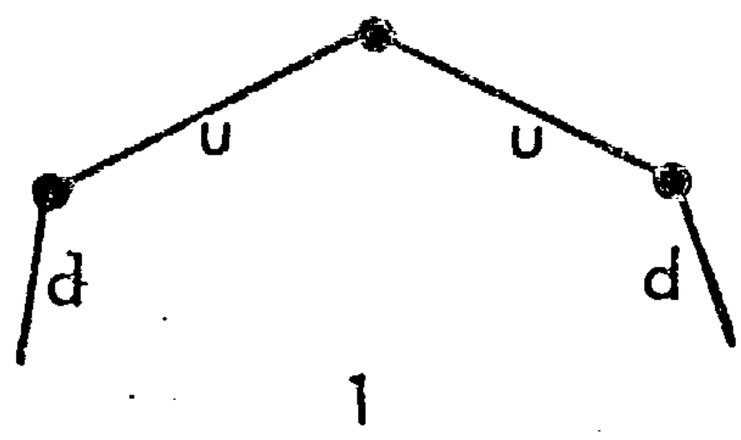

1

Type (a)

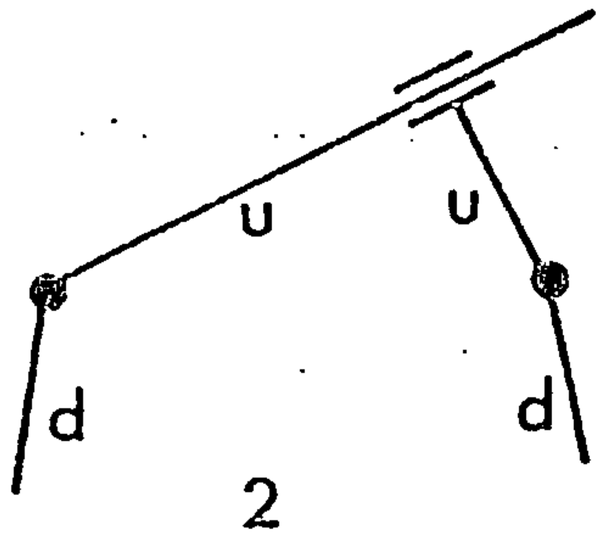

2

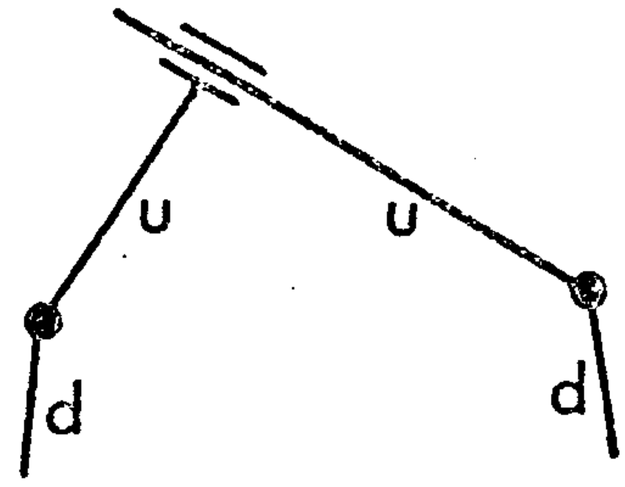

3

Group (ii)

Type (b)

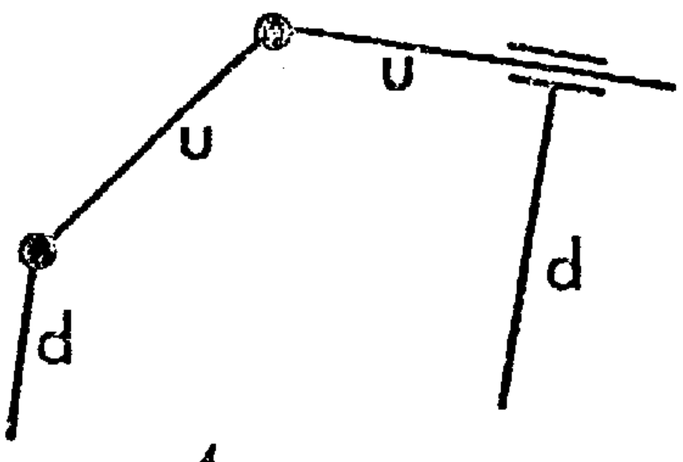

4

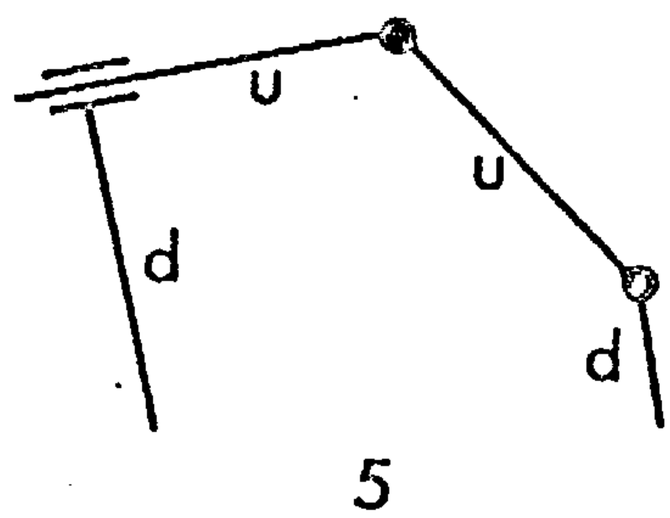

5

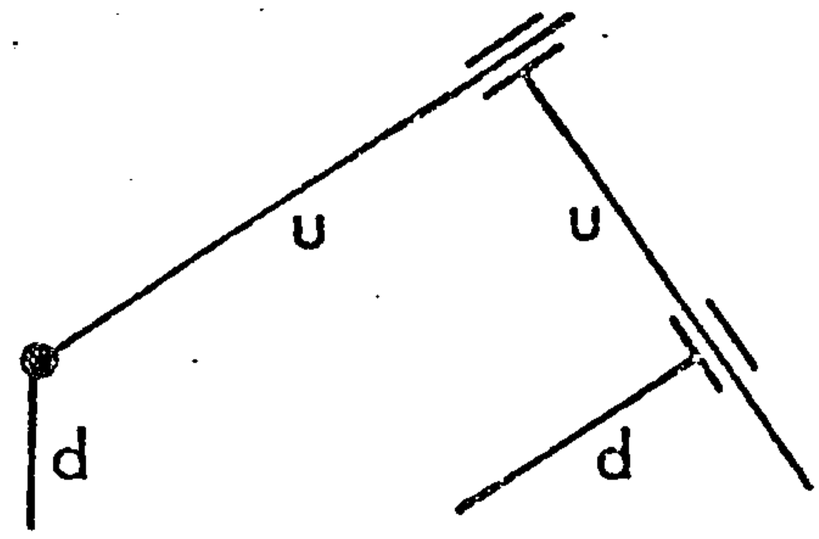

6

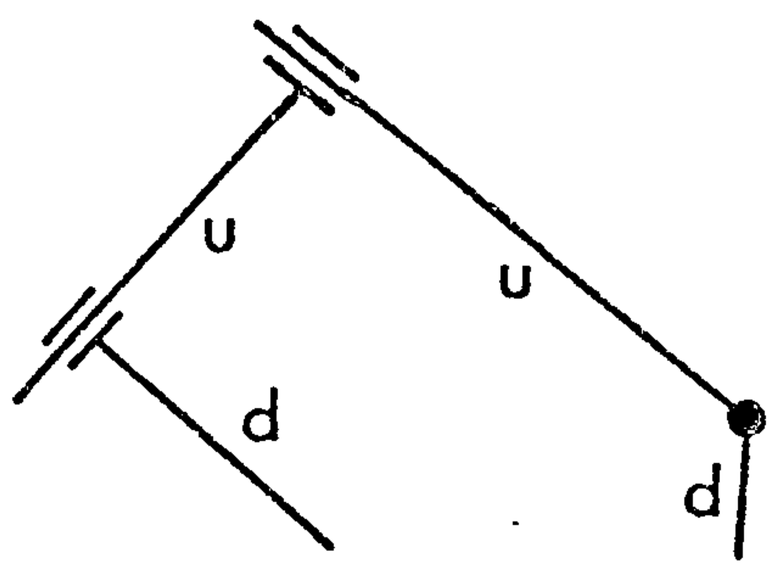

7

Group (iii)

d = determined arc
u = undetermined arc

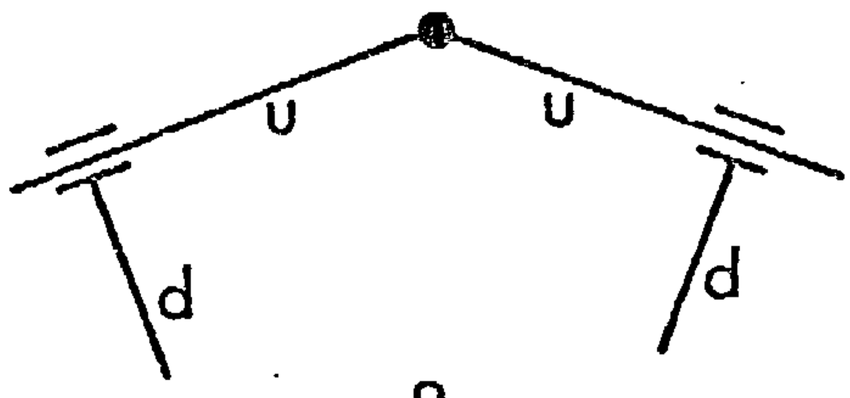

8

FIGURE 5·3 VALID UNDETERMINED DYADS

Figure 5.1, consider the loops ABCDEA and ABFGEA as vector polygons with the direction of the vectors lying along each arc as the loops are traversed in the sequence :

input link pivot, ..., frame

The reference direction for each loop is in the negative frame arc vector direction. Angles are positive when measured in the anti-clockwise sense from this direction.

Each loop will contain an undetermined dyad formed by two arcs connected together. Let one of these arcs be denoted by p and the other by q as shown in Figure 5.2 where the joints A, B and C represent any of the combinations shown in Figure 5.3. Then by resolving along and perpendicular to the frame arc we have

$$\ell_p \cos\theta_p + \ell_q \cos\theta_q + c_1 = 0$$

$$\ell_p \sin\theta_p + \ell_q \sin\theta_q + c_2 = 0 \qquad (5.10)$$

where

$$c_1 = \sum_{i=1}^{n} \ell_i \cos\theta_i \qquad i \neq p,q \qquad (5.11)$$

$$c_2 = \sum_{i=1}^{n} \ell_i \sin\theta_i$$

where ℓ refers to arc length and n is the number of arcs in the loop.

The appropriate solution of equations (5.10) depends on the nature of the joints in the undetermined dyad as outlined below.

5.2.1. Undetermined Dyad with Three Revolute Joints

The lengths of the arcs appearing in equations (5.10) are regarded as known quantities and their angular positions are to be determined. Eliminating Θ_p from equations (5.10) gives an equation of the form

$$c_3 + c_4\cos\Theta_q + c_5\sin\Theta_q = 0 \qquad (5.12)$$

where $c_3 = (c_1^2+c_2^2+\ell_q^2-\ell_p^2)$

$$c_4 = 2c_1\,\ell_q \qquad (5.13)$$

$$c_5 = 2c_2\,\ell_q$$

This leads to the following expressions for $\sin\Theta_q$ and $\cos\Theta_q$

$$\sin\Theta_q = (-c_3c_5 \pm c_4\sqrt{c_4^2+c_5^2-c_3^2})/(c_4^2+c_5^2) \qquad (5.14)$$

$$\cos\Theta_q = -(c_3+c_5\sin\Theta_q)/c_4$$

The choice of the sign to be used in the expression for $\sin\Theta_q$ is governed by the closure specified when prescribing the topology. Θ_q can then be calculated using

$$\Theta_q = \tan^{-1}(\sin\Theta_q/\cos\Theta_q) \qquad (5.15)$$

For arc p, we obtain from equations (5.10)

$$\sin\Theta_p = -(c_2+\ell_q\sin\Theta_q)/\ell_p$$

$$\cos\Theta_p = -(c_1+\ell_q\cos\Theta_q)/\ell_p \qquad (5.16)$$

$$\Theta_p = \tan^{-1}(\sin\ell_p/\cos\Theta_p)$$

Schonfeld {5.14} uses $(1-\sin^2\Theta_q)^{\frac{1}{2}}$ for $\cos\Theta_q$, thereby losing the sign which is necessary to determine the appropriate quadrant for Θ_q.

5.2.2 Undetermined Dyad with Two Revolute Joints and One Prismatic Joint

Equations (5.10) must now be solved for the length ℓ_p of the sliding link and the angle Θ_q of the other arc. Two sub-cases can be distinguished when determining Θ_q :

a) the prismatic joint connects the two arcs,
b) the guide of the sliding link constitutes a determined arc in the loop.

These are shown in group (ii) of Figure 5.3 as types (a) and (b) respectively. In both cases, the expression for the length of the sliding link is the same.

a) The guide link is an undetermined arc

The convention of perpendicularity given in Section 3.1 provides that

$$(\Theta_p - \Theta_q) = \pm \pi/2 \quad \text{radians} \qquad (5.17)$$

the sign being specified when the topology is prescribed. Eliminating ℓ_p from equations (5.10) and substituting (5.17) gives

$$\ell_q + c_1\cos\Theta_q + c_2\sin\Theta_q = 0 \qquad (5.18)$$

which is similar in form to equation (5.12). Accordingly

$$\sin\Theta_q=(-c_2\ell_q\pm c_1\sqrt{c_1^2+c_2^2-\ell_q^2})/(c_1^2+c_2^2)$$

$$\cos\Theta_q= -(\ell_q+c_2\sin\Theta_q)/c_1 \qquad (5.19)$$

$$\Theta_q = \tan^{-1}(\sin\Theta_q/\cos\Theta_q)$$

Angle Θ_p may then be determined from equation (5.17).

b) <u>The guide link is a determined arc</u>

In this case, the angle θ_p is determined directly from the angular position of its guide link which is already determined. Eliminating ℓ_p from equations (5.10) gives

$$c_6 + c_7\cos\theta_q + c_8\sin\theta_q = 0 \qquad (5.20)$$

where $c_6 = c_1\sin\theta_p - c_2\cos\theta_p$

$$c_7 = \ell_q\sin\theta_p \qquad (5.21)$$

$$c_8 = -\ell_q\cos\theta_p$$

Equation (5.20) is similar in form to equations (5.12) and (5.18). Accordingly

$$\sin\theta_q = (-c_6c_8 \pm c_7\sqrt{c_7^2+c_8^2-c_6^2})/(c_7^2+c_8^2)$$

$$\cos\theta_q = -(c_6+c_8\sin\theta_q)/c_7 \qquad (5.22)$$

$$\theta_q = \tan^{-1}(\sin\theta_q/\cos\theta_q)$$

In both cases, the length ℓ_p of the sliding link is then given from equations (5.10) by

$$\ell_p = -\frac{\{c_1+c_2+\ell_q(\sin\theta_q + \cos\theta_q)\}}{(\sin\theta_p + \cos\theta_p)} \qquad (5.23)$$

The reason for using both equations (5.10) when calculating ℓ_p is to ensure that division by zero does not occur when θ_p equals an integer multiple of $\pi/2$ radians.

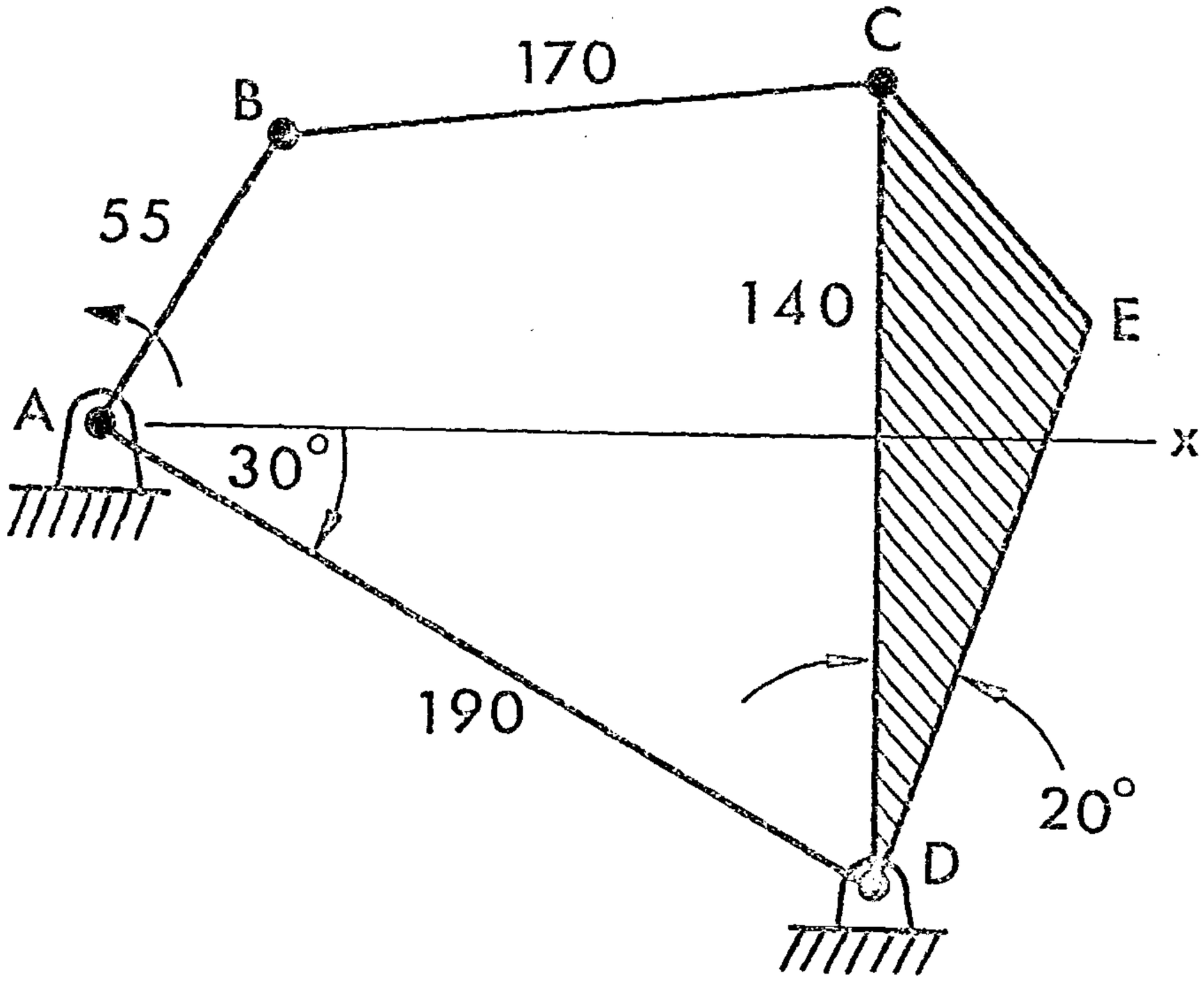

FIGURE 5·4 FOUR-BAR LINKAGE

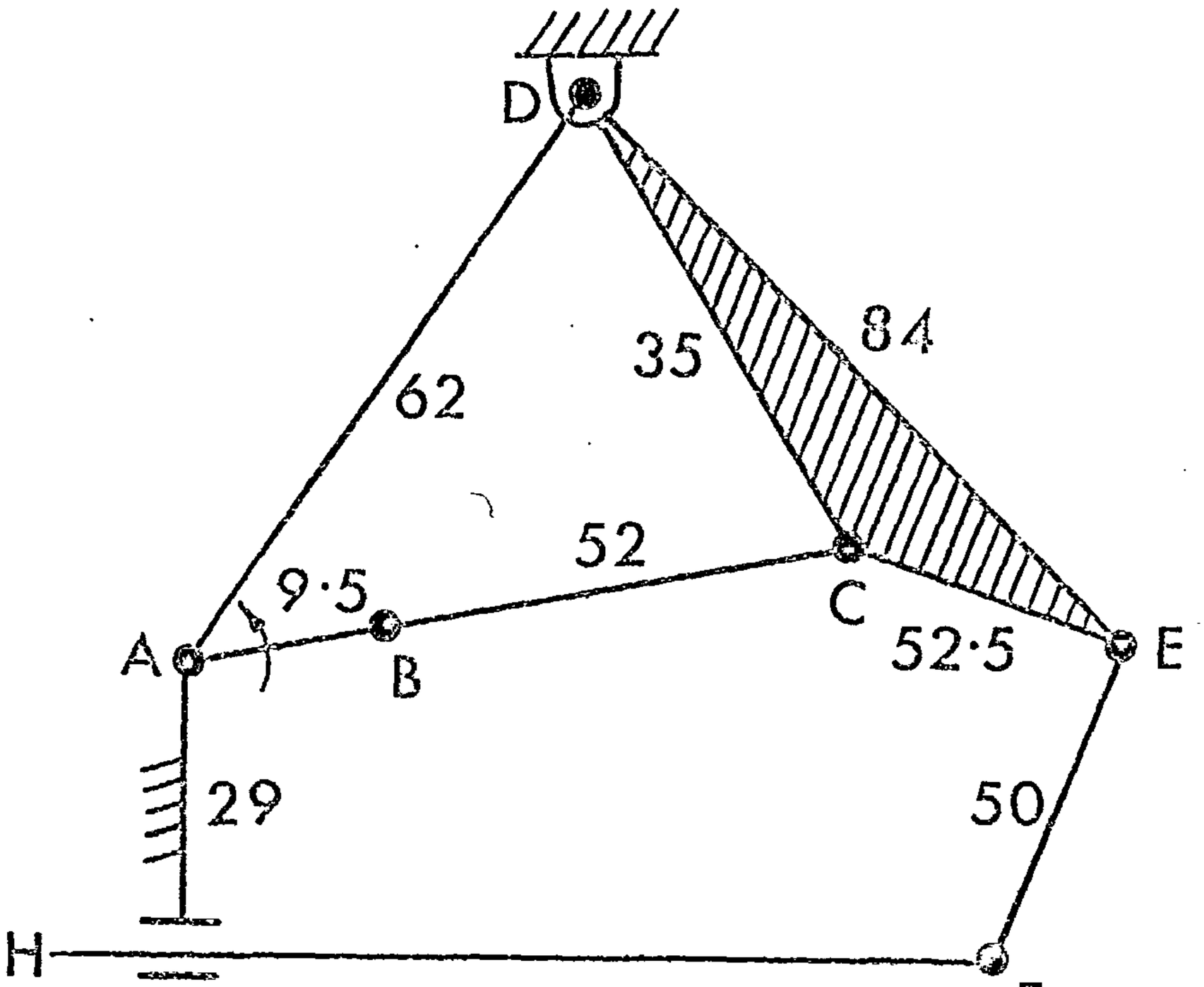

FIGURE 5·5 SIX-BAR LINKAGE

5.2.3. Undetermined Dyad with One Revolute Joint and Two Prismatic Joints

In whatever combinations the joints may occur as indicated by group (iii) of Figure 5.3, the angular positions of the two arcs appear in equations (5.10) as known quantities and it remains only to determine the corresponding arc lengths. The results are

$$\ell_q = (c_2\cos\theta_p - c_1\sin\theta_p)/\sin(\theta_p-\theta_q)$$

$$\ell_p = -\frac{\{c_1+c_2+\ell_q(\sin\theta_q + \cos\theta_q)\}}{(\sin\theta_p + \cos\theta_p)} \qquad (5.24)$$

with both equations (5.10) again being used for ℓ_p.

5.3 COMPARISONS

Two industrial linkages were used as examples to compare the various approaches. The first, shown in Figure 5.4, is a crank-rocker linkage with AB as the crank. It is used when knitting the heels and toes of socks (half-hose). The second, shown in Figure 5.5, again has AB as the input link. The output at H is used to feed paper into a duplicating machine.

Each method was programmed in double precision and then compiled using a Fortran G compiler and run on an IBM370 computer. The cpu time in seconds required to analyse each linkage at 180 equally spaced positions of the input link was determined - additional time would be required to set up the equations and print out the results.

Table 5.1. Effect of Variables on Analysis Times

Variables	Four-bar linkage	Six-bar linkage
Link angles and lengths	0.540	2.038
Joint co-ordinates	0.350	3.862

Table 5.1 shows the effect of using joint co-ordinates as the variables in the displacement equations instead of link angles and lengths. In each case, Brown's algorithm {5.9} was used to solve the equations to eight significant figures. For the four-bar linkage, both sets of variables result in two simultaneous equations and the pair involving joint co-ordinates were solved more rapidly. However, joint co-ordinates resulted in six simultaneous equations for the six-bar linkage whereas only four equations resulted from using link angles and lengths. In consequence, the time for solving the equations with joint co-ordinates as variables was higher. Since the disparity in the number of equations, and hence solution times, tends to increase with the number of links, the use of link angles and lengths as variables in equations based on a set of independent loops is to be preferred for any general program.

Four methods of solving the displacement equations were tested :

a) direct method given in Section 5.2,

b) Adams-Moulton variable order integration method as implemented by Smith {5.13},

c) Brown's iterative algorithm {5.9},

d) Newton-Raphson iterative method as implemented by Smith {5.13}.

The results are given in Table 5.2.

Table 5.2 Effect of Method on Analysis Times

Method	Four-bar linkage	Six-bar linkage
Direct	0.053	0.121
Adams-Moulton	0.474	0.981
Brown	0.540	2.038
Newton-Raphson	0.840	1.735

The direct method is at least eight times as fast as any of the other methods. This reduced computation time is the main justification for restricting the range of linkages to those for which the direct method is appropriate, namely those consisting of a basic unit and additional peelable dyads. With this selection of linkages, there are only two possible closures of each loop. This results in two other advantages. Firstly the desired closure can be prescribed by a sign convention which can be used directly in the equations in Section 5.2 and so the user does not have to supply estimates of the initial values of the variables. Secondly, if the input link is moved through a large angle between successive positions, there is no risk of an incorrect closure being obtained as could happen with an iterative method where the results for one position of the input link are used as initial estimates for the next position.

Summary

This chapter starts by considering the equations that may be used for the kinematic analysis of a linkage, the different variables that may appear in the equations and alternative methods of solution. It is noted that the use of independent loops leads to independent equations. The necessary theory is then developed for each of the valid dyads identified in the previous chapter. A direct method of solving the resulting equations is compared with other methods. This highlights the advantages of using linkages built up from dyads.

6. OPTIMIZATION

6.1 VARIABLES AND PARAMETERS

In any consideration of the use of optimization algorithms in the kinematic synthesis of linkage mechanisms, a distinction must be made between kinematic variables, linkage parameters and optimization variables. Kinematic variables are the angular positions of the links and the lengths of any sliding links which change as the input link rotates. They are the variables in the kinematic equations considered in Chapter 5. On the other hand, linkage parameters are the arc lengths and the angles between pairs of arcs in a link. The user is free to choose which of these may be altered, i.e. which are optimization variables, and which shall remain fixed. Two arrays, analogous to those containing the topological information, are used to register this choice as described in Appendix B3.1

6.2 OBJECTIVE

Given an estimate of the values of the optimization variables, the optimization algorithm will alter those values. An analysis of the corresponding linkage is carried out with the optimization variables appearing as (fixed) linkage parameters in the kinematic equations. If the result is closer to the desired objective, then the process is repeated until no further improvement is obtained. The algorithm is then said to have converged to a minimum. ~ There is no certainty that this will be the global minimum, i.e. the lowest of all the possible minima. A simple strategy is to define the objective solely in terms of the output motion. In this case, if the initial estimates represent links that the designer would like to use, then, as long as the output motion is acceptable, a nearby local minimum may be adequate. If the output motion is not acceptable, the process should be started from several different initial estimates.

It is assumed that the desired motion can be represented in one of the following forms for a prescribed set of absolute or relative angular positions, θ_i, of the input link :

a) the output link shall occupy prescribed angular positions, θ_o, relative to the machine frame,

b) a point on the output link shall occupy prescribed positions, (x_o, y_o), relative to a set of Cartesian axes fixed in the machine frame,

c) a point on the output link shall be at a prescribed distance, d_o, from the origin of the Cartesian axes fixed in the machine frame.

The desired values may be written as $f_d(\theta_i)$, $i = 1,2,...t$ where θ_i are the t given positions of the input link which are equivalent to intervals of time if the input link rotates at constant velocity. The method of supplying these values is described in Appendix B3.2.

The question arises of a suitable value for t - the higher the value, the more accurate the representation of the actual (continuous) motion but the longer the time for analysis. Porter and Sanger {6.1} have shown that a very close approximation to the forces in a four-bar linkage over a cycle is obtained if 36 positions of the input link are used. However, they also present a graph which shows that 18 and 12 positions give results within 1% and 10% of the true value respectively. Youssef {6.2} recommends that only a few positions should be used initially with the number being increased as the optimization proceeds.

For use with an optimization algorithm, an objective function must be defined to represent the quality of a linkage by a single number. If the actual values produced by that linkage for the given positions of the input link are written as $f_a(\theta_i)$, $i = 1,2, \ldots t$, then

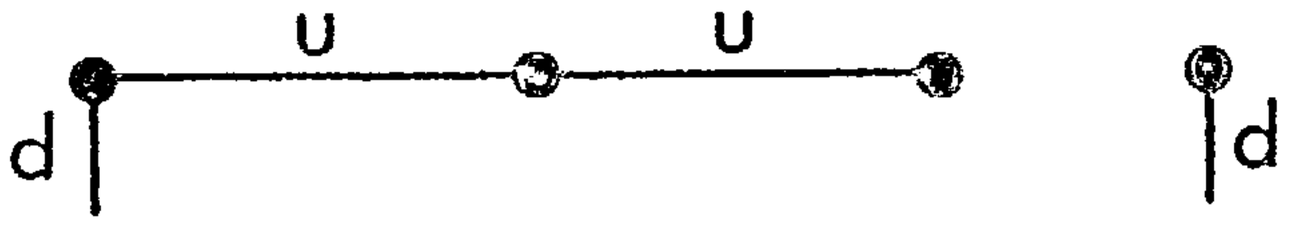

(a) Sum of arc lengths too small

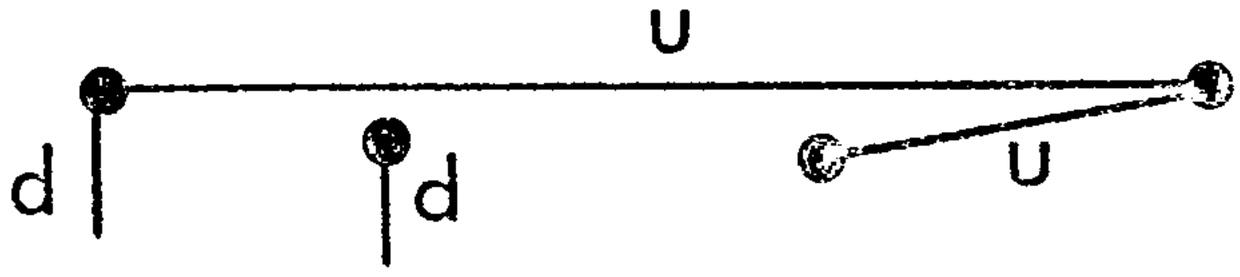

(b) Difference in arc lengths too large

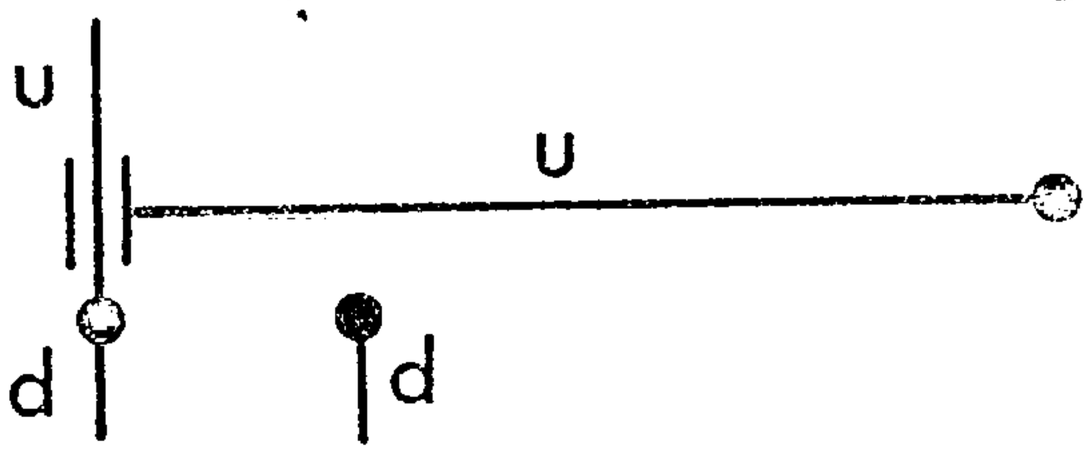

(c) Guide link too long

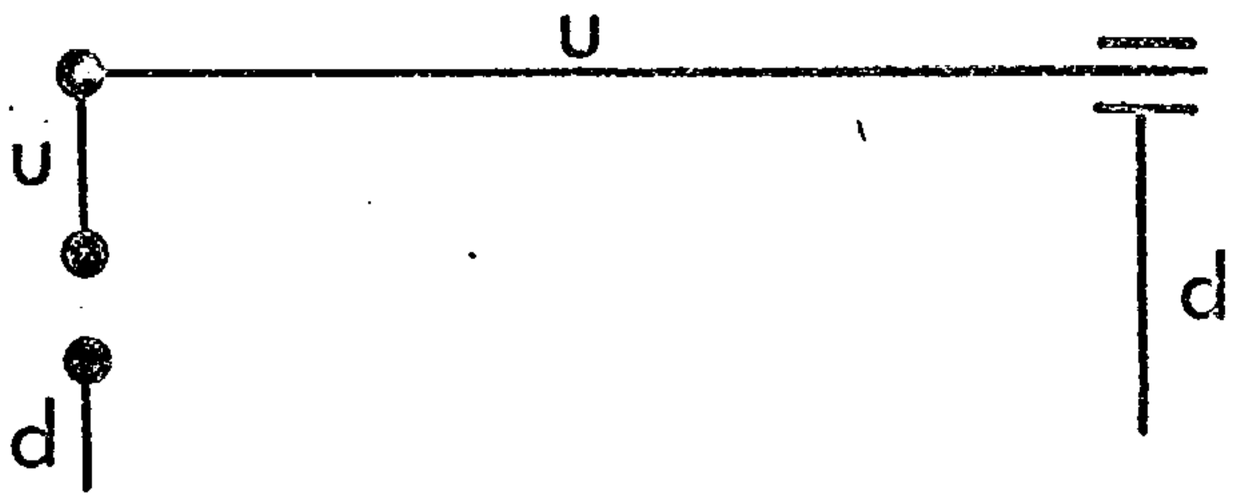

(d) Fixed length arc too short

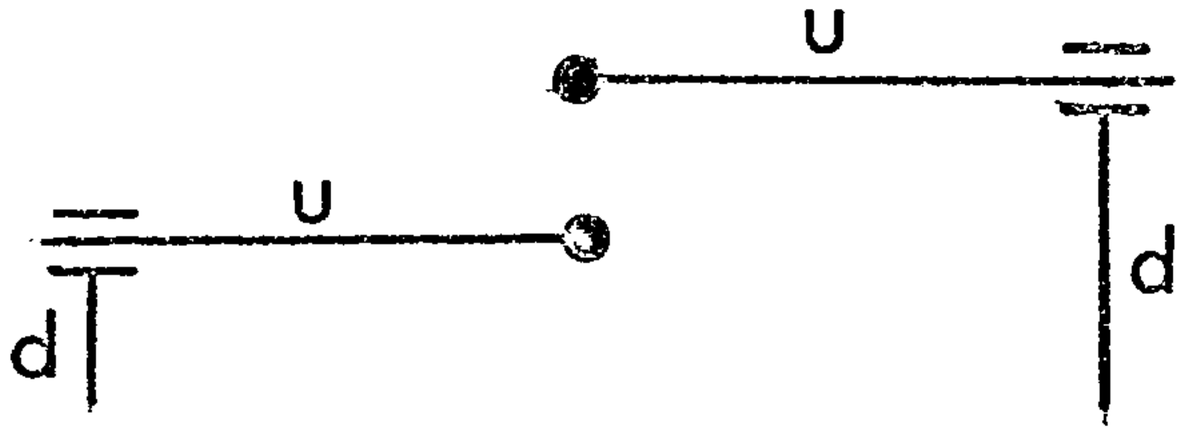

(e) Infinite sliding links

u=undetermined arc

d=determined arc

FIGURE 6·1 CONDITIONS FOR UNCLOSED LOOPS

a suitable objective function is given by :

$$F(v) = \sum_i w_i \{f_d(\theta_i) - f_a(\theta_i)\}^2 \qquad (6.1)$$

where v = optimization variables,

w_i = a weighting factor which may be different for each position of the input link.

A weighting factor greater than unity can be prescribed for positions that are more critical than others. Alternatively the input link positions can be closely spaced in the relevant region if the resulting total number of positions is not too large. The objective is to minimize $F(v)$ by altering the values of the optimization variables.

6.3 CONSTRAINTS

6.3.1. Loop Closure

There is one constraint that every linkage mechanism must satisfy if it is to provide constrained motion. The constraint is that every independent loop in the linkage must remain closed without a change of closure throughout the motion of the linkage. As a result, optimization applied to the kinematic synthesis of linkages can never be truly unconstrained.

The conditions under which a pair of undetermined arcs will not close a loop are illustrated in Figure 6.1. When the program is used for analysis, an appropriate warning message is printed out. However, in synthesis the undetermined arcs will often be optimization variables, in which case their lengths can be altered. The appropriate action can be determined by relating the conditions to the equations given in Chapter 5.

Let h be the distance between the 'free' ends of the determined arcs. Then, from equation (5.11)

$$h^2 = c_1^2 + c_2^2 \qquad (6.2)$$

Group (i), three revolute joints.

Substituting from equations (5.13) and (6.2), equation (5.14) yields imaginary values if

$$(h^2 + \ell_q^2 - \ell_p^2)^2 > 4\, h^2 \ell_q^2 \qquad (6.3)$$

where ℓ_p and ℓ_q are the lengths of the undetermined arcs.

If the two sides of this inequality are equal, the links are in a toggle position with the attendant risk of change of loop closure. Since the right-hand side of the inequality is always positive, the inequality may be written as

$$h^4 - 2h^2(\ell_p^2 + \ell_q^2) + (\ell_q^2 - \ell_p^2)^2 > 0$$

This factorizes to give

$$\{h^2 - (\ell_q + \ell_p)^2\}\{h^2 - (\ell_q - \ell_p)^2\} > 0 \qquad (6.4)$$

This is satisfied if either both terms are positive or both negative.

Case a) Both terms positive.

If $(\ell_q + \ell_p)^2 < h^2$, then $(\ell_q - \ell_p)^2$ will be less than h^2 and both terms will be positive. This condition is illustrated in Figure 6.1a and can be remedied by lengthening both arcs equally. This is preferable to lengthening them in proportion to their lengths as it reduces the likelihood of case (b) occurring at another part of the motion. The necessary alterations to the arc lengths are determined in Section 6.3.2.

Case b) Both terms negative.

If $(\ell_q - \ell_p)^2 > h^2$, then $(\ell_q + \ell_p)^2$ will be greater than h^2 and both terms will be negative. This condition is illustrated in Figure 6.1b and can be remedied by lengthening the shorter arc. This is preferable to shortening the longer arc as it reduces the likelihood of case (a) occurring at another part of the motion.

Group (ii), two revolute joints and one prismatic joint

In the equations for this group, ℓ_p and ℓ_q are the lengths of the sliding link and fixed length arc respectively.

Case a) The guide link is an undetermined arc.
Equation (5.19) yields imaginary values if

$$\ell_q^2 > h^2 \qquad (6.5)$$

This condition is illustrated in Figure 6.1c and can be remedied by shortening the guide link.

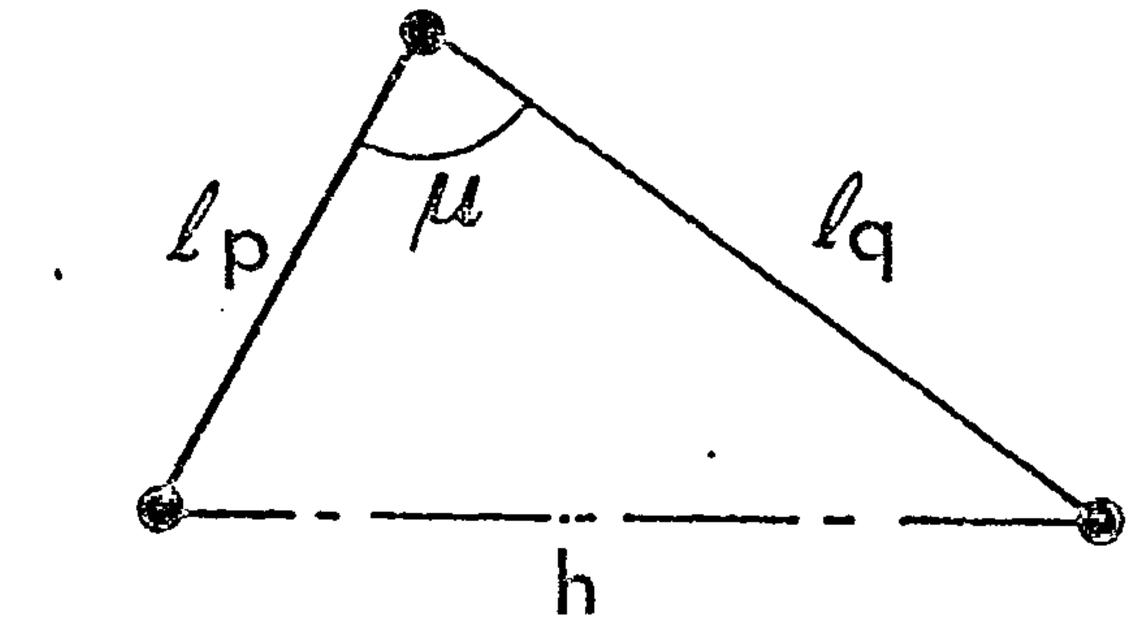

(a) Undetermined dyad

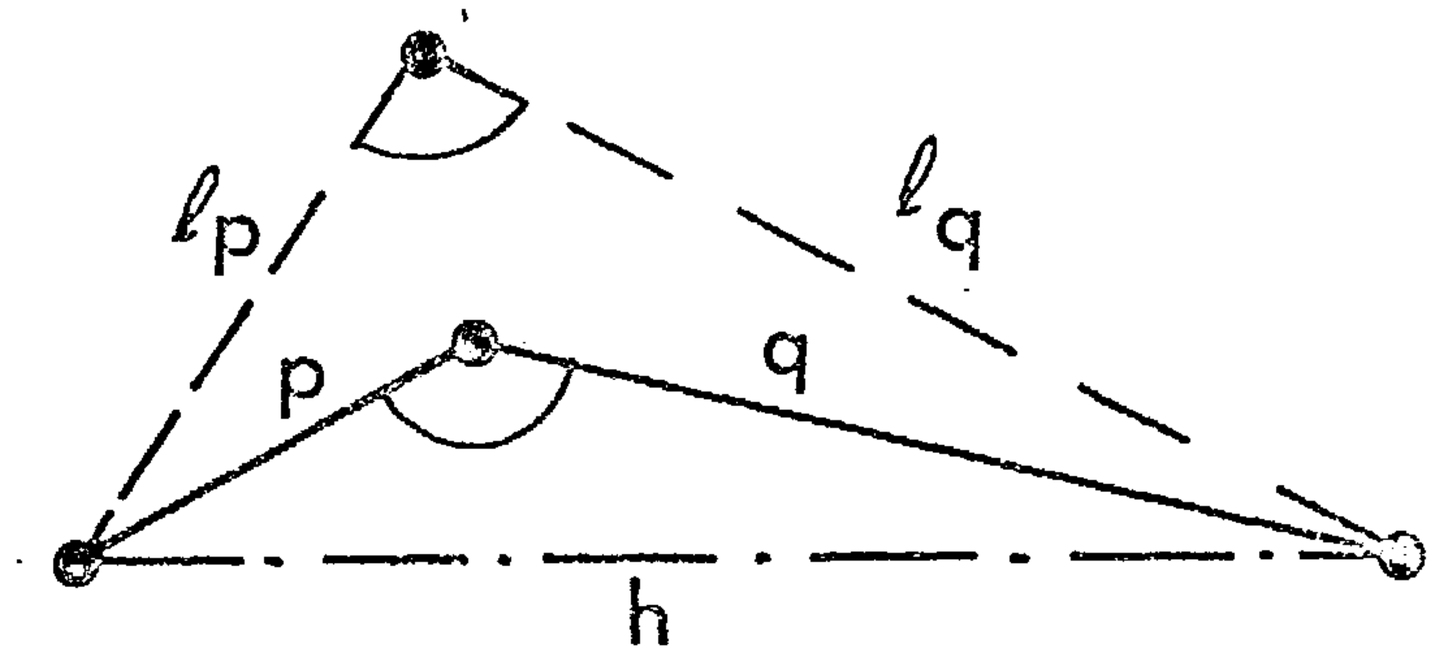

(b) Longer arcs reduce angle

(c) Longer arc increases angle

FIGURE 6·2 TRANSMISSION ANGLE

Case b) The guide link is a determined arc.
Substituting the values from equations (5.21), equation (5.22) yields imaginary values if

$$(c_1 \sin \Theta_p - c_2 \cos \Theta_p)^2 > \ell_q^2 \qquad (6.6)$$

This condition is illustrated in Figure 6.1d and can be remedied by lengthening the fixed length arc.

Group (iii), one revolute joint and two prismatic joints

Equation (5.24) yields an infinite length for one of the sliding links if

$$\Theta_p - \Theta_q = \pm k\pi \text{ radians, } k = 0,1,2 \ldots. \qquad (6.7)$$

The condition for this to occur is shown in Figure 6.1e and cannot be remedied by altering either undetermined arc. It cannot occur with the other two dyads in this group as the two undetermined arcs are mutually perpendicular by convention.

6.3.2. Transmission Angle

In the foregoing discussion relating to an undetermined dyad with three revolute joints, it was noted that there is a risk of a change of loop closure if the two arcs concerned assume an in-line configuration. Moreover,any such dyad that approaches too close to that configuration will be very sensitive to errors in the lengths of the arcs and will also have poor force transmission characteristics. Hain {6.3} therefore recommends that the transmission angle, i.e. the angle between the two arcs, should be in the range $90 \pm 50^{\circ}$. This can be related to the test for loop closure as follows. Let the transmission angle be μ, then, from Figure 6.2a

$$\ell_p^2 + \ell_q^2 - h^2 = 2\ell_p \ell_q \cos\mu \qquad (6.8)$$

$$4\ell_p^2\ell_q^2 - (\ell_p^2+\ell_q^2 - h^2)^2 = 4\ell_p^2 \ell_q^2 (1-\cos^2\mu)$$

$$\{(\ell_p+\ell_q)^2 - h^2\}\{h^2 - (\ell_q-\ell_p)^2\} = (2\ell_p\ell_q \sin\mu)^2 \qquad (6.9)$$

The left hand side of equation (6.9) is identical to the left hand side of inequality (6.4) apart from a change of sign and the right hand sides are equal if μ equals 0^o or 180^o. Since higher values of the left hand side of equation (6.9) give transmission angles closer to the optimum value of 90^o, an acceptable dyad will be such that :

$$\{(\ell_p+\ell_q)^2 - h^2\}\{h^2-(\ell_q-\ell_p)^2\} \geq (2\ell_p\ell_q\sin\mu)^2 \qquad (6.10)$$

As in the case of loop closure, there are two conditions for which this inequality is not satisfied. The corrective action to be taken is given below.

Case a) Both arcs too short.

If the two arcs are too short compared to h, the transmission angle will be too large as shown in Figure 6.2b. Let

p,q = unacceptable arc lengths,

ℓ_p, ℓ_q = corresponding acceptable arc lengths,

k = correction such that

$$\ell_p = p+k \quad \text{and} \quad \ell_q = q+k \qquad (6.11)$$

Substitution in equation (6.8) gives

$$2(p+k)(q+k)\cos\mu = (p+k)^2 + (q+k)^2 - h^2$$

$$k^2\{2(1-\cos\mu)\} + k\{2(p+q)(1-\cos\mu)\}$$

$$+ \{p^2+q^2 - h^2 - 2\cos\mu.pq\} = 0$$

Thus both links should be extended by

$$k = -\frac{(p+q)}{2} + \left\{\frac{2h^2 - (1+\cos\mu)(p-q)^2}{4(1-\cos\mu)}\right\}^{\frac{1}{2}} \qquad (6.12)$$

If $\mu = 180^o$, $k = (h-p-q)/2$

Case b) Difference in arc lengths too great.

If the difference in the arc lengths is too great compared to h, the transmission angle will be too small as shown in Figure 6.2c. Let

p = length of the arc that is too short,
ℓ_p = acceptable length of shorter arc,
ℓ_q = length of longer arc,
k = correction such that

$$\ell_p = p + k \tag{6.13}$$

Then, from equation (6.8)

$$2(p+k)\ell_q\cos\mu = (p+k)^2 + \ell_q^2 - h^2 \tag{6.14}$$

$$k^2 + 2k(p-\ell_q\cos\mu) + (p^2+\ell_q^2 - h^2 - 2p\ell_q\cos\mu) = 0$$

$$k = \ell_q\cos\mu - p - (h^2-\ell_q^2\sin^2\mu)^{\frac{1}{2}}$$

Thus the corrected arc length is

$$\ell_p = \ell_q\cos\mu - (h^2 - \ell_q^2\sin^2\mu)^{\frac{1}{2}} \tag{6.15}$$

If $\mu = 0$, $\ell_p = \ell_q - h$.

This approach fails if

$$\ell_q\sin\mu > h$$

This represents the situation where, even if the angle between the undetermined arcs is the minimum transmission angle, the distance between the 'free' ends of the determined arcs is shorter than the perpendicular distance from the end of the longer undetermined arc to the line of the shorter arc. To give the largest sum of the arc lengths while satisfying the constraints, both ℓ_p and ℓ_q are changed to $h/\{2\sin(\mu/2)\}$. It follows that ℓ_q cannot be lengthened subsequently at another point in the cycle.

6.3.3. Limits for Optimization Variables

The user is free to prescribe upper and lower limits for the lengths of arcs other than sliding links as described in Appendix B4.2. An equality constraint, i.e. that an arc shall have a certain length, is handled by specifying that that arc shall not be an optimization variable. Angles between arcs may be treated in a similar manner.

6.4 SIMPLEX METHOD

6.4.1. Choice of Algorithm

The objective is to minimize the objective function (6.1) subject to the constraints of loop closure, transmission angle and possibly limiting values of arc lengths and angles. Since both the function and the constraints are nonlinear, this represents a nonlinearly constrained nonlinear optimization problem.

Optimization algorithms can be divided into two types - gradient and direct search methods. The use of derivatives of the function involves extra work, both in obtaining formulae and coding, but experience has shown that explicit knowledge of the gradient reduces the time required to solve a problem and increases the size of problem that can be tackled successfully {6.4}. However, in a general kinematic synthesis program, the calculation of the objective function and constraints involves solving the kinematic equations for each loop for a series of input link positions. Hence it is difficult to derive explicit expressions for the partial derivatives of both the objective function and the constraints with respect to each of the possible optimization variables. In these circumstances, derivative values can only be obtained by means of finite-difference approximations. However, this approach can introduce truncation and/or cancellation errors which may nullify the theory underlying the chosen algorithm and lead the search astray so that it converges to the solution only very slowly, or possibly not at all (Swann {6.5}). Accordingly a direct-search method which does not call for derivative values is used.

Nonlinear constraints can be handled in two ways. In the first, values of variables that violate the constraints are permissible but a penalty term, the value of which increases rapidly as the degree of violation increases, is added to the objective function. In the second, only feasible sets of values which do not violate the

constraints are permissible. Since it is not possible to calculate the objective function for a linkage in which a loop does not close, the second approach is adopted here.

In view of these considerations and in the absence of a clear 'best' algorithm for this type of problem, a variant of the simplex method for unconstrained optimization proposed by Spendley, Hext and Himsworth {6.6} has been adopted. This method derives its name from its use of a regular simplex to explore the parameter space, a regular simplex in n dimensions being $n+1$ mutually equidistant points. The basic method is just to replace the worst vertex in the simplex, i.e. the one having the highest value of $F(v)$, by its reflection in the centroid of the others, thereby producing a new simplex so that the procedure can be repeated. Nelder and Mead {6.7} improved the performance of the method by allowing the simplex to rescale itself according to the local geometry of the function by incorporating expansion and contraction moves. Parkinson and Hutchinson {6.8} proposed unlimited expansion followed by translation of the simplex to avoid undue distortion. Both of these features have been incorporated into the program.

Box {6.9} found that, in the presence of constraints, allocating a large positive function value to non-feasible points often led to the simplex flattening itself against a constraint and remaining thereafter in the corresponding subspace. He therefore developed a new constrained simplex method using $q \geq n+1$ vertices, where n is the number of optimization variables, and termed his figure a 'complex'. The extra vertices were introduced to prevent the simplex losing dimensions when confronted with constraints {6.5}. If the only constraints are those of loop closure and transmission angle, the flattening of the simplex is unlikely to occur as the value of a variable on the constraint boundary depends on the values of (some of) the other variables. Hence the number of vertices used in

this program is (n+1). However, if the program is used with explicit bounds on the variables, this number should be increased.

6.4.2. Initial Simplex

The initial simplex is usually generated in the manner proposed by Box {6.9}. The user supplies values for the linkage parameters corresponding to one linkage (see Appendix B2.6). The values that are optimization variables form the set of values that defines the first vertex. Effectively the user also supplies upper and lower bounds for each variable (see Appendix B3.3). Let these be u_i and ℓ_i respectively for the i^{th} variable. Then the remaining n vertices are obtained one at a time from

$$v_i^{(j)} = \ell_i + r_i(u_i - \ell_i) \quad i = 1,2,..,n; \quad j = 2,3,.., n+1 \quad (6.16$$

where r_i is a pseudo-random deviate uniformly distributed over the interval (0, 1). Using this approach, the simplex is roughly scaled to the orders of the variables, reducing the need for any scaling by the user. This is aided by any angular variables being in degrees rather than radians so that the scale of these variables is comparable to that of any variable arc lengths.

The random numbers are generated using the power residue method {6.10}. The sequence of numbers depends on a user-supplied integer so that a completely different initial simplex (apart from the first vertex), can be obtained merely by changing the value of this integer. In addition, the results of other runs can be used for some, or all, of the vertices as recommended by Youssef {6.2}.

6.4.3. Strategy

As soon as the set of values, i.e. co-ordinates, for a vertex is available, the value of the objective function for that vertex is calculated with the co-ordinate values being altered if necessary so that constraints are not violated. When the simplex is complete, the method proceeds in a series of stages which together constitute

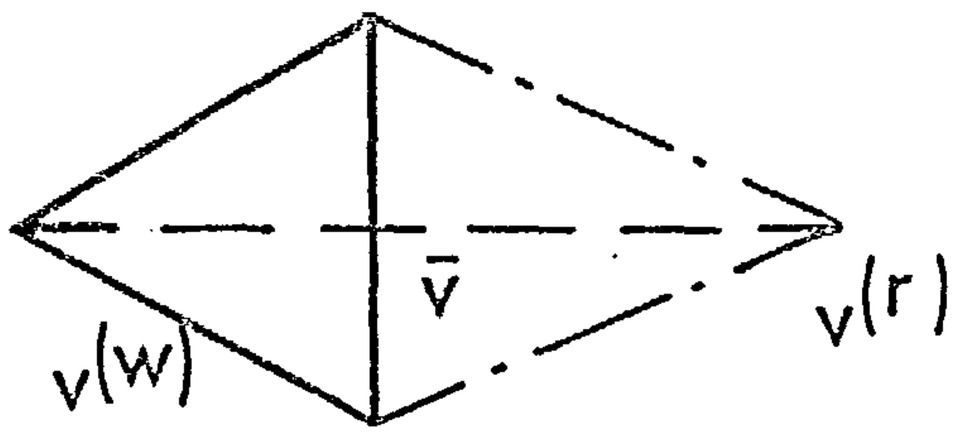

$$\alpha = \frac{v(r) - v(w)}{\bar{v} - v(w)}$$

(a) Reflection

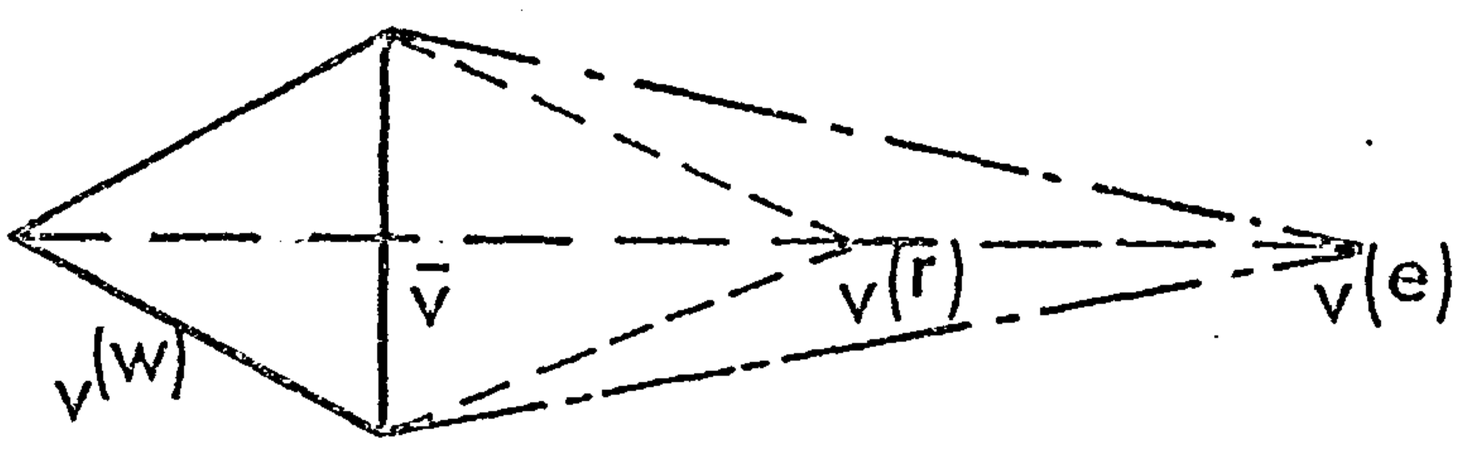

$$\beta = \frac{v(e) - v(w)}{v(r) - v(w)}$$

(b) Expansion

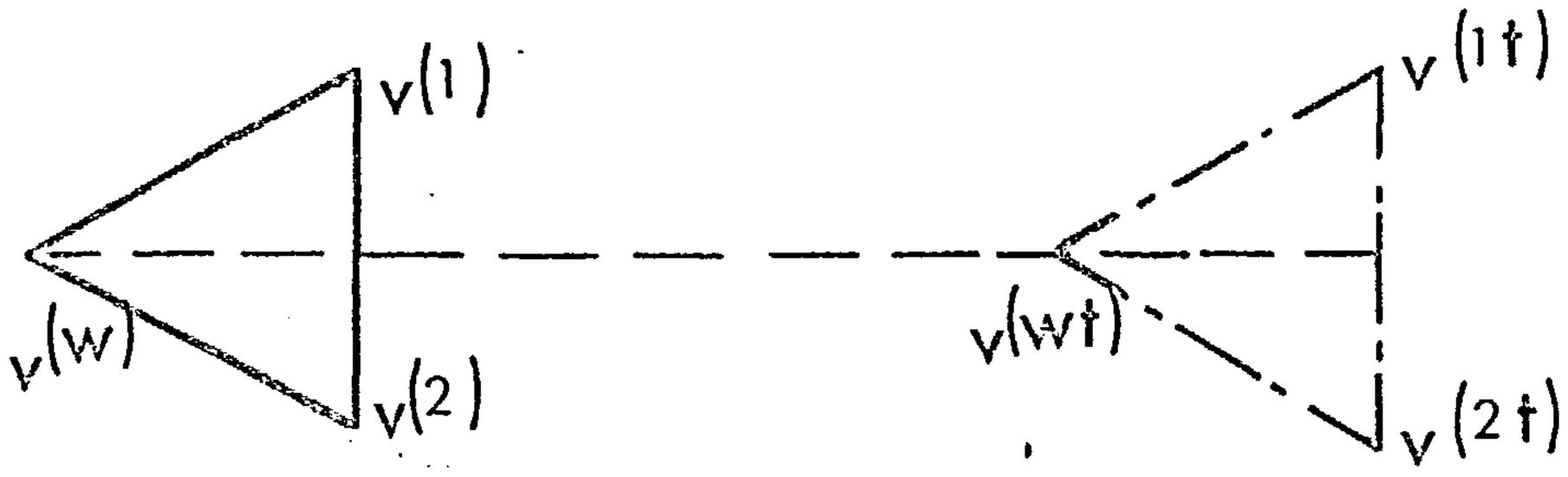

(c) Translation

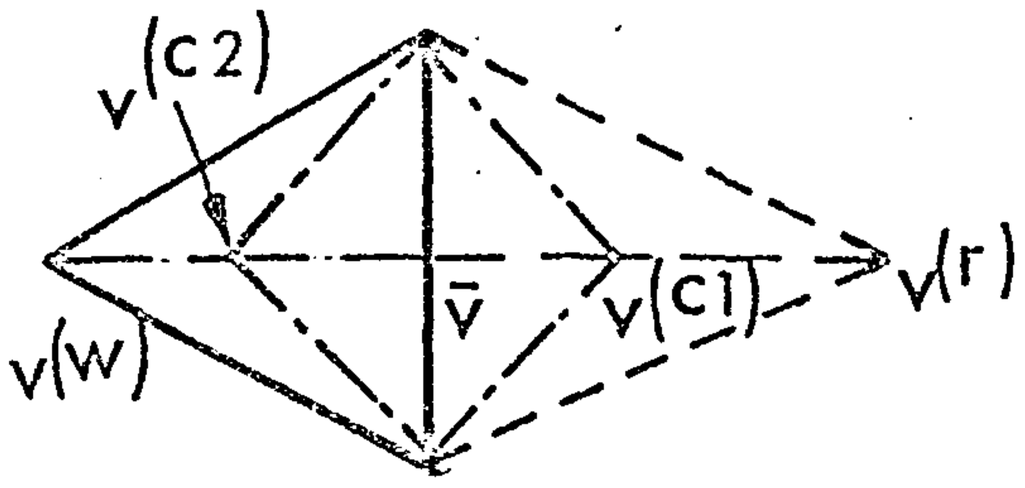

If $F(r) < F(w)$, then $v(w) \rightarrow v(c1)$

If $F(r) \geq F(w)$, then $v(w) \rightarrow v(c2)$

$$\delta = \frac{v(c1) - \bar{v}}{v(r) - \bar{v}} \text{ or } \frac{v(c2) - \bar{v}}{v(w) - \bar{v}}$$

(d) Contraction

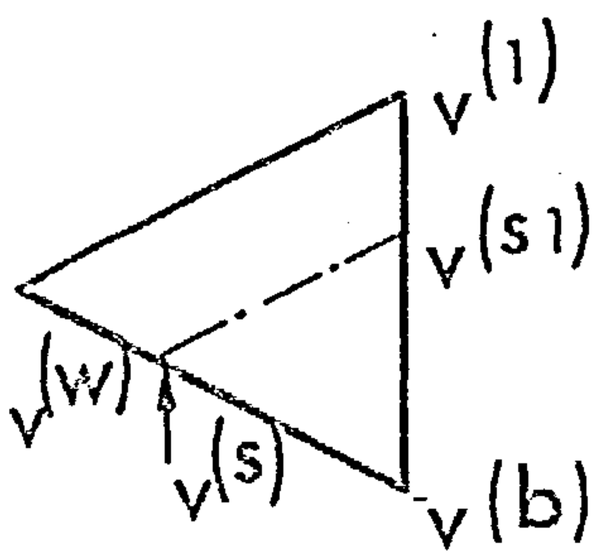

$$v(w) \rightarrow v(s), \quad v(1) \rightarrow v(s1)$$

$$\zeta = \frac{v(b) - v(s)}{v(w) - v(b)}$$

(e) Shrinkage

FIGURE 6·3 SIMPLEX OPERATIONS

an iteration. In each iteration, the worst vertex, i.e. the vertex having the highest value of the objective function, is replaced.

(i) Vertex ordering

In the first stage, the vertices are ordered so that

$$F^{(w)} > F^{(w-1)} > \ldots > F^{(b)} \qquad (6.17)$$

where $F^{(w)}$ is the value of the objective function for the worst vertex with co-ordinates $v^{(w)}$

$F^{(b)}$ is the value for the best vertex with co-ordinates $v^{(b)}$

(ii) Trial values

A new set of values is calculated by reflecting the worst vertex about the centroid of the other values. Thus

$$v^{(r)} = \alpha\bar{v} + (1-\alpha)\, v^{(w)} \qquad (6.18)$$

where α is the reflection coefficient,

$\bar{v}$ is the centroid of all $v^{(i)}$ excluding $v^{(w)}$ and is given by

$$\bar{v} = \frac{1}{n} \sum_{\substack{i=1 \\ i \neq w}}^{n+1} v^{(i)} \qquad (6.19)$$

The associated objective function value, $F^{(r)}$, is then calculated and, depending on that value, one or more of the following operations ensues.

(iii) Replacement

(a) Reflection

If $F^{(w-1)} > F^{(r)} \geq F^{(b)}$, $v^{(w)}$ is replaced by $v^{(r)}$ as illustrated in Figure 6.3a for a two-variable problem for which the simplex has three vertices.

(b) Expansion

If $F^{(r)} < F^{(b)}$, then $F^{(e)}$ is calculated where

$$v^{(e)} = \beta v^{(r)} + (1-\beta)\, v^{(w)} \qquad (6.20)$$

β is the expansion coefficient

If $F^{(e)} \geq F^{(r)}$, then $v^{(w)}$ is replaced by $v^{(r)}$, If $F^{(e)} < F^{(r)}$, then the calculation is repeated with $v^{(e)}$ being substituted for $v^{(r)}$ in equation (6.20) until the objective function starts to increase. Control then passes to the next operation.

(c) Translation

If the lowest value found during expansion is $F^{(\ell)}$ then if $F^{(\ell)} > \gamma.F^{(b)}$, where γ is the translation coefficient, $v^{(w)}$ is replaced by $v^{(\ell)}$ as illustrated in Figure 6.3b. If $F^{(\ell)} \leq \gamma.F^{(b)}$, the complete simplex is translated to the new position as shown in Figure 6.3c. This prevents the simplex from becoming too elongated but it involves re-calculating the objective function for all of the vertices. The larger the number of vertices, i.e. optimization variables, the longer this operation takes and the translation coefficient should be correspondingly small.

(d) Contraction

If, at stage (ii), $F^{(r)} \geq F^{(w-1)}$, a comparison is made between $F^{(r)}$ and $F^{(w)}$. If $F^{(r)} < F^{(w)}$, then $v^{(c)}$ is calculated using

$$v^{(c)} = (1-\delta)\bar{v} + \delta.v^{(r)} \qquad (6.21)$$

where δ is the contraction coefficient.
If $F^{(r)} \geq F^{(w)}$, then $v^{(w)}$ is used instead of $v^{(r)}$ as follows.

$$v^{(c)} = (1-\delta)\bar{v} + \delta.v^{(w)} \qquad (6.22)$$

In either case, if $F^{(c)} < F^{(w)}$, $v^{(w)}$ is replaced by $v^{(c)}$ as shown in Figure 6.3d. If $F^{(c)} \geq F^{(w)}$, the next operation is invoked.

(e) Shrinkage

If the contraction move fails, the complete simplex is retracted towards the best vertex as shown in Figure 6.3e. The new values are calculated using

$$v^{(e)} = \zeta v^{(i)} + (1-\zeta)v^{(b)} \qquad (6.23)$$

where ζ is the shrinkage coefficient.
Again, the objective function must be re-calculated for all of the vertices.

(iv) Convergence

After each iteration, the simplex may be tested for convergence at the discretion of the user. If convergence has not been achieved, the next iteration is started at stage (i). The user is also free to prescribe the values of the coefficients to be used in the various operations as described in Appendix B3.4. The default values correspond to those recommended by Parkinson and Hutchinson {6.8}.

6.4.4. Convergence Criteria

A set of criteria are used to cater for different circumstances. The tests are carried out in the following order.

(i) Excessive Number of Iterations

If the number of iterations exceeds a user-prescribed number (see Appendix B3.5), the program stops.

(ii) Acceptable Value of Objective Function

If $F^{(b)}$ is less than a user-prescribed value, the program assumes that success has been achieved.

(iii) Simplex has Converged to a Minimum

This test is carried out in two stages :

(a) If $F^{(w)} - F^{(b)} > \varepsilon.F^{(b)}$, continue with next iteration. If not, apply test (b).

(b) The simplex is assumed to have converged if

either $$|v_i^{(w)} - v_i^{(b)}| \leq \varepsilon.|v_i^{(b)}| \qquad (6.24)$$

or $$|v_i^{(b)}| \leq \varepsilon$$

for all $i(=1,2,....,n)$ where ε is a small constant. This test becomes more stringent as the value of the objective function decreases.

6.5 COMMENT

One of the most popular methods which does not require the calculation of derivatives is that by Powell {6.11} . This method (as implemented in the

NAG Library {6.4}) and the chosen simplex method were both used to determine the dimensions for the brake-reaction links described in Chapter 8. There were four optimization variables and the only constraints were those of loop closure. The results are given in Table 6.1.

Table 6.1 Comparison of Simplex and Powell Algorithms

Method	Value of Objective Function	Cpu Time, secs
Simplex	28.66	2.31
Powell	28.71	5.8

The simplex method is robust so that its operation is unaffected if values are altered when constraints are transgressed. This approach cannot be used with Powell's method as this searches along conjugate directions and changing the values would destroy the conjugacy.

Smith and Reed {6.12} have compared Powell's method with the complex method of Box {6.9} and conclude that the complex method is preferable for linkage synthesis in the presence of both implicit and explicit constraints. The simplex method used here can be readily changed to the complex method if explicit constraints on link dimensions prove a problem.

Dixon {6.13} proposed combining the simplex method with a quadratic hill-climbing technique but in the light of later experience does not recommend its use for more than four optimization variables {6.14}. Although the examples above contain only four and two variables respectively, Parkinson and Hutchinson {6.15} have shown that the competitiveness of the simplex method improves as the dimensionality of the problem increases.

One other advantage of the simplex direct search method is that the objective function is calculated for points scattered throughout the space corresponding to

the optimization variables. This increases the likelihood of finding the global minimum rather than the nearest local minimum to which gradient methods often converge.

One of the main changes to the simplex method, which has been made in the present work, is the action that is taken when any of the operations results in a linkage that violates the constraints. The program attempts to satisfy the constraints by changing the values of the pair of optimization variables that represent the lengths of the links forming the current undetermined dyad. This may not be possible. For example, it may result in contradictory changes such as lengthening the links at one point in the cycle and shortening them at another. The action then taken depends on the current operation. If this is either a reflection or a contraction, the program tests whether the centroid of the simplex, excluding the worst vertex, represents a feasible linkage. If so, the vertex under consideration is moved towards the centroid. Otherwise it is moved towards the best vertex. When the operation is an expansion, the attempted move is abandoned and the result of the previous operation is adopted. For translation and shrinkage operations, the vertex is moved towards the best vertex.

Summary

After making a distinction between parameters and variables, an objective function that is suitable for kinematic synthesis is defined. The theory to cater for the non-linear constraints of loop closure and transmission angle is then developed in detail. The reasons for choosing the Simplex, direct-search algorithm are given and are followed by a description of its operation. After a comparison with an alternative algorithm, the chapter concludes with a discussion of how the Simplex algorithm has been developed to operate with the non-linear constraints.

7. PSALM

7.1 SCOPE

The foregoing theory has been incorporated into a computer program called PSALM - Program for the Synthesis and Analysis of Linkage Mechanisms. PSALM is applicable to those single degree-of-freedom, planar linkages having revolute and prismatic joints which consist of a basic unit and additional dyads (see Section 3.3). It is assumed that the linkage has :

a) rigid links,
b) no clearance at the joints,
c) a pivoted input link with a prescribed motion.

The basis of PSALM depends on the definition of the linkage in terms of a number of loops, each of which contains not more than two undetermined links which must be connected together (see Section 4.3). If the topology of a linkage can be prescribed in this manner, the program will either :

(i) calculate the displacement of any point or link in the linkage at prescribed positions of the input link using the theory in Section 5.2, or

(ii) determine the optimal dimensions of the links so as to achieve a required function, motion or path output (see Section 6.2) subject to constraints of loop closure, transmission angle and, maybe, link dimensions (see Section 6.3) using the method given in Section 6.4.

In writing PSALM, the aim has been to produce a program that is easy to use and efficient whilst providing the flexibility required for research. To this end, default values are provided for many of the input data parameters (which are defined in Appendix B) and the structure of the program is modular so that alternative

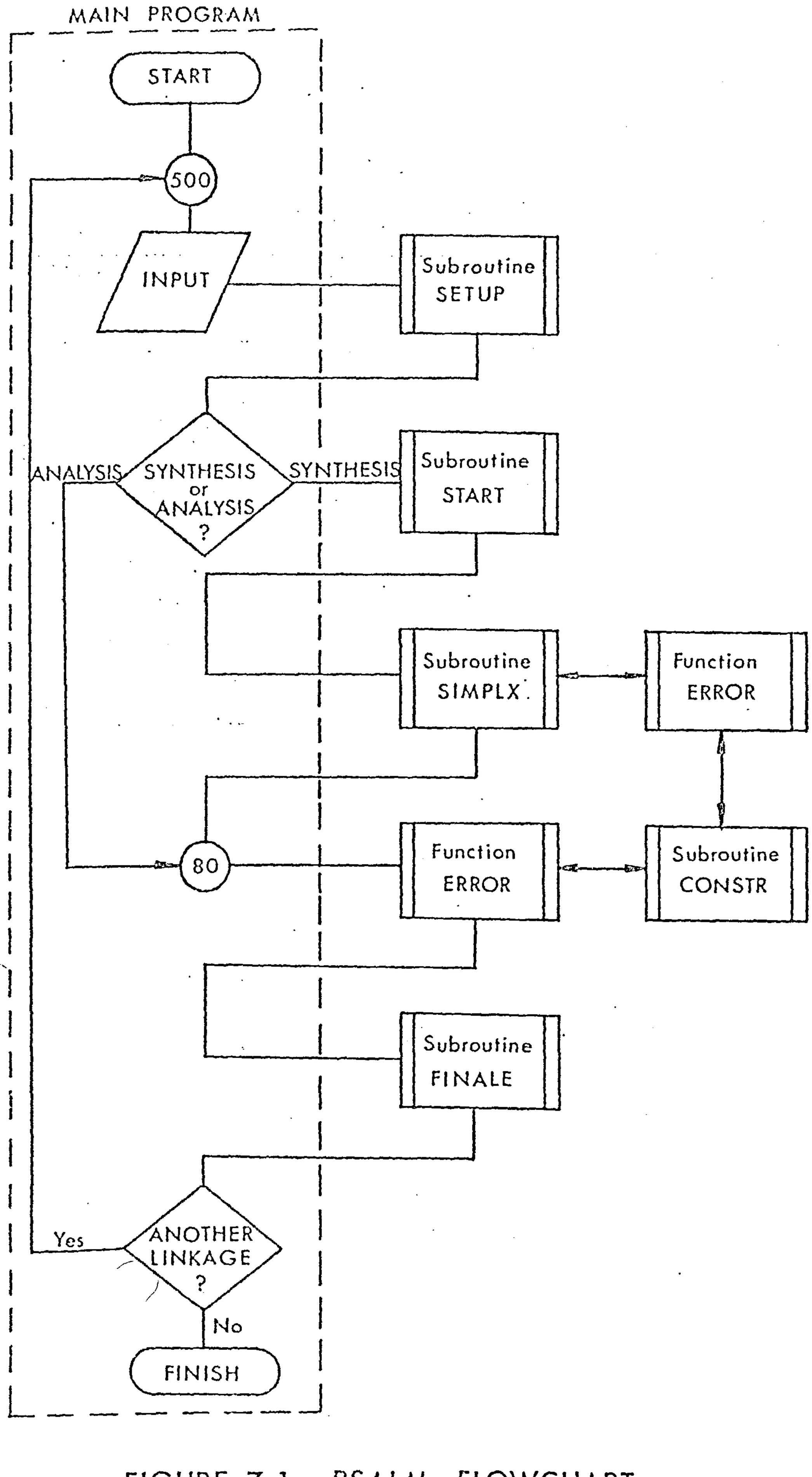

FIGURE 7·1 PSALM FLOWCHART

techniques could be incorporated without too much disruption of the program.

7.2 CODING

7.2.1 Language

PSALM consists of a main program and six subprograms as shown in Figure 7.1. It is written in standard Fortran IV with two exceptions. Firstly, all real (non-integer) numbers are in double precision which is specified by IMPLICIT statements as the program has been developed on an IBM 370 computer. Secondly, most of the input data is read in in the main program using NAMELIST statements. Words are included with the numbers which improves comprehension.

7.2.2 Namelist

Since NAMELIST statements are non-standard, a brief description follows. The data is divided into data sets, each of which is given a different name. PSALM uses three data sets called LINKS, METHOD and LIMITS. They are associated with topology, optimization and constraints respectively and details are given in Appendix B. Each data set consists of one or more records. Typically a record will take the form of a punched card or a line in a file. Each record contains data items which consist of a parameter name and one or more associated values. Items may be entered in any order within a data set.

The first character of each record must be a blank. The remainder of the first record of a set takes the form :

```
&name parameter1=value,parameter2=value,.....
```

where 'name' is the name given to the data set, e.g. LINKS. It is followed by a blank and appears only on the first record. 'Parameter' may be an array name, in which case 'value' should consist of sufficient entries to fill the array. Each record must end with a value followed by a comma, apart from the last record for the set. This must terminate with &END with a space between the last value and the ampersand.

One advantage is that the user need only supply values for those parameters which are used in a particular run. In addition, default values are included in the main program and the user can utilize any of those values merely by not entering that data item.

7.2.3 Operation

The main program controls the sequence of operations. After the input data has been read in, subroutine SETUP is called to translate the topological information (see Appendix B2) into a form that is more suitable for the kinematic subprogram ERROR (see Appendix C). In addition, SETUP establishes the correspondence between the linkage parameters and any optimization variables (see Section 6.1 and Appendix B3.1) so that there is a rapid transfer of data between the optimization subroutine SIMPLX and ERROR. At the same time, SETUP checks for consistency of the input data wherever possible. This aspect is considered in more detail in Section 7.3.

If there are no optimization variables, the program jumps to statement number 80 from which the function subprogram ERROR is called. This sets up and solves the kinematic equations for each loop in turn at the prescribed positions of the input link to determine the angular position of the output link or the co-ordinates of the output point.

Alternatively, when there are some optimization variables, subroutine START is called either to read in or to generate the values required for the initial simplex (see Section 6.4.2). As each set of co-ordinates, i.e. values of the optimization variables, becomes available, the objective function is calculated and written to a data file together with the associated co-ordinates. The subroutine RANDU {7.1} has been incorporated into START to generate random numbers as

necessary. It is specific to computers with the same word size as IBM360-370 computers and will produce 2^{29} terms before repeating. An integer initiates each sequence of random numbers. The integer at the start of each set of co-ordinates is printed out. Together with the co-ordinate values written to the file, this enables a run to be interrupted and restarted without repetition.

The optimization subroutine, SIMPLX, then minimizes the objective function (see Section 6.2) which is calculated in the subprogram ERROR taking into account any weighting. The current version of SIMPLX was developed from the corresponding routine given by Youssef {7.2}.

If any of the constraints are violated, subroutine CONSTR is called to change the values of the appropriate optimization variables if this is possible. If the constraints concerned are bounds on the link dimensions, this is straightforward. However, if the relevant constraints are those of loop closure and transmission angle, the procedure is more complicated. The expressions in Section 6.3 hold only for a given position of the input link. Consequently, when the input link is indexed to the next prescribed position, the same constraint may be violated again even though the values of the relevant optimization variables were changed to suit the previous position. Accordingly, once one of these constraints is transgressed, calculation of the objective function is suspended. The loops in the linkage up to and including the loop that contains the offending dyad are analysed at each of the prescribed positions of the input link and the values of the one or two variables concerned adjusted as necessary. Sometimes mutually exclusive conditions are met. For example, in order to satisfy the loop closure or transmission angle constraints, a given arc may have to be lengthened at one position and shortened at another. Alternatively, either of these actions may violate any bounds on the length of that arc.

TEN-BAR NEEDLE LINKAGE

ARRAY OF ARC LENGTHS,ARCL

L1	L2	L3	L4	L5	L6
19.000	95.000	104.500	112.468	0.0	0.0
19.000	105.000	31.000	110.064	0.0	0.0
19.000	105.000	61.000	12.500	24.000	112.468
19.000	105.000	61.000	245.500	85.000	352.715

ARRAY OF ARC ANGLES,GAMA

G1	G2	G3	G4	G5	G6
0.0	0.0	0.0	238.359	0.0	0.0
0.0	0.0	0.0	33.593	0.0	0.0
0.0	0.0	0.0	0.0	47.384	0.0
0.0	0.0	0.0	0.0	0.0	20.443

THE REFERENCE CRANK ANGLE
180.000
POLAR CO-ORDINATES (LENGTH,ANGLE) OF
INPUT PIVOT 0.0 0.0
OUTPUT LINK 121.600 131.6893
OUTPUT ARC IS MEASURED FROM THE FINISH OF ARC 5 IN LOOP 4

INPUT PIVOT (X,Y)
0.0 0.0
ARRAY OF LINK X DIMENSIONS,XLINK

L1	L2	L3	L4	L5	L6
19.000	95.000	104.500	59.000	0.0	0.0
19.000	105.000	31.000	-3.750	0.0	0.0
19.000	105.000	61.000	12.500	16.250	59.000
19.000	105.000	61.000	245.500	85.000	68.500

ARRAY OF LINK Y DIMENSIONS,YLINK

L1	L2	L3	L4	L5	L6
0.0	0.0	0.0	95.750	0.0	0.0
0.0	0.0	0.0	110.000	0.0	0.0
0.0	0.0	0.0	0.0	17.662	95.750
0.0	0.0	0.0	0.0	0.0	346.000

OUTPUT LINK (X,Y)
-80.875 90.806

CRANK ANGLE	DESIRED ANGLE	ACTUAL ANGLE	ERROR
180.0000	149.9900	150.0895	-0.9952564D-01
165.0000	150.7000	150.9822	-0.2822028
150.0000	150.9600	151.0511	-0.9110027D-01
135.0000	150.5600	150.2382	0.3218115
120.0000	149.3500	148.8832	0.4668423
90.00000	146.4600	146.3305	0.1294986
60.00000	145.5800	145.1543	0.4256596
45.00000	145.5500	145.1043	0.4457206
30.00000	145.5500	145.2963	0.2536952
15.00000	145.5500	145.4760	0.7402939D-01
345.0000	145.2700	144.8644	0.4056288
330.0000	144.8500	144.2441	0.6058859
315.0000	144.3300	143.9171	0.4129023
309.0000	144.2300	143.9312	0.2987571
300.0000	144.4000	144.1132	0.2867810
285.0000	144.6800	144.7241	-0.4413467D-01
270.0000	145.8500	145.3991	0.4509391
255.0000	146.1700	145.8676	0.3023922
240.0000	146.2300	146.2187	0.1131700D-01
210.0000	147.2000	147.5994	-0.3994360

TOTAL ERROR
5.698467

FIGURE 7·2 SYNTHESIS RESULTS

In such cases, all of the values associated with that vertex are moved one quarter of the distance towards a feasible linkage (see Section 6.5).. Once this is complete, calculation of the objective function is restarted with the input link reset to its initial position. The linkage could still violate the constraints at positions of the input link in between those prescribed. Thus either the limiting values should be set on the safe side or the final linkage should be checked throughout the motion of the input link. The linkage is checked automatically at one degree increments of the input link position if the plotting parameter is used (see Appendix B4.4).

The progress of the optimization may be printed out at intervals at the discretion of the user (see Appendix B4.3). If the optimization routine performs a prescribed number of iterations without either reducing the error to an acceptable value or converging to a minimum,the current values will be written to a file so that the program may be re-started with those values as initial values. Otherwise the kinematic subprogram ERROR will be called to calculate the kinematics using the link dimensions that give the least value of the objective function.

At the end of any successful run (either synthesis or analysis), subroutine FINALE is called to print out the linkage details as well as the required output positions, the actual positions and the errors in a tabular format as shown in Figure 7.2. The link dimensions are printed out in both polar and Cartesian form. The former corresponds to that of the input data whilst the latter is more suitable for manufacturing purposes and for dynamic analysis using the DRAM program {7.3}. If a graphic output is required, linkage output values may be stored in a data file for subsequent use in a conversational plotting program.

Finally, the program checks whether another linkage is to be read in and, if so, repeats the procedure. Otherwise it stops.

7.2.4 Input/Output Devices

Usually all of the input data is read in from device 5. However, if values from an earlier run are to provide some, or all, of the co-ordinates for the initial simplex, these values are read in from device 4.

The results from a run (Figure 7.2) and any error messages are written to device 6. The co-ordinates and objective function values for the initial simplex and the final simplex are written to device 7. They are then available for re-use as input data for a later run. All of the information (apart from any error messages) that provides a check on the input data (see Section 7.3) is written to device 8. Any information required for subsequent plotting is written to device 9. The remainder of the information is written to devices 1 and 2. The starting integer for the sequence of random numbers to generate the co-ordinates of a vertex for the initial simplex is written to device 1. If the generated co-ordinates violate the constraints, subroutine CONSTR will be called to modify them. The corresponding set of acceptable values, together with the value of the objective function, is written to device 7. Notification that this has occurred is written to device 1. It is followed by reports on the progress of the optimization and loop closure and transmission angle violations (see Appendix B4.3). On device 2 are written the limits within which the initial simplex will be generated and the subsequent sets of co-ordinates (before any modification that may prove to be necessary).

7.2.5 Efficiency and Size

A conscious effort has been made to produce an efficient coding. For example, in addition to keeping the number of calculations within DO-loops to a minimum, variables are passed between subroutines via COMMON rather than as arguments. Also the co-ordinates which

define the simplex are stored sequentially, vertex by vertex, in a one-dimensional array. A pointer is then used to mark the start of each set. As mentioned previously, the correspondence between these co-ordinates and the linkage parameters is established at the outset in the subroutine SETUP so that a simple table look-up procedure may be used once optimization is under way.

Which subprograms have the greatest effect on the execution time (and so should be the most efficient) was determined in the following way. The program was compiled using the IBM Fortran IV G compiler and then run with two sets of data. The first set corresponded to analysing the six-bar linkage in Figure 5.5 for 180 positions of the input link and the second resulted in 357 iterations for a ten-bar linkage with 16 optimization variables. The runs were analysed using *TIMETALLY which periodically inspects the computer to determine the current operation. The results are given in Table 7.1

Table 7.1 Time in Each Subprogram as a Percentage of the Total cpu Time.

Subprogram	Analysis of Six-bar Linkage	Synthesis of Ten-bar Linkage
MAIN	8.22	0.34
SETUP	0.0	0.02
START	0.0	0.01
SIMPLX	0.0	2.81
CONSTR	0.0	0.21
ERROR	46.28	81.74
FINALE	23.14	3.60
(System)	22.36	11.27
Total cpu time, s	0.523	37.625

The input to MAIN and the output from FINALE are slightly greater for the synthesis run. However they occupy a much smaller proportion of the run time since the synthesis run is over seventy times longer than the

```
*** PSALM,DEC.1976 ***

          TEN-BAR NEEDLE LINKAGE

  MOTION  NLOOP  MAXARC ILKOUT INGOUT  ICRK  IORIG  KTHETA IPLOT
     1       4       6       0       1       1       0       0       1
ARRAY OF ARC LENGTHS,ARCL
    19.000    95.000   104.500   112.468     0.0       0.0
    19.000   105.000    31.000   110.064     0.0       0.0
    19.000   105.000    61.000    12.500    24.000   112.468
    19.000   105.000    61.000   245.500    85.000   352.715
ARRAY OF ARC ANGLES,GAMA
     0.0       0.0       0.0     238.359     0.0       0.0
     0.0       0.0       0.0      33.593     0.0       0.0
     0.0       0.0       0.0       0.0      47.384     0.0
     0.0       0.0       0.0       0.0       0.0      20.442
THE REFERENCE CRANK ANGLE
   180.000
POLAR CO-ORDINATES (LENGTH,ANGLE) OF
INPUT PIVOT          0.0       0.0
OUTPUT ARC       121.6003  131.6893
OUTPUT ARC IS MEASURED FROM THE FINISH OF ARC  5 IN LOOP  4

NUMBER OF DESIRED POSITIONS,NDES =  20
THE DESIRED OUTPUT ANGLE
  149.9900      150.7000      150.9600      150.5600      149.3500
  146.4600      145.5800      145.5500      145.5500      145.5500
  145.2700      144.8500      144.3300      144.2300      144.4000
  144.6800      145.8500      146.1700      146.2300      147.2000
WEIGHTING FACTORS FOR THE VALUES ABOVE
  1.000000      1.000000      1.000000      1.000000      1.000000
  1.000000      1.000000      10.00000      1.000000      10.00000
  1.000000      1.000000      1.000000      1.000000      1.000000
  5.000000      5.000000      10.00000      10.00000      1.000000
THE DESIRED CRANK INPUT ANGLE
 0.0           -15.00000     -30.00000     -45.00000     -60.00000
 -90.00000     -120.0000     -135.0000     -150.0000     -165.0000
 -195.0000     -210.0000     -225.0000     -231.0000     -240.0000
 -255.0000     -270.0000     -285.0000     -300.0000     -330.0000

TOPOLOGICAL ARRAY,ILINK
  1  2  3  4  0  0
  1  2  3 -4  0  0
  1  2 -3 -4 -3  4
  1  2  3 -4 -5 -4
TOPOLOGICAL ARRAY,ILOOP
  1  0  0  1  0  0
  1  0  0  1  0  0
  1  2  0  0  1  1
  1  2  3  0  0  1
ARRAY OF VARIABLE ARC LENGTHS,IVA
  0  1  1  1  0  0
  0  1  1  1  0  0
  0  0  1  1  1  0
  0  0  0  1  1  0
ARRAY OF VARIABLE ARC ANGLES,IVG
  0  0  0  1  0  0
  0  0  0  1  0  0
  0  0  0  0  1  0
  0  0  0  0  0  0
```

FIGURE 7·3 ANNOTATED INPUT DATA

analysis run. Thus, if we discount the time for input and output, the remarkable feature of both runs is the high proportion of time spent in calculating the kinematics in ERROR. Therefore any attempt to improve the speed of the program should be aimed at either speeding up the calculation of the kinematics or, in the case of optimization, reducing the number of times the objective function is calculated.

PSALM contains 1412 statements. With the comment cards which are interspersed through the program, the source program is 1966 lines long. When compiled using WATFIV, the object code requires 62K bytes and the arrays a further 36K bytes. When the IBM Fortran IVG compiler is used, the object code requirement is reduced to 40K bytes. The array requirement can be reduced by a quarter if the following reductions are made in the maximum values of :

a) number of desired positions, 181 to 41,
b) product of number of loops and arcs within a loop, 100 to 42,
c) number of optimization variables, 30 to 25.

With these reductions, the program might just operate in a 64K computer without overlaying.

7.3 DATA CHECKING

There is a possibility with any program, but more so with a general program, that a mistake in the input data will result in a worthless run. To guard against this, several features have been incorporated into PSALM.

Firstly, the input data is printed out in an annotated tabular format as shown in Figure 7.3. In the arrays, each line corresponds to a different loop. This effect is obtained by using variable format statements.

Secondly, as the subroutine SETUP translates the topological data into an intermediate set of arrays that are more suitable for the kinematic subprogram ERROR, it checks for the following inadmissible conditions :

INPUT LINK POSITION 5 ARC LENGTHS AND ANGULAR POSITIONS

L1	L2	L3	L4	L5	L6
24.425	24.390	24.425	24.390	0.0	0.0
9.992	21.975	9.293	4.425	24.390	0.0
9.992	21.975	3.750	13.290	15.000	41.383
41.383	42.000	10.538	35.030	27.000	0.0
T1	T2	T3	T4	T5	T6
120.000	-7.380	-60.000	172.620	0.0	0.0
90.000	0.000	-90.000	-60.000	172.620	0.0
90.000	0.000	0.000	3.614	-81.568	174.442
354.442	98.432	270.000	180.000	270.000	0.0

INPUT LINK POSITION 6 ARC LENGTHS AND ANGULAR POSITIONS

L1	L2	L3	L4	L5	L6
24.425	24.390	24.425	24.390	0.0	0.0
9.992	20.356	10.912	4.425	24.390	0.0
9.992	20.356	3.750	13.290	15.000	41.383
41.383	42.000	9.620	30.542	27.000	0.0
T1	T2	T3	T4	T5	T6
150.000	-7.380	-30.000	172.620	0.0	0.0
90.000	0.000	-90.000	-30.000	172.620	0.0
90.000	0.000	0.000	2.199	-75.316	174.442
354.442	104.684	270.000	180.000	270.000	0.0

INPUT LINK POSITION 7 ARC LENGTHS AND ANGULAR POSITIONS

L1	L2	L3	L4	L5	L6
24.425	24.390	24.425	24.390	0.0	0.0
9.992	19.800	12.557	4.425	24.390	0.0
9.992	19.800	3.750	13.290	15.000	41.383
41.383	42.000	9.184	28.998	27.000	0.0
T1	T2	T3	T4	T5	T6
180.000	0.005	-7.375	172.620	0.0	0.0
90.000	0.000	-90.000	-7.375	172.620	0.0
90.000	0.000	0.000	1.527	-73.128	174.442
354.442	106.872	270.000	180.000	270.000	0.0

INPUT LINK POSITION 8 ARC LENGTHS AND ANGULAR POSITIONS

L1	L2	L3	L4	L5	L6
24.425	24.390	24.425	24.390	0.0	0.0
9.992	19.799	12.559	4.425	24.390	0.0
9.992	19.799	3.750	13.290	15.000	41.383
41.383	42.000	9.184	28.998	27.000	0.0
T1	T2	T3	T4	T5	T6
210.000	30.028	-7.352	172.620	0.0	0.0
90.000	0.000	-90.000	-7.352	172.620	0.0
90.000	0.000	0.000	1.527	-73.127	174.442
354.442	106.873	270.000	180.000	270.000	0.0

INPUT LINK POSITION 9 ARC LENGTHS AND ANGULAR POSITIONS

L1	L2	L3	L4	L5	L6
24.425	24.390	24.425	24.390	0.0	0.0
9.992	19.799	12.561	4.425	24.390	0.0
9.992	19.799	3.750	13.290	15.000	41.383
41.383	42.000	9.184	28.997	27.000	0.0
T1	T2	T3	T4	T5	T6
240.000	60.055	-7.325	172.620	0.0	0.0
90.000	0.000	-90.000	-7.325	172.620	0.0
90.000	0.000	0.000	1.527	-73.126	174.442
354.442	106.874	270.000	180.000	270.000	0.0

FIGURE 7.4 ARC LENGTHS AND ANGULAR POSITIONS

a) there are either too many or too few undetermined arcs,

b) the undetermined arcs are not adjacent within a loop,

c) an arc other than a guide link is common (see Section 4.5) with another arc in the same loop.

If one of these conditions is encountered, the run is stopped after all of the topological data has been checked. When the program is being used for optimization, warning messages are printed out if the following arcs are identified as optimization variables :

(i) identical arcs (see Appendix B3.1),

(ii) sliding links,

(iii) non-existent arcs.

A message is also printed out if arcs are found that are identical apart from being traced in opposite directions. None of these latter conditions is fatal. The intermediate set of arrays is also printed out (see Appendix C).

The most difficult condition to detect is that of incorrect loop closure. This condition is also likely to occur as it depends on a sign convention. Two approaches have been adopted depending on the equipment available. If only alphanumeric facilities, e.g. line-printer, are available, a parameter (see Appendix B4.3) may be set so that the length and angular position of each arc, including sliding links, is printed out for each position of the input link as shown in Figure 7.4. In this case, there should be no optimization variables as it uses a lot of paper. Alternatively, if a graphic terminal is available, the program PICTUR, developed in conjunction with Dr. M.R. Smith, can be used. PICTUR is an amalgam of the relevant parts of PSALM and the plotting routines developed by the author {7.4, 7.5}. Exactly the same input data as for PSALM is supplied to PICTUR and the linkage is then drawn on the screen for each position of the input link. Unfortunately, since the input link pivot is common to all of the loops, this

program cannot be used with a graph plotter as the pen would carve a hole in the paper around the input link pivot. Yet another approach would be to use a printer plot as is done in the DRAM program {7.3}. This can become rather confused if the linkage contains more than a few links.

Another condition which is difficult to check within the program can arise if the desired linkage output is the angular position of a link. In this case, the value of the objective function changes markedly if either the angular position of the frame arc in the first loop or the output arc angle is changed by 360 degrees as this gives an apparent 'error' at the output of the order of 360 degrees for each position of the input link. This condition is best checked for by letting the program run for one iteration and then examining the print-out.

7.4 PROGRAM TESTING

Any computer program must be tested to ensure that it contains no errors. PSALM has been used to analyze linkages that contain examples of all the valid undetermined dyads as listed on page 4-8. The results have been checked by comparison with graphical analyses. The program has been changed where the test runs have indicated that this is necessary. For example, equations (5.14), (5.19) and (5.22) become ill-conditioned if the denominator in the expressions for $\cos\theta_q$ becomes small. Accordingly, PSALM was altered to detect this condition and to use an alternative method when it occurs. In the case of equations (5.14) and (5.19), the alternative method uses the cosine rule to solve the triangle formed by the undetermined dyad. It then adds on the angular position of the pseudo-arc connecting the 'free' ends of the dyad. This approach is more akin to that proposed

by Talbourdet {7.6} but takes longer than the method given in Chapter 5. PSALM has also been used for the synthesis of several linkages as described in the next chapter.

Summary

A computer program called PSALM - Program for the Synthesis and Analysis of Linkage Mechanisms - has been written to satisfy the need identified in earlier chapters. After the scope has been reviewed, the language, structure and operation of the program are given. The time taken by, and the size of, the various parts of the program have been determined. The problems of testing the input data for errors and the program for the conditions where ill-conditioned equations may give erroneous results are then considered in more detail. Apart from the random number generator and part of the optimization routine, the program is completely new.

8. CASE STUDIES

8.1 INTRODUCTION

In addition to testing the individual parts of a computer program, the complete program should be tested to ensure that there is no undesirable interaction between the various parts. For example, the manner in which the constraints are handled may affect the optimization routine. PSALM was used therefore in two case studies which are reported in the following sections. These case studies were chosen to demonstrate the use of PSALM for the kinematic synthesis of linkages for path generation, motion generation and function generation. One case study concerns the synthesis of a completely new linkage whereas the other considers the modification of two existing linkages.

8.2 MOTORCYCLE REAR SUSPENSION

8.2.1 Background

This case study demonstrates the synthesis of a new linkage for the rear suspension of a moto-cross machine. Such machines require a wheel travel of about 250 mm which is much longer than that for a road machine. With a conventional design, the rear road and sprocket wheels are mounted on a swinging arm. This is pivoted on the machine frame some distance behind the gearbox output shaft on which the driving sprocket wheel is mounted. As a result, the centre distance between the sprocket wheels changes as the suspension deflects and there is a danger that the chain will leave the sprocket wheels at maximum wheel deflection when the chain is at its slackest. PSALM was used to synthesize a suspension linkage that avoids this problem. A full account of the various stages in the synthesis is given in Appendix D. Three aspects that provide a comparison between PSALM and other methods are now considered further.

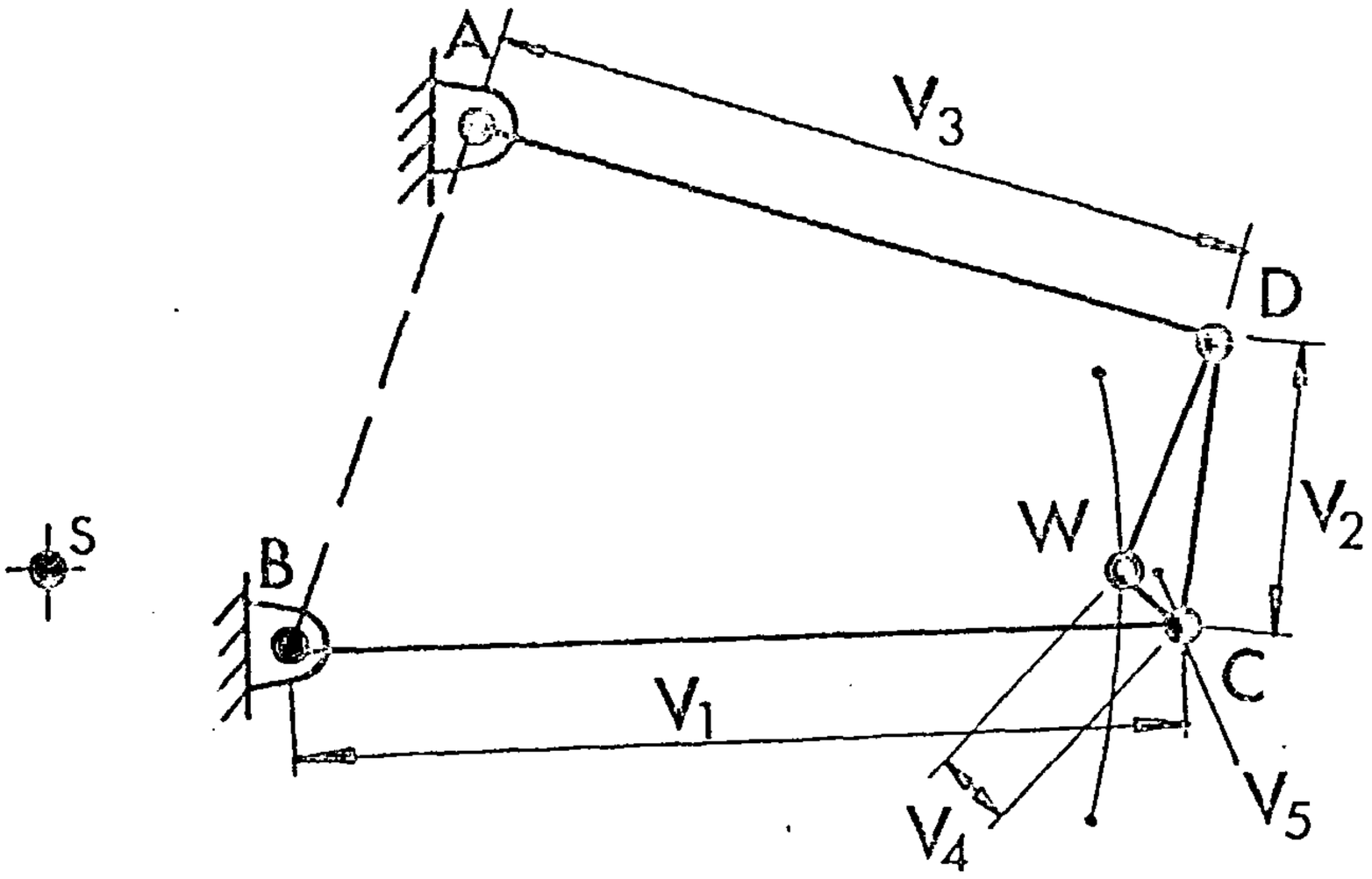

(a) Generation of a Circular Arc

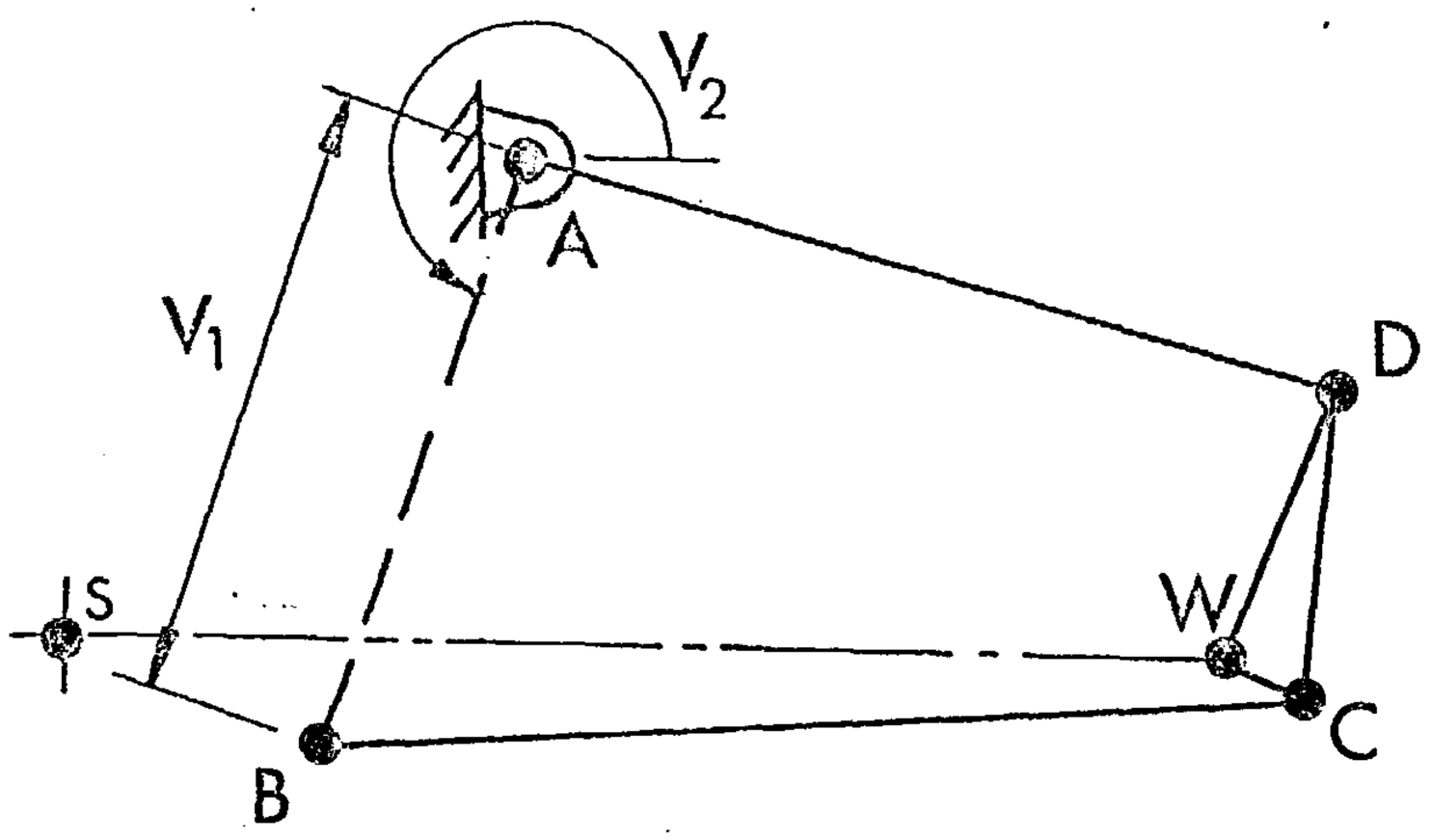

(b) Adjustment for Chain Wear

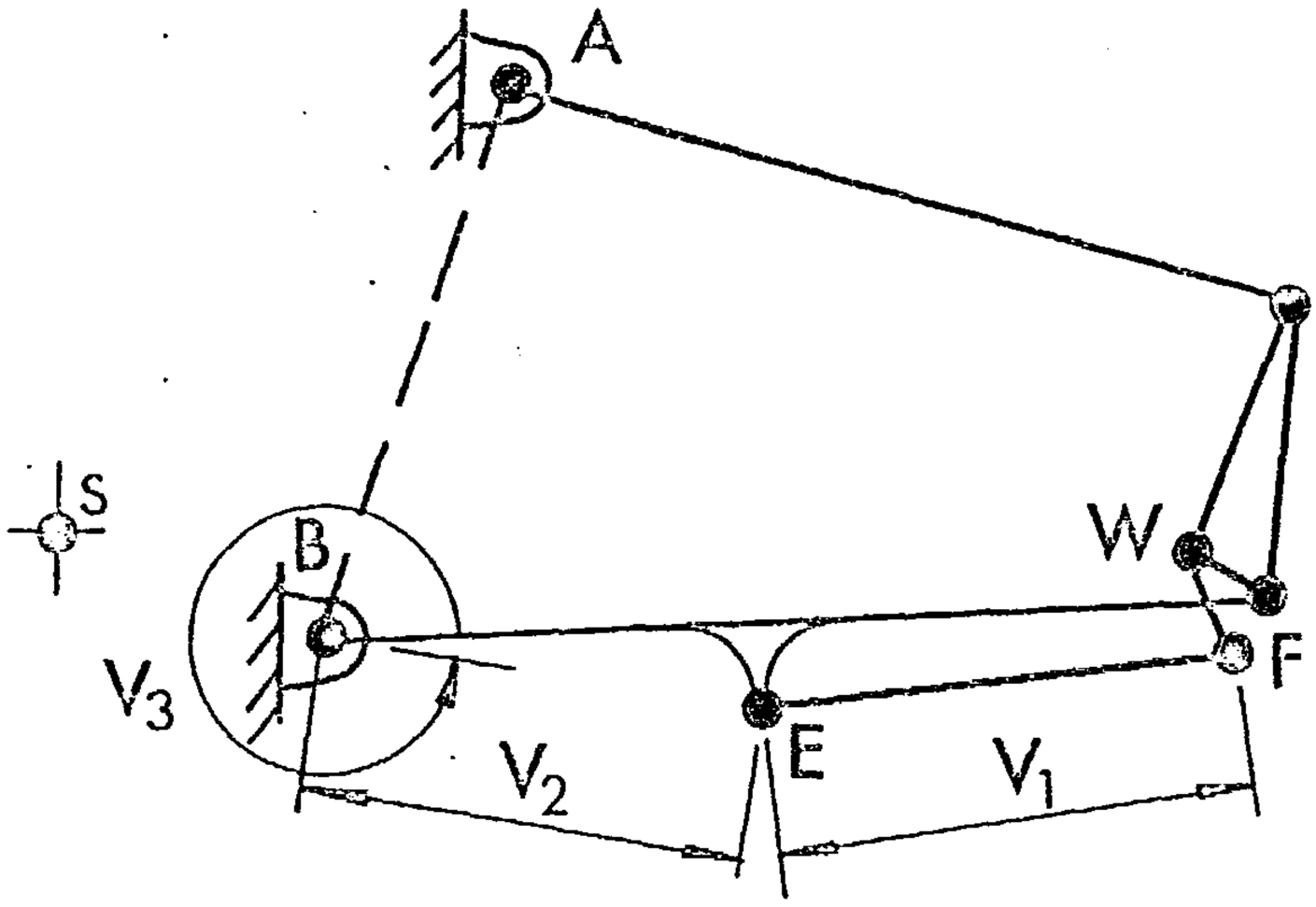

(c) Brake Reaction Linkage

FIGURE 8·1 MOTORCYCLE REAR SUSPENSION

8.2.2 Generation of a Circular Arc

The first stage was the synthesis of a four-bar linkage to generate a circular arc centred on the gearbox output shaft shown at S in Figure 8.1. The moving links were to consist of upper and lower links, AD and BC, pivoted to the machine frame at prescribed mounting points, A and B, and connected by a coupler, CDW. The road wheel was to be attached to the coupler at W. Five dimensions were available as optimization variables as indicated in Figure 8.1a.

Several runs were carried out to cater for different specifications. The initial and final values for a typical run are given in Table 8.1. In reducing the value of the objective function, the program made significant changes in the dimensions of the moving links whilst maintaining the prescribed points of attachment to the frame.

Table 8.1. Synthesis of a Four-bar Linkage

		Initial values	Final values
V_1	Lower link length, mm	530.0	496.9
V_2	Coupler length, mm	125.0	170.2
V_3	Upper link length, mm	425.0	429.2
	Polar co-ordinates of wheel centre		
V_4	- distance from lower link joint, mm	60.0	44.6
V_5	- angular position on coupler, deg	400.0	420.0
	Objective function, mm^2	20013.4	0.2
	Number of iterations		165

Prescribing the frame pivot positions relative to the centre of the circular arc makes it difficult to synthesize the linkage graphically. If a precision point

approach is used, not more than four precision points may be prescribed if the resulting equations are to be solved using a desk calculator. Freudenstein and Sandor {8.1} used a computer to synthesize a four-bar linkage to generate a circular arc of a given radius using five precision points. However, to use this number of precision points, ten dimensions must be variable since each point is defined by two co-ordinates. Prescribing the frame pivot positions fixes four of the dimensions that Freudenstein and Sandor used as variables. Accordingly the maximum number of precision points that could be used in the present example to define the desired arc would be three. There would be no control over the motion between these points. For example, if the Freudenstein and Sandor linkage is scaled to trace a circular arc of radius 610 mm, the variation in the radius is 3.46 mm between the precision points. This quality of arc is maintained over a vertical movement of 610.5 mm. On the other hand, up to 28 positions were used with PSALM which ensured a much closer correspondence overall between the desired and actual motion. With the final linkage, the variation in centre distance over the desired wheel travel of 250 mm is 0.26 mm on a nominal value of 610 mm. This compares with variations over the same travel of 2.0 mm for the scaled Freudenstein and Sandor linkage and 5.39 mm for the conventional design. Thus a much improved arc has been obtained as a result of using PSALM.

8.2.3 Adjustment for Chain Wear

During use, a roller chain wears and so some adjustment must be provided to compensate for this. In the conventional design, the swinging arm is mounted on an eccentric. Accordingly PSALM was used to analyze the effect of mounting the lower link pivot on an eccentric. However the deviations from circularity of the resulting paths of the wheel centre were unacceptably large. PSALM was then used in the synthesis mode to determine the

positions to which the lower link pivot, B, should be moved to give a centre distance 6.5mm shorter than, and longer than, the nominal distance. There were two optimization variables as indicated in Figure 8.1b. The co-ordinates that give the nominal centre distance were used as initial values. The results are given in Table 8.2. The nominal and the other two pivot positions lie on a straight line and so offer a convenient mechanical solution.

Table 8.2 Pivot Adjustment for Chain Wear

	Centre distance, mm Values	603.5		616.5	
		Initial	Final	Initial	Final
V_1	Distance between pivots, mm	325.7	331.7	325.7	320.1
V_2	Relative angular position, deg.	251.4	250.3	251.4	252.5
	Objective function, mm^2	1400.4	0.1	1388.4	0.3
	Number of iterations		40		31

This stage could be tackled graphically. Links SA,AD and CDW, together with the desired centre distance WS, can be considered as a four-bar linkage. If the wheel centre, W, is placed near to one end of its travel and the lower link, BC, is rotated about C, joint B will trace a circular arc. If the process is repeated with W near to the other end of its travel, a second arc will be traced. Where these arcs intersect is the desired position for the frame pivot. However this will guarantee the correct centre distance at the two positions only. In addition, if the corresponding positions of C are close together compared to the length of BC, the arcs will intersect at a small angle so that it would be difficult to determine the point of intersection accurately. Using PSALM, the resulting variation in centre distance is less than 0.4mm.

8.2.4 Brake Reaction Linkage

In addition to maintaining the rear wheel in the correct position for the chain drive, the suspension provides

the torque reaction during braking. In the standard design, the brake reaction is taken by attaching the brake backplate to the swinging arm. If the backplate were anchored directly to the coupler, its possible angular rotation would be much greater than that of the original layout and this could upset the braking performance. To overcome this problem, it was decided to connect the brake backplate to the lower link in such a way that the orientation of the backplate remains constant as the wheel deflects. This effectively converts the four-bar linkage into a six-bar linkage as shown in Figure 8.1c. The length of the backplate, FW, was set at its current value. This left four optimization variables - the three indicated in Figure 8.1c and the angle of the brake reaction linkage to the vertical. The problem is one of motion generation rather than one of path generation as for the previous stages. The initial and final values are given in Table 8.3. The total variation in backplate angle for the final linkage throughout the wheel travel is 3.26 degrees. This is much less than with the standard design.

Table 8.3 Synthesis of Brake Reaction Linkage

		Initial values	Final values
V_1	Connecting link length, mm	211.1	261.2
	Point of attachment to lower link		
V_2	- distance from frame pivot, mm	261.6	238.8
V_3	- angular position, deg	360.0	348.2
V_4	Angle between brake reaction link & the vertical, deg	360.0	337.0
	Total error, deg^2	287.7	28.7
	Number of iterations		74

This is a difficult problem to tackle using other methods as the angle of the brake backplate to the vertical is not prescribed, the requirement is merely that it shall

be constant. However this rather more uncommon inversion of a Watt's six-bar linkage poses no difficulty for PSALM.

8.2.5 Tolerancing

In the account given in Appendix D, PSALM was used to determine the effect of small changes in the length of one link at a time. The user can then decide on suitable tolerances either on the basis of these results alone or by using the algorithm developed by Sutherland and Roth {8.2} which takes the relationship between accuracy and manufacturing costs into account. The corresponding limiting dimensions can be fed into PSALM as limiting values for a complete set of optimization variables. Generating an initial simplex within these limits using the random number generator will then give an indication of the effect of manufacturing errors on the output from the linkage.

8.2.6 Implementation

The convenient lengths of the links and the method of adjusting the position of the lower link pivot offer a very practical linkage. When the quality of the circular arc traced by the wheel centre is considered as well, there is a considerable incentive to adopt the linkage. The problem in implementing it lies in the form design of the links and bearings to give the same unsprung weight and lateral rigidity as the conventional design. This is particularly important for a moto-cross machine which is used on rough ground. This aspect is currently receiving attention from CCM Ltd., Bolton.

8.3. WARP KNITTING MECHANISMS

8.3.1 Background

This case study is concerned with a problem in function generation. A manufacturer of warp knitting machines wished to modify the existing sinker and needle

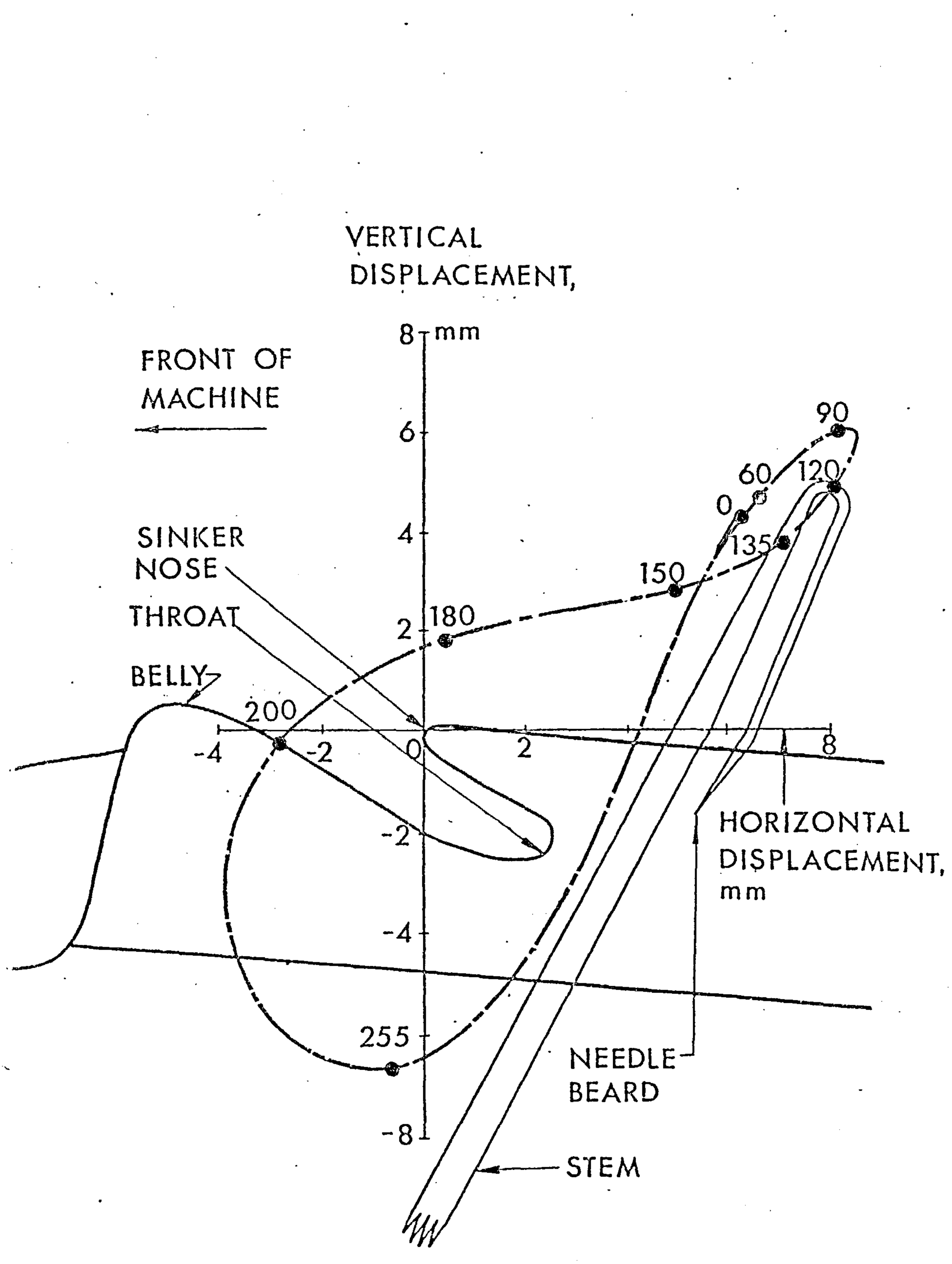

FIGURE 8·2 MOTION OF NEEDLE RELATIVE TO SINKER

mechanisms to provide a better knitting action. These are two of the fundamental mechanisms in the machine as they control the sinkers and needles which co-operate in forming the knitted loops. In a typical machine, the sinkers and needles are spaced evenly at 28 per inch along bars which run the full machine width of 3.3m (130 in).

The active parts of a sinker and needle are shown in Figure 8.2. The needle is of the bearded type invented by Rev. William Lee in 1589. Also shown is the motion of the needle relative to the sinker. The numbers around the curve are the angular positions of the machine crankshaft measured from the start of the knitting cycle and are referred to in the description which follows of the knitting process. At the start of the cycle, the needles are at a mid-height position with loops of yarn wrapped round their stems. They dwell there until 60^{o} while the guide bars (not shown) which carry the yarns swing between the needles from the front of the machine and move sideways one needle pitch behind the needles before returning to the front of the machine. After the guide bars have completed this movement and so wrapped yarns round the needle beards, the needles rise to full height by 90^{o} so that the yarns slip on to the needle stems. The needles then descent and the newly wrapped yarns move inside the beards at 120^{o}. After the needle points have passed the upper edge of the sinker at 135^{o}, the presser (not shown) presses the points into grooves in the stems of the needles. The needles dwell in this position while the sinkers move backwards so that the slope of the sinker belly lifts the old loops; which were lower down the stems of the needles, and lands them on the needle beards (150^{o} - 180^{o}). The presser is then withdrawn and the needles continue to move downwards to pull the wrapped yarns through the old loops. As the needles pass below the level of the sinker at 200^{o}, the old loops slip off the needles and the sinkers begin to move forward. The needles descent further to pull sufficient yarn from the warp beam to form the new loops. The sinkers continue to move forward so that the fabric is held in the sinker throat and is prevented from

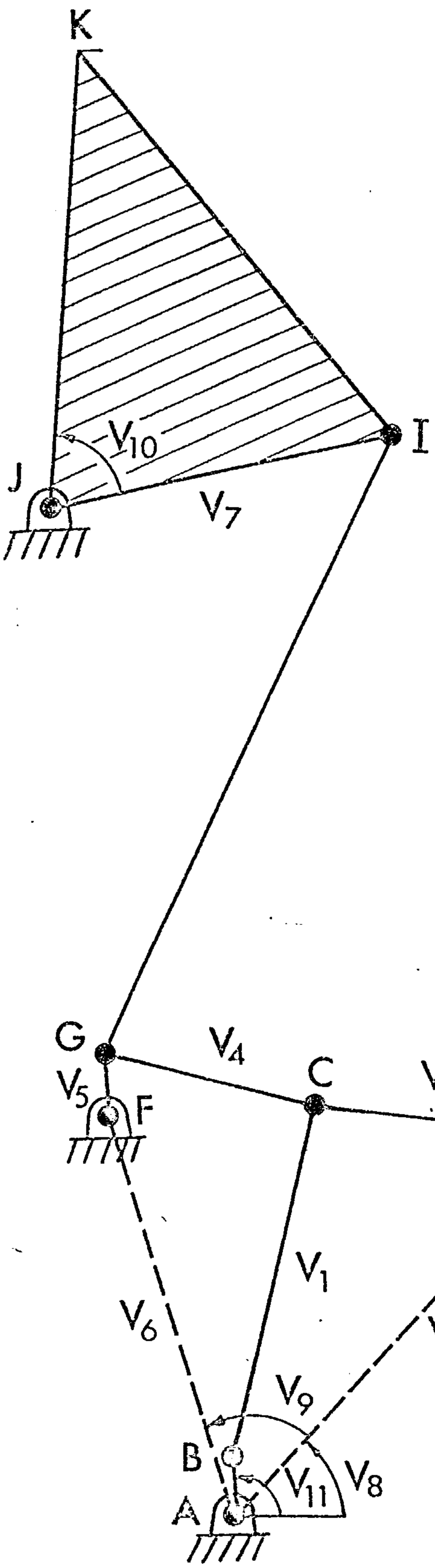

(a) Original Linkage showing Optimization Variables

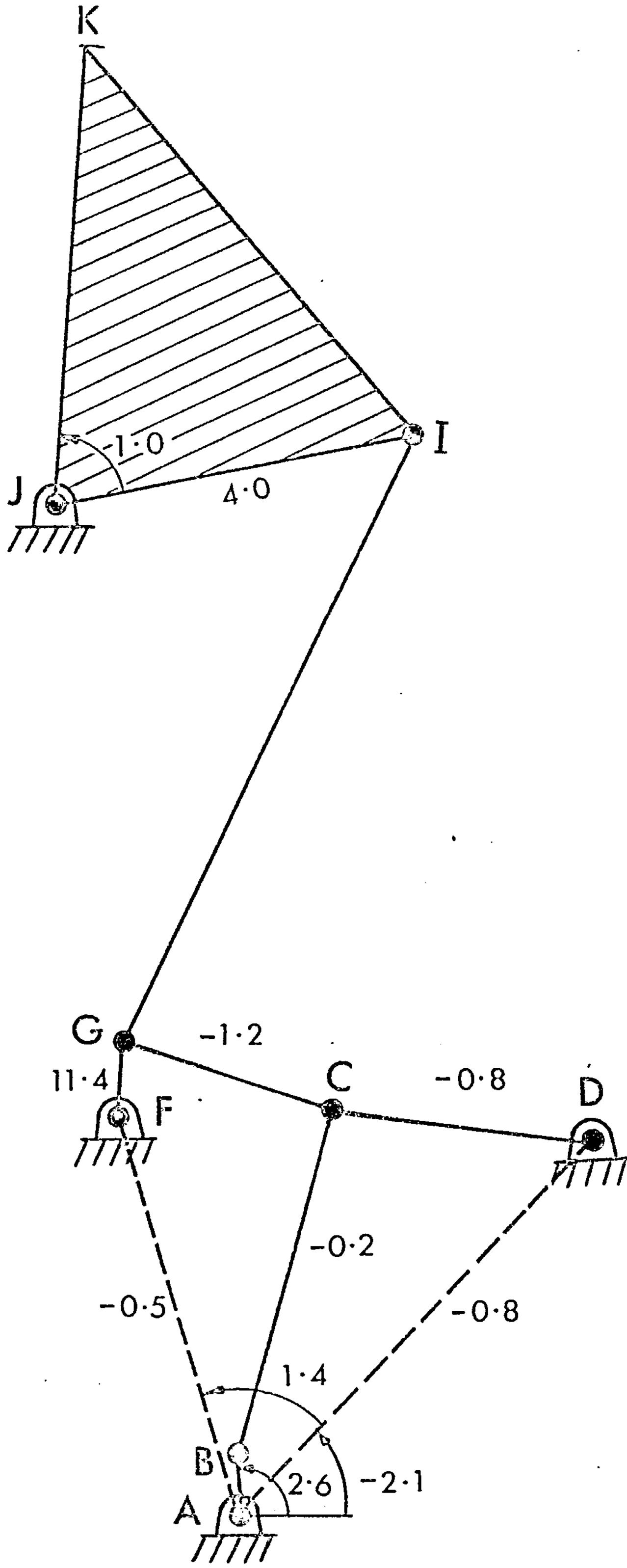

(b) Modified Linkage showing % changes in dimensions

FIGURE 8·3 SINKER MECHANISM

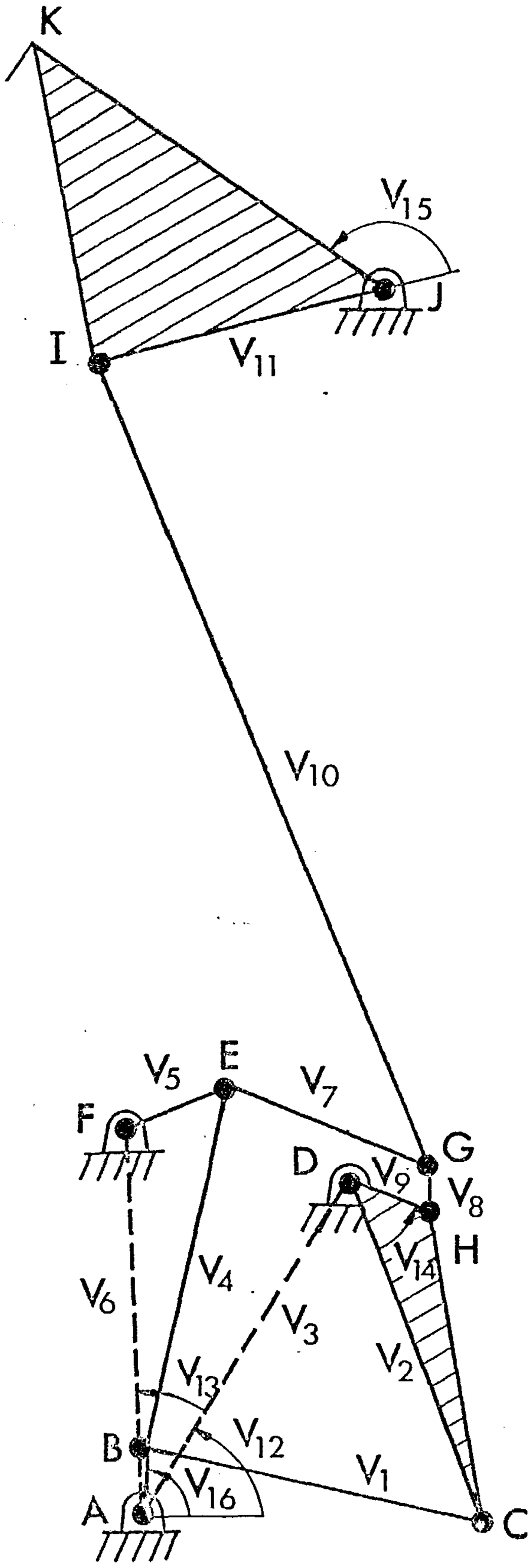

(a) Original Linkage showing Optimization Variables

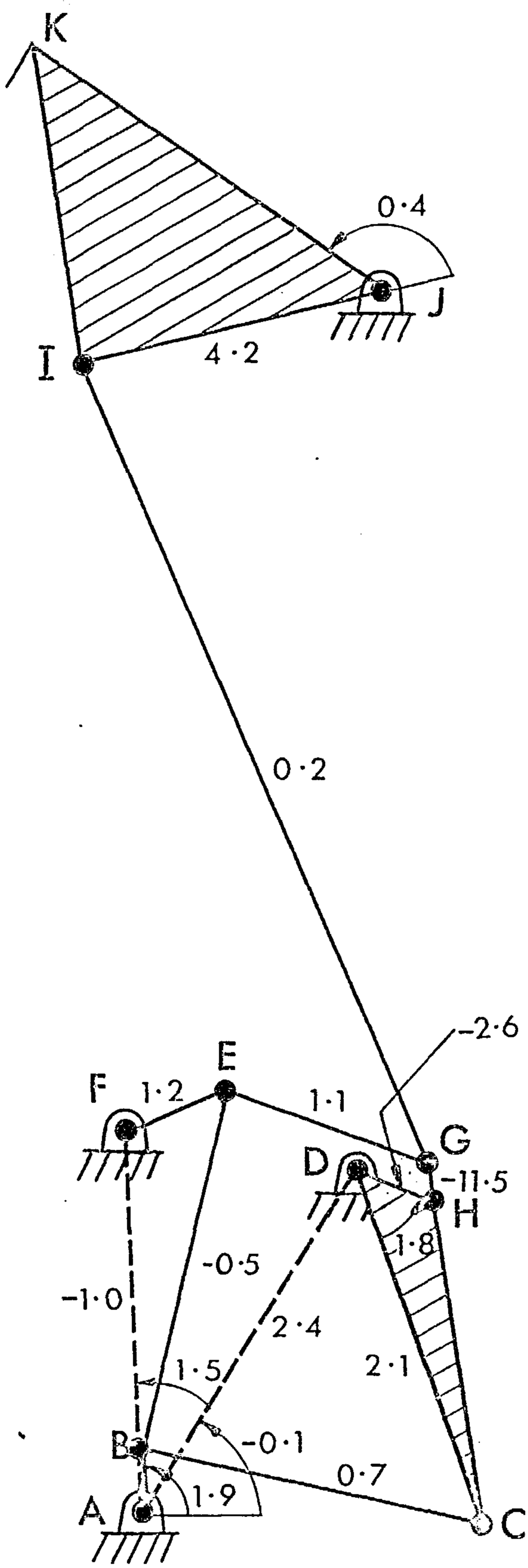

(b) Modified Linkage showing % changes in dimensions

FIGURE 8·4 NEEDLE MECHANISM

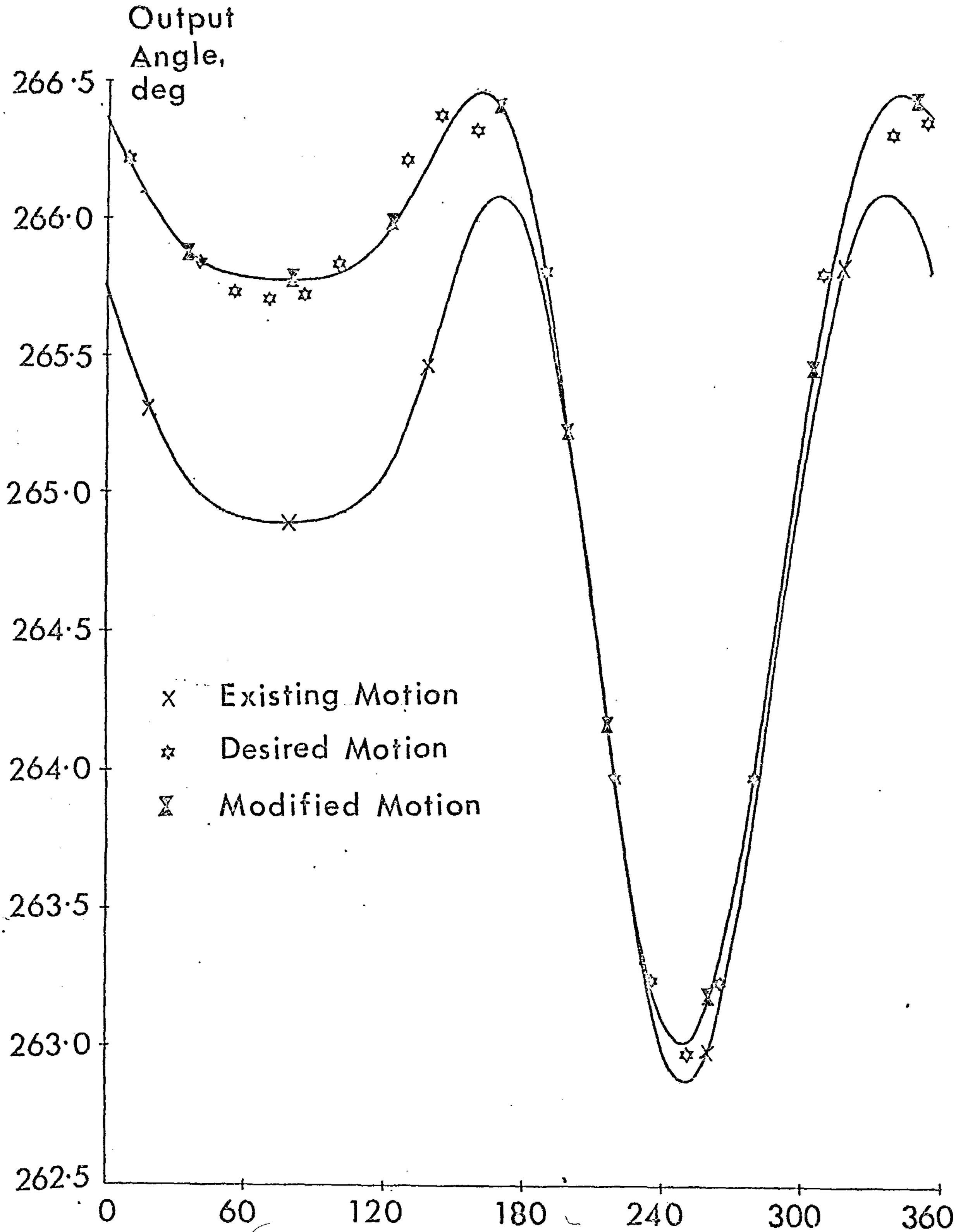

FIGURE 8·5 SINKER LINKAGE OUTPUT MOTION

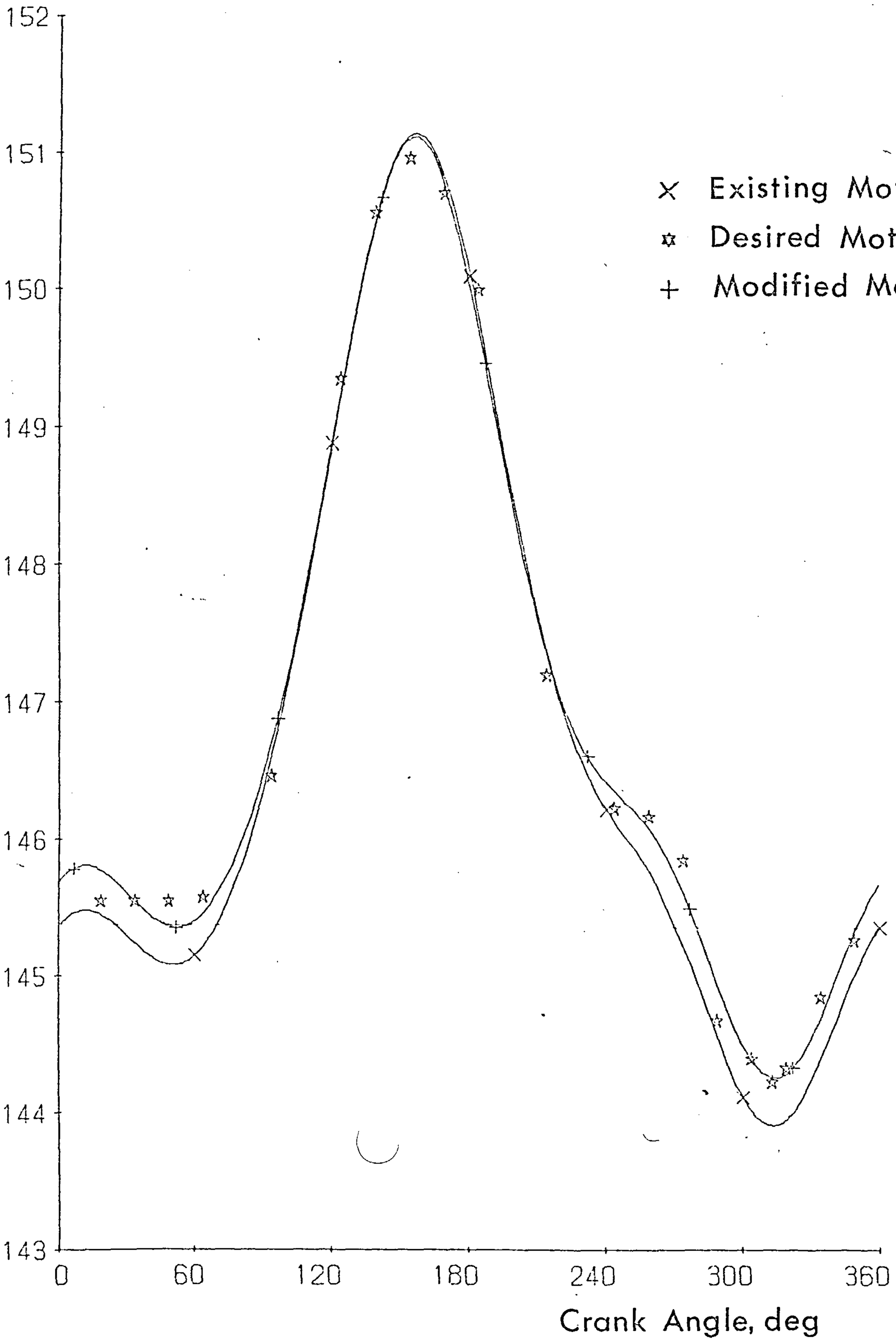

FIGURE 8·6 NEEDLE LINKAGE OUTPUT MOTION

rising as the needles start to rise at 255°. As the needles rise, the guide bars move sideways in front of the needles ready for the next cycle.

The existing mechanisms take the form of an eight-bar and a ten-bar linkage as shown in Figures 8.3a and 8.4a respectively. In both cases, AB is the input crank attached to the machine crankshaft and the output is taken from point K which represents the tip of the sinker nose and the tip of the needle. Joints A to G are contained within an oil bath. The motion is transferred from there to the knitting area via links GI which protrude through seals. This arrangement is designed to meet two requirements which apply to any fabric-producing machine. The first is that linkage mechanisms should be well lubricated for reliable high-speed operation. Secondly, no lubricating oil should get on to the fabric as an extra operation is necessary to remove it and non-staining oils are not such good lubricants as other oils.

8.3.2 Analysis of Existing Linkages

The first stage was to analyse the existing linkages. Table 8.4 shows their topological properties. Each double joint is equivalent to two simple joints as it connects three links. Each independent loop includes the crankshaft, A. If FG is chosen as a chord instead of CG for the sinker linkage, the third loop becomes ABCGIJA. This contains six arcs compared with five for loop AFGIJA. As a result, the time to analyse the linkage is increased by 10%. Thus the chords should be chosen to give the set of independent loops that contain the minimum number of arcs as well as the input link pivot. The results of analysing the two linkages are given in Figures 8.2, 8.5 and 8.6 There is a phase shift and a change in direction of the crank angle in Figures 8.5 and 8.6 compared with the crankshaft angles in Figure 8.2.

Table 8.4 Topological Properties of Sinker and Needle Linkages

Property	Equation	Linkage	
		Sinker	Needle
Number of links, ℓ		8	10
Number of single joints		6	7
Number of double joints		2	3
Number of simple joints, p	(3.9)	10	13
Degrees of freedom, λ	(3.8)	1	1
Number of independent loops, L	(4.1)	3	4
Spanning tree		ADFJ,AB, BC,FG,IJK	ADFJ,AB,BE, CDH,EG,IJK
Chords		CD,CG,GI	BC,EF,GH,GI
Independent loops		ABCDA, ABCGFA, AFGIJA	ABCDA, ABEFA, ABEGHDA, ABEGIJA

8.3.3 Synthesis of Modified Linkages

The desired output motions were represented by eighteen points for the sinker mechanism and twenty points for the needle mechanism as indicated by the stars in Figures 8.5 and 8.6 respectively. The use of the angular position of a link rather than the Cartesian co-ordinates of a point on that link is preferable for this purpose as the former is calculated more quickly. Since other mechanisms operate in the knitting area, it was decided to maintain the present positions of the pivot shafts, J, as well as the crankshaft, A. In addition, the input cranks, AB, were to remain unchanged as they are eccentrics. Link GI in the sinker linkage was also to be unchanged. This left eleven and sixteen optimization variables as indicated in Figures 8.3a and 8.4a respectively.

The program converged to the linkages shown in Figures 8.3b and 8.4b. The output motion from the

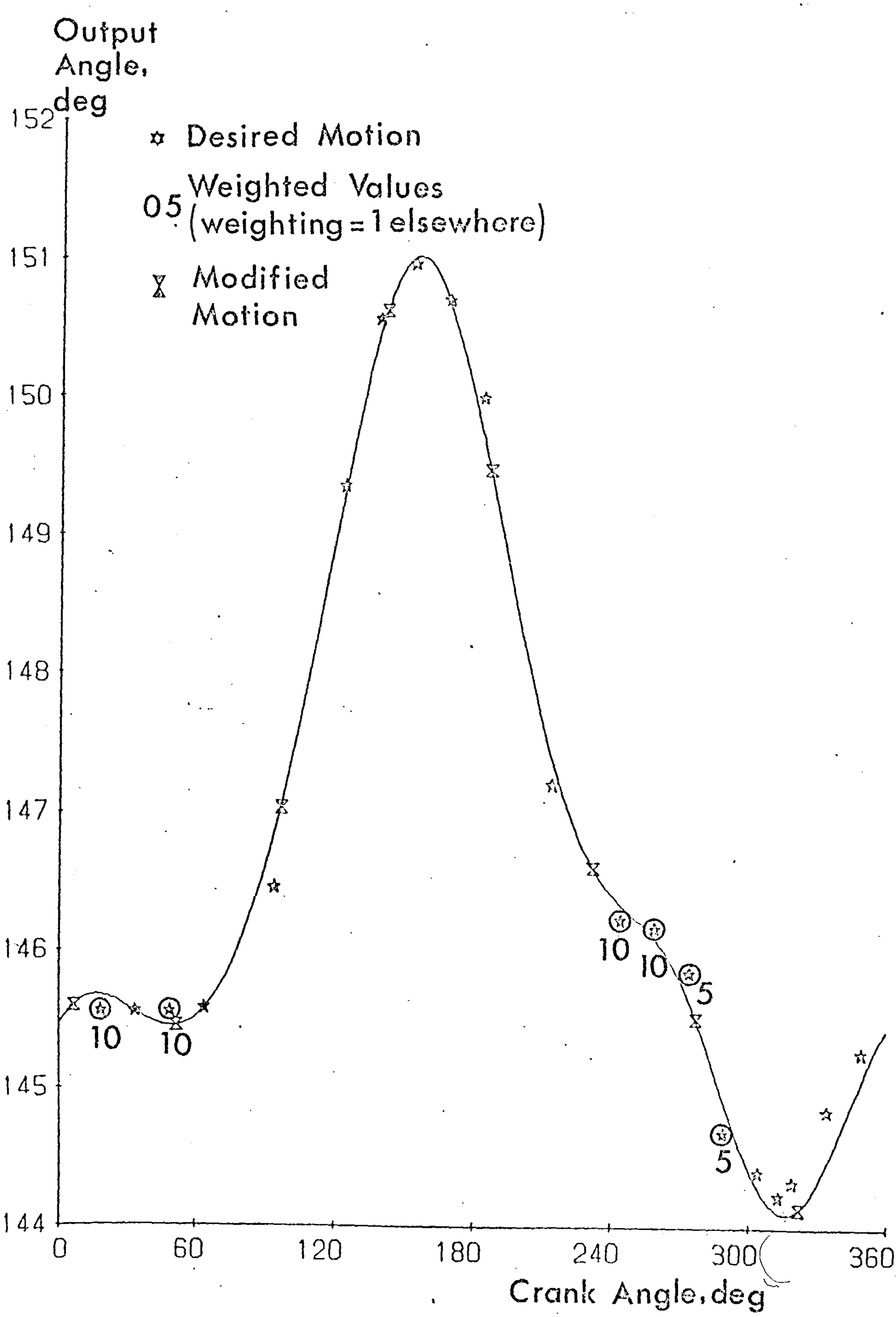

FIGURE 8·7 NEEDLE MOTION WITH WEIGHTING

modified sinker linkage is shown in Figure 8.5 and is a very close fit to the desired motion. The output motion from the modified needle linkage is shown in Figure 8.6. In this case, the desired motion includes a dwell for a crank angle of 0 to 60 degrees. This is the position where the presser depresses the needle beard so that the old loop of yarn on the stem of the needle can slip over the beard. Thus any movement of the needle at this time will result in wear of the presser and the needle beard. However the linkage in Figure 8.4b produces a needle bar movement of 0.4 degrees, which is equivalent to a needle movement of 0.85 mm, during the desired dwell. It was therefore decided to apply weighting factors to the desired motion as shown in Figure 8.7. The program was run using the linkage in Figure 8.4b as an initial guess. The resulting linkage produced the output motion shown in Figure 8.7. The needle movement during the desired dwell has been nearly halved and a closer approximation to the desired motion at a needle position of 151 degrees obtained.

8.3.4 Effect of Simplex Coefficients on the Optimization

As noted in Section 6.4.3, the default values for the simplex coefficients are those recommended by Parkinson and Hutchinson {8.3}. The effect of using the values recommended by Nelder and Mead {8.4} for the reflection and contraction coefficients is shown in Table 8.5 for the runs associated with Figures 8.3 and 8.4.

Table 8.5 Effect of Simplex Coefficients

Linkage	Sinker		Needle	
Simplex Coefficients	N&M	P&H	N&M	P&H
Reflection, α	2.0	3.0	2.0	3.0
Contraction, δ	0.5	0.25	0.5	0.25
Final value of objective function	0.14	0.13	0.48	0.47
Cpu time, seconds	10.89	15.11	25.13	39.69
Number of iterations	274	249	419	421
Objective function calculations	447	634	650	1033
Calls to constraint subroutine	28	69	67	150

The comparison was repeated for the runs where weighting factors were applied to the desired output motion of the needle linkage. In Table 8.5, the default values resulted in slightly lower final values of the objective function, but in the other runs the reverse was true (1.49 and 1.56 compared with 1.59 and 1.96 respectively). However the cpu times to reach these values were generally longer for the default values even though the number of iterations was usually less. The reason for the difference is that, on average, the objective function is calculated 2.3 times per iteration using the default values and only 1.5 times per iteration with the other values. In addition, the constraints are violated twice as often using the default values. If the simplex is not favourably aligned, the larger reflection coefficient attempts to move the worst vertex too far so that a contraction must take place. With a smaller value, the reflections are generally acceptable. In the absence of theoretical guidelines, the Nelder and Mead values are well worth a run if the number of optimization variables is large and the space to be searched is convoluted and has boundaries.

8.3.5 Comment

The use of PSALM has resulted in two mechanisms whose output motion closely matches the desired motion whilst maintaining some of the existing dimensions. If a more radical re-design of the machine were undertaken at a later date, it would be a relatively easy matter with PSALM to investigate the use of simpler linkages to produce the desired motion.

Summary

This chapter contains two case studies of PSALM in use as a design aid. The first is the synthesis of a new motorcycle rear suspension and involves both path and motion generation. In the second, two linkages with up to ten links are modified, using existing links where desirable. They are used for function generation in a warp knitting machine. In all cases,the output motion closely matches the desired motion. The approach compares favourably with alternative methods.

9. DISCUSSION

9.1. PRESENT VERSION OF PSALM

Several conclusions were drawn in Chapter 2 about the role of a computer in the kinematic synthesis of linkage mechanisms. These conclusions are now stated and discussed in relation to PSALM.

9.1.1. Types of Synthesis Problem

Conclusion : Only a digital computer program offers a general approach to kinematic synthesis.

Synthesis problems may be divided into two types. In the first, certain conditions must be met exactly and then the use of precision points and/or their derivatives is essential. Thus exact correspondence in displacement, velocity and either acceleration or path curvature requires the use of precision points, first derivatives and second derivatives respectively. First derivatives also indicate the sensitivity of a linkage to tolerances in the link dimensions. The second group consists of those problems where there is some latitude in the requirements. Typical examples are given in the case studies in the previous chapter. For instance, some variation in centre distance is acceptable for the sprocket wheels in the motorcycle rear suspension considered in Section 8.2.2. In this situation, the optimization approach provided by PSALM is ideal. However a precision point approach using second derivatives to give the required path curvature may well be the best way to obtain an initial linkage for PSALM for this example. Thus the ideal situation would be to have two computer programs. Both would cater for the same selection of linkages but one would use a precision point approach whereas the other would use optimization techniques. The first would be useful in its own right for the first type of synthesis problem and as an adjunct to the existing program, PSALM, for the second type of problem.

9.1.2. Selection of Linkages

Conclusion : Such a program as described above should be restricted to the dimensional synthesis of a well defined and easily identified group of linkages.

The case studies demonstrate PSALM being used as a design tool in the dimensional synthesis of several linkages. It caters for planar linkages that can be formed by combining dyads. This selection includes most of the planar linkages used in industry - presumably this is because these linkages are easy to analyse graphically. This group of linkages is easily identified and enables relatively straightforward techniques to be used so that PSALM is both fast and powerful. PSALM is more general than any of the programs for the kinematic synthesis of planar linkages surveyed by Chen {9.1}.

9.1.3. Choice of Initial Linkage

Conclusion : The linkage designer should be able to make full use of his creative skill and experience by choosing an appropriate mechanism and making an initial estimate of the link dimensions.

There are two problems related to this conclusion. The first is the choice of an appropriate type of linkage. This problem is common to all methods of kinematic synthesis. The second is the choice of initial link dimensions from which to start searching. Precision point methods may help with this problem as discussed in Section 9.1.1. In both cases, PSALM offers only indirect assistance in that it enables the designer to investigate various alternatives easily.

Preferably the initial linkage should be kinematically valid, i.e. satisfy the constraints, or at least it must be such that the program can modify the undetermined dyads and thereby make it valid. The closer the initial guess is to the optimum linkage, the more likely the program is to find that linkage and the time to do so should also be shorter. However usually the optimum linkage is not known in advance, otherwise there would be no need to use PSALM. In any case, the designer should prescribe an initial linkage with dimensions similar to those which he would like to use in practice.

9.1.4. Optimization

Conclusion : Given the designer's choice of mechanism, the program should automatically set up the equations necessary to analyse that mechanism and change the link dimensions to produce an output motion closer to the desired motion whilst keeping certain dimensions fixed if the designer so wishes.

When changing the link dimensions, PSALM makes use of valid linkages only. It achieves this by ensuring that the arc lengths are always positive and that the constraints of loop closure and transmission angle are satisfied. These latter constraints give bounds on the values of certain optimization variables. These bounds vary during optimization according to the lengths of the other arcs in the loop. By using the Simplex algorithm for optimization rather than any of the other methods surveyed by Root and Ragsdell {9.2}, PSALM accommodates the constraints in a physically meaningful way without invalidating the search method.

Kramer and Sandor {9.3} recommend that linkages composed of dyads should be synthesized dyad by dyad as this results in several short runs rather than one much longer run. However the method that they advocate for this raises two problems. The first is that function generating linkages must be inverted so that the motion generating inversion can be used for synthesis. Secondly the designer is not free to fix the dimensions of certain links and so the method is not suitable for modifying existing linkages. While catering for the same group of linkages, PSALM avoids these problems. At the same time, it enables the designer to prescribe limits on transmission angles and to work with as many or as few optimization variables as he wishes. Consequently it can be used to synthesize a linkage dyad by dyad if this is appropriate. Thus PSALM offers the same advantages without the disadvantages of the alternative method.

In any optimization program, it is assumed that the desired result can be specified completely by the objective function and prescribed constraints. In the case of PSALM,

it is not possible to prescribe directly the space within which the linkage must operate. In addition, it may not always be possible to prescribe realistic values for certain constraints. For example, the link lengths determine the kinematics which affect the forces at the joints and hence the size of the joints. This, in turn, determines the minimum lengths of the links. In these situations, the designer may prefer the program to give a variety of linkages rather than just one 'optimum' linkage. Several linkages for a given application can be obtained in two ways using PSALM. Firstly the program periodically prints out the values of the optimization variables (after every so many iterations as prescribed by the designer). Secondly a different initial simplex or different values of the simplex coefficients may result in different linkages. A different initial simplex can be obtained either by using a different starting integer or by allowing the simplex to be generated within different limits. A useful improvement to PSALM would be for the program to write the data for these different linkages to a data file in such a manner that the linkages could be displayed using the PICTUR program. This program enables the linkage corresponding to the input data to be displayed on the screen of a graphic computer terminal.

9.1.5. User's Manual

Conclusion : The program should be easy to use.

For a program to be widely used, not only must it be reliable and efficient, but it should be easy to supply the necessary input data. The more general the program, the more likely is this to be a problem. Thus there is a possibility of using 55 different data items with PSALM, each consisting of a name and one or more numerical values. Although default values are provided for 40 of these data items, the options can be bewildering at first sight. In addition, the concepts, particularly those for prescribing the topology, may be unfamiliar to a potential user. Thus a good user's manual is essential for any program of this

type. Such a manual is being written for PSALM. It will be divided into two parts. The first will be a self-instruction manual. It will introduce the concepts and the use of the program by means of simple examples. In effect it will be a simplified and shortened version of the preceding chapters in this thesis. The second part will be a reference manual giving definitions of all of the data items as in Appendix B. The program PICTUR will form a useful adjunct to this manual by providing a check on the input data for PSALM.

9.1.6. Transfer to Other Computers

Conclusion : It should be easy to transfer the program to other computers.

If PSALM is to be transferred to a type of computer other than an IBM 360/370 series, five changes may have to be made. If the associated compiler does not cater for NAMELIST statements, these can be replaced by suitable standard Fortran statements although this would add to the length of the program. Some compilers do not maintain values in labelled COMMON if a routine is used that does not contain a COMMON statement for that set of values. If this is the case, all of the labelled COMMON statements should be combined into the blank (unlabelled) COMMON statement which appears in the main program and each of the subroutines. When doing this, boundary alignment should be maintained by ordering all of the real variables before any integer variables. The IMPLICIT statements can either be replaced by DOUBLE PRECISION statements or removed altogether and also the random number generator changed depending on the word size of the machine. Finally the functions for $\sin^{-1}$ and $\cos^{-1}$, i.e. DARSIN and DARCOS, may have to be changed.

If PICTUR and the conversational plotting program are to be transferred as well, they will have to be changed as they use plotting routines which are specific to the NUMAC installation.

9.2. FURTHER DEVELOPMENT

Further development of PSALM will be considered under the following headings :

(a) topology,

(b) kinematics,

(c) constraints.

9.2.1. Topology

The scope of PSALM could be extended in three ways. The first would be to increase the range of admissible actuator pairs to include :

(a) a translating pair such as a solenoid or a pneumatic cylinder,

(b) more than one actuator pair in the linkage to cater for linkages with more than one degree of freedom.

Some geared linkages would come within the latter category. The basic unit would consist of the frame link and the input link(s). The remainder of the linkage would still consist of additional peelable dyads and so the present method of prescribing the linkage could still be used.

The second extension would permit the use of actuator pairs that did not include the frame link as one of the two links. Such actuator pairs are used in fork lift trucks for tilting the mast. Further work would be needed to clarify the implications of this extension.

The third extension would permit other Assur groups in addition to the binary group to be added to the basic unit. Since there are more than two possible closures for these other Assur groups, a sign convention would no longer suffice to prescribe the appropriate closure. However the estimates of the initial angular positions of the links and the lengths of the sliding links that would be necessary to prescribe the closure could be supplied using the existing ARCL and GAMA arrays. The present method for prescribing the topology could remain otherwise unchanged except that there would not necessarily be two undetermined arcs in each loop. Thus, with relatively minor changes, the present method of prescribing

the topology of a linkage can cater for a much larger group of linkages. However, since the topology is prescribed in terms of arcs rather than links, it would be difficult to apply the method in a dynamics program where the masses and inertias of the links would be required.

9.2.2. Kinematics

The analysis routine used to calculate the objective function for an optimization program should be efficient. One of the time-consuming features in PSALM is the summation of the projections of the determined arcs in each loop on to the co-ordinate axes for that loop. However the use of Assembler code for this part of the program did not appear to offer a significant improvement because the time is taken in calculating the sine and cosine of the angular positions of the arcs. An efficient code for these calculations is automatically supplied by the compiler.

The present version of PSALM uses the loops prescribed by the user when analysing a linkage. If the user has not identified the loops with the minimum number of arcs, the run time will be longer than is necessary. However the linkage will still be completely specified and therefore it should be possible for the program to choose the optimal set of independent loops irrespective of those prescribed by the user. The advantage of using independent loops in this context is that it ensures that the kinematic equations are also independent.

A similar facility would be required to recognise the different Assur groups if PSALM were altered to cater for these. The advantage of using Assur groups is that they give the minimum number of simultaneous equations to be solved at each stage in analysing a linkage. It may be possible to use special techniques for particular groups - this, of course, is one of the features of PSALM. One method of analysing inversions of the present selection of linkages would be to analyse the currently acceptable inversion and then invert. However this poses the problem of what position to choose for the assumed input link to

achieve the desired position of the actual input link. In addition, it would be possible to choose a position for the assumed input link that was outside its actual range of motion. Thus this approach is felt to be unacceptable for a general purpose program.

9.2.3. Constraints

In certain applications, the designer will want a linkage to operate within a given space. For example, the purchaser of an up-and-over garage door would not want the linkage to poke through the roof of the garage. Similarly linkages in fabric-producing machines must not intersect the fabric. Further work is required to cater for this type of constraint.

9.3. OTHER APPLICATIONS OF APPROACH

9.3.1. Kinematic Analysis of Planar Linkages

When used for analysis, PSALM will give only the displacement of the output point or link corresponding to the prescribed positions of the input link. However the theory given in Chapter 5 can be easily extended to give velocities and accelerations of the output as long as the velocity and acceleration of the input are prescribed. This extended theory and details of an analysis-only program that incorporates it are given by Oldham {9.4}.

9.3.2. Cam Synthesis

As discussed in Chapter 1, cams are used to drive many linkages. The designer of such a mechanism will be concerned with the motion at the output of the linkage rather than that of the cam follower. Accordingly the foregoing analysis program has been combined with a cam synthesis program by Oldham {9.5}. The result is a three-part program for the synthesis of rotating cams with swinging roller followers. The first part fits a trig-type law to the output motion. The law may be any variation on a modified trapezoidal acceleration law such as skewed modified trapezoidal, cycloidal, modified sine and constant acceleration. The program also caters for dwells and ramps (constant velocity). The second part

accounts for the transfer characteristics of the linkage and may be omitted if the cam follower provides the output motion directly. The third part calculates the cutter-centre co-ordinates necessary to manufacture the cam. The cutter need not be the same diameter as the roller follower. This part also calculates the radius of curvature of the cam profile and the pressure angle between the roller and the cam. The co-ordinates of the cam profile are available for plotting. Cutter-centre co-ordinates and profile information may be produced for conjugate profiles on request. The program also caters for the situation where two cams are used to drive the same linkage. In this case, the program will calculate the co-ordinates for both cams.

Summary

The discussion about the kinematic synthesis program, PSALM, falls into three parts. The first is concerned with how well its characteristics match the desirable features of a general method for kinematic synthesis established in Chapter 2. The second part discusses possible developments of the program. Some of these have since been implemented. The third part considers the application of the approach used in PSALM to the kinematic analysis of planar linkages and the synthesis of cams that drive linkages of this type.

10. CONCLUSIONS

10.1. COMPUTER PROGRAMS

Contacts with industry showed that there was a need for a computer program to assist machine designers in the kinematic synthesis of linkage mechanisms. Accordingly a program called PSALM - Program for the Synthesis and Analysis of Linkage Mechanisms - has been written for the dimensional synthesis of a wide range of planar linkages used for path, motion or function generation. The range of linkages includes most of those used in industry. The program has been written to run on digital computers since these are more widely available and generally applicable than analogue computers. The language of the program is Fortran IV so that it may be transferred easily from the IBM 360/370 computers on which it was developed to other models of computer.

Four other programs have been written. Two are concerned with plotting and use routines that are specific to the NUMAC installation. The other two are for related applications. Their roles in relation to PSALM are given later.

10.2. SELECTION OF LINKAGES

PSALM caters for single degree-of-freedom planar linkages that can be formed by adding pairs of links to an initial pair consisting of a frame link with an input link pivoted to it. At each stage in the building up, the linkage must have one degree of freedom. The linkages may contain prismatic joints as well as revolute joints. These linkages form a large, but easily identified, group so that a designer does not have to change his approach if there is a change in the form of the linkage being designed.

The form of the linkage is prescribed by the user in terms of a set of independent loops formed by the links. These loops lead to a set of independent equations which can be solved sequentially loop by loop. This has permitted the development of a rapid method of analysis for these linkages so that the use of an optimization

technique becomes practicable. At present PSALM relies on the user to choose the set of loops that gives the shortest analysis time. It would be beneficial if the program removed the onus for this from the user.

The selection of linkages could be extended to include linkages with more than one input link. Few changes would have to be made to the program for this. A major change to the analysis subroutine would be necessary if the program were to cater for linkages where the additional units contain more than two links.

10.3. OPTIMIZATION

By adopting an optimization approach for PSALM, the designer is able to make full use of his creative skill and experience in choosing the form of a linkage and the initial set of dimensions which the program requires. PSALM offers only limited assistance with these aspects in that alternative linkages and sets of dimensions can be investigated quickly. Another program, catering for the same selection of linkages but using a precision point approach, should be written as it would offer help with this problem and be useful in its own right for linkages where there is no latitude in the output motion requirements.

With PSALM, the user is free to prescribe which of the link dimensions shall remain fixed and which shall be optimization variables. The desired motion is expressed in terms of the positions of the output for prescribed positions of the input link. If some parts of the desired motion are more critical than others, the user may apply weighting factors to the critical parts.

The modified Simplex optimization routine enables the non-linear constraints of loop closure and transmission angle to be taken into account directly without invalidating the search procedure. In this way, PSALM makes use of only those linkages which satisfy the constraints. If it is found that the simplex flattens itself against a constraint boundary when bounds are placed on the link lengths, then the number of vertices in the simplex should be increased.

Further work is required to cater for situations where the space within which the linkage must operate is limited.

10.4. EASE OF USE

The aim has been to write a versatile program which is easy to use. This is achieved by providing default values for much of the input data. In addition, the program sets up the equations for analyzing the linkage automatically from the input data. A user's manual is also being written. A conscious effort has been made to write an efficient program. The result is a fast and powerful program which is applicable to a wide range of linkages and which offers advantages over alternative approaches.

Another program, called PICTUR, has been written to display the linkage corresponding to the input data on the screen of a graphic computer terminal. This enables a user to check his data for errors before carrying out a synthesis run. At the end of a synthesis run, the output motion from the final linkage may be plotted on a graph plotter using a conversational program.

10.5. OTHER APPLICATIONS

Two other programs have been written using the same methods as PSALM. The first is for the kinematic analysis of the same selection of linkages as PSALM. It gives the output velocity and acceleration as well as the displacement thereby complementing the displacement-only capability of PSALM. The second is for cam synthesis where one cam or a pair of cams drives a linkage. Thus the methods developed for PSALM, as well as being fast, are capable of wider application than the dimensional synthesis of linkages.

Summary

The main conclusion about the kinematic synthesis program is that it meets a widespread need in industry. It caters for planar linkages that can be assembled from pairs of links. Such linkages can be analyzed rapidly which makes an optimization approach feasible. Non-linear constraints of transmission angle and loop closure are satisfied and the designer is free to choose which link dimensions shall be optimization variables. Plotting options are also available.

PART B

FORCE

BALANCING

11. FORCE BALANCING

11.1 INTRODUCTION

Once a designer has determined the lengths of the links to give the required motion from a linkage mechanism, he will choose the material and cross-sectional areas of the links. When the resulting linkage is run, the linear acceleration of the link masses will produce inertia forces and the angular acceleration of the link inertias will produce inertia couples. If the linkage is to be run at high speed, these inertia forces and couples may be significant compared to any external loads. In this case, the designer may wish to balance the linkage such that the net force on the frame is zero i.e. the linkage is force-balanced. This raises the following questions :

1) Can the linkage be force-balanced using simple counterweights?
2) If so, how many counterweights are required?
3) To which links should the counterweights be attached?
4) What conditions must each counterweight satisfy?

Lowen and Berkof {11.1} have surveyed various approaches to balancing planar linkages. Of the various techniques reviewed, attaching simple counterweights is the most straightforward. Accordingly Berkof and Lowen {11.2} developed the 'Method of Linearly Independent Vectors' and Smith {11.3} has applied this to the ten-bar linkage considered in Chapter 8. The position of the centre of mass of each moving link is expressed in vector form and then the time-dependent terms eliminated to give the necessary counterweight conditions. However, by using the concept

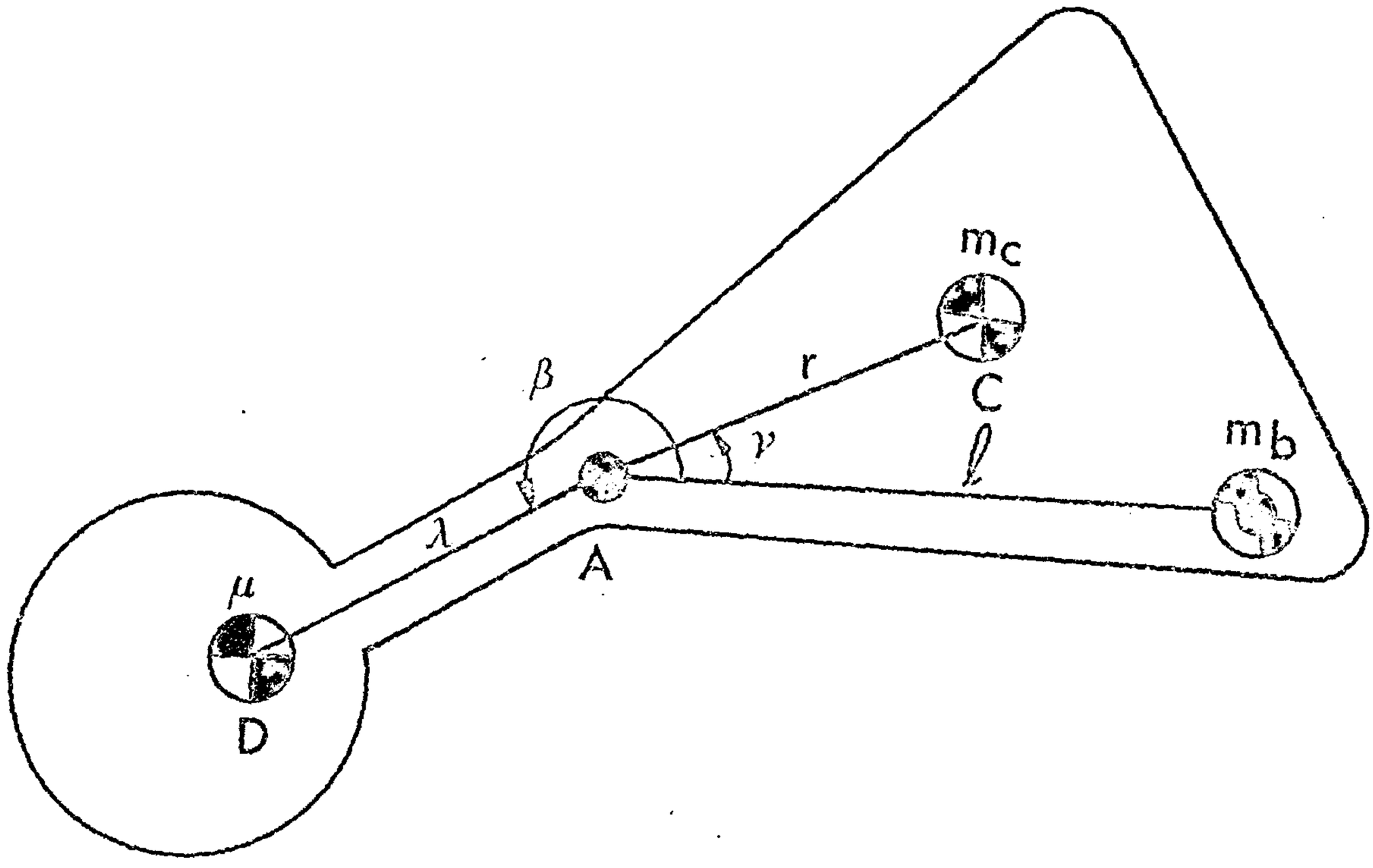

FIGURE 11·1 COUNTERWEIGHTED LINK

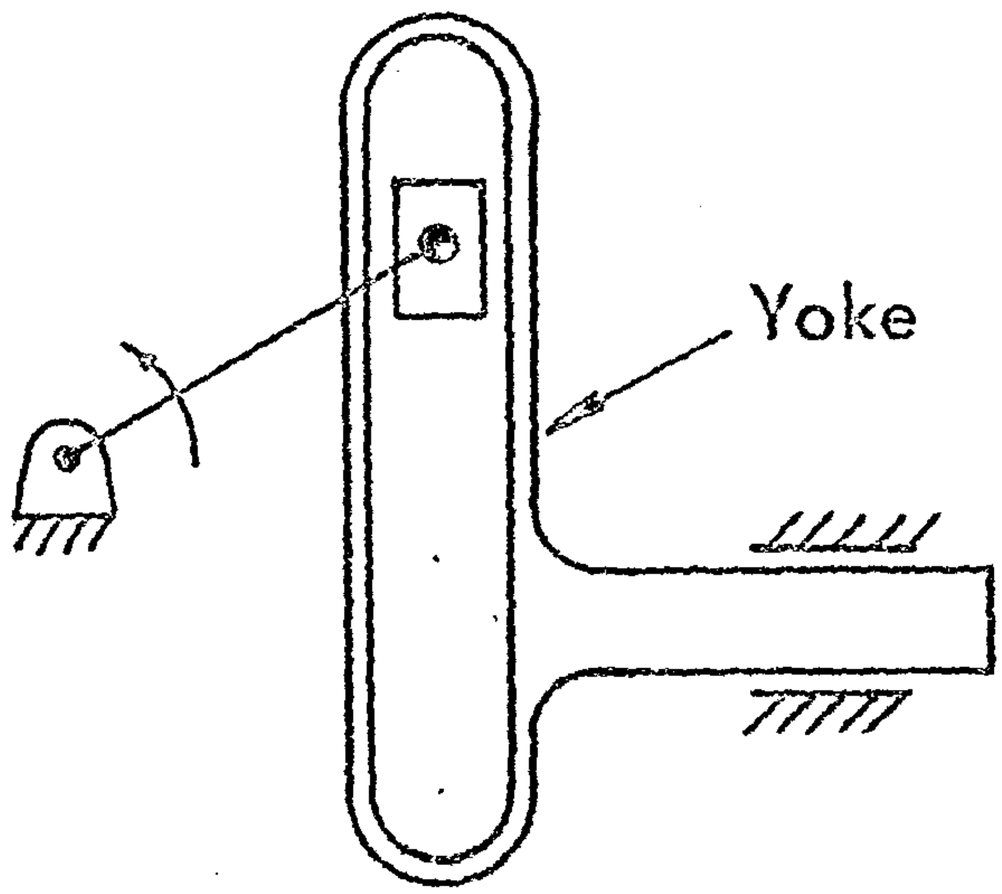

FIGURE 11·2 SCOTCH YOKE MECHANISM

of independent loops developed by Paul {11.4}, the choice of which links to leave uncounterweighted is clarified. In addition, the counterweight conditions can be obtained more simply using the procedure given in Section 11.4. This procedure also gives a clearer insight into the relationship between link and counterweight masses. The procedure and the example in Sections 11.4 and 11.5 respectively may be read before the theory given in Sections 11.2 and 11.3.

11.2 CONDITIONS FOR FORCE BALANCE

Since the trajectory of the centre of mass of a linkage mechanism is a closed curve, a necessary and sufficient condition for a force-balance is that the centre of mass is stationary (Tepper and Lowen {11.5}). The possibility of achieving this for a general planar linkage using simple counterweights depends on two facts.

Firstly the axis of relative motion of links connected by a revolute joint remains fixed relative to each of those links. Consequently any mass on that axis may be ascribed to any of those links. The same does not apply to a prismatic joint as there is no common point that remains fixed in both links connected by that joint.

Secondly the centre of mass of a link and any masses ascribed to that link may be moved to any point fixed relative to the link by the attachment of a suitable counterweight provided that the masses and geometry are not affected by the link motion. Consider the link shown in Figure 11.1 with a revolute joint at A. The mass of the link alone is m_c at C with an ascribed mass m_b at B and a mass of μ at D due to a counterweight with its attachment link. For the combined centre of mass to be at A, we have

$$\mu.\lambda.e^{i\beta} + m_c.r.e^{i\gamma} + m_b.\ell.e^{iO} = O \qquad (11.1)$$

where the lengths and angles are depicted in Figure 11.1. That this produces the desired effect will be proved in the next Section. If μ and λ are constants, i.e. the counterweight is rigidly attached to the link, this expression holds only if m_b and ℓ are constant assuming that the link itself is rigid. Thus the expression holds if there is a revolute joint at B. If there is a prismatic joint at B, the expression holds only if m_b is zero since, for such a joint, either m_b or ℓ would vary. Consequently no mass may be ascribed from one link to another via a prismatic joint directly.

If the expression is true throughout the motion of the linkage,the effective mass at A, namely $(m_b + m_c + \mu)$, may be ascribed to any other link connected to the revolute joint at A. If this second link contains another revolute joint, the addition of a suitable counterweight to it will result in the combined centre of mass being at this latter joint. This second counterweight will then balance the mass of the first link with its counterweight as well as the mass of the second link. It follows that if a link is connected by a chain of revolute jointed links to a stationary point, such as a frame pivot, the addition of a suitable counterweight to each link in the chain will result in the centre of mass of the chain as a whole being at that stationary point. Each counterweight balances the mass of the link to which it is attached and the masses of any links and counterweights in the chain that are more remote from the frame. Consequently there is a progressive build-up in the size of counterweight required for each link as the stationary point is approached.

In a linkage that can be force-balanced, there will be at least one chain of revolute-jointed links connecting the frame link to each moving link. By definition, such a chain cannot traverse a prismatic

joint. In the case of a linkage containing the maximum number of prismatic joints for which a force-balance is possible using simple counterweights, each chain will start from a link with at least one prismatic joint and only one revolute joint and finish at the frame link. These chains, together with the prismatic joints, will form loops of links which may or may not include the frame link. If not, the loops will be connected to the frame link by a revolute-jointed chain of links. If all of the prismatic joints in this limiting case are disconnected, then no loops will remain. However, all of the links will still be connected together through the frame link. The reconnection of any one of the disconnected prismatic joints will result in the formation of only one loop. If each prismatic joint is reconnected individually, then a set of loops will be formed. The loops so formed constitute a complete set of independent loops for the linkage (Deo {11.6}).

For a planar linkage, the number of independent loops, L, is given by (Chapter 3) :

$$L = j - n \qquad (11.2)$$

where j = effective number of simple joints, a joint connecting k links is counted as (k-1) joints,

n = number of moving links

If a set of loops can be chosen such that every link appears in at least one loop but no loop includes more than one prismatic joint, then the linkage can be force-balanced. Furthermore, if all of the prismatic joints are disconnected, no links become detached from the chain that includes the frame link. This forms the basis of the simple check given in the procedure in Section 11.4 for the feasibility of achieving a force-balance. There are certain linkages that, although they fail this test, can be force-balanced using simple counterweights. In linkages that fail the check, links become detached from the chain that includes the frame link. Accordingly,

there is no revolute-jointed chain of links connecting them to a stationary point. If, however, the combined centre of mass of the detached links remains stationary during the motion of the linkage, no counterweights are required for these links. In the limit, no counterweights whatsoever are required for a force balance if a duplicate mirror image linkage is provided (Davies {11.7}). If this is impracticable, the mass of the detached links should be kept as low as possible. For example, the scotch yoke mechanism shown in Figure 11.2 cannot be force-balanced using simple counterweights because the yoke becomes detached when the prismatic joints are disconnected. The mass of the yoke should therefore be minimized.

11.3 NUMBER OF COUNTERWEIGHTS

If all of the prismatic joints in a linkage that can be force-balanced are disconnected, any remaining loops will contain only revolute joints. Not every link within such a loop has to be counterweighted. Severing a joint in a revolute-jointed loop from a link in that loop by cutting the link will break the loop in a similar manner to disconnecting a prismatic joint. The maximum number of revolute joints, s, that may be severed in this way without any link becoming detached from the chain that includes the frame link is given by

$$s = L - p \tag{11.3}$$

where p = number of prismatic joints.

As will be shown below, the links from which these joints are severed may be left uncounterweighted.

Consider a link in a revolute-jointed loop. The acceleration of any mass at a point fixed in that link, which will have at least two revolute joints, is a constant linear function of the accelerations of those joints, so suitable constant masses ascribed to those joints will produce the same inertia forces as the

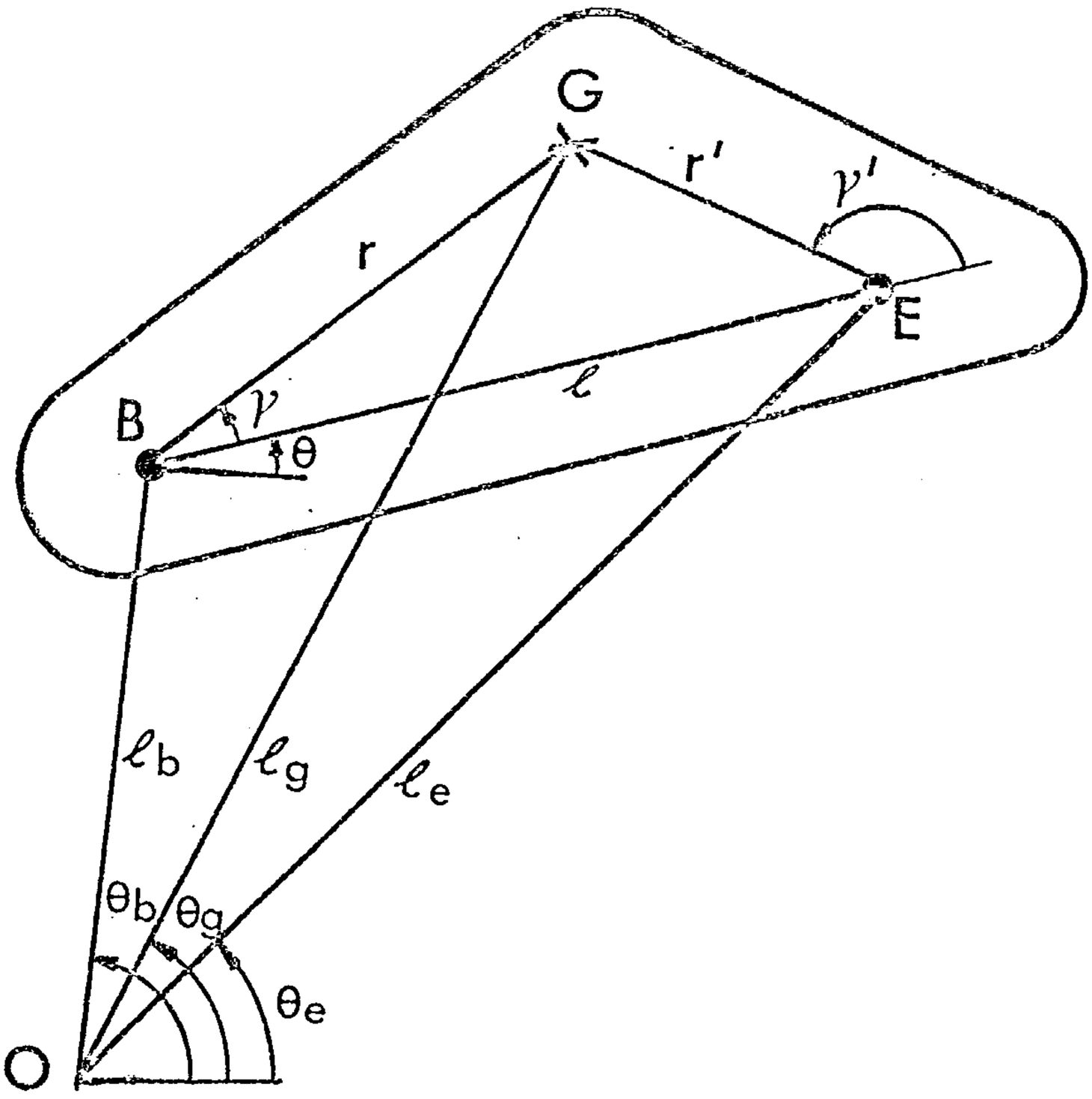

FIGURE 11·3 UNCOUNTERWEIGHTED LINK

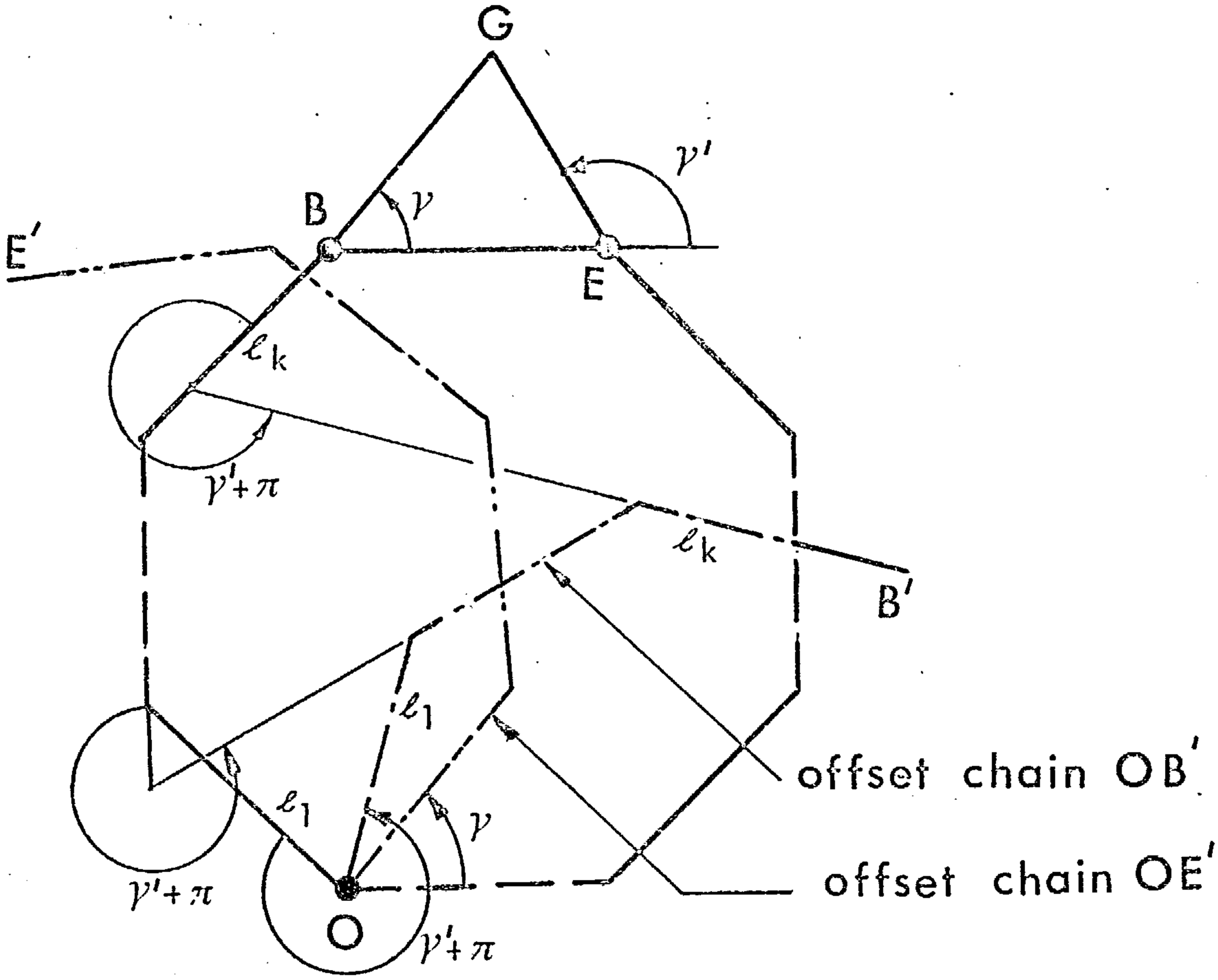

FIGURE 11·4 OFFSET CHAINS

original mass. The ascribed masses can be balanced down the respective chains from those joints to the frame. Replacing the original mass by the ascribed masses is equivalent to cutting that link since it has the effect of breaking the loop. Occasionally one of the revolute joints concerned connects that link directly to the frame link. In this case, one of the chains will be of zero length.

The general case may be demonstrated in the following manner. Consider the link shown in Figure 11.3 with a mass of m_g at G and connected to the frame by revolute-jointed chains from the revolute joints at B and E. The positions of B and E relative to some stationary point O are (ℓ_b, Θ_b) and (ℓ_e, Θ_e) respectively. Then

$$\ell_b.e^{i\Theta_b} + \ell.e^{i\Theta} = \ell_e.e^{i\Theta_e} \qquad (11.4)$$

If the co-ordinates of G with respect to O, B and E are (ℓ_g,Θ_g), (r,γ) and (r',γ') respectively, then

$$\ell_g.e^{i\Theta_g} = \ell_b.e^{i\Theta_b} + r.e^{i(\Theta+\gamma)}$$

$$= \ell_b.e^{i\Theta_b} + \ell.e^{i\Theta} . r.e^{i\gamma}/\ell \qquad (11.5)$$

and $$\ell - r.e^{i\gamma} = r'. e^{i(\gamma'+\pi)} \qquad (11.6)$$

From equations (11.4 - 11.6), we have

$$\ell_g.e^{i\Theta_g} = \ell_b.e^{i\Theta_b} + \frac{r}{\ell}.e^{i\gamma}\{\ell_e.e^{i\Theta_e} - \ell_b.e^{i\Theta_b}\}$$

$$= \{1-\frac{r}{\ell}.e^{i\gamma}\}.\ell_b.e^{i\Theta_b} + \frac{r}{\ell}.e^{i\gamma}.\ell_e.e^{i\Theta_e}$$

$$= \frac{r'}{\ell}.e^{i(\gamma'+\pi)}.\ell_b.e^{i\Theta_b} + \frac{r}{\ell}.e^{i\gamma}.\ell_e.e^{i\Theta_e} \qquad (11.7)$$

If points B, E and G are fixed relative to each other, then ℓ, r, r', γ and γ' are constant and the relationship holds under differentiation i.e. the acceleration of G is the same linear combination of the accelerations of B and E.

Equation (11.7) can be written in the form

$$\ell_g.e^{i\Theta_g} = \frac{r'}{\ell}.\ell_b.e^{i(\Theta_b+\gamma'+\pi)} + \frac{r}{\ell}.\ell_e.e^{i(\Theta_e+\gamma)} \qquad (11.8)$$

Now $\ell_b.e^{i(\Theta_b+\gamma'+\pi)}$ represents a vector OB' with the same length as OB but rotated through a constant angle of $(\gamma'+\pi)$. It may be considered therefore to be a chain of links in which each link has the same length as, and is at a constant angle to, the corresponding link in the chain OB as shown in Figure 11.4. Similarly $\ell_e.e^{i(\Theta_e+\gamma)}$ may be regarded as a chain of links OE' in which each link is at a constant angle of γ to the corresponding link of equal length in the chain OE. As a result, a mass of $m_g.r'/\ell$ at B' and a mass of $m_g.r/\ell$ at E' will produce the same inertia forces as a mass of m_g at G.

Let there be k links in the chain OB with the kth link (see, for example, Figure 11.4) connected to B by a revolute joint. Also let

$$m_b = m_g.r'/\ell;\ \psi'=\gamma'+\pi \text{ and } \alpha = \dot{\Theta}^2 - i\ddot{\Theta} \qquad (11.9)$$

Then the inertia force, F_b, at O due to the acceleration of the ascribed mass at B' is given by

$$F_b = -m_b.\frac{d^2}{dt^2}\{\ell_b.e^{i(\Theta_b+\psi')}\}$$

$$= m_b.\alpha_k.\ell_k.e^{i(\Theta_k+\psi')} + m_b.\sum_{j=1}^{k-1}\alpha_j\{\ell_j.e^{i(\Theta_j+\psi')}\} \qquad (11.10)$$

If a counterweight is added to the kth link to satisfy the following condition (which is the same as equation (11.1) except for the presence of ψ'),

$$\mu_k.\lambda_k.e^{i\beta_k} + m_k.r_k.e^{i\gamma_k} + m_b.\ell_k.e^{i\psi'} = 0 \quad (11.11)$$

then the inertia force, F_k, at O due to m_b and the kth link with its counterweight, namely

$$F_k = m_b\{\alpha_k.\ \ell_k.e^{i(\psi'+\Theta_k)} + \sum_{j=1}^{k-1} \alpha_j(\ell_j.e^{i(\psi'+\Theta_j)})\ \}$$

$$+ m_k\{\alpha_k.r_k.e^{i(\gamma_k+\Theta_k)} + \sum_{j=1}^{k-1} \alpha_j(\ell_j.e^{i\Theta_j})\ \}$$

$$+ \mu_k\{\alpha_k.\lambda_k.e^{i(\beta_k+\Theta_k)} + \sum_{j=1}^{k-1} \alpha_j(\ell_j.e^{i\Theta_j})\ \} \quad (11.12)$$

will reduce to

$$F_k = \{m_b.e^{i\psi'} + m_k + \mu_k\} \sum_{j=1}^{k-1} \alpha_j(\ell_j.e^{i\Theta_j}) \quad (11.13)$$

This is equivalent to a mass of $(m_k + \mu_k)$ at the joint connecting links k and (k-1) in the original chain, OB, and a mass of m_b at the corresponding joint in the offset chain, OB´. By adding the counterweight according to equation (11.11), the time-varying kth term in equation (11.10) has been eliminated as shown by equation (11.13). Similarly, adding appropriate counterweights to the other links in the chain will eliminate the other time-varying terms. Thus, the force due to m_b at B´ is balanced by the addition of counterweights to each link in the chain OB. Accordingly, m_b can be ascribed to B as long as the offset angle, ψ', is taken into account at each balancing stage. Similarly the mass of $m_g.r/\ell$ at E´ can be ascribed to E, the offset angle in this case being γ. Thus there is no need to add a counterweight to link BEG since the counterweights added to the moving links in chains

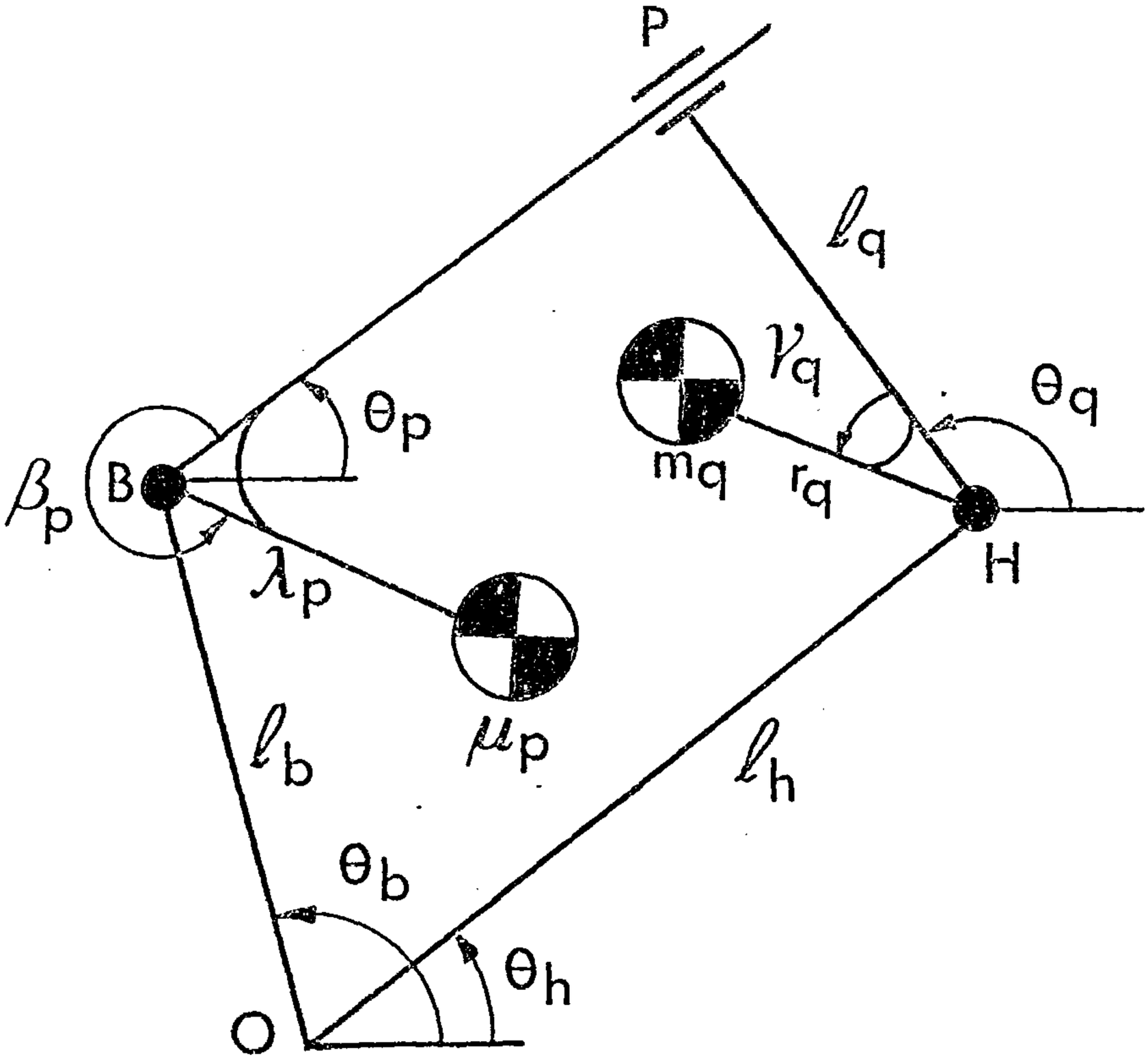

(a) Counterweight on the Sliding Link

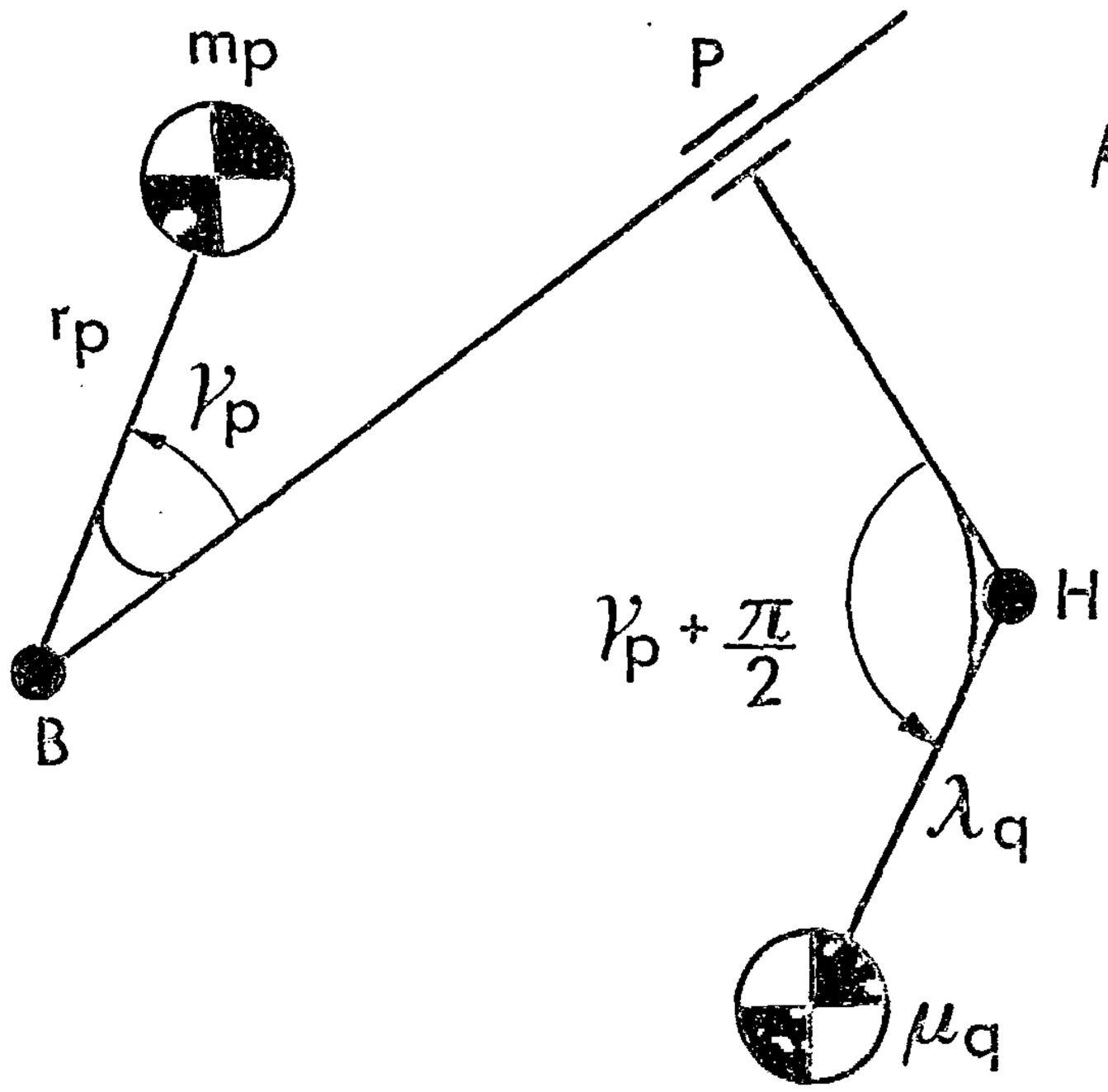

$$\mu_q \cdot \lambda_q = m_p \cdot r_p$$

(b) Counterweight on the Guide Link

FIGURE 11·5 PRISMATIC JOINTS

OB and OE will balance it.

If G represents another revolute joint in the link, then m_g may be a mass (with an associated offset angle) ascribed to the link BEG from a chain incident to that link at G. This ascribed mass in ascribed in turn to the revolute joints at B and E as before. There will be an associated double offset angle to be taken into account at each stage of chains OB and OE. Thus a chain incident to another revolute joint in an uncounterweighted link splits into two at that joint.

If the loop contains a prismatic joint, one of the two links connected by that joint may be left uncounterweighted. Consider a sliding link BP and a guide link PH connected by a prismatic joint at P and with revolute joints at B and H as shown in Figure 11.5a. The inertia force at some stationary point O due to the mass m_q of the guide link PH (or any mass ascribed to it) is

$$m_q\{r_q.\alpha_q e^{i(\theta_q + \gamma_q)} - \frac{d}{dt^2}(\ell_h.e^{i\theta_h})\}$$

where the lengths and angles are as illustrated in the Figure. If a counterweight is added to the sliding link BP as shown such that

$$\mu_p.\lambda_p = m_q.r_q \quad \text{and} \quad \beta_p = \gamma_q + \frac{3\pi}{2}$$

then the inertia force at O due to this counterweight will be

$$\mu_p\{\lambda_p.\alpha_p.e^{i(\theta_p+\gamma_q+\frac{3\pi}{2})} - \frac{d}{dt^2}(\ell_b.e^{i\theta_b})\}$$

The inertia force at O due to the counterweight on the sliding link and the mass on the guide link will be

$$m_q.r_q.\alpha_q\{e^{i(\theta_q+\gamma_q)} + e^{i(\theta_q-\frac{\pi}{2}+\gamma_q+\frac{3\pi}{2})}\}$$

$$-\frac{d}{dt^2}\{\mu_p.\ell_b.e^{i\theta_b}+m_q.\ell_h.e^{i\theta_h}\}$$

$$= - \frac{d}{dt^2}\{\mu_p . \ell_b . e^{i\theta_b} + m_q . \ell_h . e^{i\theta_h}\}$$

since $\theta_q = \theta_p + \pi/2$, $\alpha_q = \alpha_p$ and $e^{i\pi} = -1$.

This is equivalent to a mass of μ_p at B and a mass of m_q at H and there is no offset angle associated with either mass. If the joints B and H are connected by revolute-jointed chains of links to stationary points, the equivalent masses can be balanced by adding suitable counterweights to the links in the chains. Thus a guide link may be left uncounterweighted if a suitable counterweight is added to the associated sliding link. Conversely, by a similar argument, a sliding link may remain uncounterweighted if a suitable counterweight is added to the corresponding guide link. This case is illustrated in Figure 11.5b. Again there is no offset angle associated with the masses ascribed to the revolute joints. Since a counterweight is necessary to transfer a mass across a prismatic joint, the transfer is indirect rather than direct.

As noted above, there is usually a choice as to which link shall be left uncounterweighted in a revolute-jointed loop. Leaving a link uncounterweighted has the same effect as cutting the link since it breaks the loop. The selection should therefore be such that any uncounterweighted link is, in effect, only cut once. In a loop containing a prismatic joint, the uncounterweighted link must be one of the two links connected by that joint and the corresponding cut coincides with the joint. Thus, for a linkage containing links with an arbitrary mass distribution, the maximum number of uncounterweighted links equals the number of independent loops. Consequently the minimum number of counterweights, c, is the total number of moving links less the number of independent loops. Using equation (11.2), this gives

$$c = 2n - j \qquad (11.14)$$

11.4. PROCEDURE

The two preceding sections contain the basis for the following procedure which applies to any planar linkage with one or more degrees of freedom and with revolute, and maybe some prismatic, joints.

11.4.1. Check on force-balancing

If for any reason, such as space limitations, a link cannot be counterweighted, that link is considered to be proscribed. For the purposes of this procedure, one of the joints of a proscribed link is treated as a prismatic joint. If the link contains only revolute joints, the appropriate joint is the one that is connected to the frame link by the revolute-jointed chain containing the fewest links.

All of the prismatic joints, both actual and assumed, are disconnected. If this results in any link becoming detached from the chain of links that includes the frame link, then the linkage cannot be force-balanced using simple counterweights. The only exception to this is where the mass centre of the detached links remains stationary throughout the motion of the linkage.

11.4.2. Link ordering

There is a progressive increase in the size of the counterweights required in a revolute-jointed chain of links connecting an uncounterweighted link to the frame link. These chains should therefore be kept short. To this end, all of the moving links are ordered. Those pivoted to the frame are order one links. The (unordered) links connected to the first order links by revolute joints are order two links. This process is continued along each chain until the end of a chain is met due to either the disconnection of a prismatic joint or two chains meeting at a revolute joint. When all of the moving links have been ordered, the prismatic joints, both actual and assumed, are reconnected.

11.4.3. Uncounterweighted links

An uncounterweighted link, i.e. a link which is to remain uncounterweighted, is chosen from each independent loop of links as follows. Each link of the highest order in a separate loop is chosen to be an uncounterweighted link. It is identified as such in one of two ways. If it does not contain a prismatic joint, a cut is made extending from its centre of mass to intersect the arc between the two joints that connect it to lower or equal order links. If the link contains an actual prismatic joint, that joint is disconnected but, for brevity, the link is still regarded as having been cut. If there are two links of the highest order in the same loop, the choice of which link to cut is arbitrary unless one of the two links is proscribed. In this latter case the proscribed link is chosen. Each cut will break at least one loop. If any loops remain, the process is repeated, cutting links of the next highest order and so on, until no loops remain. During this process, no link may be cut more than once. The cut links are the links that are left uncounterweighted.

In a linkage with an arbitrary mass distribution, the number of cut links equals the number of independent loops, namely j-n where j is the effective number of simple joints and n is the effective number of moving links. A simple joint has one degree of freedom and connects two links. Thus a joint connecting k links is counted as (k-1) simple joints. Similarly a joint with two degrees of freedom is counted as two simple joints with an additional moving link. Since this additional link has zero length, it is, of necessity, proscribed. If the corresponding set of independent loops is required, the cuts should be extended until one joint is completely severed from each cut link. The independent loops are formed one at a time when individual severed joints are reconnected.

11.4.4. Chains

Two chains are traced from the mass centre of each link that is to remain uncounterweighted and one chain from the mass centre of each other link to the frame link. The chains run from high order links to links of lower or equal order. A chain may only pass directly from one link to another if a revolute joint connects them and then only through that joint. If a prismatic joint connects them, one of the two links will remain uncounterweighted and the chain may only pass from an actual or effective mass centre in this link to a revolute joint in the other link. The fact that the chain does not pass through the prismatic joint indicates that the transfer is indirect and that a counterweight is necessary to effect it. Apart from this one exception, a chain must pass in a straight line within a link from either a mass centre or a revolute joint to a revolute joint in the same link. A chain may not traverse a cut nor pass through more than two joints in the same link without splitting. A chain splits into two at a revolute joint in an uncounterweighted link that is connected to lower or equal order links by two other joints. For this reason, the cut in that link is regarded as severing only the arc connecting these latter two joints. Chains merge at multiple joints. They may also merge at revolute joints connecting a link to a lower or equal order link.

11.4.5. Counterweight conditions

The links are considered in turn starting with those of the highest order. Before any link is considered, all of the masses ascribed to that link (as a result of chains being incident to the link) must have been determined.

At each of the (j-n-p) uncounterweighted links connected by revolute joints, say B and E as shown in Figure 11.3, to lower or equal order links, masses are ascribed to the revolute joints. A mass of $m_g.r'/\ell$ is ascribed to joint B with an associated offset angle of $(\gamma'+\pi)$ and a mass of $m_g.r/\ell$ is ascribed to

joint E with an associated offset angle of γ where the angles and lengths are as shown in the Figure. If G is the centre of mass of the link, m_g is the mass of the link. Similarly, if G is a revolute joint connecting link BEG to a higher order link, then m_g is the mass ascribed to G from that link and any other links higher than that in the same chain. Any offset angle associated with this mass must be added to the offset angles associated with the masses ascribed to joints B and E. If BEG is an axisymmetric binary link, then γ is zero and the ascribed masses are $m_g.r'/\ell$ at B and $m_g.r/\ell$ at E where m_g is the mass of the link. There are no offset angles associated with these masses in this case.

At each of the p uncounterweighted links containing a prismatic joint, a mass is ascribed to the revolute joint connecting that link to lower or equal order links. The mass is equal to the mass of the link and any masses ascribed to the link. There is no additional offset angle associated with these masses.

The minimum number of counterweighted links, c, is given by

$$c = 2n-j \qquad (11.14$$

Some of these links will contain only revolute joints. At each of these revolute-jointed links, the counterweight must satisfy the condition that

$$\mu.\lambda.e^{i\beta}+m_c.r.e^{i\gamma}+\sum_{k=1}^{h} m_k.\ell_k.e^{i(\gamma_k+\psi_k)}=0 \qquad (11.15$$

where μ = mass of the counterweight,
m_c = mass of the link,
h^c = number of revolute joints to which masses, m_k, have been ascribed from higher order links.
λ, r, ℓ_k = distances measured to the mass centres of μ, m_c and m_k respectively from the revolute joint at which the combined centre of mass may be considered to be,
β, γ, γ_k = corresponding angles measured from a common reference direction as shown in Figure 11.1,
ψ_k = offset angle associated with an ascribed mass, m_k, arising from a revolute-jointed uncounterweighted link.

If h is zero, the corresponding summation is zero.

If a link that is to be counterweighted contains one or more prismatic joints, say s, the counterweight condition contains an extra term to account for the uncounterweighted links connected by those joints. The full condition is

$$\mu.\lambda.e^{i\beta} + m_c.r.e^{i\gamma} + \sum_{k=1}^{h} m_k.\ell_k.e^{i(\gamma_k+\psi_k)} - \sum_{q=1}^{s} \{m_q.r_q.e^{i\gamma_q} + \sum_{u=1}^{v} m_u.\ell_u.e^{i\psi_u}\}\ e^{\pm i\frac{\pi}{2}} = 0 \qquad (11.16$$

where, for the uncounterweighted link connected by the q^{th} prismatic joint to the link being counterweighted, we have

m_q = mass of the link,

v = number of revolute joints in the link to which masses, m_u, have been ascribed from higher order links,

r_q, ℓ_u = distances measured to the mass centres of m_q and m_u respectively from the revolute joint to which those masses are ascribed (this joint is referred to below as the revolute joint),

γ_q, ψ_u = angles between the line from the revolute joint to the prismatic joint and the lines from the revolute joint to the mass centres of m_q and m_u respectively,

$\pm \frac{\pi}{2}$ = angle turned through when traversing from the revolute joint in the uncounterweighted link to the revolute joint in the counterweighted link via the prismatic joint.

Again, if h, s or v are zero, the corresponding summations are zero.

The designer is free to choose the relative values of μ and λ. The mass ascribed to the next lower link in the chain is

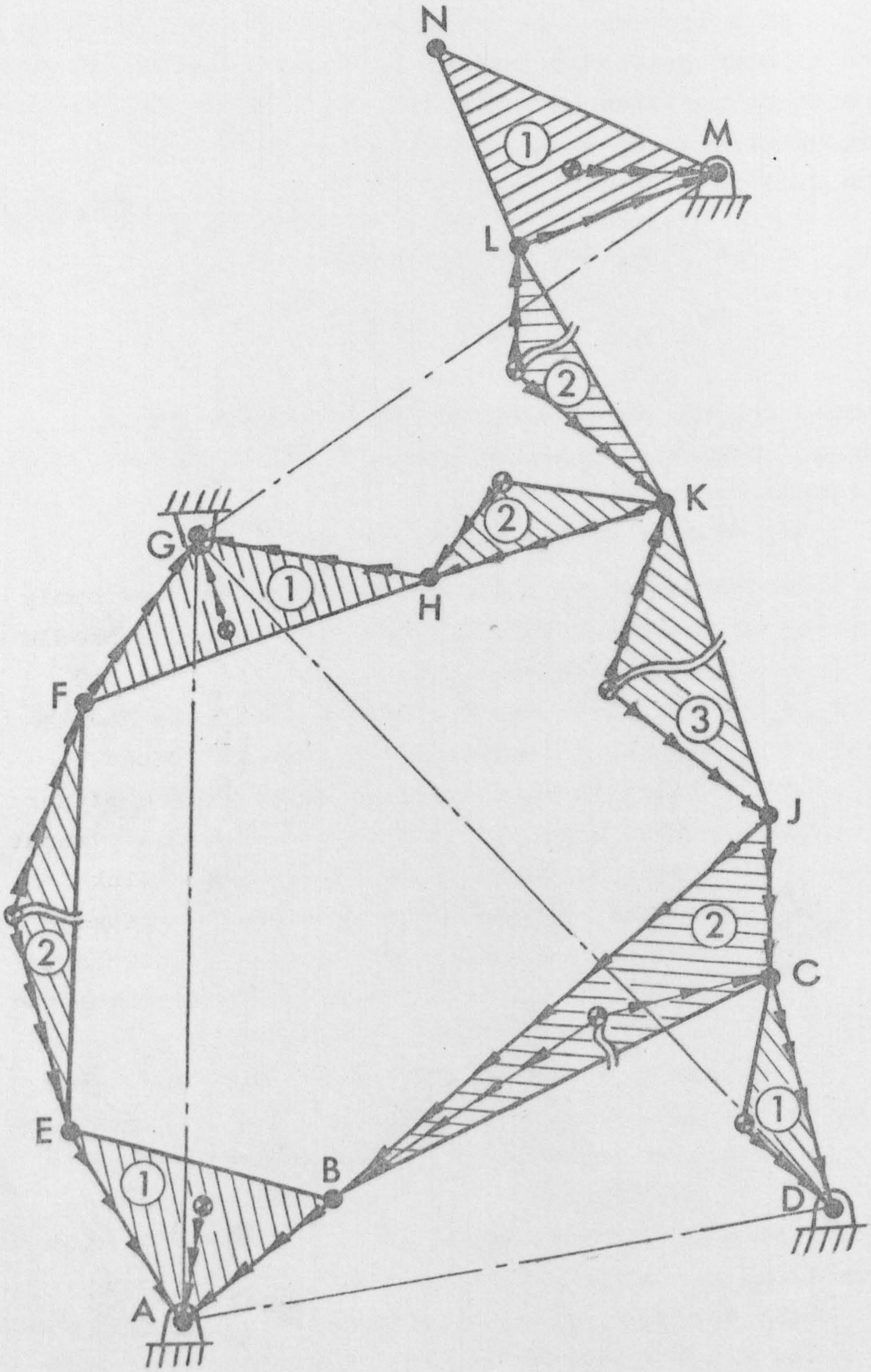

FIGURE 11·6 LINK ORDERING AND CHAINS

$$\mu + m_c + \sum_{k=1}^{h} m_k$$

with offset angles being associated with any of the masses m_k which arise from a revolute-jointed uncounterweighted link other than an axisymmetric binary link.

This process is continued until all of the moving links have been accounted for. The complete set of conditions necessary to obtain a full force-balance of the linkage will then have been obtained.

11.5. EXAMPLE

Figure 11.6 shows the ten-bar linkage previously considered by Smith {11.3}. It is based on the needle mechanism of a warp knitting machine. The original linkage is an earlier version of the needle mechanism used as an example in Section 8.3 and illustrated in Figure 8.4. Both versions of the mechanism are planar linkages with one degree of freedom. The ternary input link, ABE in Figure 11.6, has become a binary link with a double joint in the later version, as has the ternary link FGH. The other difference is that the output from the first loop, ABCD, is now taken from the rocker instead of the coupler. The output member, i.e. the needle, is at point N. The motion of the needle is similar to that shown in Figure 8.6.

All of the joints in the linkage are revolute. In order to provide a direct comparison with Smith {11.3}, each link is assumed to have an offset centre of mass as indicated by the half-filled circles in Figure 11.6. The following description of the process by which the counterweight conditions are obtained is divided into sections which are numbered according to the various stages in the balancing procedure.

11.5.1 Check on force-balancing

Since there are no proscribed links and no prismatic joints, the linkage can be force-balanced.

11.5.2 Link ordering

The moving links are ordered as shown by the numbers in circles. The frame link, ADGM, is left unordered - alternatively it may be considered to be of zero order.

11.5.3 Uncounterweighted links

From equation (11.14), the number of links to be cut and so remain uncounterweighted is four since there are effectively thirteen simple joints, nine moving links and no prismatic joints. The highest ordered link is JK, so this is cut as indicated by the double wavy line in Figure 11.6. There are four second order links - BCJ, EF, HK and KL - remaining in loops. Arc BC of link BCJ is cut and link EF is also cut. Either HK or KL may be cut and we choose KL arbitrarily. Four links have now been cut and, as predicted by equation (11.14), no loops remain. The links that are to remain uncounterweighted are BCJ, EF, JK and KL.

If the cut in BCJ is assumed to sever joint B from that link, then the set of independent loops formed by individually reconnecting the cut links are as follows :

Reconnected link	JK	KL	EF	BCJ
Independent loop	DCJKHGD	GHKLMG	AEFGA	ABCDA

The associated spanning tree consists of the frame link, ADGM, links ABE, CD, FGH, HK, LMN and arc CJ of link BCJ.

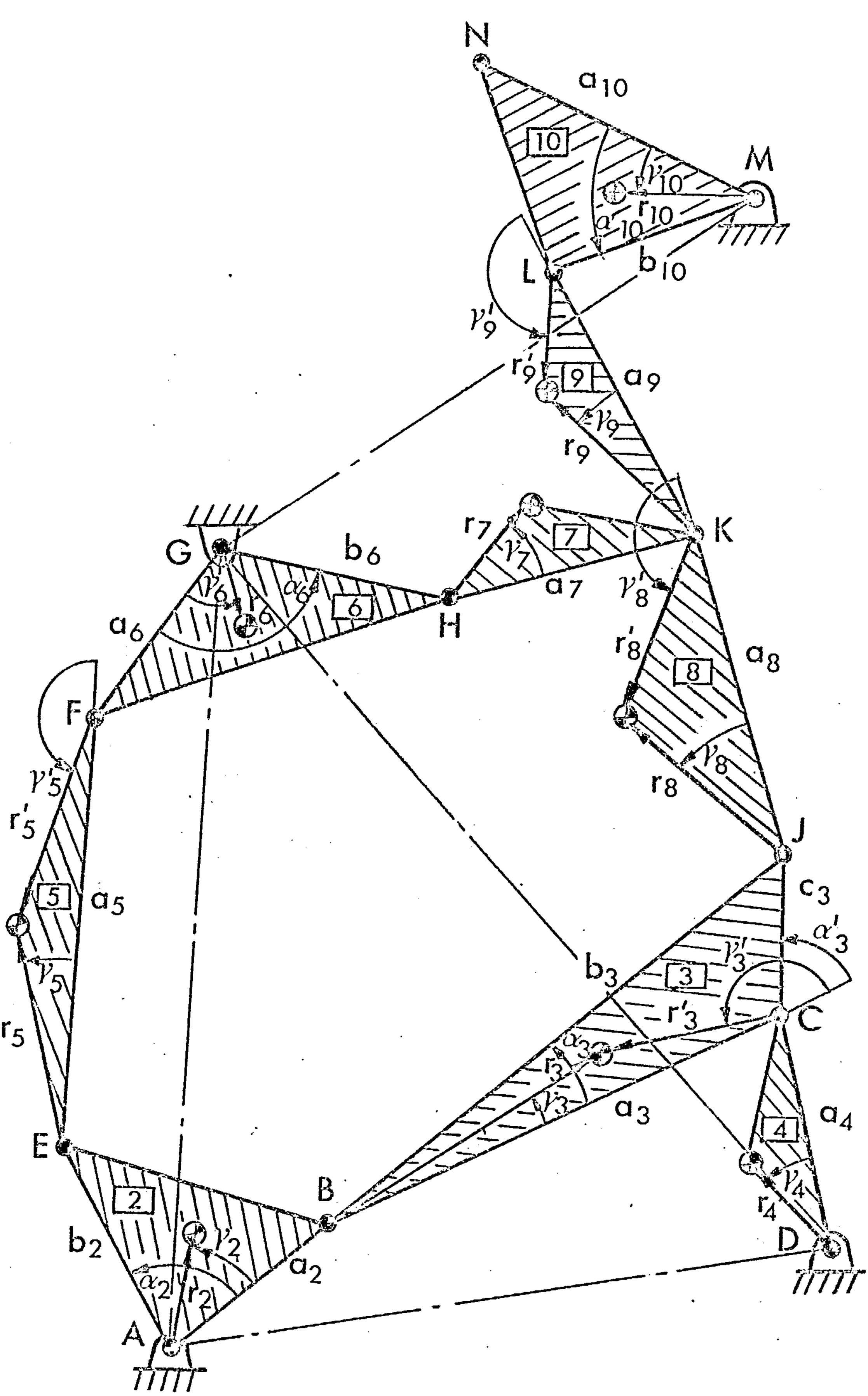

FIGURE 11·7 LINK CONSTANTS

11.5.4. Chains

Two chains are traced from the mass centre of each uncounterweighted link and one chain from the mass centre of each other link to the frame as indicated by the arrowheads in Figure 11.6.

11.5.5. Counterweight conditions

To aid identification of the various quantities used in the counterweight conditions, each link is given a different number. The numbers in rectangles in Figure 11.7 agree with those used by Smith {11.3} and are in no way related to the order numbers. The links are considered in turn. From equation (11.14), four links are to remain uncounterweighted thereby leaving five links to be counterweighted.

(i) Link 8, JK

Starting at the highest ordered link, JK, which is uncounterweighted, a mass of $m_8.r_8'/a_8$ with an offset angle of $(\gamma'_8+\pi)$ is ascribed to J and a mass of $m_8.r_8/a_8$ with an offset angle of γ_8 is ascribed to K.

(ii) Link 9, KL

This link is also uncounterweighted. A mass of $m_9.r_9'/a_9$ with an offset angle of $(\gamma_9'+\pi)$ is ascribed to K and a mass of $m_9.r_9/a_9$ with an offset angle of γ_9 is ascribed to L.

(iii) Link 10, LMN

Since the mass ascribed to this link has been determined, the counterweight condition for this link may be written as follows :

$$\mu_{10}.\lambda_{10}.e^{i\beta_{10}} + m_{10}.r_{10}.e^{i\gamma_{10}} + m_9.\frac{r_9}{a_9}.b_{10}.e^{i(\gamma_9+\alpha_{10})} = 0 \qquad (11.17)$$

where the angles are measured from MN and the lengths from M.

(iv) Link 7, HK

Two masses have been ascribed to K, one from link JK and one from KL. The counterweight for this link must therefore satisfy the following condition :

$$\mu_7 \cdot \lambda_7 \cdot e^{i\beta_7} + m_7 \cdot r_7 \cdot e^{i\gamma_7} + m_8 \cdot \frac{r_8}{a_8} \cdot a_7 \cdot e^{i\gamma_8} + m_9 \cdot \frac{r_9'}{a_9} \cdot a_7 \cdot e^{i(\gamma_9' + \pi)} = 0 \qquad (11.18)$$

where β_7 is measured from HK and λ_7 from H. The effective mass at H is $\{\mu_7 + m_7 + m_8 \cdot r_8/a_8 + m_9 \cdot r_9'/a_9\}$ with offset angles of γ_8 and $(\gamma_9' + \pi)$ associated with the last two terms.

(v) Link 3, BCJ

This is an uncounterweighted link with a mass ascribed to J from link JK. Two masses are ascribed to B, namely $m_3 \cdot r_3'/a_3$ with an offset angle of $(\gamma_3' + \pi)$ from link BCJ and $m_8 \cdot \frac{r_8'}{a_8} \cdot \frac{c_3}{a_3}$ with an offset angle of $(\gamma_8' + \alpha_3')$ from link JK. The corresponding masses ascribed to C are $m_3 \cdot r_3/a_3$ with an offset angle of γ_3 from BCJ and $m_8 \cdot \frac{r_8'}{a_8} \cdot \frac{b_3}{a_3}$ with an offset angle of $(\alpha_3 + \gamma_8' + \pi)$ from link JK.

(vi) Link 4, CD

Taking into account the two masses ascribed above to C, the counterweight for this link must satisfy the condition :

$$\mu_4.\lambda_4.e^{i\beta_4}+m_4.r_4.e^{i\gamma_4}+m_3.\frac{r_3}{a_3}.a_4.e^{i\gamma_3}+m_8.\frac{r_8'}{a_8}.\frac{b_3}{a_3}.a_4.e^{i(\alpha_3+\gamma_8'+\pi)}$$

$$= 0 \qquad (11.19)$$

where β_4 is measured from DC and λ_4 from D.

(vii)Link 5, EF

This is the last uncounterweighted link. A mass of $m_5.r_5'/a_5$ with an offset angle of $(\gamma_5'+\pi)$ is ascribed to E and a mass of $m_5.r_5/a_5$ with an offset angle of γ_5 is ascribed to F.

(viii) Link 6, FGH

Masses have been ascribed to this link at F from link EF and at H from link HK and indirectly links JK and KL. The counterweight for this link must therefore satisfy the condition :

$$\mu_6.\lambda_6.e^{i\beta_6}+m_6.r_6.e^{i\gamma_6}+m_5.\frac{r_5}{a_5}.a_6.e^{i\gamma_5}+(\mu_7+m_7).b_6.e^{i\alpha_6}$$

$$+m_8.\frac{r_8}{a_8}.b_6.e^{i(\alpha_6+\gamma_8)}+m_9.\frac{r_9'}{a_9}.b_6.e^{i(\alpha_6+\gamma_9'+\pi)} = 0 \qquad (11.20)$$

where the angles are measured from GF and the lengths from G.

(ix) Link 2, ABE

Masses have been ascribed to this link at E from link EF and at B from link BCJ and indirectly link JK. The counterweight condition for this link is :

$$\mu_2.\lambda_2.e^{i\beta_2} + m_2.r_2.e^{i\gamma_2} + m_5.\frac{r_5'}{a_5}.b_2.e^{i(\alpha_2+\gamma_5'+\pi)}$$

$$+ m_3.\frac{r_3'}{a_3}.a_2.e^{i(\gamma_3'+\pi)} + m_8.\frac{r_8'}{a_8}.\frac{c_3}{a_3}.a_2.e^{i(\gamma_8'+\alpha_3')} = 0 \quad (11.21)$$

where the angles are measured from AB and the lengths from A.

All of the nine moving links have now been considered, so equations (11.17 - 11.21) are a necessary and sufficient set of conditions for a force balance.

Comparison of this example with Reference {11.3} demonstrates the advantages of using the procedure. The number and complexity of the counterweight conditions is the same in both cases. However the procedure avoids the necessity of deriving the kinematic equations and eliminating the time-dependent terms from them.

11.6 ADDITIONAL MASS

The counterweight conditions govern only the product of the mass of the counterweight and its offset from the combined centre of mass for the link and the counterweight. Hence, to a certain extent, the designer is free to choose the shape and mass of the counterweight. In consequence, no general statement can be made about the increase in mass and inertia when simple counterweights are used to obtain a force balance. However, certain deductions may be made if the effect of various assumptions are observed.

Epstein and Steinvolf {11.8} have shown that for minimum additional inertia, a counterweight should be cylindrical and tangential to the combined centre of mass of the counterweight and the link to which it is attached. This will reduce the increase in the inertia couples due to force-balancing. Assume that the link is rectangular,

of length ℓ and breadth b, and that the counterweight is cylindrical, of radius r with material and thickness the same as those of the link. Assume also that the combined centre of mass is to be at one end of the link. Taking moments about this end, we have

$$\pi r^2 . r = b . \ell^2/2 \qquad (11.22)$$

If the areas and hence masses of the counterweight and link are equal

$$\pi r^2 = b\ell \quad \text{and} \quad r = \ell/2 \qquad (11.23)$$

Substituting for r yields

$$b = \ell . \pi/4 \qquad (11.24)$$

Thus if the breadth of the link is less than $\pi/4$ times its length, then the mass of the counterweight will be greater than that of the link.

Let us assume, therefore, that the mass of any counterweight is equal to or greater than the mass of the link to which it is attached and any masses ascribed to that link. Then, for the linkage in Figure 11.7, we have, from equations (11.17 - 11.21) :

$$\mu_{10} \geq m_{10} + m_9 . r_9/a_9$$

$$\mu_7 \geq m_7 + m_8 . r_8/a_8 + m_9 . r_9'/a_9$$

$$\mu_4 \geq m_4 + m_3 . r_3/a_3 + m_8 . r_8' . b_3/(a_8 . a_3)$$

$$\mu_6 \geq m_6 + m_5 . r_5/a_5 + 2 . m_7 + 2 . m_8 . r_8/a_8 + 2 . m_9 . r_9'/a_9$$

$$\mu_2 \geq m_2 + m_5 . r_5'/a_5 + m_3 . r_3'/a_3 + m_8 . r_8' . c_3/(a_8 . a_3)$$

Adding these gives

$$\Sigma\mu \geq m_2+m_3(r_3+r_3')/a_3+m_4+m_5(r_5+r_5')/a_5$$

$$+m_6+3.m_7+m_8\{3.r_8+r_8'(b_3+c_3)/a_3\}/a_8$$

$$+m_9(r_9+3r_9')/a_9 +m_{10}$$

i.e. $\Sigma\mu \geq \Sigma m + 2\{m_7+m_8.r_8/a_8+m_9.r_9'/a_9\}$

since (r_3+r_3') is greater than a_3 etc. Thus the increase in mass is more than the mass of the original linkage. In particular, it rises as the offset, γ, of any floating link, i.e. not pivotted to the frame, is increased. Furthermore, if a floating link is counterweighted, then the increase in mass is yet higher. The additional mass is equal to the mass of that link and any masses ascribed to it times (2^q-2) where q is the number of counterweighted links in the chain connecting the link concerned to a frame-pivot. This confirms the desirability of keeping the chains short.

The purpose of force-balancing is to prevent the out-of-balance inertia forces due to a mechanism affecting the remainder of the machine of which it forms part. In achieving this aim by adding simple counter-weights, the mass of the linkage may be more than doubled. There will be a corresponding increase in the forces at certain joints. In addition, there will be a considerable increase in the inertia of the links which is likely to result in increased shaking couples. The input torque fluctuations are also likely to be greater. The effect of a full force balance on the forces and moments in a range of four-bar linkages have been considered in detail by Lowen et al. {11.9}. Their conclusions support the deductions above.

Thus in any linkage mechanism that is to be run at high speed, whether force-balanced or not, the links should be as light as possible. This will reduce the

inertia forces and couples due to the link masses and inertias and hence the need for counterweights. If the links are too slender, they may vibrate due to elasticity or even break. Accordingly the remainder of this thesis is concerned with the analysis of vibration in planar linkage mechanisms.

Summary

A linkage in motion is subject to inertia forces and couples arising from the mass and inertia of the moving links. This part of the thesis is concerned with whether these forces can be balanced using simple counterweights. The theory of obtaining a force-balance is presented. It is followed by a procedure which determines how many counterweights are required, to which links they should be attached and what conditions they must satisfy. An example shows that the method is straightforward and simpler than alternative approaches. The discussion leads to the conclusion that, in general, the counterweights will double the mass of a linkage and therefore the original links should be as light as possible.

12. BACKGROUND

12.1. INTRODUCTION

Force-balancing as defined in the preceding chapter is aimed at reducing the vibration in a machine due to out-of-balance forces arising from the mass of the moving links in a constituent linkage mechanism. However the addition of mass for this purpose can cause an increase in the amplitude of the variations in the driving torque, the forces at the joints of the linkage and the shaking moment acting on the frame of the machine. A preferable approach therefore is to reduce the mass of appropriate links. If this is carried too far, it will cause a loss in stiffness which will result in unacceptable vibrations and possibly fatigue of the links themselves. This final part of the thesis is concerned therefore with assessing how light a link may be without the vibration becoming excessive.

The literature on vibration in linkage mechanisms was reviewed by Lowen and Jandrasits {12.1} and Erdman and Sandor {12.2} in 1972. Accordingly the survey that follows is mainly concerned with literature published during the last five years. It is divided into four sections. The first two are devoted to the analysis of linkages containing elastic links. A distinction is drawn between a lumped and a distributed representation of the mass of the links. These sections are followed by one on related investigations and another on the implications of the various investigations for mechanism designers.

Before surveying the literature, it is convenient to delineate the degree of elasticity more closely. It is assumed that the mechanism designer would like every link to be perfectly rigid. Since this is unobtainable in practice, it is assumed that the deflections of the links will be small. Small deflections are said to occur when ϵ^2 is negligible in comparison with ϵ where ϵ is is the strain in a link. Accordingly links as flexible

as those surveyed by Shoup and McLarnan {12.3} are not considered further.

In the case of small deflections, two beam theories are commonly used, namely Euler-Bernoulli and Timoshenko. These theories differ in that the effects of shear deformation and rotary inertia are neglected in the former and taken into account in the latter. The difference in the natural frequencies in bending of a simply supported uniform beam calculated using the two theories is given by McCallion {12.4} as

$$\frac{\omega_{en} - \omega_{tn}}{\omega_{en}} = \frac{\pi^2 n^2 I}{2L^2 A} \left(1 + \frac{E}{kG}\right) \qquad (12.1)$$

where ω_{en} = n th natural frequency using Euler-Bernoulli theory,
ω_{tn} = n th natural frequency using Timoshenko theory,
I = second moment of area of the beam cross-section,
A = cross-sectional area of beam,
L = length of beam,
E = Young's modulus,
G = modulus of rigidity,
k = shear coefficient which depends on the shape of the cross-section, see Cowper {12.5}.

For the difference to be less than 5% for a beam with a rectangular cross-section, this reduces to

$$L/d > 13n \qquad (12.2)$$

where d = depth of cross-section.

Thus the difference in the natural frequencies predicted by the two theories is more pronounced for higher modes of vibration and for beams with a lower length to depth ratio.

12.2. LUMPED MASS REPRESENTATION OF ELASTIC LINKS

The lumped mass approach {12.6 - 12.33} is a finite element technique based on the use of matrices for the analysis of structures. Any linkage may be considered as an instantaneous structure if its rigid body, kinematic degrees of freedom are removed by locking the actuator pairs (defined on page 3-9). Every position of the mechanism corresponds to a different structure and, in addition, the rigid body inertia forces due to the gross

motion of the links must be taken into account.

The linkage is divided into segments and the mass of each segment is lumped at prescribed co-ordinate positions. The segments may correspond to complete links or to parts of the links. Three methods have been used for lumping the mass and these methods may be called end mass, central mass and consistent mass methods respectively.

In the end mass method, half of the mass of each segment is lumped at each end of the segment. If the segment corresponds to the complete link, the masses will be lumped at the joints of each link. The use of this approach for linkage analysis was mooted by Oldham {12.6} in 1964 and later adopted by Erdman {12.7 - 12.9}.

In the central mass method, the mass of each segment is lumped either at the geometric centre or at the centre of mass of the segment. These two positions will coincide for a uniform binary link. Furthermore, if the segments are of equal length as they usually are, the lumped masses will also be equal. This method is favoured by Sadler {12.10 - 12.14} and has been applied by Kohli and Sandor {12.15} to a spatial linkage.

The consistent mass method is based on energy considerations. A mode shape is assumed for the deflected link and the mass is lumped at the prescribed co-ordinates so that the resulting inertia forces produce the assumed deflections at those points. Generally it is assumed that a polynomial can be used to represent the mode shape. Archer {12.16} used a cubic polynomial which gives continuity of displacement and slope at the segment boundaries within a beam. He determined the corresponding mass matrix for a segment of an Euler-Bernoulli beam and compared this method with the end and central mass methods. He found that the percentage difference of the computed natural frequencies from the actual natural frequencies for a uniform beam was an order of magnitude lower using his method. Later {12.17}, he extended this approach to a Timoshenko beam element. Different Timoshenko beam elements have been compared by

D.L. Thomas et al {12.18} and J. Thomas and Abbas {12.19}. All use Hermite interpolation or osculating polynomials.

Boronkay and Mei {12.20} used the Archer {12.16} element suitably modified with a linear function to account for end loading. Imam {12.23 - 12.26} also assumed a cubic polynomial for the transverse deflections and included terms to account for rotary inertia but not shear deformation. Alexander and Lawrence {12.27 - 12.30} and Jones {12.31} used a similar approach. Bahgat and Willmert {12.32} also included rotary inertia effects but used a fifth degree polynomial for the transverse mode shape to maintain continuity of curvature as well as displacement and slope between segments. However, Khan and Willmert {12.33} found that a harmonic series gave better results than a polynomial for constant length segments.

In each case, the elements of the flexibility matrices used by Oldham {12.6} and Erdman {12.7 - 12.9} and the stiffness matrices used by Sadler {12.10 - 12.14} and others {12.21 - 12.33} correspond to the flexibility and stiffness respectively of the segments connecting the co-ordinate positions.

In most of the published work, a damping matrix is used to account for internal damping of the links. This matrix is based on the stiffness and mass matrices. Its elements, C, are given by

$$C_{ii} = 2\zeta_i (K_{ii}/M_{ii})^{\frac{1}{2}} \qquad (12.3)$$

$$C_{ij} = 0, \; i \neq j$$

where ζ = damping factor
K = stiffness matrix element,
M = mass matrix element

Winfrey {12.21} arbitrarily chose a value of 0.15 for the damping factor and this value was adopted by Imam {12.23 - 12.26} . However Alexander and Lawrence {12.27 - 12.29} found that more suitable values for an experimental four-bar linkage with aluminium links were 0.015 for the crank and coupler and 0.03 for the rocker. Accordingly Sadler {12.13} used a value of 0.02.

The simplest method of calculating the elastic deflections in a linkage with elastic links is to assume that the elastic deflections have no influence on the gross motion of the linkage {12.6, 12.7 and 12.21}. The inertia forces and resulting deflections can then be estimated on the basis of a rigid body analysis. However Erdman et al.{12.8} showed that the accelerations due to the elasticity of the links can be of the same order of magnitude as the rigid body accelerations. They therefore solved the differential equations of motion by numerical integration using a fourth order Runge-Kutta algorithm. This method was also adopted by Sadler {12.10 - 12.14} and by Alexander and Lawrence {12.27 - 12.30}. The latter workers assumed that axial deflections can be neglected having found experimentally {12.28} that the peak axial strains were less than 5% of the corresponding peak bending strains. This assumption removes the high frequency components from the equations which can then be solved more rapidly. Imam {12.23 - 12.26} proposed the 'Rate of Change of Eigenvalues and Eigenvectors Method' to speed up the calculation process. Willmert {12.32, 12.33} used harmonic series to obtain the steady state solution.

Golebiewski and Sadler {12.14} investigated the effect of the number of lumped masses per link on the computation time and on the accuracy of the results. They found that the computation time was approximately proportional to $10^{n/3}$, where n is the number of lumped masses per link. Jones {12.31} states that the time is proportional to the cube of the number of degrees of freedom. Consequently there is a considerable incentive to keep the number of lumped masses as low as possible consistent with obtaining the desired accuracy. Imam {12.23 - 12.26} and Alexander and Lawrence {12.27 - 12.30} represented each link by a single segment with two lumped masses. However the resulting deflections are then those corresponding to the first mode of vibration only. The frequency characteristics of the bending strains calculated

by Sadler {12.13} using a three-mass representation for each link in a four-bar linkage are much closer to the experimental results for links with a length/depth ratio of 170 than those obtained by Lawrence and Alexander {12.30} using only two masses per link. Bahgat and Willmert {12.32} concluded that one segment per link is sufficient for a revolute-jointed link but that at least five segments are required if there are any prismatic joints. Golebiewski and Sadler {12.14} felt that five masses per link are desirable when modelling the connecting rod in a slider-crank mechanism. Winfrey {12.22}and Imam {12.23} both proposed methods for reducing the number of co-ordinates to those associated with the points of particular interest in the linkage but noted that the results would be approximate.

One of the problems inherent in the matrix approach is that forces can act only at the co-ordinate positions. The lumped masses can be chosen to give inertia forces that will produce the correct deflections at those points. However the stress distribution resulting from those forces may be completely different from that due to a distributed load such as occurs in practice. Two methods have been proposed to overcome this problem. Sadler {12.10, 12.11} used a comparatively large number (5) of masses per link. The alternative is to assume a mode shape which corresponds to the calculated deflections. The distributed inertia forces which would produce this mode shape can then be calculated and hence the stresses. Imam {12.23 - 12.26} and Bahgat and Willmert {12.32} utilized the polynomials used earlier for determining the consistent mass matrices whereas Alexander and Lawrence {12.27 - 12.30} used the first two normal modes of vibration of a simply-supported uniform beam. This latter approach is commonly used with distributed mass models.

12.3. DISTRIBUTED MASS REPRESENTATION OF ELASTIC LINKS

In the distributed mass approach, each elastic link is treated as an elastic continuum. Certain authors

{12.34 - 12.40} considered just one link in a mechanism to be elastic. Zorzi and Frohrib {12.38} investigated the effect of laminating the elastic material with a viscoelastic layer. Thompson and Barr {12.41} considered both the crank and the connecting rod of a slider-crank mechanism to be elastic whilst Sutherland {12.42, 12,43} considered all three moving links of a four-bar linkage to be elastic. In each case, the effects of gravity and friction at the joints are neglected. In general, the input crank is assumed to rotate at constant speed. The exception is Thompson and Barr {12.41} but these authors did not attempt to solve the final equations of motion.

The elastic links are assumed to vibrate in the plane of the mechanism only. The equations of motion governing the vibrations are derived using either a vectorial or a variational technique. Vectorial techniques are based on Newton's theory which uses two vectors, force and momentum, as fundamental quantities. Thus Smith {12.34 - 12.36} and others {12.37 - 12.39} used a force and moment balance of an element of an elastic link when deriving the equations of motion. On the other hand, variational techniques are based on two scalar quantities - kinetic energy and work function. Thompson and Barr {12.40, 12.41} used Hamilton's principle to formulate the equations of motion. This approach assumes that initial and final positions and times are given. The Hamilton principle of least action then asserts that the actual motion between these end conditions will be that motion for which the time integral of the difference between the kinetic and potential energies is a minimum. The determination of a function to minimize an integral is the essence of variational problems. If the system is conservative, the principle of Euler-Lagrange may be used and this approach was adopted by Sutherland {12.42, 12.43}.

The resulting equations of motion are partial integro-differential equations in time and at least one space variable. Consequently simplying assumptions are made to

make the problem more tractable. Typical assumptions are that the elastic deflections are small so that linear theory is applicable. Furthermore, attention is restricted to the first few (i.e. three or less) modes of vibration so that rotary inertia effects may be neglected. Accordingly Euler-Bernoulli beam theory is used. Longitudinal extension is commonly neglected when calculating joint motion. Smith {12.34 - 12.36} and Sutherland {12.42, 12.43} further assumed that only terms that are linear in the transverse direction and their derivatives should be retained in the equations of motion. This is equivalent to assuming that the distributed axial forces may be calculated on the basis of a rigid body force analysis. However, Vinogradov {12.44} showed that as the input speed of a particular four-bar linkage is varied between 600 and 1800 rev/min the bearing loads are between 1.07 and 2.22 times those due to rigid body calculations alone. In each case, the effect of the axial forces on the transverse deflections is taken into account. Since the axial forces vary with time, they can give rise to parametric instability in addition to the possibility of resonance due to the transverse forces. This aspect has been investigated by several authors {12.34 - 12.39}.

Reference is made in the literature under review to two methods for solving the simplified equations of motion. The methods are those of Galerkin and Kantorovich and a brief description follows based on Kantorovich and Krylov {12.45} and Forray {12.46}. It is assumed that a partial differential equation with two independent variables, say x and t, and one dependent variable, say y, is to be solved subject to boundary conditions which define a domain D.

In the Galerkin method, an approximate solution of n terms is assumed. Substitution of this into the differential equation will yield a residual $R_n(x,t)$ which can be regarded as an error function. The solution is assumed to be of the form :

$$Y_n = \sum_{k=1}^{n} a_k \cdot \phi_k(x,t) \qquad (12.4)$$

where a_k = constants to be determined,
$\phi_k(x,t)$ = set of co-ordinate functions that satisfy the boundary conditions and are orthogonal to each other and $R_n(x,t)$.

Since the functions are orthogonal, we have

$$\iint_D R_n(x,t) \cdot \phi_k(x,t) \cdot dx.dt = 0 \quad (k = 1,2,...n) \qquad (12.5)$$

which results in a system of n linear equations in the n unknowns, $a_1, a_2, \ldots, a_n$. This method is equivalent to the requirement that the virtual work due to the external loads acting on the elements of a system shall be zero for n virtual displacements.

In the Galerkin method, the complete form of the solution is chosen a priori and only constants are to be determined. In contrast, Kantorovich proposed that a more accurate solution would be obtained by leaving the function of one or more variables (rather than constants) to be determined. Thus a solution is assumed of the form

$$y_n = \phi_o(x,t) + \sum_{k=1}^{n} c_k(t) \cdot \phi_k(x,t) \qquad (12.6)$$

where $\phi_o(x,t)$ = a function that accommodates nonhomogeneous boundary conditions,
$c_k(t)$ = functions to be determined of the variable t.

The determination of a set of functions to minimize the residual is a variational problem. The functions must therefore satisfy the corresponding Euler equations. This method reduces the solution of a partial differential equation to that of solving sets of ordinary differential equations.

In practice a modified Kantorovitch method has been used with

$$\phi_k(x,t) = \sin k\pi x/\ell \qquad (12.7)$$

where ℓ is the length of the link.
However, instead of obtaining the solution of the resulting ordinary differential equations analytically, the response

is obtained numerically using either a Kutta Merson algorithm {12.36, 12.42, 12.43} or a fourth order Runge Kutta algorithm {12.37}. As alternatives to these algorithms, Smith {12.36} used an algorithm by de Vogelaere while Chu and Pan {12.37} used a piecewise polynomial technique. Sutherland {12.43} considered the use of

$$c_k(t) = \frac{a_o}{2} + \sum_{j=1}^{m} (a_j \cos_j \omega t + b_j \sin_j \omega t) \qquad (12.8)$$

He would then have been using the Galerkin method. However he decided that he would have required a large number of terms to obtain reasonable accuracy so he concluded that a numerical integration approach was preferable.

Sutherland {12.42, 12.43} compared his theoretical results with experimental results from a four-bar linkage where the brass coupler and rocker had a length/depth ratio of 320. The phase relationship for the rocker motion was within two degrees of crank rotation and the magnitude of the deviation from rigid body calculations was within 10%. High speed photographs showed that the actual deflected shapes corresponded closely to the sinusoidal shape assumed in equation (12.7) with k equal to one i.e. first mode only. Smith {12.36} using steel couplers with length/depth ratios of 240, 320 and 480 found that the second and third mode shapes became visible at the onset of instability but at that stage the assumption of small deflections was no longer valid. Thus the restriction of the deflected shape to the first mode is valid only if the linkage is operated in a stable region.

12.4. RELATED INVESTIGATIONS

So far the effect on the motion of a linkage mechanism of one or more moving links being elastic has been considered in this review. Related investigations have also been carried out during the same period. Rose and Schrepfer {12.47} and Funabashi and Ogawa {12.48} investigated experimentally the effect of using spring-loaded telescopic links. A variety of elastic connections have been considered.

Thus Meyer zur Capellen and Krumm {12.49} elastically suspended the coupler of a four-bar linkage while Chakraborty and Khare {12.50} flexibly attached the slider to a crank-slider mechanism. Davidson {12.51} mounted a four-bar linkage on flexible supports while Kohli and Sandor {12.52} combined this with torsionally elastic input and output shafts. Thompson and Ashworth {12.53} considered the effect of vibrating the frame in a direction perpendicular to the plane of the mechanism. Finally Dubowsky et al.{12.54 - 12.56} have investigated the effects of clearance at the joints in addition to link elasticity.

12.5. IMPLICATIONS FOR DESIGN

Imam et al. {12.8, 12.23, 12.25, 12.26} have proposed that high-speed linkages should be designed in two stages. The first consists of a kinematic synthesis to determine the link lengths. Freudenstein {12.57} recommended that, for high-speed operation of a crank-rocker four-bar linkage, the coupler and rocker should be of equal length, the crank should be short compared to the frame link and the transmission angle should be as close to a right angle as possible. Sutherland {12.43} showed that the last conclusion is still valid when the moving links are elastic. The links should also be as short as possible.

The second stage is to optimize the cross-sections of the links using elastodynamic criteria such as stress and deflection. Imam {12.23, 12.26} found that a rectangular cross-section gives much lighter links (about 1/7 of the mass) than a circular cross-section for a criterion of maximum deflection. Sadler {12.10, 12.11} investigated the effect of varying the cross-section along the length of the connecting rod in a crank-slider mechanism. A link with a single taper along its length scarcely reduced the stress levels compared with a uniform link of the same mass. In contrast, a uniform strength link which, in effect, is tapered at both ends reduced the maximum stress and deflection by about 30%.

12.6. COMMENTS

All of the reported experimental work has been carried out on slender links with length/depth ratios between 120 and 480 since it is then easier to obtain measurable strains. Consequently Euler-Bernoulli beam theory is shown to be applicable. However industrial linkages tend to contain links with much lower length/depth ratios. Typical values in linkages operating at 1000 rev/min or above seem to be in the range 2 to 22. With these values, particularly at the lower end of the range, vibration of the links is likely to be less of a problem than out-of-balance and clearance effects. The question still remains however of how slender the links could be.

The survey has shown that there are a variety of methods available for analyzing a linkage with elastic links. Before employing these techniques, the machine designer will want a reasonable estimate of the cross-section of the links. The emphasis in the chapters that follow is therefore on the development of guidelines for machine designers to enable them to choose suitable cross-sections for links that are to be operated at high speed.

Summary

If the stiffness of a link is reduced too far in an effort to lighten the link, the link will vibrate. This is likely to affect detrimentally the performance of the linkage containing it. This chapter surveys the literature published during the last five years about linkages containing elastic links. Two approaches have been used. The lumped mass representation is a finite element method. The number and characteristics of the elements are considered. The distributed mass approach treats the link as an elastic continuum. The use of the Galerkin and Kantorovich methods to solve simplified forms of the partial integro-differential equations of motion is reviewed. The implications of this work for linkage designers is noted.

13. GENERAL THEORY

13.1. SCOPE

The preceding chapter has shown that there is a need for a method to assess, assuming stability, the forced vibration of a link that may be regarded as a Timoshenko beam with an end-load varying with time. Accordingly the equations of motion for a revolute-jointed, uniform, binary link satisfying this requirement are derived in this chapter. These equations are complicated and the designer, before applying them, will wish to check that any cross-section proposed for the link is reasonable. A simplified equation of motion is derived therefore for an Euler-Bernoulli link and the corresponding equations that define the regions of stable operation for the link are given. This leads to a logical procedure for designing a linkage.

Before deriving these equations, the effect of damping should be considered. Lazan {13.1} suggests that the following equation gives sufficient accuracy for engineering purposes for the internal damping of most metals including grey iron, mild steel, aluminium, magnesium and titanium alloys:

$$D = (\sigma_a/\sigma_f)^{2.3} + 6(\sigma_a/\sigma_f)^8 \qquad (13.1)$$

where D = energy absorbed per unit volume of material per cycle of loading,
σ_a = amplitude of induced stress,
σ_f = fatigue strength of the material at 2×10^7 cycles.

The equation applies in cases where σ_a/σ_f is greater than 0.05. Thus the higher the stress level, the more significant is material damping. Its effect is to increase the stable regions of operation of the mechanism. Consequently a theory that neglects material damping will err on the safe side. The same argument applies to

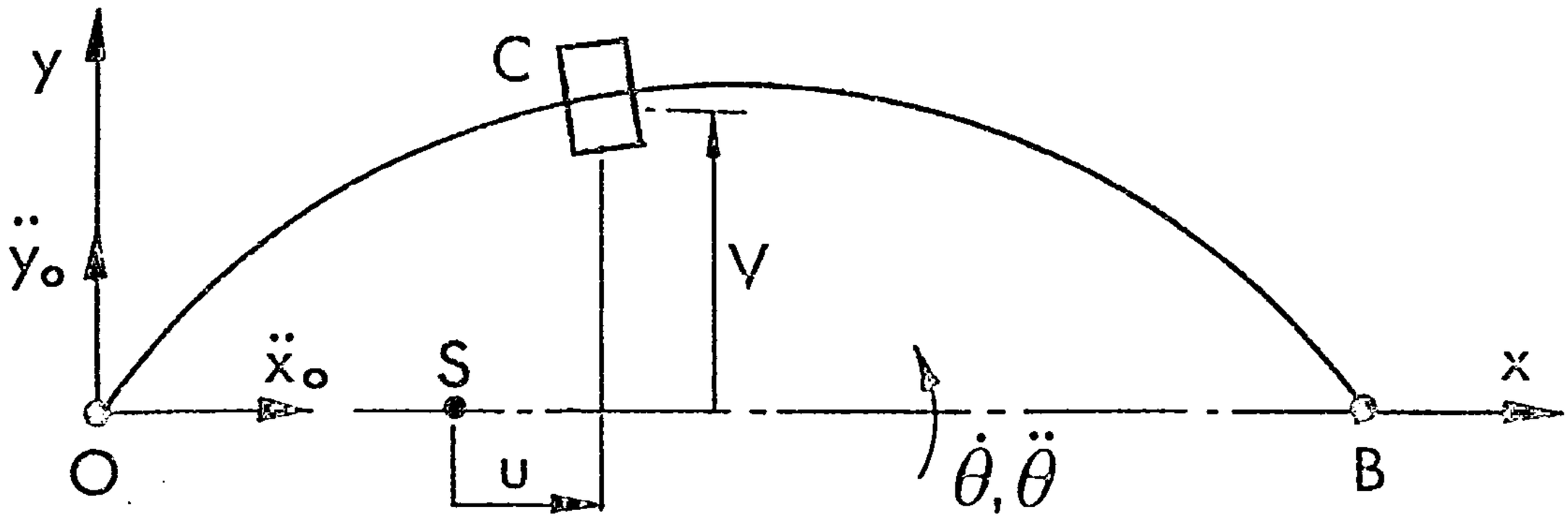

FIGURE 13.1 REVOLUTE - JOINTED BINARY LINK

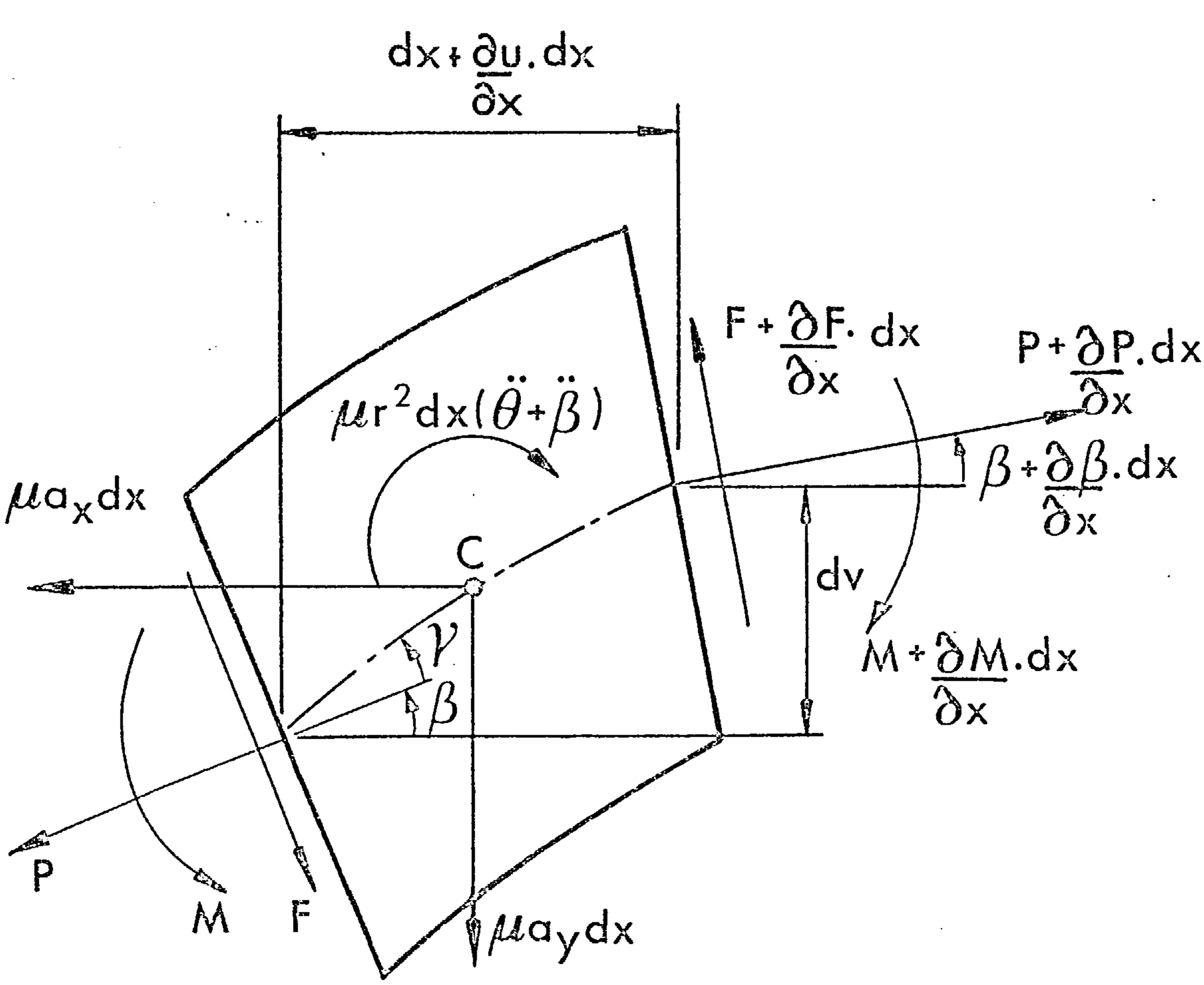

FIGURE 13.2 BINARY LINK ELEMENT

damping at the joints of a mechanism. Hence these aspects of damping and friction are neglected in the theory which follows.

Since beam-like links are being considered, the effects of Poisson's ratio are neglected. Accordingly it is assumed that the following relationships hold for link materials:

$$\sigma = E.\varepsilon$$
$$\tau = G.\gamma \qquad (13.2)$$

where σ, ε = direct stress and strain,
τ, γ = shear stress and angle of shear at the neutral axis of the link,
E, G = Young's modulus and shear modulus of the link material.

13.2. TIMOSHENKO LINK

Consider the binary link shown in Figure 13.1 with revolute joints at O and B. Assume that its width is small compared to its length. Define a Cartesian co-ordinate system such that O is the origin and the x-axis passes through B. Let the components of the absolute acceleration of O be $\ddot{x}_o$ and $\ddot{y}_o$ as shown. Let the centre of mass of the short element originally at S with co-ordinates (x,O) move to C with co-ordinates (x+u,v) under the action of the various forces. Then the absolute acceleration of the element equals the sum of the acceleration of O and the acceleration of the element relative to O. Using a dot to denote differentiation with respect to time, the components of this acceleration are:

$$a_x = \ddot{x}_o + \ddot{u} - v\ddot{\theta} - (x+u)\dot{\theta}^2 - 2\dot{v}\dot{\theta} \qquad (13.3)$$
$$a_y = \ddot{y}_o + \ddot{v} - v\dot{\theta}^2 + (x+u)\ddot{\theta} + 2\dot{u}\dot{\theta}$$

where a_x, a_y = absolute acceleration of the element in the x and y directions respectively,
$\dot{\theta}, \ddot{\theta}$ = angular velocity and acceleration respectively of the x-axis.

An enlarged view of the element is shown in Figure 13.2. Let

dx = unstressed length of the element,
μ = mass per unit length,
A = area of cross-section,
k = radius of gyration of cross-section,
P = longitudinal force at x,
F = shear force at x,
M = bending moment at x,
β = angle between the cross-section at x and the y-axis.

The positive directions of the forces acting on the element are as shown. Resolving the forces parallel to the x-axis, we have:

$$\mu a_x.dx + P\cos\beta + (F+\frac{\partial F}{\partial x}.dx)\sin(\beta+\frac{\partial \beta}{\partial x}.dx)$$

$$= F\sin\beta + (P+\frac{\partial P}{\partial x}.dx)\cos(\beta+\frac{\partial \beta}{\partial x}.dx) \qquad (13.4)$$

Resolving the forces parallel to the y-axis, we have:

$$\mu a_y.dx+P\sin\beta + F\cos\beta = (F+\frac{\partial F}{\partial x}.dx)\cos(\beta+\frac{\partial \beta}{\partial x}.dx)$$

$$+ (P+\frac{\partial P}{\partial x}.dx)\sin(\beta+\frac{\partial \beta}{\partial x}.dx) \qquad (13.5)$$

One effect of the shear force is to increase the angle between the x-axis and the line of centroids (shown chain-dotted) from β to (β+γ). As a result, the longitudinal forces, P, produce a moment acting on the element. Taking moments about the centre of mass, C, of the element, we have:

$$\{P\sin\gamma/\cos(\beta+\gamma)+(P+\frac{\partial P}{\partial x}.dx)\sin(\gamma+\frac{\partial \gamma}{\partial x}.dx)$$

$$/\cos(\gamma+\frac{\partial \gamma}{\partial x}.dx+\beta+\frac{\partial \beta}{\partial x}.dx)-F\cos\gamma/\cos(\beta+\gamma)$$

$$-(F+\frac{\partial F}{\partial x}.dx)\cos(\gamma+\frac{\partial \gamma}{\partial x}.dx)/\cos(\gamma+\frac{\partial \gamma}{\partial x}.dx+\beta+\frac{\partial \beta}{\partial x}.dx)\}$$

$$.\{1+\frac{\partial u}{\partial x}\}\frac{dx}{2}+\frac{\partial M}{\partial x}.dx+\mu k^2(\ddot{\theta}+\ddot{\beta})dx = 0 \qquad (13.6)$$

The direct strain, ε, is given by:

$$dx(1+\varepsilon) = dx(1+\partial u/\partial x)\ \cos\gamma/\cos(\beta+\gamma) \qquad (13.7)$$

As implied above, the total deflection of the line of centroids is the sum of the deflections due to the bending moment and the shear force. Thus if the deflections are small enough for the simplified expression for the radius of curvature to be used, we have:

$$M = -AEk^2 \frac{\partial \beta}{\partial x} \qquad (13.8)$$

Another effect of shear is to warp the cross-section. The resulting non-uniform distribution of shear stress and strain is accounted for by introducing a dimensionless shear coefficient, s, which depends on the shape of the cross-section. Accordingly the effective shear strain is taken to be equal to the average shear stress over a cross-section divided by the product of the shear modulus and the shear coefficient (see Cowper {13.2}), i.e.

$$\gamma = \frac{F}{sAG} \qquad (13.9)$$

Equations (13.4-13.8) simplify if we assume that the deflections are small as well as the length of the element. In this case, β, $\frac{\partial \beta}{\partial x}$, γ, $\frac{\partial \gamma}{\partial x}$ and dx are small so that we may take:

$$\sin\beta = \beta \qquad \beta+\gamma = \frac{\partial v}{\partial x}\left(1-\frac{\partial u}{\partial x}\right)$$

$$\cos\beta = \cos\left(\frac{\partial \beta}{\partial x}.dx\right) = 1 \qquad \sin\left(\frac{\partial \beta}{\partial x}.dx\right) = \frac{\partial \beta}{\partial x}.dx \qquad (13.10)$$

$$\cos\gamma = \cos\left(\frac{\partial \gamma}{\partial x}.dx\right) = 1 \qquad \sin\left(\frac{\partial \gamma}{\partial x}.dx\right) = \frac{\partial \gamma}{\partial x}.dx$$

In general, F and P may differ by an order of magnitude. Accordingly, when equations (13.10) are substituted in equations (13.4-13.8), terms that differ by only one order of magnitude are retained. This yields:

$$\mu a_x + \frac{\partial}{\partial x}(F\beta) = \frac{\partial P}{\partial x}$$

$$\mu a_y = \frac{\partial F}{\partial x} + \frac{\partial}{\partial x}(P\beta)$$

$$\frac{\partial M}{\partial x} + \mu k^2(\ddot{\theta}+\ddot{\beta}) + (P\gamma-F)(1+\frac{\partial u}{\partial x}) = 0 \qquad (13.11)$$

$$\frac{\partial u}{\partial x} = \varepsilon - \frac{\beta^2}{2} - \beta\gamma$$

$$M = AEk^2\{\frac{\partial \gamma}{\partial x} + \frac{\partial v}{\partial x}.\frac{\partial^2 u}{\partial x^2} - \frac{\partial^2 v}{\partial x^2}(1 - \frac{\partial u}{\partial x})\}$$

The fourth of these equations shows that the effect of bending is to draw the ends of the link towards each other and is increased by the effect of shear. Thus the total elongation of the element equals the direct extension minus the bending and shear displacements. From this equation and equation (13.2), it follows that:

$$P = AE(\frac{\partial u}{\partial x} + \frac{\beta^2}{2} + \beta\gamma) \qquad (13.12)$$

Eliminating, P, M, β and γ from equations (13.11) and (13.12) and substituting for a_x and a_y from equations (13.3) leads to:

$$\frac{\partial}{\partial x}(\frac{F}{\mu}.\frac{\partial v}{\partial x}) - \frac{F}{\mu sAG}.\frac{\partial F}{\partial x}(2+\frac{E}{sG}) - \frac{AE}{\mu}(\frac{\partial^2 u}{\partial x^2} + \frac{\partial v}{\partial x}.\frac{\partial^2 v}{\partial x^2})$$

$$+ \ddot{x}_o + \ddot{u} - v\ddot{\theta} - (x+u)\dot{\theta}^2 - 2\dot{v}\dot{\theta} = 0 \qquad (13.13)$$

$$\frac{1}{\mu}\cdot\frac{\partial F}{\partial x}\left(\frac{E}{sG}\cdot\frac{\partial u}{\partial x}-1\right)+\frac{F}{\mu}\cdot\frac{E}{sG}\cdot\frac{\partial^2 u}{\partial x^2}-\frac{AE}{\mu}\cdot\frac{\partial}{\partial x}\left(\frac{\partial u}{\partial x}\cdot\frac{\partial v}{\partial x}\right)$$

$$+\ddot{y}_o+\ddot{v}-v\dot{\theta}^2+(x+u)\ddot{\theta}+2\dot{u}\dot{\theta}=0 \qquad (13.14)$$

$$\frac{F}{\mu k^2}\left(\frac{E}{sG}\cdot\frac{\partial u}{\partial x}-\frac{\partial u}{\partial x}-1\right)+\frac{E}{\mu sG}\cdot\frac{\partial^2 F}{\partial x^2}-\frac{AE}{\mu}\left\{\frac{\partial^3 v}{\partial x^3}-\frac{\partial^2}{\partial x^2}\left(\frac{\partial u}{\partial x}\cdot\frac{\partial v}{\partial x}\right)\right\}$$

$$+\ddot{\theta}+\frac{\partial\ddot{v}}{\partial x}-\frac{\partial}{\partial t^2}\left(\frac{\partial u}{\partial x}\cdot\frac{\partial v}{\partial x}\right)-\frac{\ddot{F}}{sAG}=0 \qquad (13.15)$$

These equations assume that the cross-sectional properties, A, k and s, and the material properties, E, G and μ, are constant along the length of the link.

If the joints are at the ends of the link so that there is no moment at a joint caused by an overhanging portion of the link, some of the boundary conditions for these equations are:

$$u = 0 \text{ at } x = 0,$$

$$v = 0 \text{ at } x = 0 \text{ and } L, \qquad (13.16)$$

$$\frac{\partial^2 v}{\partial x^2} = \frac{1}{sAG}\cdot\frac{\partial F}{\partial x}\left(1+\frac{\partial u}{\partial x}\right) \quad \text{at } x = 0 \text{ and } L$$

where L = length of the link.
The other boundary conditions are determined by the remainder of the linkage of which the link under consideration forms part.

The following terms are those due to shear deformation:

$$\frac{\partial}{\partial x}\left(\frac{F}{\mu}\cdot\frac{\partial v}{\partial x}\right)-\frac{F}{\mu sAG}\cdot\frac{\partial F}{\partial x}\left(2+\frac{E}{sG}\right) \text{ in equation (13.13),}$$

$$\frac{1}{\mu}\cdot\frac{\partial F}{\partial x}\left(\frac{E}{sG}\cdot\frac{\partial u}{\partial x}-1\right)+\frac{F}{\mu}\cdot\frac{E}{sG}\cdot\frac{\partial^2 u}{\partial x^2} \text{ in equation (13.14),}$$

$\frac{F}{\mu k^2}\left(\frac{E}{sG}\cdot\frac{\partial u}{\partial x}\frac{\partial u}{\partial x}-1\right)-\frac{\ddot{F}}{sAG}$ in equation (13.15).

Similarly rotary inertia accounts for the terms:

$\ddot{\Theta}+\frac{\partial\ddot{v}}{\partial x}-\frac{\partial}{\partial t^2}\left(\frac{\partial u}{\partial x}\cdot\frac{\partial v}{\partial x}\right)-\frac{\ddot{F}}{sAG}$ in equation (13.15).

At this stage, it is desirable to check that the equations of motion reduce to a standard form in a special case. For a non-rotating link with no end load and neglecting longitudinal deformation, we have:

$$a_x = \ddot{x}_o = \ddot{y}_o = \ddot{\Theta} = \dot{\Theta} = \partial u/\partial x = 0$$

Substituting these values into equations (13.14) and (13.15) and eliminating F leads to:

$$\frac{AE}{\mu}\cdot\frac{\partial^4 v}{\partial x^4}+\frac{1}{k^2}\cdot\frac{\partial^2 v}{\partial t^2}-\left(1+\frac{E}{sG}\right)\frac{\partial^4 v}{\partial x^2\,\partial t^2}+\frac{\mu}{sAG}\cdot\frac{\partial^4 v}{\partial t^4}=0 \qquad (13.17)$$

This agrees with the equation of motion for the transverse vibration of a uniform beam including shear and rotary inertia effects as given by Timoshenko, Young and Weaver {13.3}. Equation (13.13) is concerned with longitudinal effects and is therefore not of interest in this case. Equation (13.17) has been solved by Anderson {13.4} who found that the vibrations of the lower modes in slender beams are predominantly in bending while those of the higher modes in thick beams are predominantly in shear.

Equations (13.13 - 13.15) can be used to predict the response of a straight, uniform, binary link having revolute joints at its ends and proportions as used in industry for any planar linkage where there is no offset between the links. However they are too complex to provide guide-lines for the design of such links and so further simplifying assumptions must be made for this purpose.

13.3 EULER-BERNOULLI LINK

Longitudinal deformation of a link will affect the motion of the links that are driven by the link in question. As a result, the motion of these links, even if they are rigid, cannot be calculated from a rigid-link analysis. However, longitudinal deformation is much less than the bending deformation for most revolute-jointed, binary links and so can be neglected if a first order approximation to the motion of that particular link is all that is required. Accordingly longitudinal deformation is neglected in the theory that follows. At the same time, shear deformation and rotary inertia are neglected as these are also second order effects. The result is to assume that Euler-Bernoulli beam theory is applicable. In this case, equations (13.3) and (13.11) simplify to:

$$\mu(\ddot{x}_o - v\ddot{\theta} - x\dot{\theta}^2 - 2\dot{v}\dot{\theta}) = \frac{\partial P}{\partial x} - \frac{\partial}{\partial x}\left(F.\frac{\partial v}{\partial x}\right) \qquad (13.18)$$

$$\mu(\ddot{y}_o + \ddot{v} - v\dot{\theta}^2 + x\ddot{\theta}) = \frac{\partial F}{\partial x} + \frac{\partial}{\partial x}\left(P.\frac{\partial v}{\partial x}\right) \qquad (13.19)$$

$$F + AEk^2.\ \frac{\partial^3 v}{\partial x^3} = 0 \qquad (13.20)$$

Again assuming no overhang of the link beyond the joints, the boundary conditions for v are:

$$v = \frac{\partial^2 v}{\partial x^2} = 0 \quad \text{at } x = 0 \text{ and } L \qquad (13.21)$$

Equations (13.18) and (13.19) may be reduced to ordinary differential equations using the method of Kantorovich described on page 12-9. If the mechanism is operating under steady-state conditions, it may be

assumed that the solution of the equations of motion will take the form:

$$v = \sum_j Q_j(t).f_j(x) \qquad j = 1,2,....,m \tag{13.22}$$

where Q and f are appropriate orthogonal functions. The natural modes of vibration in bending satisfy the boundary conditions given in equations (13.21) and so are appropriate functions for $f_j(x)$. Hence for a uniform, revolute-jointed, binary link with no overhang, we may assume that:

$$f_j(x) = \sin\ (j\pi x/L) \tag{13.23}$$

Substituting equations (13.22) and (13.23) into equations (13.18 - 13.20) and eliminating F leads to a second order differential equation which may be simplified by using the orthogonality condition. This involves multiplying through by $\sin(j\pi x/L)$ and integrating over the length of the link. Since equations (13.18) and (13.19) represent the change in the forces along the link, this is equivalent to using the principle of virtual work. The multiplying factor, $\sin(j\pi x/L)$, can be regarded as an arbitrary variation which satisfies the geometric constraints. The subsequent integration over the length of the link leads to virtual work expressions which must be zero. Neglecting the products of small quantities, this yields:

$$\ddot{Q}_j + \{\frac{EAk^2}{\mu}(j\frac{\pi}{L})^4 + (\frac{T}{\mu} - \ddot{x}_o.\frac{L}{2})(j\frac{\pi}{L})^2 + (j^2.\frac{\pi^2}{3} - \frac{5}{4})\dot{\theta}^2\}\ Q_j$$

$$+ \frac{2}{j\pi}\{\ddot{y}_o - (\ddot{y}_o + \ddot{\theta}.L)(-1)^j\} = 0 \tag{13.24}$$

where T = external, time-varying, tensile force acting longitudinally on the link at x = L.

Thus the set of three partial differential equations has been reduced to a single ordinary differential equation with time-varying coefficients.

In an earlier investigation, Smith and Maunder {13.5} neglected the variation in the axial force along the link, i.e. they assumed $\partial P/\partial x = 0$. As a result, they obtained the following equation:

$$\ddot{Q}_j + \{\frac{EAk^2}{\mu}(j\frac{\pi}{L})^4 + \frac{T}{\mu}(j\frac{\pi}{L})^2 - \dot{\theta}^2\} Q_j + \frac{2}{j\pi}\{\ddot{y}_o - (\ddot{y}_o + \ddot{\theta}.L)(-1)^j\} = 0$$

Comparison with equation (13.24) shows the assumption to be that:

$$j^2\pi^2(\frac{\dot{\theta}^2}{3} - \frac{\ddot{x}_o}{2L}) - \frac{\dot{\theta}^2}{4} << \dot{\theta}^2$$

Even for the first mode of vibration (when $j = 1$), the coefficient of $\dot{\theta}^2$, namely $(\frac{\pi^2}{3} - \frac{1}{4})$, is not negligible compared to unity and so should appear in the equation of motion. In general, it cannot be assumed that $\ddot{x}_o << \dot{\theta}^2.L$ and so the term $j^2\pi^2\ddot{x}_o/2L$ must also appear.

Returning to equation (13.24), the coefficients of the Q_j term and the inhomogeneous term (not involving Q_j) form two distinct groups. The first term in the coefficient of Q_j is related to the j^{th} Euler buckling load, P_{crj}, as follows:

$$\frac{EAk^2}{\mu}(j\frac{\pi}{L})^4 = \frac{P_{crj}}{\mu}(j\frac{\pi}{L})^2$$

It is time-invariant and is the square of the j^{th} natural frequency in bending of a stationary link with no end load. When the link is moving, there are three additional time-varying terms, all associated with forces acting along the link. The first of these terms is due to the end load arising from the reaction of the links being driven by the link under consideration.

The second and third terms result from the longitudinal acceleration and angular velocity of the link itself.

The coefficient of the inhomogeneous term contains two terms. These are associated with the two rigid-body components of transverse acceleration of the link - that due to the linear acceleration of the driven end and that due to the angular acceleration of the link. The former contributes only to the odd modes of vibration. This is consistent with the linear acceleration acting on the uniform link to produce a uniformly-distributed inertia load for which the Fourier half-series contains only odd terms. In contrast, the angular acceleration contributes to both odd and even modes since it produces a sawtooth-distributed inertia load for which the Fourier series contains both odd and even terms.

Equation (13.24) takes the form of an inhomogeneous Hill's equation with three periodic terms in the coefficient of Q_j. To examine the conditions for the equation to yield stable solutions, the homogeneous form of the equation is considered. If the elastic link forms part of a linkage with prescribed kinematic characteristics and also drives links with fixed dynamic characteristics, this may be written as:

$$\ddot{Q}_j + \{\Omega^2 + e\,.g(t) + h(t)\}\, Q_j = 0 \qquad (13.25)$$

where $\Omega = (j\frac{\pi}{2})^2 \,.\, (\frac{E}{\rho}k^2)^{\frac{1}{2}}$, the j^{th} natural frequency in bending,

$$e = (j\frac{\pi}{L})^2 . \frac{1}{\rho A},$$

ρ = mass density of the link material.

The two periodic terms dependent on the kinematics of the linkage have been subsumed into the one term h(t). It is necessary to determine those combinations of values of the two independent parameters, Ω^2 and e, which

cause instability to occur. For a link of a given material, this depends on the relationship between the area, A, and the radius of gyration, k, of the cross-section. The parameter Ω^2 is related to the Euler buckling load and therefore e will be small in comparison if the link is not to buckle. For a linkage with a single rigid-body degree of freedom and an input link with a periodic motion, the functions g and h will be doubly differentiable functions with the same period as the input link. The following series representations may be used therefore:

$$g(t) = \sum_{n=0}^{\infty} (a_n.e^{int} + \bar{a}_n.e^{-int}) \qquad (13.26)$$

$$h(t) = \sum_{n=0}^{\infty} (b_n.e^{int} + \bar{b}_n.e^{-int})$$

where i is the square root of minus one, a bar over a letter denotes complex conjugate and the unit of time is the periodic time for the input link.

Rubenfeld {13.6} has derived the equations of the stability surfaces for a general Hill's equation of period 2π with several small parameters. His findings may be applied to equation (13.25) in conjunction with equations (13.26). Thus, to a first order approximation, the equations of the instability boundaries are given by:

$$\Omega^2 = p^2/4 - e(a_o+\bar{a}_o)-(b_o+\bar{b}_o) \pm |e.a_p + b_p| \qquad (13.27)$$

where p = 0, 1, 2, ...
| | denote absolute value.

To a second order approximation, the equations of the instability boundaries are given by:

$$\Omega^2 = p^2/4 - e(a_o+\bar{a}_o) - (b_o+\bar{b}_o)$$

$$+ \frac{p^2}{2} - \frac{p^2}{2}\left[1 + \frac{4}{p^2}\left\{ \frac{3}{2p^2} \left| e.a_p + b_p \right|^2 \right.\right.$$

$$\left.\left. + 2 \sum_{\substack{n=1 \\ n\neq p}}^{\infty} \frac{\left| e.a_n + b_n \right|^2}{(n^2 - p^2)} \pm |B| \right\}\right]^{\frac{1}{2}} \qquad (13.28)$$

where $B = e.a_p + b_p + \sum_{n=1}^{p-1} (e.a_n + b_n)(e.a_{p-n} + b_{p-n})/\{n(n-p)\}$

$$+ 2\sum_{n=1}^{\infty} (e.\bar{a}_n + \bar{b}_n)(e.a_{p+n} + b_{p+n})/\{n(n+p)\}$$

The regions of instability lie between the boundaries defined by this equation for each value of p.

The foregoing theory suggests the following sequence of operations in the design of a linkage mechanism:

a) determine the link lengths to give an acceptable kinematic performance,

b) choose a material for the links and also any counterweights for the rigid links that may be necessary to modify the force loci,

c) calculate the coefficients in equations (13.26) for the elastic link that is driving the fewest links,

d) use equation (13.28) to plot stability boundaries in the Ω^2, e plane,

e) choose values of k and A that are stable for all modes; if the resulting mass is significantly different from that used when determining the counterweights in step (b), modify the counterweights and re-check stability,

f) if there is more than one elastic link repeat steps (c-e) for the elastic link driving the next smallest number of links,

g) once a stable linkage is predicted, check that the kinematic performance is not adversely affected by the dynamic response which may be calculated using either equations (13.13-13.15) or equation (13.24) as appropriate.

To examine the feasibility of this approach, the next chapter is devoted to the consideration of a four-bar linkage with an elastic coupler.

14. FOUR-BAR LINKAGE

14.1 CHOICE OF LINKAGE

The simplest planar linkage with one degree of freedom has four links and four joints. A variety of arrangements of revolute and prismatic joints is possible as noted in Chapter 3. However, that with four revolute joints is not only used in its own right but also forms a basic part of more complicated linkages such as the warp-knitting mechanisms described in Section 8.3. Of the four links, only the coupler has both ends moving and therefore has the most general motion. Accordingly a four-bar linkage with four revolute joints and an elastic coupler is used to investigate further the theory given in the previous chapter.

14.2 THEORY

The use of equations (13.25 - 13.28) to predict the boundaries of stable operation is based on Euler-Bernoulli beam theory being applicable. In that case, equation (13.24) can be used to predict the response. Furthermore the change in length of the link is neglected and so the accelerations required to determine the coefficients in those equations may be calculated using rigid-body theory.

For a given position of the input link, the angular positions of the coupler and rocker can be determined from equations (5.15) and (5.16) respectively. The first time-derivative of equations (5.11) is:

$$\dot{c}_1 = \sum_{i=1}^{n} (\dot{\ell}_i \cos\Theta_i - \ell_i \dot{\Theta}_i \sin\Theta_i)$$

$$i \neq p,q \qquad (14.1)$$

$$\dot{c}_2 = \sum_{i=1}^{n} (\dot{\ell}_i \sin\Theta_i + \ell_i \dot{\Theta}_i \cos\dot{\Theta}_i)$$

where, as before, ℓ refers to arc length and n is the

number of arcs in the loop. The second time-derivative is:

$$\ddot{c}_1 = \sum_{i=1}^{n} (\ddot{\ell}_i \cos\theta_i - 2\dot{\ell}_i\dot{\theta}_i \sin\theta_i - \ell_i\ddot{\theta}_i \sin\theta_i - \ell_i\dot{\theta}_i^2 \cos\theta_i)$$

$$i \neq p,q \quad (14.2)$$

$$\ddot{c}_2 = \sum_{i=1}^{n} (\ddot{\ell}_i \sin\theta_i + 2\dot{\ell}_i\dot{\theta}_i \cos\theta_i + \ell_i\ddot{\theta}_i \cos\theta_i - \ell_i\dot{\theta}_i^2 \sin\theta_i)$$

For an undetermined dyad with three revolute joints, the angular velocity of link q may be obtained by differentiating equation (5.12) with respect to time giving:

$$\dot{\theta}_q = (\dot{c}_3 + \dot{c}_4\cos\theta_q + \dot{c}_5\sin\theta_q)/(c_4\sin\theta_q - c_5\cos\theta_q) \quad (14.3)$$

where
$$\dot{c}_3 = 2c_1.\dot{c}_1 + 2c_2.\dot{c}_2$$

$$\dot{c}_4 = 2\ell_q.\dot{c}_1 \quad (14.4)$$

$$\dot{c}_5 = 2\ell_q.\dot{c}_2$$

Similarly the angular acceleration of link q may be obtained by taking the second time-derivative of equation (5.12) to give:

$$\ddot{\theta}_q = (\ddot{c}_3 + \ddot{c}_4\cos\theta_q + \ddot{c}_5\sin\theta_q - 2\dot{c}_4\dot{\theta}_q\sin\theta_q + 2\dot{c}_5\dot{\theta}_q\cos\theta_q - c_4\dot{\theta}_q^2\cos\theta_q - c_5\dot{\theta}_q^2\sin\theta_q) \div (c_4\sin\theta_q - c_5\cos\theta_q) \quad (14.5)$$

where $\ddot{c}_3 = 2\dot{c}_1^2 + 2\dot{c}_2^2 + 2c_1.\ddot{c}_1 + 2c_2.\ddot{c}_2$

$$\ddot{c}_4 = 2\ell_q.\ddot{c}_1 \quad (14.6)$$

$$\ddot{c}_5 = 2\ell_q.\ddot{c}_2$$

For link p, we differentiate equations (5.16) with respect to time giving:

$$\dot{\theta}_p = -\{\dot{c}_2 - \dot{c}_1 + \ell_q \dot{\theta}_q (\cos\theta_q + \sin\theta_q)\} / \ell_p (\cos\theta_p + \sin\theta_p) \qquad (14.7)$$

Using the equations for both $\sin\theta_p$ and $\cos\theta_p$ when deriving equation (14.7) ensures that division by zero does not occur when θ_p is an integer multiple of a right angle. The time-derivative of equation (14.7) gives the angular acceleration of link p:

$$\ddot{\theta}_p = -\{\ddot{c}_2 - \ddot{c}_1 + \ell_q \ddot{\theta}_q (\cos\theta_q + \sin\theta_q) + \ell_q \dot{\theta}_q (\cos\theta_q - \sin\theta_q) + \ell_p \dot{\theta}_p^2 (\cos\theta_p - \sin\theta_p)\} / \ell_p (\cos\theta_p + \sin\theta_p) \qquad (14.8)$$

These general expressions may be simplified for a four-bar linkage. Let us denote the crank, coupler, rocker and frame by the subscripts 1, 2, 3 and 4 respectively. If we assume that the crank rotates at a constant angular velocity, equations (14.3), (14.5), (14.7) and (14.8) become:

$$\begin{aligned}
\dot{\theta}_2 &= \dot{\theta}_1 \{\ell_1 . \sin(\theta_1 - \theta_3)\} / \{\ell_2 . \sin(\theta_3 - \theta_2)\} \\
\dot{\theta}_3 &= \dot{\theta}_1 \{\ell_1 . \sin(\theta_1 - \theta_2)\} / \{\ell_3 . \sin(\theta_2 - \theta_3)\} \qquad (14.9) \\
\ddot{\theta}_2 &= \{\dot{\theta}_1^2 . \ell_1 . \cos(\theta_1 - \theta_3) + \dot{\theta}_2^2 . \ell_2 . \cos(\theta_2 - \theta_3) + \dot{\theta}_3^2 . \ell_3\} / \\
&\qquad \{\ell_2 . \sin(\theta_3 - \theta_2)\} \\
\ddot{\theta}_3 &= \{\dot{\theta}_1^2 . \ell_1 . \cos(\theta_1 - \theta_2) + \dot{\theta}_2^2 . \ell_2 + \dot{\theta}_3^2 . \ell_3 . \cos(\theta_2 - \theta_3)\} / \\
&\qquad \{\ell_3 . \sin(\theta_2 - \theta_3)\}
\end{aligned}$$

Taking moments about the crank pin for the coupler and using equations (13.3), (13.22) and (13.23), we have:

$$\begin{aligned}
F_L . \ell_2 &= \int_o^{\ell_2} \mu a_y . x . dx \\
&= \mu \{\frac{\ddot{y}_o}{2} . \ell_2^2 + \frac{\ddot{\theta}_2}{3} . \ell_2^3 - \sum_j (\ddot{Q}_j - \dot{\theta}_2^2 . Q_j) . \ell_2^2 \frac{(-1)^j}{j\pi}\} \qquad (14.10)
\end{aligned}$$

where F_L = transverse force on the coupler at $x = \ell_2$.

Taking moments about the frame pivot for the rocker yields:

$$I_{3p}.\ddot{\Theta}_3 + T.\ell_3.\sin(\Theta_3-\Theta_2) = F_L.\ell_3.\cos(\Theta_3-\Theta_2) \qquad (14.11)$$

where I_{3p} = moment of inertia of the rocker about its frame pivot. Eliminating F_L from equations (14.10) and (14.11) gives:

$$T=\mu\ell_2\{\frac{\ddot{y}_o}{2} + \frac{\ell_2}{3}.\ddot{\Theta}_2 + \frac{(-1)^j}{j\pi}\sum_j(\dot{\Theta}_2^2.Q_j-\ddot{Q}_j)\}\cot(\Theta_3-\Theta_2)$$
$$+ I_{3p}.\ddot{\Theta}_3.\operatorname{cosec}(\Theta_2-\Theta_3)/\ell_3 \qquad (14.12)$$

where $\ddot{y}_o = \ell_1.\dot{\Theta}_1^2.\sin(\Theta_2-\Theta_1)$

Substituting for T from equations (14.12) and neglecting the product of small quantities, the coefficient of Q_j in equation (13.24) becomes:

$$\frac{EAk^2}{\mu}\left(j\frac{\pi}{\ell_2}\right)^4 + \{\ell_2(\frac{\ddot{y}_o}{2} + \frac{\ell_2}{3}.\ddot{\Theta}_2)\cot(\Theta_3-\Theta_2)$$
$$+ \frac{I_{3p}}{\mu\ell_3}.\ddot{\Theta}_3.\operatorname{cosec}(\Theta_2-\Theta_3) - \frac{\ell_2}{2}.\ddot{x}_o\}\left(j\frac{\pi}{\ell_2}\right)^2 + \left(j^2\frac{\pi^2}{3}-\frac{5}{4}\right)\dot{\Theta}_2^2$$

Noting that $\ddot{x}_o$ equals $\{-\ell_1.\dot{\Theta}_1^2.\cos(\Theta_2-\Theta_1)$ and using equations (14.9), this coefficient may be written as:

$$\frac{EAk^2}{\mu}\left(j\frac{\pi}{\ell_2}\right)^4 + j^2\frac{\pi^2}{\ell_2}\left(\frac{\ell_3}{3} + \frac{I_{3p}}{m_2\ell_3}\right)\ddot{\Theta}_3.\operatorname{cosec}(\Theta_2-\Theta_3)$$
$$-\frac{5}{4}\dot{\Theta}_2^2 - j^2\frac{\pi^2}{6}\dot{\Theta}_1\dot{\Theta}_2$$

where $m_2 = \mu\ell_2$, the mass of the coupler.

Equation (13.24) therefore becomes for the coupler of a four-bar linkage:

$$\ddot{Q}_j+\{\frac{EAk^2}{\mu}\left(j\frac{\pi}{\ell_2}\right)^4 + j^2\frac{\pi^2}{\ell_2}\left(\frac{\ell_3}{3} + \frac{I_{3p}}{m_2\ell_3}\right)\ddot{\Theta}_3.\operatorname{cosec}(\Theta_2-\Theta_3)$$
$$-\frac{5}{4}\dot{\Theta}_2^2 - j^2\frac{\pi^2}{6}\dot{\Theta}_1\dot{\Theta}_2\}Q_j + \frac{2}{j\pi}\{\ddot{y}_o-(\ddot{y}_o+\ell_2.\ddot{\Theta}_2)(-1)^j\} = 0 \qquad (14.13)$$

This equation may be used to predict the response of slender couplers.

Before doing this, the various quantities required to predict the regions of stable operation should be determined. Comparison of equation (14.13), after division by $\dot{\theta}_1^2$ to give non-dimensional coefficients, with equation (13.25) shows that for a four-bar linkage:

$$\Omega = \left(j\frac{\pi}{\ell_2}\right)^2 . \left(\frac{Ek^2}{\rho}\right)^{\frac{1}{2}}$$

$$e = j^2 . I_{3p} / \{\rho A \ell_2 . \ell_2 \ell_3\}$$

$$g(t) = \pi^2 . \text{cosec}(\theta_2 - \theta_3) . \ddot{\theta}_3 / \dot{\theta}_1^2 \qquad (14.14)$$

$$h(t) = j^2 \frac{\pi^2}{3} \left\{ \frac{\ell_3}{\ell_2} \text{cosec}(\theta_2 - \theta_3) . \frac{\ddot{\theta}_3}{\dot{\theta}_1^2} - \frac{1}{2} . \frac{\dot{\theta}_2}{\dot{\theta}_1} \right\} - \frac{5}{4} \left(\frac{\dot{\theta}_2}{\dot{\theta}_1}\right)^2$$

The series corresponding to g(t) and h(t), as given in equations (13.26), must be determined before the stability boundaries can be obtained using either equation (13.27) or equation (13.28). The series for θ_3 and $\dot{\theta}_3$ have been obtained algebraically by Denavit and Hasson {14.1}. They note that the approach fails if the linkage passes through a dead-centre position as the series do not then converge due to indeterminancy in the kinematic expressions. This can be seen in equations (14.9) where, in each case, the denominator becomes zero when θ_2 and θ_3 are equal. Thus the approach fails for parallelogram and anti-parallelogram linkages. Since there are several series to be determined, it is more convenient to use a numerical rather than an algebraic approach. The Cooley-Tukey algorithm {14.2} was therefore incorporated into a computer program to predict the stability boundaries for the coupler.

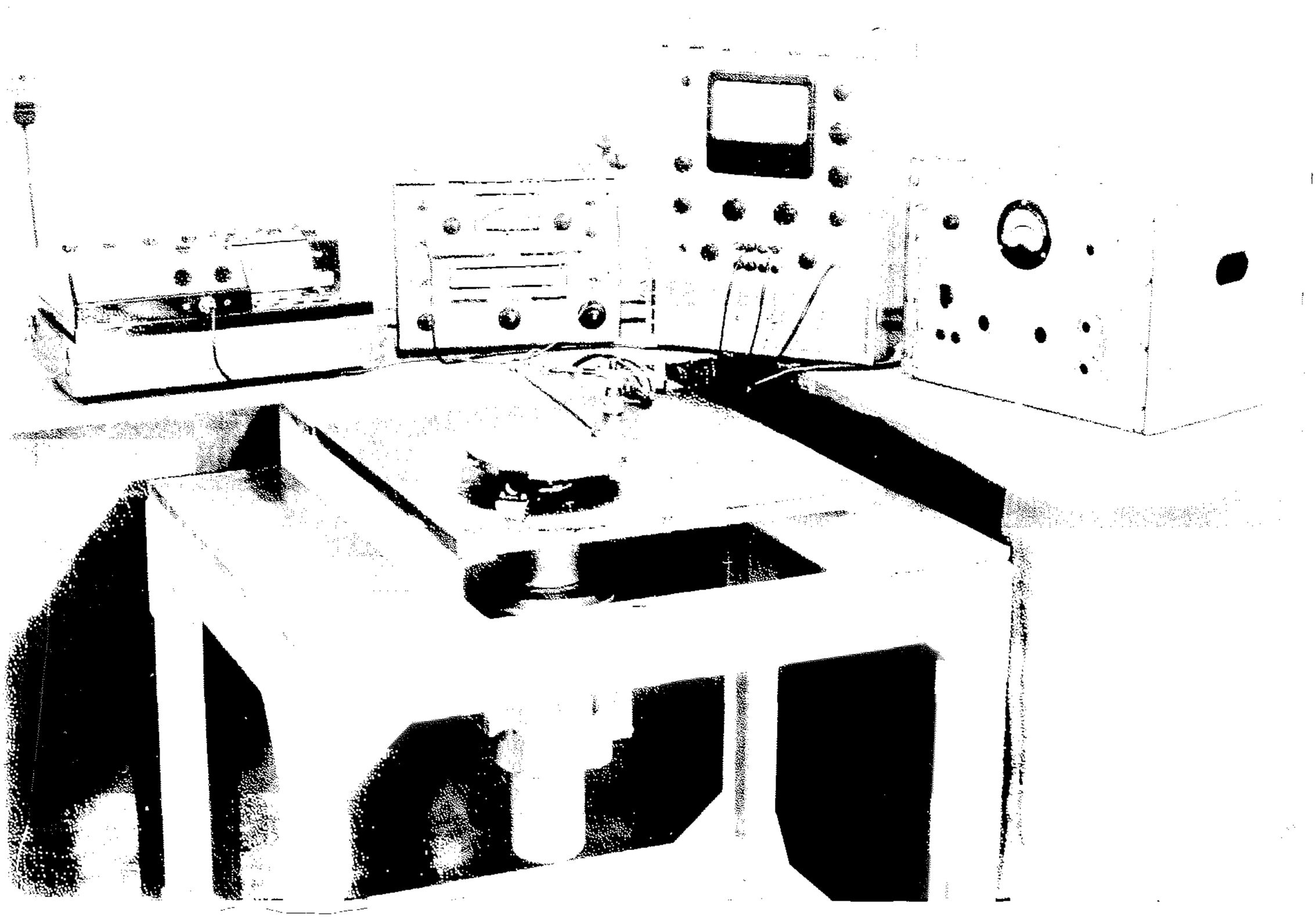

FIGURE 14.1 EXPERIMENTAL SET-UP

14.3 EXPERIMENTAL SET-UP AND PROCEDURE

In view of the number and nature of the assumptions made in the preceding theory, any theoretical predictions must be compared with experimental results to check whether the predictions are borne out in practice. The main prediction, since the design procedure depends upon it, is the existence of the stability boundaries and the nature of the coupler response close to them. Magnus and Winkler {14.3} show that on the stability boundaries the solution to equation (14.13) will be neutrally stable with period equal to or twice that of the input crank as p in equations (13.27) and (13.28) is even or odd respectively. In the simpler case of Mathieu's equation, McLachlan {14.4} shows that, in the stable regions between the boundaries, the response is non-periodic. The experimental results to be obtained therefore are the detection of the stability boundaries and the nature of the coupler response close to those boundaries.

The set-up shown in Figure 14.1 was used to provide the experimental results. The test rig has been described in detail by Smith {14.5}. Briefly it consists of a four-bar linkage mounted in a horizontal plane. The linkage is of the crank-rocker type and each of the links may be considered to be rigid except for the coupler. The details of the links are:

crank: length = 76 mm (3 in),

coupler: length = 381 mm (15 in),
cross-section = 6.35 mm (0.25 in) perpendicular to the plane of the mechanism by 1.24 mm (0.049 in) or 0.82 mm (0.032 in) in the plane of the linkage,
material = steel gauge plate,

rocker: length = 152 mm (6 in),
moment of inertia about the frame pivot = 1.92 g.m^2 (6.57 lb. in^2).

frame : length = 381 mm (15 in).

The ratio of the link lengths (1:5:2:5) is similar to that of the basic four-bar linkages used in the warp knitting mechanisms described in Section 8.3 and of other four-bar linkages used in industry.

The crank is driven by a 373 watt (0.5 H.P.) D.C. motor controlled by a Servomex Motor Controller type MC47 which appears on the right of Figure 14.1. A pair of strain gauges was attached back-to-back to the coupler at 50 mm from the rocker joint. All of the signal conditioning equipment, shown to the left of the motor controller, was manufactured by Bruel and Kjaer. The strain gauges were connected to a Strain Gage Apparatus type 1516. The harmonic content of the signal was determined using a Frequency Analyzer type 2120 which provides a frequency analysis down to 2 Hz. The result was recorded on a Level Recorder type 2305 which was mechanically coupled to the Frequency Analyzer to provide synchronization. The switch settings were those recommended for the analysis of complex sinusoidal signals as shown in Table 14.1.

Table 14.1 Settings for Frequency Analyzer and Level Recorder

Frequency Analyzer		Level Recorder		
Frequency Hz	Bandwidth %	Lower Lim. Freq.,Hz.	Writing Speed,mm/s	Paper Speed,mm/s
2-6.3	3	2	4	0.03
6.3-20	3	2	8	0.1
20-63	1	20	8	0.03
63-200	1	50	31.5	0.1

To determine the crank speeds at which instability and resonance occur, Smith {14.5} fed the signal from the Strain Gage Apparatus directly to a U.V. recorder. He used nine values of rocker inertia with the thinner coupler given above and eight values with both the thicker coupler and a coupler of thickness 1.64 mm (0.064 in).

14.4 RESULTS AND DISCUSSION

The coefficients in the Fourier series for g(t) and h(t), equations (14.14), reduced rapidly as the harmonic number, i.e. n in equations (13.26), increased. For example, the coefficients for the 32nd harmonic were of the order of 10^{-14} times those for the first harmonic. Accordingly n was limited to a maximum value of 32 when using equations (13.26).

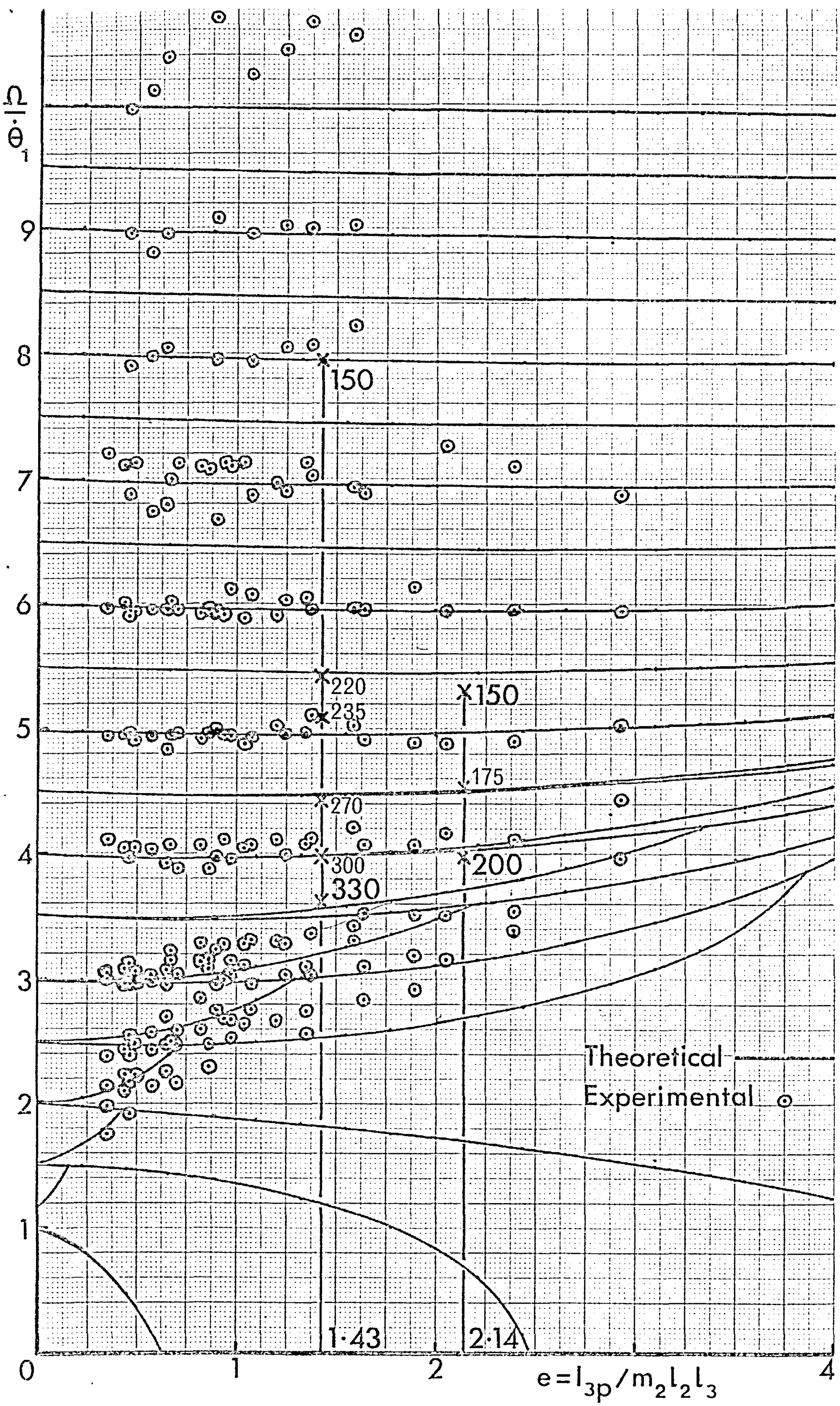

FIGURE 14·2 STABILITY BOUNDARIES

The second order stability boundaries for the first mode of vibration obtained using equations (13.26), (13.27) and (14.14) are shown in Figure 14.2. If the axial force is assumed to be constant along the link as discussed on page 13-10, the predicted stability boundaries occur at higher input crank speeds, i.e. lower values of $\Omega/\dot{\theta}_1$, than those shown. The magnitude of the effect varies with the value of p in equation (13.28), ranging from 16% for p equal to one to 0.1% for p equal to twenty. (The ordinate values in the Figure are approximately equal to p/2).

Also shown in the Figure are the experimental results obtained by Smith {14.5}. For each value of coupler thickness and rocker inertia, the input crank speed was changed slowly and note taken of the speeds at which instability and resonance occurred. No experimental evidence of instability corresponding to odd values of p was found for values of p greater than seven. Apart from this, the results from the three couplers form a single pattern which agrees well with the theoretical boundaries.

If the linkage is run at speeds higher than those indicated for the experimental results, the coupler deflections become excessive, sometimes resulting in a change in the closure of the four-bar loop. Thus, for practical purposes, the limiting speed for this linkage can be approximated by a linear relationship of the form:

$$\Omega/\dot{\theta}_1 = 1.4 + 0.85e \qquad 0 \leqslant e \leqslant 4 \qquad (14.15)$$

This is just above the speeds at which the various unstable regions merge to form one continuous region.

The input crank speeds at which frequency analyses of the strain gauge signals were made are given in Table 14.2. They are indicated by crosses in Figure 14.2 with the highest and lowest speed being marked for each coupler. All of the values are close to a stability boundary except perhaps for the lowest speed for the thinner coupler. The corresponding analyses are given

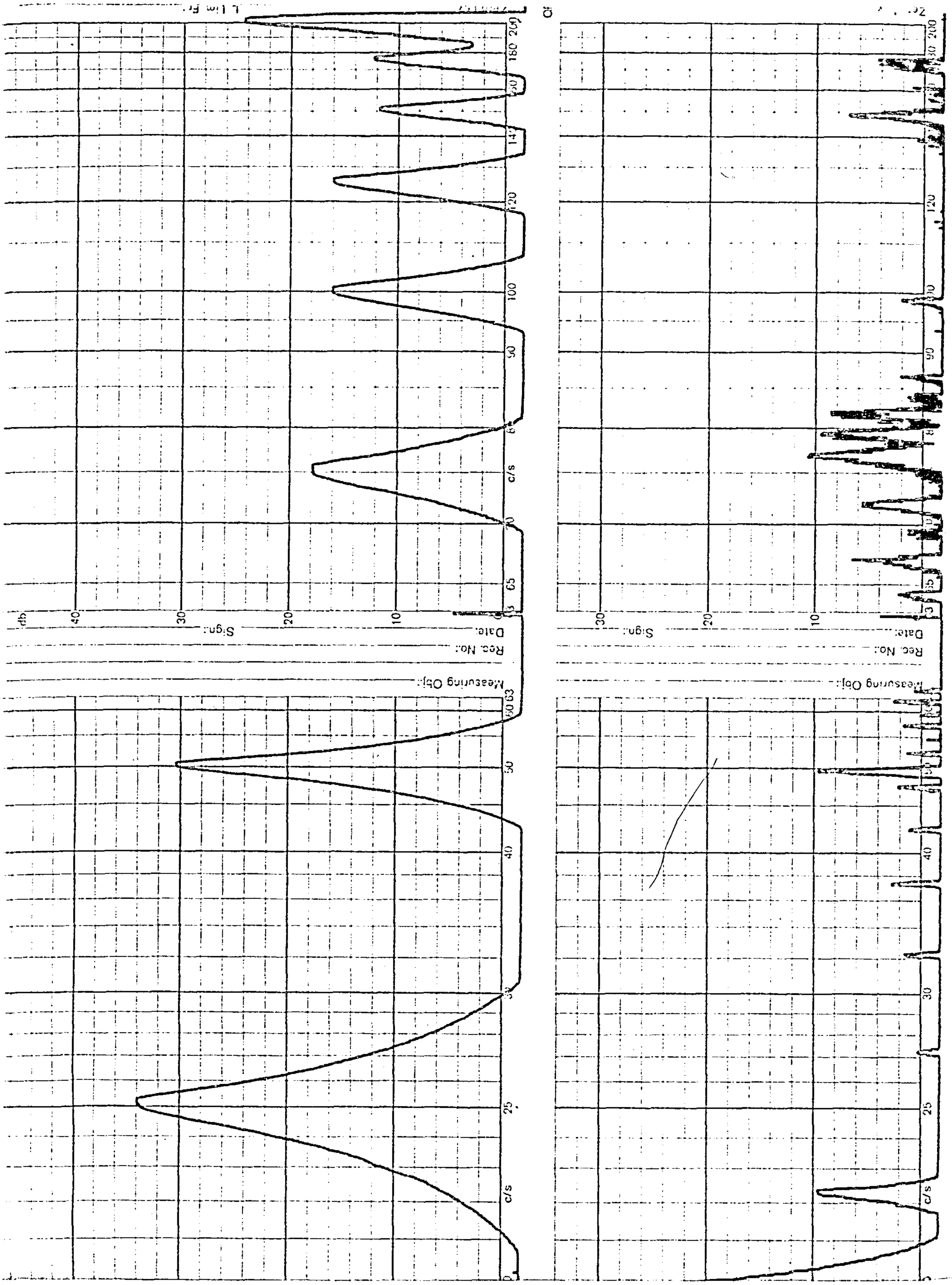

FIGURE 14.3 FREQUENCY ANALYSIS

(a) e = 1·43, 150 rev/min

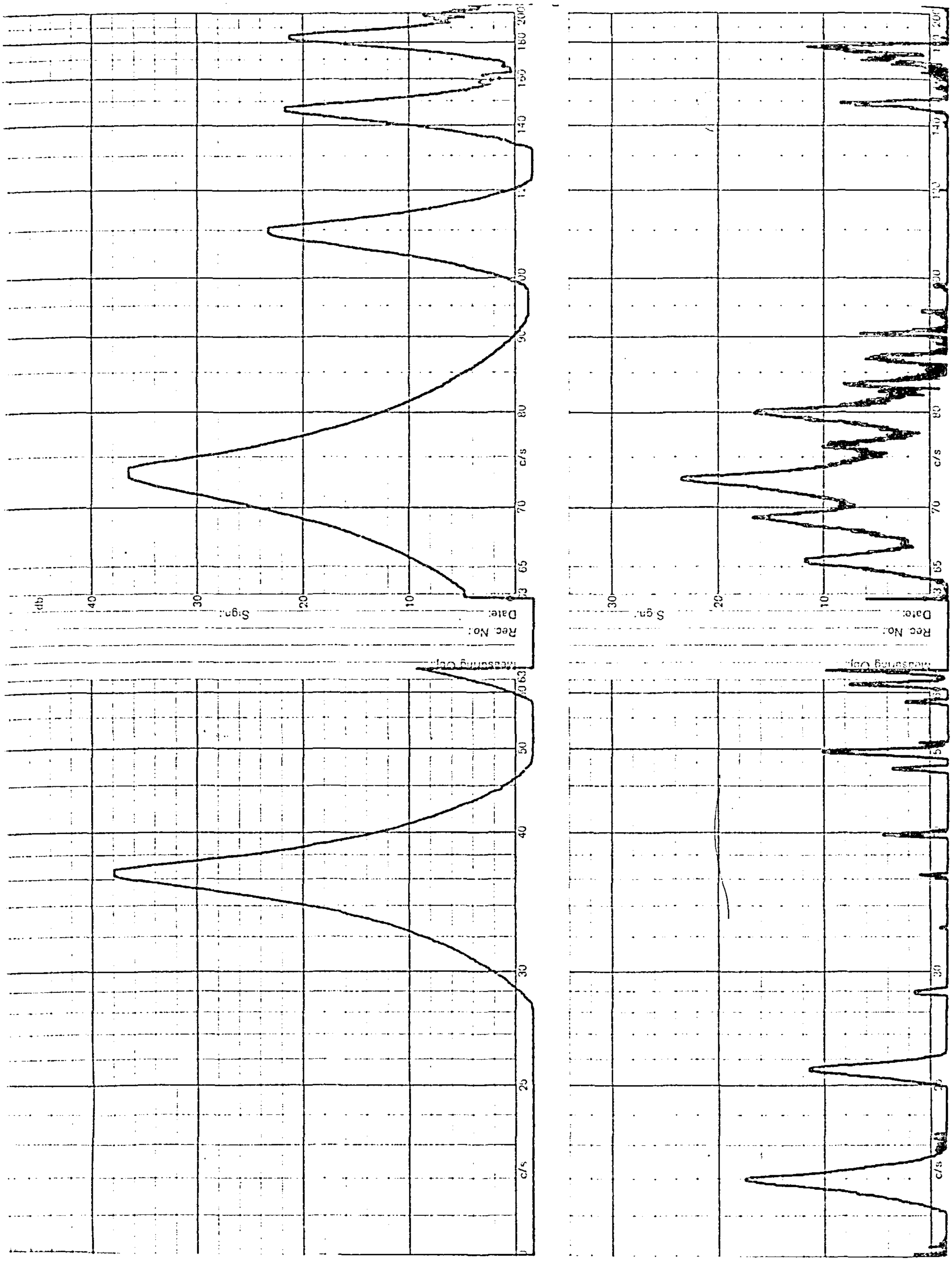

FIGURE 14.3 FREQUENCY ANALYSIS

(b) e = 1·43,220 rev/min

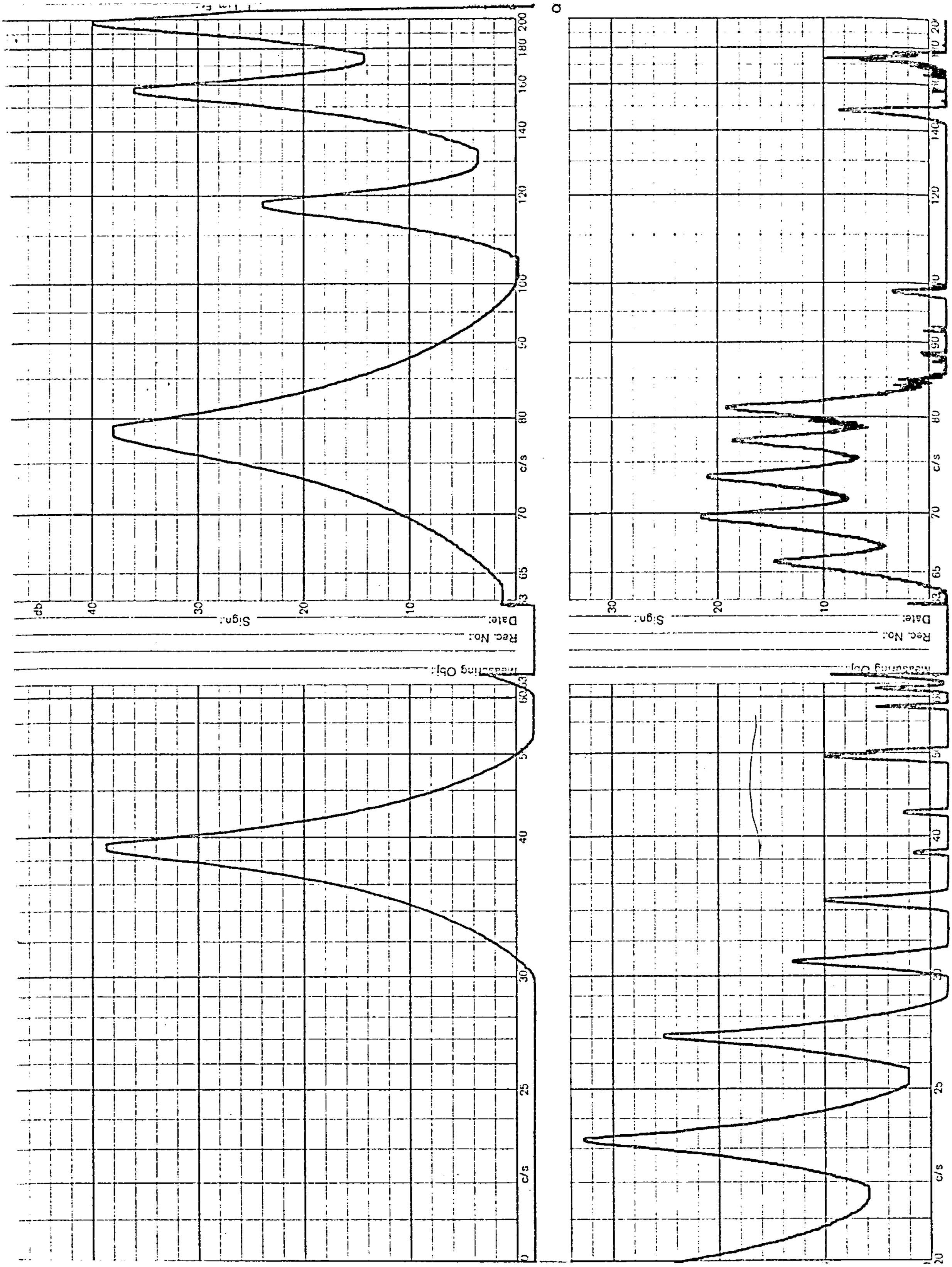

FIGURE 14.3 FREQUENCY ANALYSIS

(c) e = 1·43,235 rev/min

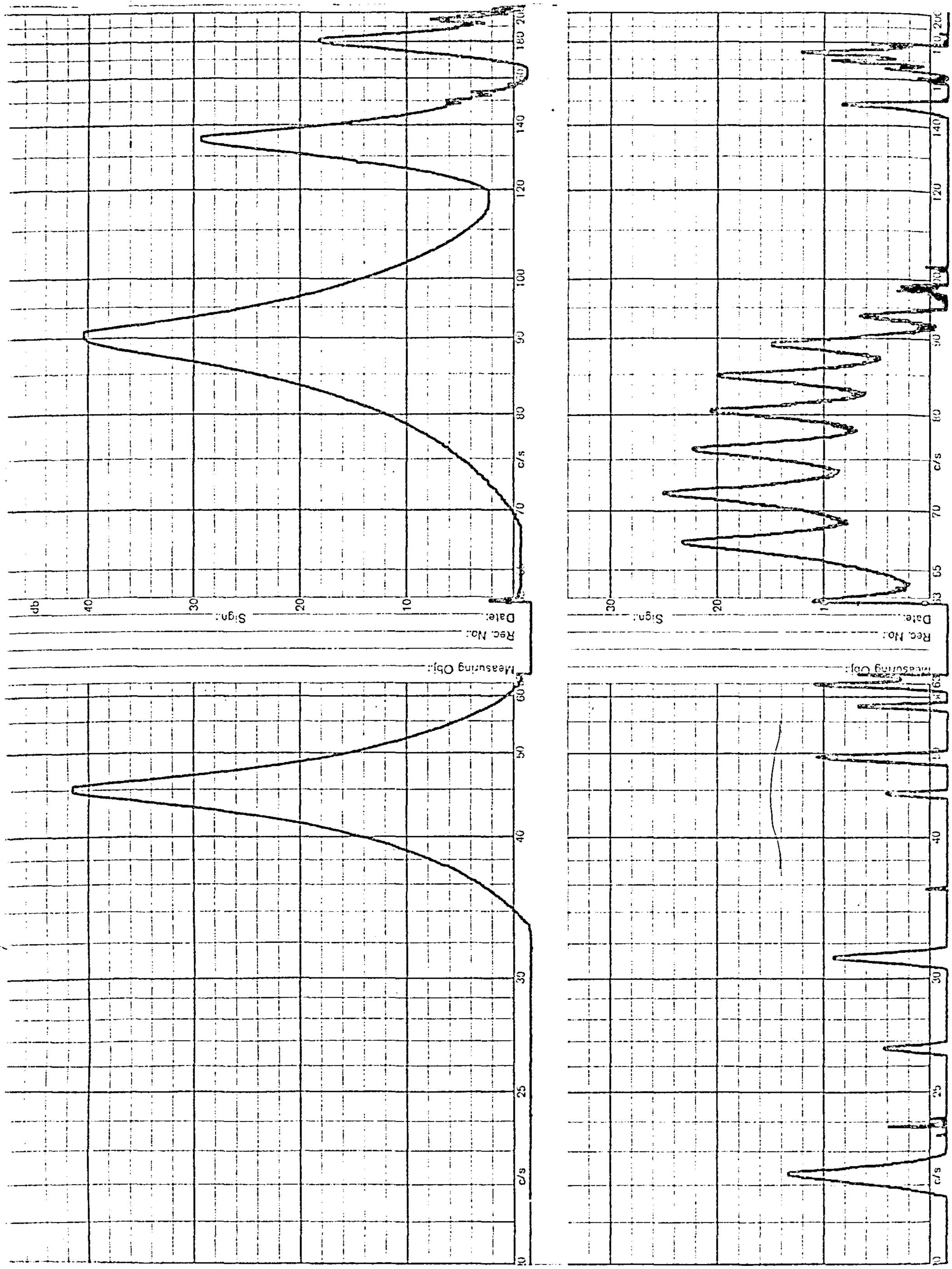

FIGURE 14.3 FREQUENCY ANALYSIS

(d) e = 1·43,270 rev/min

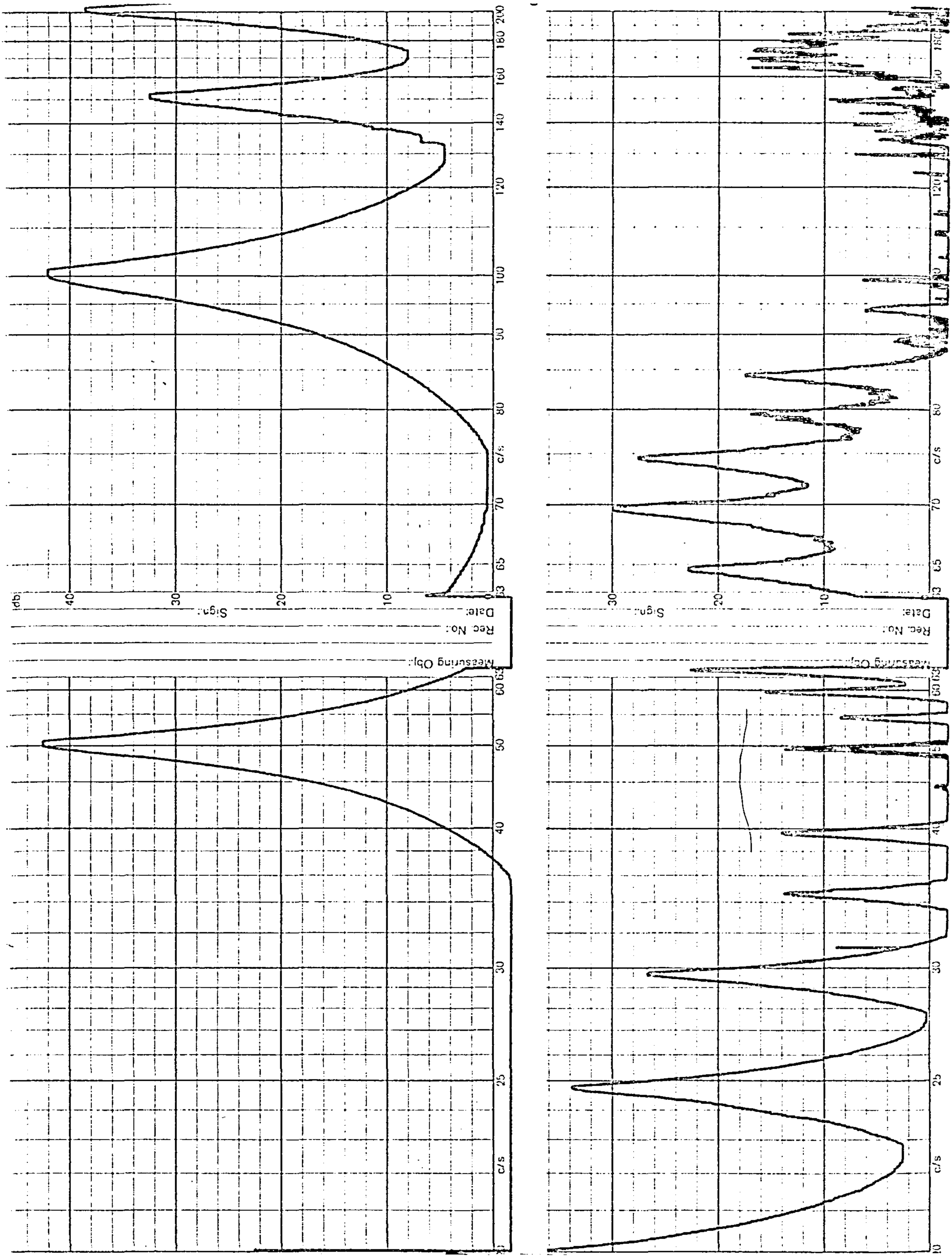

FIGURE 14.3 FREQUENCY ANALYSIS

(e) e = 1·43,300 rev/min

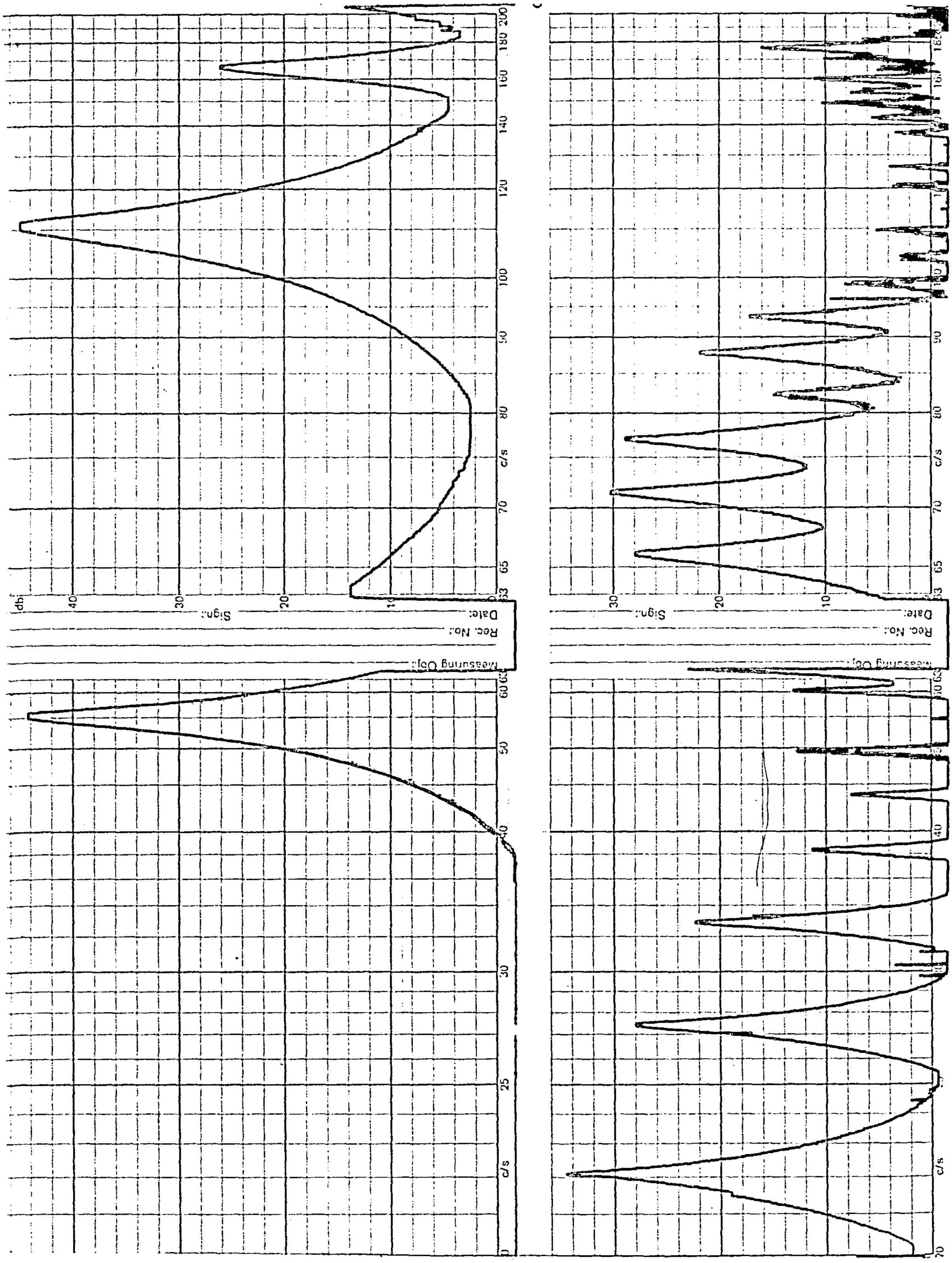

FIGURE 14.3 FREQUENCY ANALYSIS

(f) e = 1·43,330 rev/min

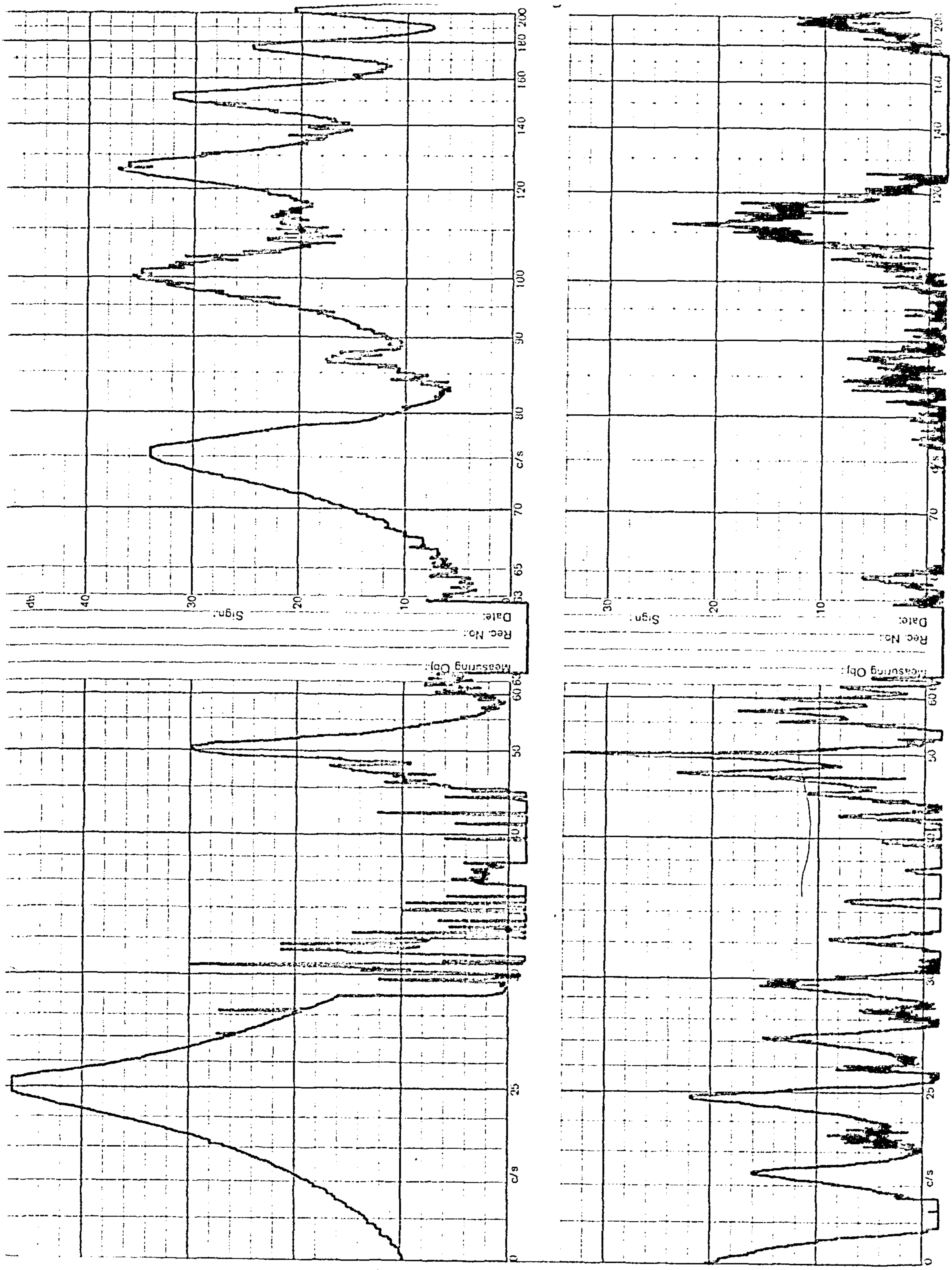

FIGURE 14.4 FREQUENCY ANALYSIS

(a) e = 2·14 , 150 rev/min

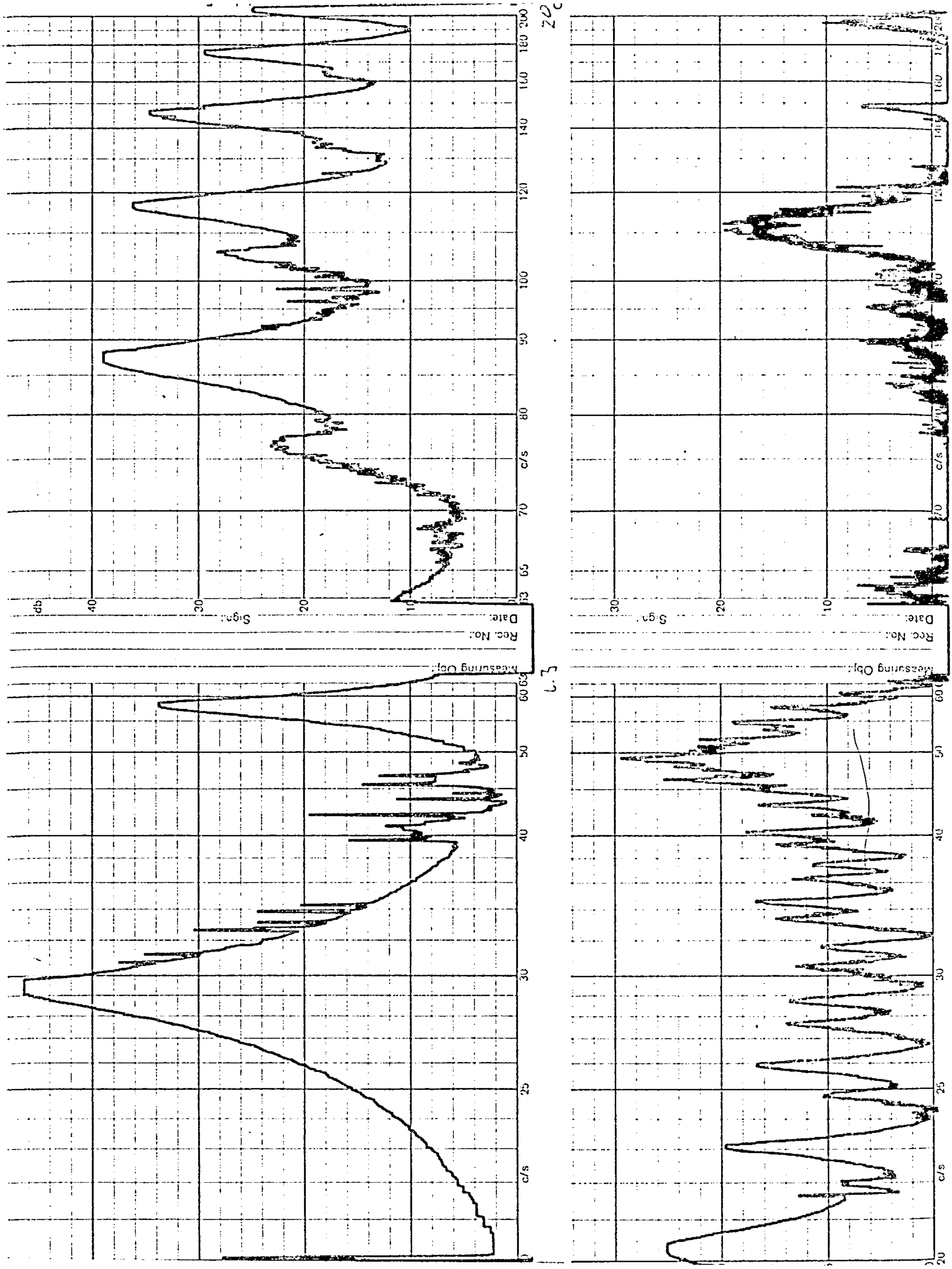

FIGURE 14.4 FREQUENCY ANALYSIS

(b) e = 2·14 ; 175 rev/min

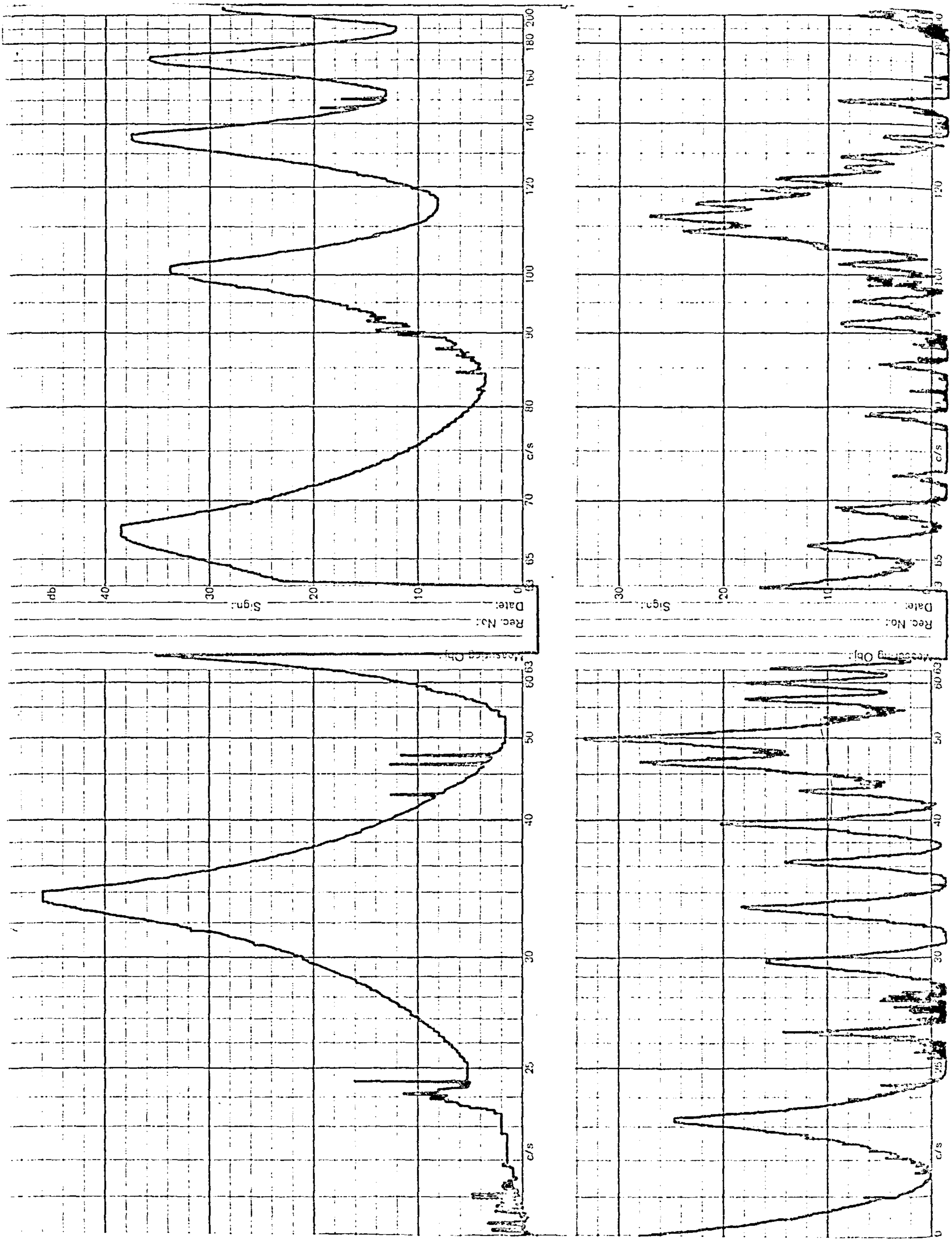

FIGURE 14.4 FREQUENCY ANALYSIS

(c) e = 2·14,200 rev/min

in Figures 14.3 and 14.4. Each Figure represents a continuous trace, the upper part covering the frequency range 2-20Hz and the lower part 20-200Hz. The relative speeds were such that 1mm along the trace represents at least 25 revolutions of the input crank. The ordinate axis is logarithmic with one major division representing 10 dB.

Table 14.2 Values for Frequency Analyses

a) Thicker Coupler, e = 1.43

Input crank speed, rev/min	150	220	235	270	300	330
$\Omega/\dot{\theta}_1$	7.96	5.42	5.08	4.42	3.98	3.62
Nearest boundary,p	16	11	10	9	8	7

b) Thinner Coupler, e = 2.14

Input crank speed, rev/min	150	175	200
$\Omega/\dot{\theta}_1$	5.3	4.54	3.98
Nearest boundary,p	11	9	8

The results for the thicker coupler in Figure 14.3 show a very stable response consisting entirely of harmonics of the input crank speed. The dynamic magnifying effect of the second and third natural frequencies can be clearly seen at about 75 Hz and 169 Hz respectively, corresponding to a first natural frequency of 19 Hz.

The results for the thinner coupler in Figure 14.4 show a slightly different pattern in that odd half-multiples of the input crank speed are visible in the range 25-55 Hz for a crank speed of 175 rev/min but not for the other crank speeds. This may be due to the operating speed lying close to a stability boundary with an odd value of p. In each trace for the thinner coupler, the dynamic magnifying effect of the second, third and

fourth natural frequencies can be seen at 50, 112 and 198 Hz respectively corresponding to a first natural frequency of 12.4Hz.

The experimental results agree well with the theoretical predictions for values of e between 0 and 4. The magnitude of e depends on the ratio of the rocker inertia to the rocker length and the size of the coupler. In the four-bar linkages used in hose knitting machines that have been analysed by Penney {14.6}, the effective rocker inertia is high (1.4 - 8 $kg.m^2$) compared to an average link length of 125 mm. As a result, the corresponding value of e is in the order of 200. Further work is required to determine whether the theory is still applicable in this range.

14.5 CONCLUSIONS

The experimental results from the coupler of a four-bar linkage confirm the theoretical predictions of stability boundaries for values of the parameter e between 0 and 4. In the stable regions close to these boundaries, the response consists of harmonics of the input crank speed. The linkage can be accelerated through the unstable regions up to the speed at which the unstable regions merge to form one continuous region. Further work is required to determine whether the conclusions are valid for higher values of the parameter e.

Summary

The previous chapter develops the equations of motion for a link that can be regarded either as a Timoshenko link or as an Euler-Bernoulli link in general planar motion and subject to time-varying end loads. The equations of the boundaries of the regions of stable operation of the latter type of link are also given together with a proposed design procedure. This chapter applies this theory to a four-bar linkage. The theoretical predictions agree well with experimental results.

PART D

FURTHER WORK

15. FURTHER WORK

15.1 KINEMATIC SYNTHESIS

The scope of PSALM and the associated analysis program, KALM, has been increased since the earlier chapters in this thesis were written. The input data sets for both programs have been harmonized so that a composite data set may be supplied to either program which will then ignore any irrelevant data. Thus, for example, PSALM will ignore data concerned with velocities and accelerations. Both programs will now accept a prismatic joint as the actuator pair although one of the two links concerned must still be a frame link. Input link lengths are supplied instead of crank angles, the parameter names remaining the same. In addition, the length of a sliding link may form the desired output value. PSALM now writes a complete data set for the final linkage to device 7 for subsequent use such as displaying the linkage or further analysis.

As noted on page 9-7, it is desirable to prescribe the topology of the linkage in terms of loops containing the minimum number of arcs. These can be determined by using the following procedure:

1. Number all of the arcs
   - those connected by the actuator pair are of order one,
   - those connected to order one arcs are of order two,
   - and so on until all arcs have been numbered.
2. Mark the order one arcs and any arcs common with them with a D to denote a determined arc.
3. (a) Find a pair of undetermined arcs which are connected together and each of which is connected to a determined arc.

   (b) From each of these two arcs proceed via the fewest links to the actuator pair using lower or equal order determined arcs. The resulting loop must not contain more than two arcs of the same order unless the loop contains a prismatic joint. The first loop must contain two first order and two second order arcs.

(c) Mark the chosen pair of undetermined arcs and any arcs common with them with a D.

(d) If one of the undetermined arcs was of variable length, i.e. a sliding link, delete from further consideration any variable length arcs that are common with it since only one variable length arc in a link is allowed to emanate from a prismatic joint.

4. Repeat step 3 until all arcs are determined.

The loops formed in step 3(b) are the required loops.

If, at any stage, a suitable pair of undetermined arcs cannot be found, the linkage must contain a higher order Assur group. It might be possible to modify PSALM to analyse such linkages in the following manner. Let us assume that the smallest loop passing through both the actuator pair and the input link contains five arcs. Then, if the linkage has one degree of freedom, fixing the input link in one of the prescribed positions will result in a structure. Replacing the output link by a sliding link with a zero-length guide link will restore this degree of freedom. The moving arc connected to the input link could then be considered as a pseudo input link. In those cases where the remainder of the linkage could be formed from pairs of undetermined arcs, PSALM could be used to vary the angular position or length of this pseudo input link until the sliding link were the same length as the actual output link. Further work is required to determine whether this approach is preferable to the other methods considered in Section 5.3.

The linkage drawing program has been developed further so that it can be used with a graph plotter as well as with a graphic display terminal. Its name has been changed from PICTUR to BALM as it now gives a Better Appreciation of Linkage Mechanisms. This program will accept the same composite data set as the other two programs. It also contains the error and warning messages from these programs. A useful extension would be to provide the user with an opportunity to change the

FIGURE 15.1 NEEDLE MECHANISM

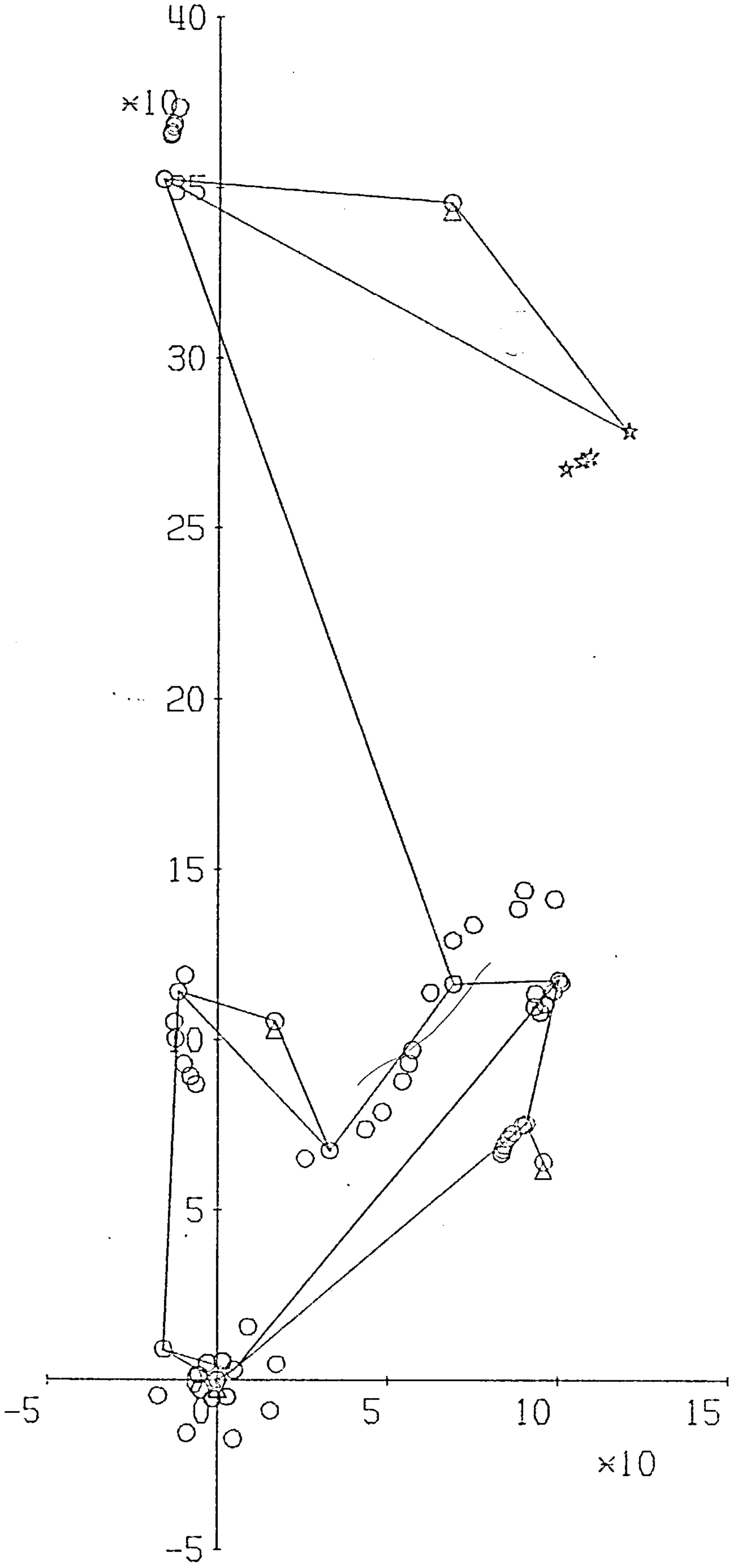

FIGURE 15.2 TEN-BAR LINKAGE

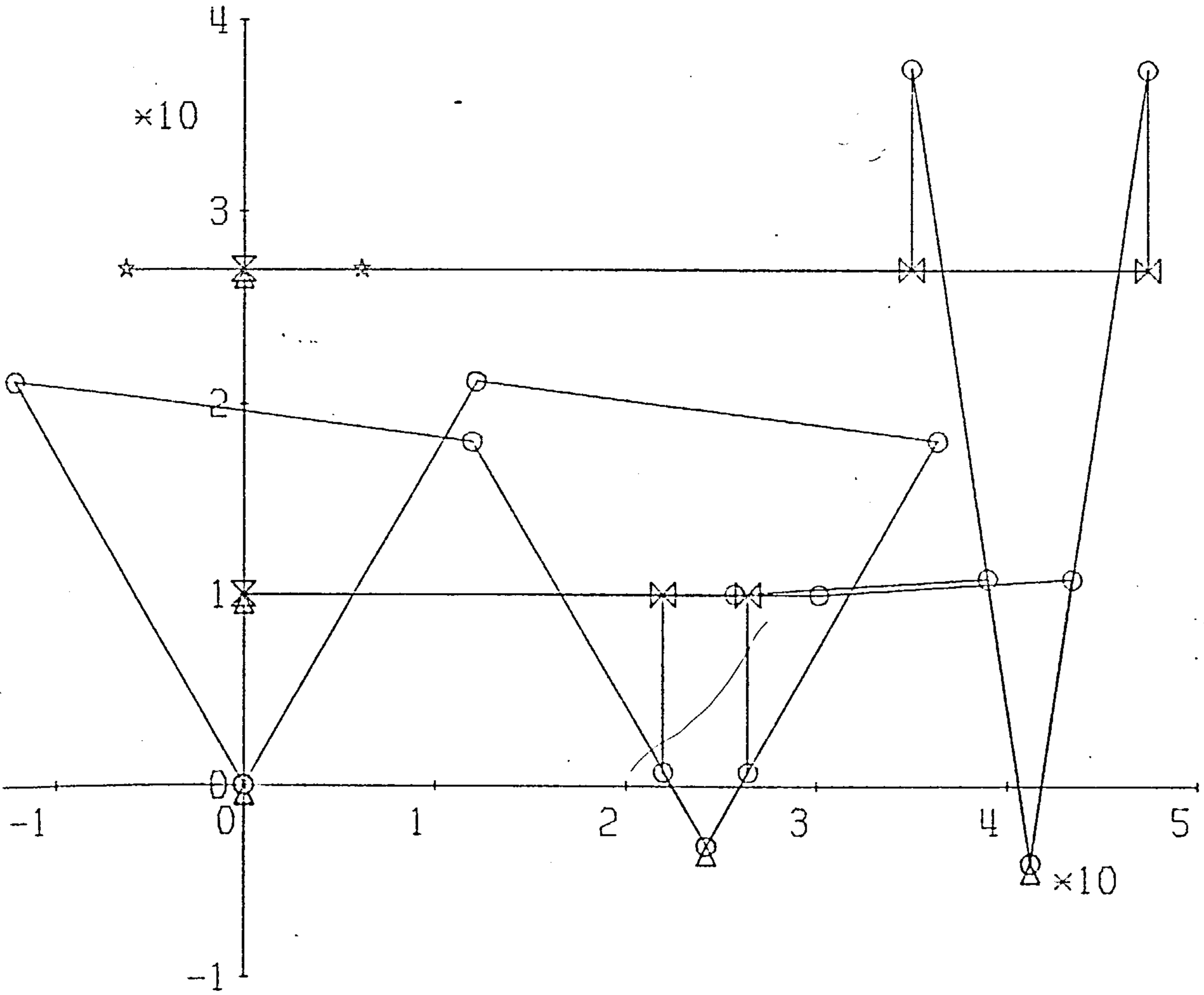

FIGURE 15.3 SCISSORS LIFT

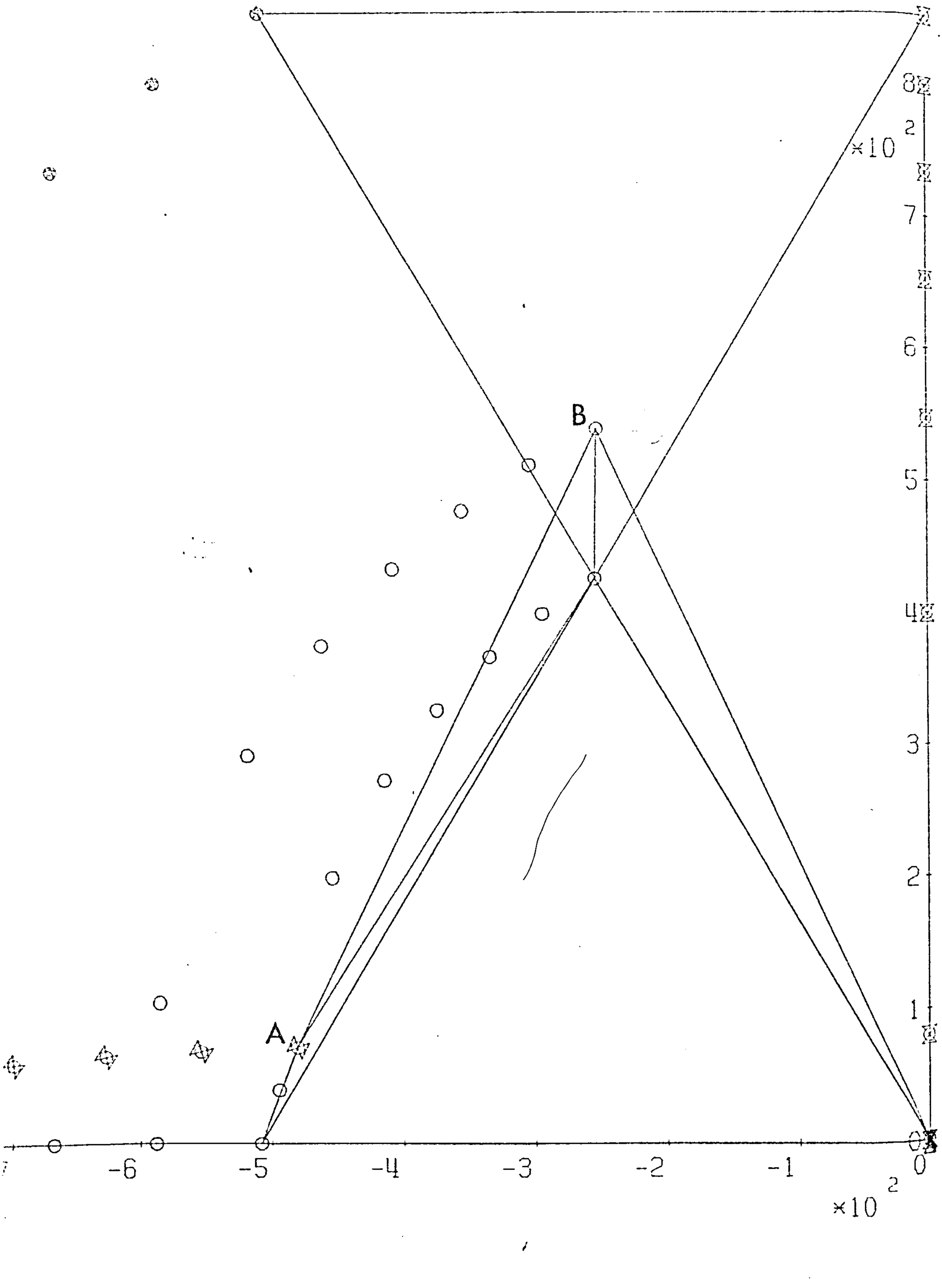

data, as a result of the messages, while the program was running. The revised data could be written to a file for subsequent use by the other programs.

Examples of the output from BALM appear in Figures 15.1 - 15.3. Circles are used to indicate revolute joints and single triangles for frame joints. Prismatic joints are represented by a pair of triangles, vertex to vertex, the direction of sliding being parallel to the bases of the triangles. Five-pointed stars indicate the output point. Figure 15.1 shows a needle mechanism similar to that considered in Chapter 11. The linkage is drawn in full in the initial position and thereafter only the moving joints and the output point are plotted. If a complete set of information for every arc at every position of the input link is requested in the input data, the linkage will be drawn in full in every position as shown in Figure 15.2. This shows the linkage used as an example in Appendix B.

The scissors lift mechanism shown in Figure 15.3 is used in a road-sweeping vehicle. The linkage is actuated by a hydraulically powered piston and cylinder mounted between points A and B. PSALM was used to determine these mounting positions such that the velocity ratio between the height of the platform and the length of the sliding input link is equal at the two ends of the stroke. Since the program does not cater for floating actuator pairs such as this, a pseudo sliding input link was assumed to connect the platform to the frame and the length of the actual input link was taken as the desired output value. Equal velocity ratios were prescribed by using two closely spaced positions at each end of the stroke. This exercise showed that if the initial simplex is some distance from the global minimum, the program is more likely to find a local minimum in a saucer-shaped depression than a global minimum at the bottom of a narrow funnel. This is a useful characteristic in that such a local minimum will be less affected by manufacturing tolerances than a global minimum of this type.

PSALM, KALM and BALM form a consistent, self-contained suite of programs. They are based on a linkage being regarded, first and foremost, as a kinematic chain with dimensions being of secondary importance. This raises the question of whether this is the 'natural' way of thinking of a linkage mechanism and further work is required to elucidate this.

An alternative form of input could be provided by developing BALM to accept as data co-ordinate information from a tablet or the cross-hairs on a Tektronix terminal. The linkage could then be drawn directly on the tablet or screen, individual arcs indicated and the dimensions etc. for that arc typed in on the terminal. BALM would then convert this data into the standard NAMELIST form.

KALM could be developed into a rigid-body dynamic analysis program. The values of mass and inertia for each link would be added to the data set. The position of the centre of mass of a link could be given relative to an arc in the same link which had been used in the topological definition of the linkage. The arc and loop number of this arc would then take the place of the part identification used in methods based on a linkage being regarded as an assembly of parts.

These changes would make possible the following sequence of operations. The initial set of kinematic data could be fed into BALM to check for correct closure etc. and modified if necessary. The revised data could be input to PSALM which would further alter it. Values of mass etc. could be added to the data set at this stage. The final set of data could be supplied to BALM for plotting showing the centre of mass of each link and to KALM for further analysis. This concept is in line with a trend towards the use of total design systems whereby a complete description of a machine is held as a data structure in a computer. The data structure is built up as the design develops and in its final form is the

design authority to be used for automatic draughting, process planning etc. Thus the composite data set used by PSALM, KALM and BALM is an embryonic form of such a data structure. More comprehensive systems are described by Gibbs et alia {15.1} and Hanratty {15.2}. Such trends should be borne in mind when further development of these and other programs is undertaken.

15.2 BALANCING

The theory and procedure in Chapter 11 give the conditions to be satisfied by a set of counterweights to obtain a frame-force balance. This is only a static balance in that the couples due to the inertia of the moving links are not balanced. In a dynamic balance, both forces and couples are balanced. Although methods of achieving this are well known for rigid rotors (see, for example, Broch {15.3}), further work is required to determine whether this is possible for linkage mechanisms.

The effect of balancing on the forces at the joints of the linkage must also be considered. It may be that an optimization approach using a composite criterion would be the answer. Preliminary results from a program restricted to four-bar linkages are encouraging {15.4}. The main difficulty in developing such a program to be as general as the kinematic programs would lie in searching the parameter space effectively. This would be increased if the program were to permit the use of additional elements such as springs or further dyads.

15.3 VIBRATION

Stability charts of the type given in Chapter 14 are valid for slender, uniform, binary links with revolute joints at each end. Further work is required to determine how small the length / depth ratio can be without invalidating the theory and whether the theory is valid for any value of the ratio of the rocker inertia to the linkage size. Extension of the theory is required to

cater for ternary links including those of the bell-crank type and links with prismatic joints. The effect of changes in the cross-section at the joints and non-uniform sections for balancing or other purposes should also be determined.

In most industrial linkages, links are more slender perpendicular to, rather than in, the plane of the linkage. Accordingly vibration out of the plane of the linkage may be more likely than in-plane vibration. This possibility is increased if the links are offset from each other. Further work is required to determine the conditions under which each type of vibration predominates.

Whatever type of vibration is anticipated the theoretical predictions will be affected by internal damping within the links, clearance and damping at the joints and flexibility of other links and the machine structure. Thus, rather than attempting to refine the theory to include the effect of all of these factors, the emphasis should be on determining the relative importance of each effect. The designer can then concentrate on the more important aspects to produce linkages that will operate efficiently and reliably at the desired speed without transmitting vibration to the remainder of the machine.

Summary

The current state of the kinematic synthesis program and two associated programs for the analysis and display of planar linkages is reviewed. This is followed by proposals to extend the scope of these programs. Adding counterweights to a linkage to obtain a frame-force balance can produce undesirable side effects. Further work is required to determine the best compromise and how it can be achieved. Finally further work should be carried out to discover when vibration is likely to be a problem and what action should be taken to avoid it.

APPENDICES

A. REFERENCES

CHAPTER 1

{1.1} Nolle, H., 'Linkage Coupler Curve Synthesis: A Historical Review - 1. Developments up to 1875', Mech. and Mach. Theory, 9(1974), 147-168.

{1.2} Kestell, T.A., 'Evolution and Design of Machinery primarily used in the Manufacture of Boots and Shoes', Proc.I.Mech.E., 178(1964), 625-683,{a} 655, {b} 647, {c} 657.

{1.3} Kraniauskas, P.V. and Maunder, L., 'Studies of Switchgear Mechanisms', Proc.IFToMM Symposium, 'University Research and its Application to Industry', Dublin, September 1974.

{1.4} Eder, W.E., 'The Kinematics and Design of Linkages: Cam or Linkage?', Mach.Des.Engng., Nov. 1967, 48-55.

{1.5} Wignall, H., 'Knitting', Sir Isaac Pitman, London, 1964, 92.

{1.6} Bloom, D., 'The Dual (or X, Y) Cam Mechanism', J. Mechanisms, 5 (1970), 11-27.

{1.7} Wray, G.R., Parry, R.M. and Pakes, H.W., 'The Mechanisms of a University - designed Textile Machine', Proc. Fourth World Congress on the Theory of Machines and Mechanisms, I.Mech.E., 1975, 1123-1129.

{1.8} Jackowski, C.S. and Dubil, J.F., 'Single-disk Cams with Positively Controlled Oscillating Followers', J. Mechanisms, 2 (1967), 157-184.

{1.9} Willkomm, G., 'Technology of Framework Knitting', translation by Rowlett, W.T., F. Hewitt, Leicester (about 1885), 249 and Fig. 339.

{1.10} Rothbart, H.A., 'Cams-Design, Dynamics and Accuracy', John Wiley and Sons Inc., New York, 1956, 174.

{1.11} Tovey, H.J. and Arnold, W.C., 'Design Progress of a Reed Mechanism and Selvedge Knitting Motion for a Loom', Proc.Mechanisms 1972 Conf., I.Mech.E., 1972, 133-139.

{1.12} VDI - Richtlinien, 2120-2147, VDI-Verlag GmbH, Dusseldorf.

{1.13} Hain, K., 'Atlas for Getriebe-Konstruktionen', Vieweg-Verlag, Braunschweig, 1972.

{1.14} ESDU, 'Kinematic and Dynamic Data for Crank-Rocker and Slider-Crank Linkages', Engineering Sciences Data Unit, London, 1976, Item 76005.

{1.15} Hrones, J.A. and Nelson, G.L., 'Analysis of the Four-bar Linkage', M.I.T. Press, Cambridge, Mass., 1951.

{1.16} Yokoyama, Y., 'Studies on the Geared Linkage Mechanisms, 1st Report, Classification and Analysis of Geared Four-Bar Linkage', Bull. JSME, 17 (1974), 1332-1339.

{1.17} Hain, K., 'Applied Kinematics', Second edition, McGraw-Hill Book Co., New York, 1967.

{1.18} Tepper, F.R. and Lowen, G.G., 'General Theorems concerning Full Force Balancing of Planar Linkages by Internal Mass Redistribution', J.Engng.Ind., Trans.ASME, Aug. 1972, 789-796.

{1.19} Oldham, K. and Walker, M.J., 'A Fundamental Approach to Balancing and Synthesizing the Forces of Multi-degree of freedom Planar Linkages', Univ. of Newcastle upon Tyne, Dept.Mech.Engng. Int. Rept. Ta 31.

{1.20} Rollason, E.C., 'Metallurgy for Engineers', 4th edn., Edward Arnold Ltd., London, 1973.

{1.21} Watt, W. and Phillips, L.N., 'Carbon Fibres for Engineering Applications', Proc.I.Mech.E., 1970, 185, 783-806.

{1.22} Paton, W. and Lockhart, A.H., 'The Structural Use of Carbon Fibre Composites', Department of Trade and Industry, NEL Report No. 555, December 1973.

{1.23} Karl Mayer Textilmaschinenfabrik G.m.b.H., Kettenwirk-Praxis, 1974, 8, No. 1, 11 (Eng.Edn.1).

{1.24} Dudley, W.M., 'A New Approach to Cam Design', Machine Design, July 1947, 143-148 and 184.

{1.25} Kanzaki, K. and Itao, K., 'Polydyne Cam Mechanisms for Typehead Positioning', J.Engng.Ind., Trans. ASME, Feb. 1972, 250-254.

{1.26} Earles, S.W.E. and Wu, C.L.S., 'Predicting the Occurrence of Contact Loss and Impact at a Bearing from a Zero-Clearance Analysis', Proc. Fourth World Congress on the Theory of Machines and Mechanisms, I.Mech.E., 1975, 1013-1018.

{1.27} Fawcett, J.N., 'Maintaining Contact brings Rewards', Engineering, September 1975, 741-743.

{1.28} Kraniauskas, P.V. and Maunder, L., 'Friction of Dry Journal Bearings subject to Periodic Loads and Speeds'. Proc. Fourth World Congress on the Theory of Machines and Mechanisms, I.Mech.E., 1975, 761-765.

CHAPTER 2.

{2.1} Reuleaux, F., 'The Kinematics of Machinery', trans. Kenedy, A.B.W., Macmillan, London, 1876 (Dover edn. 1963), 527.

{2.2} Nolle, H., 'Linkage Coupler Curve Synthesis: A Historical Review'

- I, 'Developments up to 1875', Mech. and Mach. Theory, 9 (1974), 147-168,

- II, 'Developments after 1875', Mech. and Mach. Theory, 9 (1974), 325-348,

- III,'Spatial Synthesis and Optimization', Mech. and Mach. Theory, 10 (1975), 41-55.

{2.3} Thompson, B.S., 'A Survey of Analytical Path-Synthesis Techniques for Plane Mechanisms', Mech. and Mach. Theory, 10(1975), 197-205.

{2.4} Kestell, T.A., 'Evolution and Design of Machinery primarily used in the Manufacture of Boots and Shoes', Proc.I.Mech.E., 178 (1964), 625-683.

{2.5} Dresig, H. and Pausch, E., 'Ein Programmsystem zur Kinematischen und Dynamischen Synthese ebener Koppelgetriebe', Maschinenbautechnik, 23 (1974), 3, 115-119.

{2.6} Schonfeld, S., 'Dynamische Synthese ebener Koppelgetriebe mit dem Programmsystem KOGEOP', Maschinenbautechnik, 23 (1974), 3, 119-124.

{2.7} Otto, J. and Weidauer, 'Anwendungsbeispiele des Programmsystems KOGEOP zur kinematischen Synthese und Optimierung ebener Koppelgetriebe', Maschinenbautechnik, 23 (1974), 3, 125-128.

{2.8} Kaufman, R.E., 'KINSYN - An Interactive Kinematic Design System', Proc. Third World Congress on the Theory of Machines and Mechanisms, Kupari, Yugoslavia, 1971, c17, 231-248.

{2.9} Kaufman, R.E., 'KINSYN Phase II : A Human Engineered Computer System for Kinematic Design and a New Least-Squares Synthesis Operator', Mech. and Mach. Theory, 8 (1973), 469-478.

{2.10} Bona, C., Galletti, C. and Lucifredi, A., 'Computer-Aided Automatic Design', Mech. and Mach. Theory, 8 (1973), 437-456.

{2.11} Keller, R.E., 'Mechanism Design by Electronic Analog Computer', Trans. Seventh Conf. Mechanisms, Purdue University, 1962, 11-21.

{2.12} Brat, V. and Vaclavik, M., 'Application of an Analogue Computer to the Synthesis of Plane Jointed Mechanisms', J. Mechanisms, 6 (1971), 107-118.

{2.13} Rees Jones, J., 'An Analogue Computer Aid for the Kinematic Design of a Low Impact Velocity Power Press Mechanism', Computer Aided Design, 7(1975), 250-254.

{2.14} Hartenberg, R.S. and Denavit, J., 'Kinematic Synthesis of Linkages', McGraw-Hill, New York, 1964.

CHAPTER 3

{3.1} Paul, B. 'A Unified Criterion for the Degree of Constraint of Plane Kinematic Chains', J. Appl. Mech., 27, Trans. ASME, 1960, 196-200.

{3.2} Deo, N., 'Graph Theory with Applications to Engineering and Computer Science', Prentice-Hall, Englewood Cliffs, 1974.

{3.3} Grubler, M., 'Getriebelehre', Springer, Berlin, 1917.

{3.4} Waldron, K.J., 'The Constraint Analysis of Mechanisms', J. Mechanisms, 1 (1966), 101-114.

{3.5} Manolescu, N.I., 'For a United Point of View in the Study of the Structural Analysis of Kinematic Chains and Mechanisms', J. Mechanisms, 3(1968), 149-169.

{3.6} Bagci, C., 'Degrees of Freedom of Motion in Mechanisms' J.Engng. Ind., Trans. ASME, Feb. 1971, 140-148.

{3.7} Freudenstein, F. and Alizade, R., 'On the Degree of freedom of Mechanisms with Variable General Constraint', Proc. Fourth World Congress on the Theory of Machines and Mechanisms, I.Mech.E., London, 1975, 51-56, and private Communication, March 18, 1976.

{3.8} Macmillan, R.H., 'The Freedom of Linkages', Math. Gaz., 34 (1950), 26-37.

{3.9} Grodzinski, P. and M'Ewen, E., 'Link Mechanisms in Modern Kinematics', Proc. I. Mech. E., 168 (1954), 877-896,{a} 891.

{3.10} Harrisberger, L., 'A Number Synthesis Survey of Three-Dimensional Mechanisms', J. Engng. Ind., Trans. ASME, May 1965, 213-220.

{3.11} Davies, T.H. and Umphrey, R.W., 'Self Alignment in Mechanisms', Advances in Mechanisms, vol. 1, Cranfield, 1970.

{3.12} Reuleaux, F., 'The Kinematics of Machinery', trans. Kennedy, A.B.W., Macmillan, London, 1876 (Dover edn. 1963), 551.

{3.13} Morecki, A., 'Podstawy Klasyfikacji Strukturalnej Mechanizmow Plaskich', Archiwum Budowy Maszyn, 4 (1957), 249-265.

{3.14} Crossley, F.R.E., 'The Permutations of Kinematic Chains of Eight Members of Lessfrom the Graph-Theoretic Viewpoint', Developments in Theoretical and Applied Mechanics, 2, Pergamon Press, 1965, 467-486.

{3.15} Klein, A.W., 'Kinematics of Machinery', McGraw-Hill, New York, 1917.

{3.16} Davies, T.H. and Crossley, F.R.E., 'Structural Analysis of Plane Linkages by Franke's Condensed Notation', J.Mechanisms, 1 (1966), 171-183.

{3.17} Woo, L.S., 'Type Synthesis of Plane Linkages', J. Engng. Ind., Trans. ASME, Feb. 1967, 159-172.

{3.18} Kiper, G. and Schian, D., 'Die 12 gliedrigen Grublerschen kinematischen Ketten', VDI-Z, 117 (1975), 6, 283-288.

{3.19} Uicker, J.J. and Raicu, A., 'A Method for the Identification and Recognition of Equivalence of Kinematic Chains', Mech. and Mach. Theory, 10 (1975), 375-383.

{3.20} Davies, T.H., 'An Extension of Manolescu's Classification of Planar Kinematic Chains and Mechanisms of Mobility $M \geq 1$, using Graph Theory', J. Mechanisms, 3(1968), 87-100.

{3.21} Verho, A., 'An Extension of the Concept of the Group', Mech. and Mach. Theory, 8 (1973), 249-256.

{3.22} Brat, V. and Lederer, P., 'KIDYAN: Computer-Aided Kinematic and Dynamic Analysis of Planar Mechanisms', Mech. and Mach. Theory, 8 (1973), 457-467.

{3.23} Manolescu, N.I., Antonescu, P. and Erceanu, I., 'The Methods of Formation of the Assur Groups function of the Number of Loops (circuits)(Z_g) and of the Rank of Links (J)', Bul.Institutului Politehnic"Gheorghe Gheorghiu-Dej", Bucuresti, 28(1966), 3, 59-83.

CHAPTER 4

{4.1} Hain, K., 'Applied Kinematics', 2nd edition, McGraw-Hill Book Co., New York, 1967, {a}39, {b}96,{c}302.

{4.2} Molian, S., 'Storage and Retrieval of Descriptions of Mechanisms and Mechanical Devices according to Kinematic Type', J. Mechanisms, 4 (1969), 311-323.

{4.3} Dresig, H. and Pausch, E., 'Programmsystem KOGEOP zu Analyse and Optimierung ebener Koppelgetriebe', Maschinenbautechnik, 23 (1974), 115-119.

{4.4} Taubald, R., 'Eine Moglichkeit der rechnergestutzten Strukturanalyse ebener Koppelgetriebe', Maschinenbautechnik, 21(1972), 359-361.

{4.5} Chace, M.A. and Angell, J.C., 'Users Guide to DRAM (Dynamic Response of Articulated Machinery)', 3rd edition, University of Michigan, April 1975.

{4.6} Sheth, P.N. and Uicker, J.J., 'IMP (Integrated Mechanisms Program), A Computer-Aided Design Analysis System for Mechanisms and Linkage', J. Engng.Ind., Trans. ASME, May 1972, 454-464.

{4.7} Smith, D.A., Chace, M.A. and Rubens, A.C., 'The Automatic Generation of a Mathematical Model for Machinery Systems', J.Engng.Ind., Trans. ASME, May 1973, 629-635.

{4.8} Branin, F.H., 'D.C. and Transient Analysis of Networks using a Digital Computer', IRE International Convention Record, 1962, part 2, 236-256.

{4.9} Hu, T.C., 'Integer Programming and Network Flows', Addison-Wesley Publishing Co. Inc., Cambridge, Mass., 1969.

{4.10} Kraniauskas, P.V., 'A Dynamic Analysis of Serially Connected Planar Linkages', Ph.D. Thesis, University of Newcastle upon Tyne, 1974.

{4.11} Rooney, G.T., 'Synthesis of Five-bar Geared Linkages', Ph.D. Thesis, Liverpool Polytechnic, 1970.

{4.12} Rooney, G.T., 'A Constraint Approach to Displacement Analysis of Planar Linkages', Proc. Mechanisms 1972 Conf., I.Mech.E., 1972, 60-63.

{4.13} Bitonti, F., Cooper, D.W., Frayne, D.N. and Hansen, H.H., 'A Computer-aided Linkage Analysis System', IBM Systems J., 4 (1965), 3, 200-223. See also 'Mechanism Design System - Kinematics', Application Description Manual H20-0493-1, 2nd edition, I.B.M. April 1969.

{4.14} Rosenauer, N. and Willis, A.H., 'Kinematics of Mechanisms', Dover Publications Inc., New York, 1967.

{4.15} Hannah, J. and Stephens, R.C., 'Mechanics of Machines, Advanced Theory and Examples', 2nd edition, Edward Arnold, London, 1972 , 75.

{4.16} Hartenberg, R.S. and Denavit, J., 'Kinematic Synthesis of Linkages', McGraw-Hill Book Co., New York, 1964, 66.

CHAPTER 5

{5.1} Osman, M.O.M. and Mansour, W.M., 'The Proximity Perturbation Method for the Kinematic Analysis of Six-Link Mechanisms', J. Mechanisms, 6(1971), 203-212.

{5.2} Molian, S., 'Rectangular Coordinate Methods for the Analysis of Mechanisms', ASME Paper 72-Mech-64.

{5.3} Reed, W.S. and Garrett, R.E., 'A Self-Generating Analysis Algorithm for Computer Based Design of Mechanisms', ASME Paper 74-DET-65.

{5.4} Molian, S., 'Solution of Kinematic Equations by Newton's Method', J.Mech.Engng.Sci., 10(1968), 4 360-362.

{5.5} Crossley, F.R.E. and Seshachar, N., 'Analysis of the Displacements of Planar Assur Groups by Computer', Proc. Third World Congress on the Theory of Machines and Mechanisms, Kupari, Yugoslavia, Sept. 13-20, 1971, Paper C-6, C 71-82.

{5.6} Paul, B. and Krajcinovic, D., 'Computer Analysis of Machines with Planar Motion, Part 1 - Kinematics', J.Appl.Mech., Trans. ASME, 37(1970), 3, 697-702.

{5.7} Van der Werff, K., 'Kinematics of Coplanar Mechanisms by Digital Computation', Proc. Fourth World Congress on the Theory of Machines and Mechanisms, I.Mech.E., 1975, 685-690.

{5.8} Bus, J.C.P., 'A Comparative Study of Programs for Solving Nonlinear Equations', NW25/75, Mathematisch Centrum, Amsterdam, Dec. 1975.

{5.9} Brown, K.M., 'Computer Oriented Algorithms for Solving Systems of Simultaneous Nonlinear Algebraic Equations', in Byrne, G.D. and Hall, C.A., 'Numerical Solution of Systems of Nonlinear Algebraic Equations', Academic Press, New York, 1973, 281-348.

{5.10} Powell, M.J.D., 'A Hybrid Method for Nonlinear Equations; A Fortran Subroutine for Solving Systems of Nonlinear Algebraic Equations', in Rabinowitz, P., 'Numerical Methods for Nonlinear Algebraic Equations', Gordon and Breach, London, 1970 (NAG subroutine C05NAF).

{5.11} Rooney, G.T. and Rees Jones, J., 'Curve Following in Kinematic Analysis', Proc. Fourth World Congress on the Theory of Machines and Mechanisms, I.Mech.E., 1975, 329-334.

{5.12} Fletcher, R., 'A New Approach to Variable Metric Algorithms', Computer J., 13, 3 (Aug. 1970), 317-322.

{5.13} Smith, D.A., 'Reaction Forces and Impact in Generalized Two-Dimensional Mechanical Dynamic Systems', Ph.D. Thesis, University of Michigan, 1971.

{5.14} Schonfeld, S., 'Dynamische Synthese ebener Koppelgetriebe mit dem Programmsystem KOGEOP', Maschinenbautechnik, 23(1974), 3, 119-124.

CHAPTER 6

{6.1} Porter, B. and Sanger, D.J., 'Synthesis of Dynamically Optimal Four-Bar Linkages', Proc. Mechanisms 1972 Conference, I.Mech.E., 1972, 24-28.

{6.2} Youssef, A.H., 'Dynamics and Control of Linkage Mechanisms having Two Degrees of Freedom', Ph.D. Thesis, University of Newcastle upon Tyne, April 1974, 78.

{6.3} Hain, K., 'Applied Kinematics', 2nd. edn., McGraw-Hill Book Co., New York, 1967, 642.

{6.4} Numerical Algorithms Group, 'NAG IBM 360-370 Mini Manual Mark 4', 1974.

{6.5} Swann, W.H., 'Constrained Optimization by Direct Search', in Gill, P.E. and Murray, W., 'Numerical Methods for Constrained Optimization', Academic Press, London, 1974.

{6.6} Spendley, W., Hext, G.R. and Himsworth, F.R., 'Sequential Application of Simplex Designs in Optimisation and Evolutionary Operation', Technometrics, 4 (1962), 441-461.

{6.7} Nelder, J.A. and Mead, R., 'A Simplex Method for Function Minimization', Comput.J., 7 (1965), 308-313.

{6.8} Parkinson, J.M. and Hutchinson, D., 'An Investigation into the Efficiency of Variants on the Simplex Method', in Lootsma, F.A., 'Numerical Methods for Non-linear Optimization', Academic Press, London, 1972.

{6.9} Box, M.J., 'A New Method of Constrained Optimization and a Comparison with other Methods', Comput.J., 8 (1965), 42-52.

{6.10} I.B.M., 'Random Number Generation and Testing', Manual C20-8011-O, 1959.

{6.11} Powell, M.J.D., 'An Efficient Method for Finding the Minimum of a Function of Several Variables Without Calculating Derivatives', Comput.J., 7 (1964), 155-162.

{6.12} Smith, W.D. and Reed, W.S., 'Interactive Mechanism Optimization employing Computer Graphics', Proc. Fourth World Congress on the Theory of Machines and Mechanisms, I.Mech.E., 1975, 627-632.

{6.13} Dixon, L.C.W., 'ACSIM - An Accelerated Constrained Simplex Technique', Comput. Aided Des., 5,1 (Jan. 1973), 22-32.

{6.14} Dixon, L.C.W., 'Nonlinear Optimisation : A Survey of the State of the Art' in Evans, D.J., 'Software for Numerical Mathematics', Academic Press, London, 1974.

{6.15} Parkinson, J.M. and Hutchinson, D., 'A Consideration of Non-gradient Algorithms for the Unconstrained Optimization of Functions of High Dimensionality' in Lootsma, F.A., 'Numerical Methods for Non-linear Optimization, Academic Press, London, 1972.

CHAPTER 7

{7.1} I.B.M., 'System/360 Scientific Subroutine Package, Version III, Programmer's Mannual', Manual GH20-0205-4, Fifth edition, 1970, 77.

{7.2} Youssef, A.H., 'Dynamics and Control of Linkage Mechanisms having Two Degrees of Freedom', Ph.D. thesis, University of Newcastle upon Tyne, 1974, Appendix 5.

{7.3} Chace, M.A. and Angell, J.C., 'Users Guide to DRAM', Third edition, University of Michigan, 1975.

{7.4} Smith, M.R. and Oldham, K., 'Computer Subroutine Library and a General Plotting Package', University of Newcastle upon Tyne, Dept. of Mech. Engng. Int.Rept. Te 11, Oct. 1973.

{7.5} Oldham, K., 'A General Plotting Package : Supplement to Te 11', University of Newcastle upon Tyne, Dept. of Mech. Engng. Int. Rept. Te 13, May 1974.

{7.6} Talbourdet, G.J., 'Mathematical Solution of 4-Bar Linkages, Part 1 - Analysis of Single 4-Bar Linkage', Machine Design, 13, May 1941, 65-68.

CHAPTER 8

{8.1} Freudenstein, F. and Sandor, G.N., 'Synthesis of Path-Generating Mechanisms by means of a Programmed Digital Computer', J.Engng.Ind., Trans.ASME, 1959, 159-168.

{8.2} Sutherland, G.H. and Roth, B., 'Mechanism Design: Accounting for Manufacturing Tolerances and Costs in Function Generating Problems', J.Engng. Ind., Trans. ASME, Feb. 1975, 283-286.

{8.3} Parkinson, J.M. and Hutchinson, D., 'An Investigation into the Efficiency of Variants on the Simplex Method', in Lootsma, F.A., 'Numerical Methods for Non-linear Optimization', Academic Press, London, 1972.

{8.4} Nelder, J.A. and Mead, R., 'A Simplex Method for Function Minimization', Comput.J., 7(1965), 308-313.

CHAPTER 9

{9.1} Chen, F.Y., 'A Survey of Computer Use in Mechanism Analysis and Synthesis', Proc. First Des.Engng.Tech.Conf., ASME, New York, 1974, 323-332.

{9.2} Root, R.R. and Ragsdell, K.M., 'A Survey of Optimization Methods Applied to the Design of Mechanisms', J.Engng.Ind., Trans. ASME, Aug. 1976, 1036-1041.

{9.3} Kramer, S.N. and Sandor, G.N., 'Selective Precision Synthesis - A General Method of Optimization for Planar Mechanisms', J.Engng. Ind., Trans. ASME, May 1975, 689-701.

{9.4} Oldham, K., 'KALM - Kinematic Analysis of Linkage Mechanisms', University of Newcastle upon Tyne, Department of Mechanical Engineering, Internal Rept.Ta47, June 1977.

{9.5} Oldham, K., 'Cam Design', Bentley Machine Development Co. Ltd., Leicester, Rept. 66/3, Dec. 1966.

CHAPTER 11

{11.1} Lowen, G.G. and Berkof, R.S., 'Survey of Investigations into the Balancing of Linkages', J.Mechanisms, 3(1968), 221-231.

{11.2} Berkof, R.S. and Lowen, G.G., 'A New Method for Completely Force-Balancing Simple Linkages', J.Engng.Ind., Trans. ASME, 91(1969), 21-26.

{11.3} Smith, M.R., 'Optimal Balancing of Planar Multi-bar Linkages', Proc. Fourth World Congress on the Theory of Machines and Mechanisms, I.Mech.E., 1975, 145-149.

{11.4} Paul, B., 'A Unified Criterion for the Degree of Constraint of Plane Kinematic Chains', J.Appl.Mech., Trans. ASME, Ser.E, 1960, 196-200.

{11.5} Tepper, F.R. and Lowen, G.G., 'General Theorems concerning Full Force Balancing of Planar Linkages by Internal Mass Redistribution', J.Engng.Ind., Trans.ASME., 1972, 789-796.

{11.6} Deo, N., 'Graph Theory with Applications to Engineering and Computer Science'. Prentice-Hall, Englewood Cliffs, 1974.

{11.7} Davies, T.H., 'The Kinematics and Design of Linkages, Balancing Mechanisms and Machines', Mach.Des.Engng., Mar. 1968, 40-51.

{11.8} Epstein, Yu. V. and Steinvolf, L.I., 'On the Optimum Shape of Rotating Counterweights', Trudy Seminara po TMM, 15(1955), 57, 47-60 (in Russian).
An English translation is given in Smith, M.R., 'Optimal Force-balancing of Planar Linkage Mechanisms', University of Newcastle upon Tyne, Dept. of Mech.Engng. Intl.Rept. Ta 22, Feb. 1974.

{11.9} Lowen, G.G., Tepper, F.R. and Berkof, R.S., 'The Quantitative Influence of Complete Force Balancing on the Forces and Moments of Certain Families of Four-bar Linkages', Mech. and Mach. Theory, 9(1974), 299-323.

CHAPTER 12

{12.1} Lowen, G.G. and Jandrasits, W.G., 'Survey of Investigations into the Dynamic Behaviour of Mechanisms containing Links with Distributed Mass and Elasticity', Mech. and Mach. Theory. 7 (1972), 3-17.

{12.2} Erdman, A.G. and Sandor, G.N., 'Kineto-Elastodynamics - A Review of the State of the Art and Trends', Mech. and Mach. Theory, 7 (1972), 19-33.

{12.3} Shoup, T.E. and McLarnan, C.W., 'A Survey of Flexible Link Mechanisms having Lower Pairs', J. Mechanisms, 6(1971), 97-105.

{12.4} McCallion, H., 'Vibration of Linear Mechanical Systems', Longman, London, 1973, 120.

{12.5} Cowper, G.R., 'The Shear Coefficient in Timoshenko's Beam Theory', J.Appl.Mech., Trans. ASME, June 1966, 335-340.

{12.6} Oldham, K., communication on the paper by Kestell, T.A., 'Evolution and Design of Machinery primarily used in the Manufacture of Boots and Shoes', Proc.I.Mech.E., 178 (1963-64), 670-672.

{12.7} Erdman, A.G., Sandor, G.N. and Oakberg, R.G., 'A General Method for Kineto-Elastodynamic Analysis and Synthesis of Mechanisms', J.Engng. Ind., Trans. ASME, 94 (Nov. 1972), 1193-1205.

{12.8} Erdman, A.G. Imam, I. and Sandor, G.N., 'Applied Kineto-Elastodynamics', Proc. 2nd. Appl.Mech. Conf.Stillwater, Oklahoma, Oct.1971, Paper 21.

{12.9} Erdman, A.G., 'Dynamics of High-Speed Mechanisms - an Approximate Method', Proc. 3rd. Appl.Mech.Conf., Stillwater, Oklahoma, Nov.1973, Paper 18.

{12.10} Sadler, J.P., 'A Lumped Parameter Approach to the Kineto-Elastodynamic Analysis of Mechanisms', Doctoral thesis, Rensselaer Polytechnic Institute, New York, Aug. 1972.

{12.11} Sadler, J.P. and Sandor, G.M., 'A Lumped Parameter Approach to Vibration and Stress Analysis of Elastic Linkages', J.Engng.Ind.,Trans.ASME, 95 (May 1973), 549-557.

{12.12} Sadler, J.P. and Sandor, G.N., 'Nonlinear Vibration Analysis of Elastic Four-Bar Linkages', J.Engng.Ind., Trans.ASME, May 1974, 411-419.

{12.13} Sadler, J.P., 'On the Analytical Lumped-Mass Model of an Elastic Four-Bar Mechanism', J.Engng.Ind., Trans.ASME, May 1975, 561-565.

{12.14} Golebiewski, E.P. and Sadler, J.P., 'Analytical and Experimental Investigation of Elastic Slider-Crank Mechanisms', J.Engng.Ind., Trans.ASME, Nov.1976, 1266-1271.

{12.15} Kohli, D. and Sandor, G.N., 'Lumped Parameter Approach for Kineto-elastodynamic Analysis of Elastic Spatial Mechanisms', Proc.Fourth World Congress on the Theory of Machines and Mechanisms, I.Mech.E., 1975, 253-258.

{12.16} Archer, J.S., 'Consistent Mass Matrix for Distributed Mass-Systems', J.Struct.Div., Proc. ASCE, 89, ST4(Aug.1963), 161-178.

{12.17} Archer, J.S., 'Consistent Matrix Formulations for Structural Analysis using Finite-Element Techniques', AIAA Journal, 3, 10(Oct.1965), 1910-1918.

{12.18} Thomas, D.L., Wilson, J.M. and Wilson, R.R., 'Timoshenko Beam Finite Elements', J.Sound Vibn., 31, 3(1973), 315-330.

{12.19} Thomas, J. and Abbas, B.A.H., 'Finite Element Model for Dynamic Analysis of Timoshenko Beam', J.Sound Vibn, 41,3(1975), 291-299; discussion, 46, 2(1976), 285-290.

{12.20} Boronkay, T.G. and Mei, C., 'Analysis and Design of Multiple Input Flexible Link Mechanisms', J.Mechanisms, 5, 1(1970), 29-40.

{12.21} Winfrey, R.C., 'Elastic Link Mechanism Dynamics', J.Engng.Ind., Trans.ASME, 93 (Feb.1971), 268-272.

{12.22} Winfrey, R.C., 'Dynamic Analysis of Elastic Link Mechanisms by Reduction of Co-ordinates', J.Engng.Ind., Trans.ASME, 94 (May 1972), 577-582.

{12.23} Imam, I., 'A General Method for Kineto-Elasto-dynamic Analysis and Design of High Speed Mechanisms', Ph.D. Thesis, Rensselaer Polytechnic Institute, New York, Aug. 1973.

{12.24} Imam, I., Sandor, G.N. and Kramer, S.N., 'Deflection and Stress Analysis in High Speed Planar Mechanisms with Elastic Links', J.Engng.Ind., Trans.ASME, 95(May 1973), 541-548.

{12.25} Imam, I. and Sandor, G.N., 'A General Method of Kineto-Elastodynamic Design of High Speed Mechanisms', Mech. and Mach. Theory, 8 (1973), 497-516.

{12.26} Imam, I. and Sandor, G.N., 'High-Speed Mechanism Design - A General Analytical Approach', J.Engng.Ind., Trans.ASME, May 1975, 609-628.

{12.27} Alexander, R.M. and Lawrence, K.L., 'Dynamic Strains in a Four-Bar Mechanism', Proc.3rd. Appl.Mech.Conf., Stillwater, Oklahoma, Nov. 1973, Paper 26.

{12.28} Alexander, R.M. and Lawrence, K.L., 'An Experimental Investigation of the Dynamic Response of an Elastic Mechanism', J.Engng.Ind.,Trans. ASME, 96(Feb.1974), 268-274.

{12.29} Alexander, R.M. and Lawrence, K.L., 'Experimentally determined Dynamic Strains in an Elastic Mechanism', J.Engng.Ind., Trans.ASME, Aug. 1975, 791-794.

{12.30} Lawrence, K.L. and Alexander, R.M., 'Elastic Mechanism Dynamic Strains', Proc.Fourth World Congress on the Theory of Machines and Mechanisms, I.Mech.E., 1975, 133-137.

{12.31} Jones, D.N., 'Modal Analysis of Elastic Four-Bar Mechanisms', M.Sc. Thesis, The University of Texas at Arlington, Aug.1976.

{12.32} Bahgat, B.M. and Willmert, K.D., 'Finite Element Vibrational Analysis of Planar Mechanisms', Mech. and Mach. Theory, 11(1976), 47-71.

{12.33} Khan, M.R. and Willmert, K.D., 'Vibrational Analysis of Mechanisms using Constant Length Finite Elements', J.Engng.Ind., Trans. ASME, Paper No. 76-WA/DE-21.

{12.34} Smith, M.R. and Maunder, L., 'Stability of a Four-bar Linkage with Flexible Coupler', J.Mech. Engng.Sci., 13(1971), 237-242.

{12.35} Smith, M.R., 'Determination of the Stability of Vibrations in Mechanisms by a Modified Perturbation Method', Proc.Third World Congress on the Theory of Machines and Mechanisms, Kupari, 1971, B, 225-234.

{12.36} Smith, M.R., 'The Dynamics of Rigid and Flexible Four-bar Linkage Mechanisms', Ph.D. Thesis, University of Newcastle upon Tyne, May 1972.

{12.37} Chu, S.C., and Pan, K.C., 'Dynamic Response of a High-Speed Slider-Crank Mechanism with an Elastic Connecting Rod', J.Engng.Ind.,Trans. ASME, May 1975, 542-550.

{12.38} Zorzi, E.S. and Frohrib, D.A., 'Stability and Response of a Viscoelastic Shear damped Kineto-elastodynamic Mechanism', Proc.Fourth World Congress on the Theory of Machines and Mechanisms, I.Mech.E., 1975, 1045-1050.

{12.39} Barr, A.D.S., 'Some General Aspects of the Analysis of the Vibration and Stability of Mechanisms', Euromech 22, Dynamics of Mechanisms, 1970, Paper 1.

{12.40} Thompson, B.S. and Barr, A.D.S., 'A Variational Principle for the Motion of Components of Elastic Mechanisms', Proc.Fourth World Congress on the Theory of Machines and Mechanisms, I.Mech.E., 1975, 235-239.

{12.41} Thompson, B.S. and Barr, A.D.S., 'A Variational Principle for the Elastodynamic Motion of Planar Linkages', J.Engng.Ind., Trans.ASME, Nov. 1976, 1306-1312.

{12.42} Sutherland, G.H., 'Analytical and Experimental Study of a High-Speed Elastic Mechanism', Proc.Fourth World Congress on the Theory of Machines and Mechanisms, I.Mech.E., 1975, 533-536.

{12.43} Sutherland, G.H., 'Analytical and Experimental Investigation of a High-Speed Elastic-Membered Linkage', J.Engng.Ind., Trans.ASME, Aug. 1976, 788-794.

{12.44} Vinogradov, V.S., 'Force Analysis of a Four-bar Linkage with an Elastic Coupler' (in Russian), Mashinostroenia (Moscow), 1967, 8, 12-16.

{12.45} Kantorovich, L.V. and Krylov, V.I., 'Approximate Methods of Higher Analysis', P. Noordhoff Ltd., Groningen, 1958.

{12.46} Forray, M.J., 'Variational Calculus in Science and Engineering', McGraw-Hill, New York, 1968.

{12.47} Rose, W. and Schrepfer, W., 'Experimentelle Untersuchungen an ebenen Koppelgetrieben mit mehreren Freiheitsgraden', Maschinenbautechnik, 23(1974), 3, 129-132.

{12.48} Funabashi, H. and Ogawa, K., 'A Dynamic Synthesis of Non-uniform Motion Mechanisms', Bull. JSME, 19, 130 (April 1976), 446-453.

{12.49} Meyer zur Capellen, W. and Krumm, H., 'Oscillations of an Elastically suspended Coupler of a Four-bar Linkage', J.Mechanisms, 6(1971), 4, 351-365.

{12.50} Chakraborty, J. and Khare, A.K., 'Kineto-Elastodynamic Analysis of Slider-crank Mechanism with a Flexibly attached Slider', J.Engng.Ind., Trans. ASME, Feb. 1975, 308-313.

{12.51} Davidson, I., 'Dynamic Instability in Flexibly Mounted Mechanisms', Proc. Fourth World Congress on the Theory of Machines and Mechanisms, I.Mech.E., 1975, 241-246.

{12.52} Kohli, D. and Sandor, G.N., 'Elastodynamics of Planar Linkages including Torsional Vibrations of Input and Output Shafts and Elastic Deflections at Supports', Proc. Fourth World Congress on the Theory of Machines and Mechanisms, I.Mech.E., 1975, 247-252.

{12.53} Thompson, B.S. and Ashworth, R.P., 'Resonance in Planar Linkage Mechanisms mounted on Vibrating Foundations', J. Sound Vibn., 49,3(Dec.1976), 403-414.

{12.54} Dubowsky, S. and Young, S.C., 'An Experimental and Analytical Study of Connection Forces in High-speed Mechanisms', J.Engng.Ind., Trans. ASME, Nov. 1975, 1166-1174.

{12.55} Dubowsky, S. and Gardner, T.N., 'Dynamic Interactions of Link Elasticity and Clearance Connections in Planar Mechanical Systems', J.Engng.Ind., Trans. ASME, 1975, 652-661.

{12.56} Dubowsky, S. and Gardner, T.N., 'Design and Analysis of Multi-link Flexible Mechanisms with Multiple Clearance Connections', ASME Paper No. 76-DET-9.

{12.57} Freudenstein, F., 'Harmonic Analysis of Crank and Rocker Mechanisms with Application', J.Appl.Mech., Trans. ASME, Dec. 1959, 673-675.

CHAPTER 13

{ 13.1 } Lazan, B. J., 'Damping of Materials and Members in Structural Mechanics', Pergamon Press, 1968.

{ 13.2 } Cowper, G. R., 'The Shear Coefficient in Timoshenko's Beam Theory', J. Appl. Mech., Trans. ASME, June 1966, 335-340.

{ 13.3 } Timoshenko, S., Young, D. H. and Weaver, W., 'Vibration Problems in Engineering', Fourth edn., John Wiley and Sons, 1974.

{ 13.4 } Anderson, R. A., 'Flexural Vibrations in Uniform Beams According to the Timoshenko Theory', J. Appl. Mech., Trans. ASME, Dec. 1953, 504-510.

{ 13.5 } Smith, M. R. and Maunder, L., 'Stability of a Four-bar Linkage with Flexible Coupler', J.Mech. Engng. Sci., 13(1971), 4, 237-242.

{ 13.6 } Rubenfeld, L. A., 'The Stability Surfaces of a Hill's Equation with Several Small Parameters', J. Appl. Mech., Trans. ASME, Dec. 1973, 1107-1109.

CHAPTER 14

{14.1} Denavit, J. and Hasson, S., 'On the Harmonic Analysis of the Four-bar Linkage', Proc. Int. Conf. Teachers of Mechanisms, Yale Univ., Shoe String Press, 1961, 170-185.

{14.2} Cooley, J.W. and Tukey, J.W., 'An Algorithm for the Machine Calculation of Complex Fourier Series', Mathematics of Computation, 19,90(1965), 297-301. (NAG subroutine C06AAF).

{14.3} Magnus, W. and Winkler, S., 'Hill's Equation', Interscience Publishers, John Wiley and Sons, 1966, 73.

{14.4} McLachlan, N.W., 'Theory and Application of Mathieu Functions', Oxford Univ. Press, 1947, 59.

{14.5} Smith, M.R., 'The Dynamics of Rigid and Flexible Four-bar Linkage Mechanisms', Ph.D. thesis, Univ. Newcastle upon Tyne, May 1972.

{14.6} Penney, G., 'Four-bar Linkages',Bentley Machine Development Co., Leicester, Report 67/2, June 1967.

CHAPTER 15

{15.1} Gibbs, P.J., Gilbert, D. and Stevens, D.T., 'A System for Describing Mechanical Engineering Components', CAD 76 Proceedings, 182-187.

{15.2} Hanratty, P.J., 'AD-2000, Automated Design and Drafting for 2000 AD', Manufacturing and Consulting Services Inc., Costa Mesa, California.

{15.3} Broch, J.T., 'Mechanical Vibration and Shock Measurements', Bruel and Kjaer, revised edn. May 1972, 220-233.

{15.4} Walker, M.J., Smith, M.R. and Oldham, K., 'Linkage Design, Finding the Optimum Solution', Engng. Mat. Des., 21, 10(Oct. 1977), 29-31.

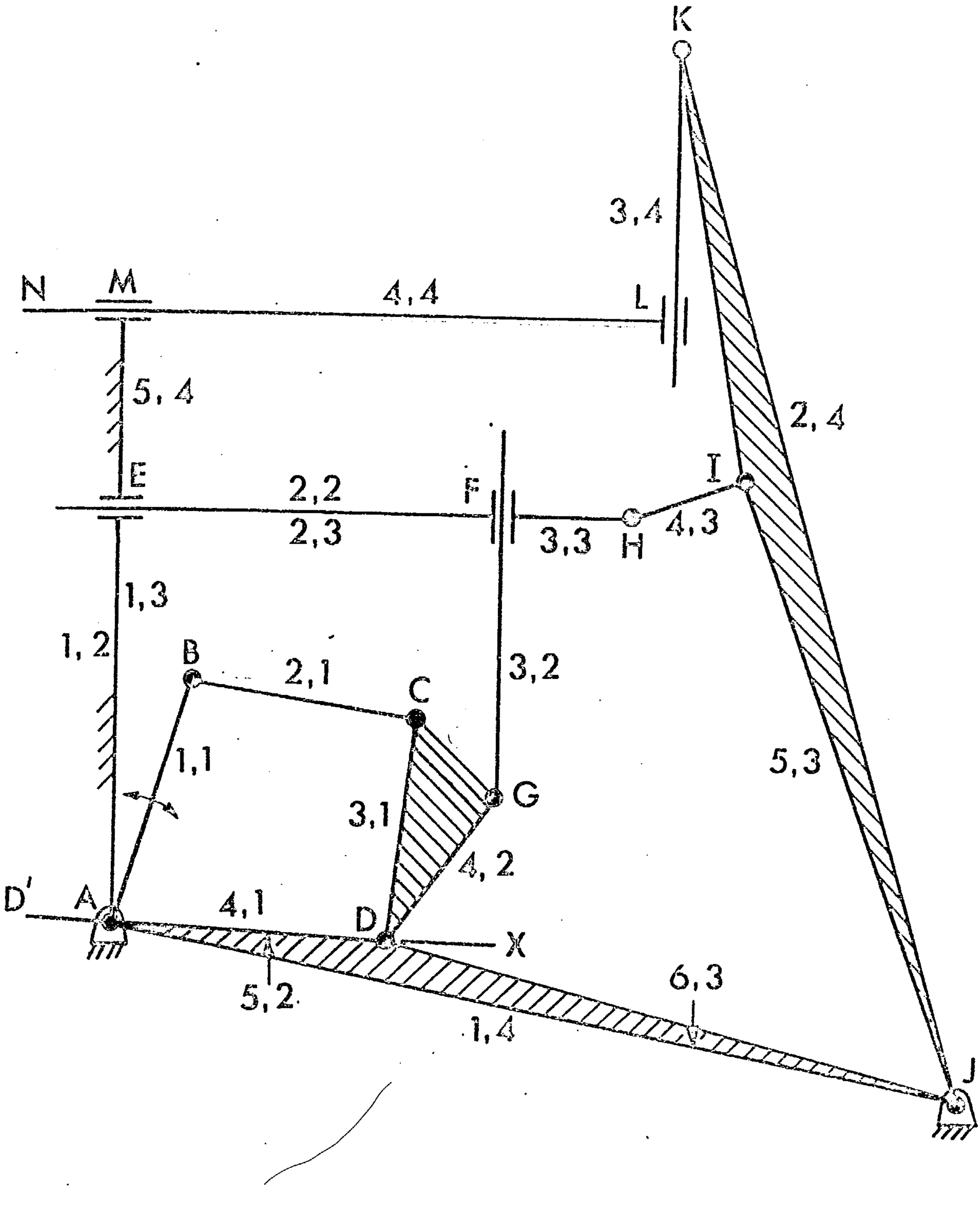

FIGURE B1 TEXTILE TEN-BAR LINKAGE

B. PSALM INPUT DATA

B1 TITLE

The first record in the data set for any linkage contains the title which is printed out at the top of the output. The title may contain any valid characters up to a maximum of 72. Thus, for example, the title for the linkage in Figure B1 could be :

```
TEXTILE TEN-BAR LINKAGE,FIGURE B1
```

B2 TOPOLOGICAL DATA SET - LINKS

The topological data set, called LINKS, is read in using a NAMELIST statement (see Section 7.2) and contains the information that defines the topology, the link dimensions and related items.

B2.1 Topological Data

The topology of the mechanism is defined by two parameters, NLOOP and MAXARC, and two arrays, ILINK and ILOOP, each containing locations for 100 entries.

NLOOP The number of loops in the linkage. In single degree-of-freedom linkages for which PSALM caters, the number of independent loops is $(\ell-2)/2$ where ℓ is the total number of links, equation (4.1). Maximum NLOOP is 10.

MAXARC The maximum number of arcs in any of the loops. The maximum value of MAXARC is 100/NLOOP.

Thus for the linkage in Figure B1 which has four loops and six arcs in the third loop, the start of the first record of the data set would be :

```
&LINKS NLOOP=4,MAXARC=6,
```

The two arrays each consist of NLOOP rows with MAXARC columns. The position of an entry in each array defines for which arc the entry provides information. Thus the entry in the third column of the second row will provide information for the third arc in the second loop.

ILINK contains the arc numbers as defined below.

ILOOP contains either loop or guide link numbers.

B2.2 Numbers for Determined Arcs

A determined arc is one associated with a link whose length and orientation either are known from a previous loop or are prescribed e.g. the input link.

For the input link, the first entries in ILINK and ILOOP respectively are 1 and 1 for a revolute actuator pair and ± 1 and -4 for a prismatic actuator pair.

Group (i)

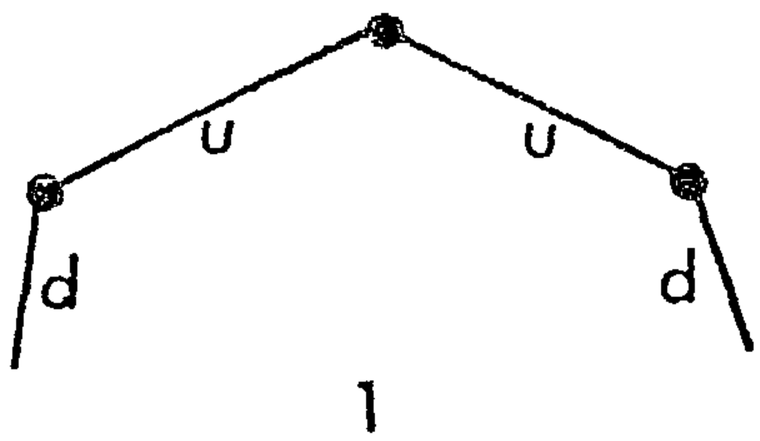

1

Type (a)

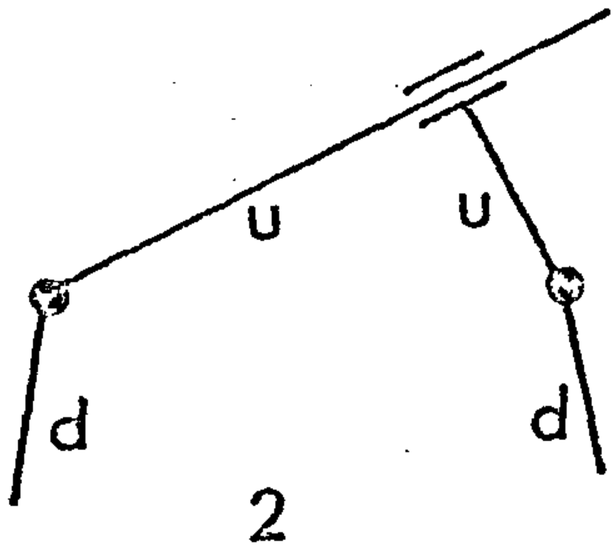

2

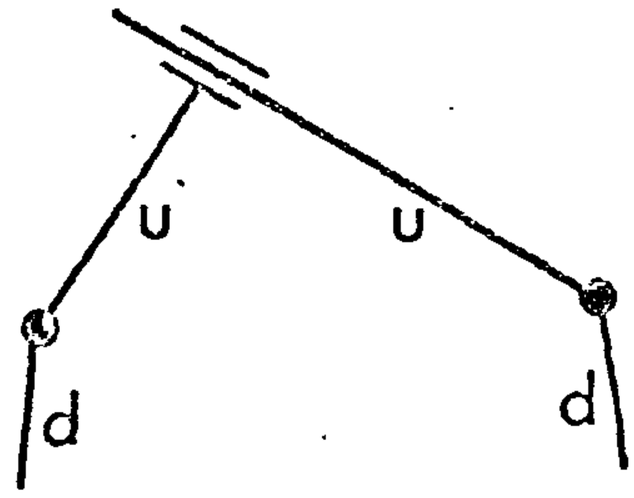

3

Group (ii)

Type (b)

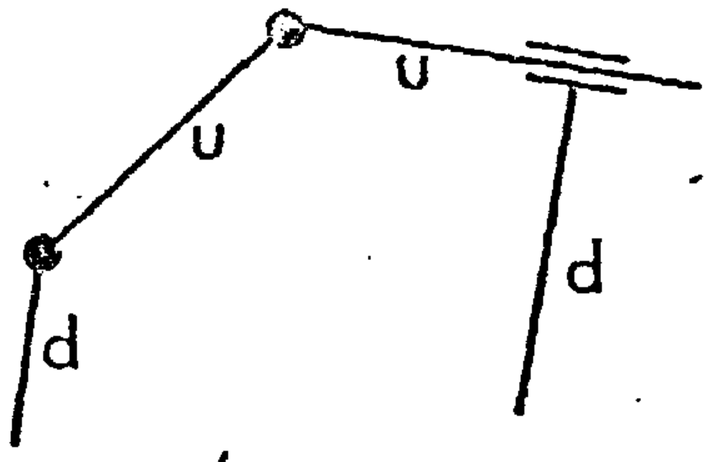

4

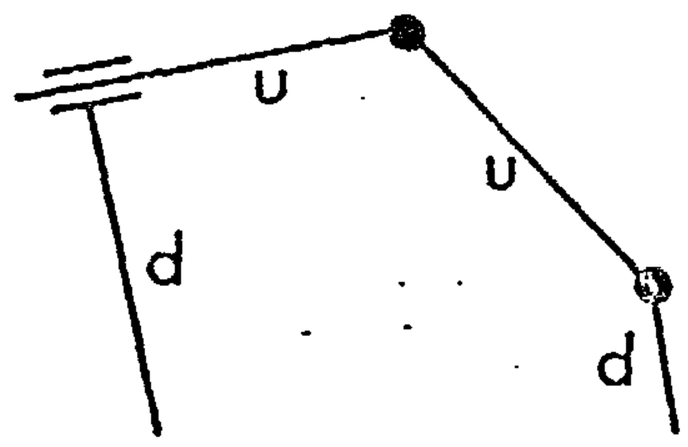

5

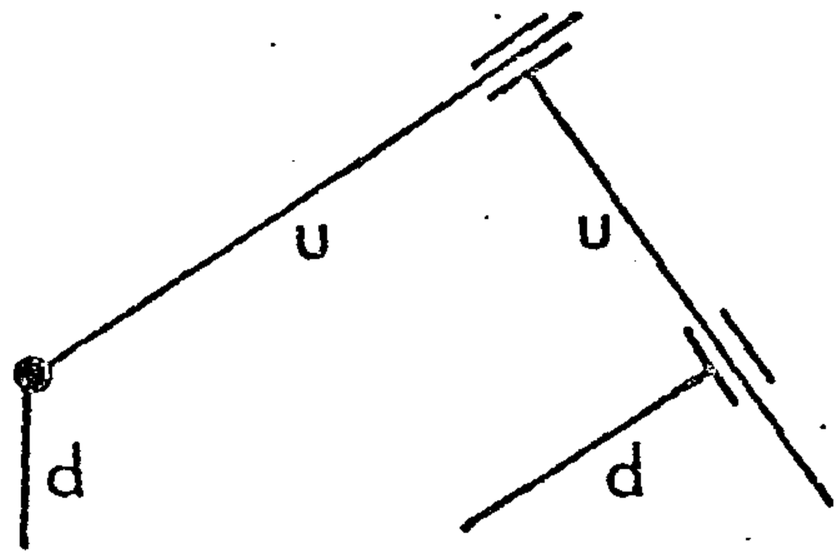

6

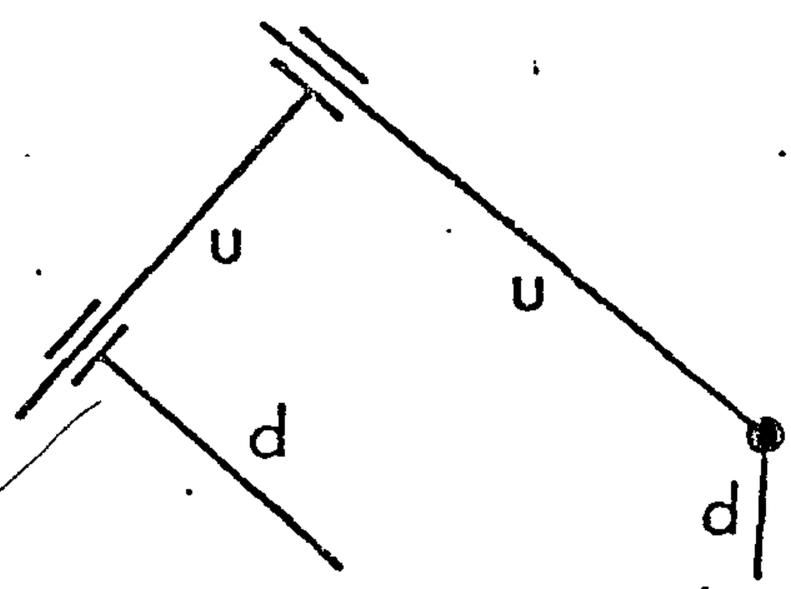

7

Group (iii)

d = determined arc
u = undetermined arc

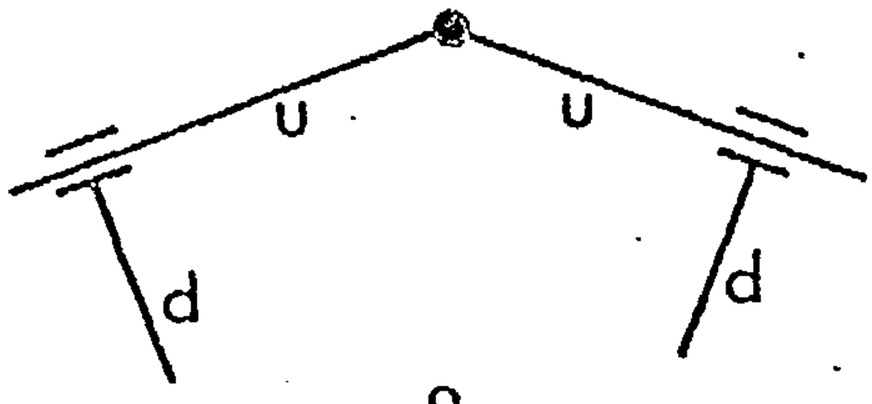

8

FIGURE B2 VALID UNDETERMINED DYADS

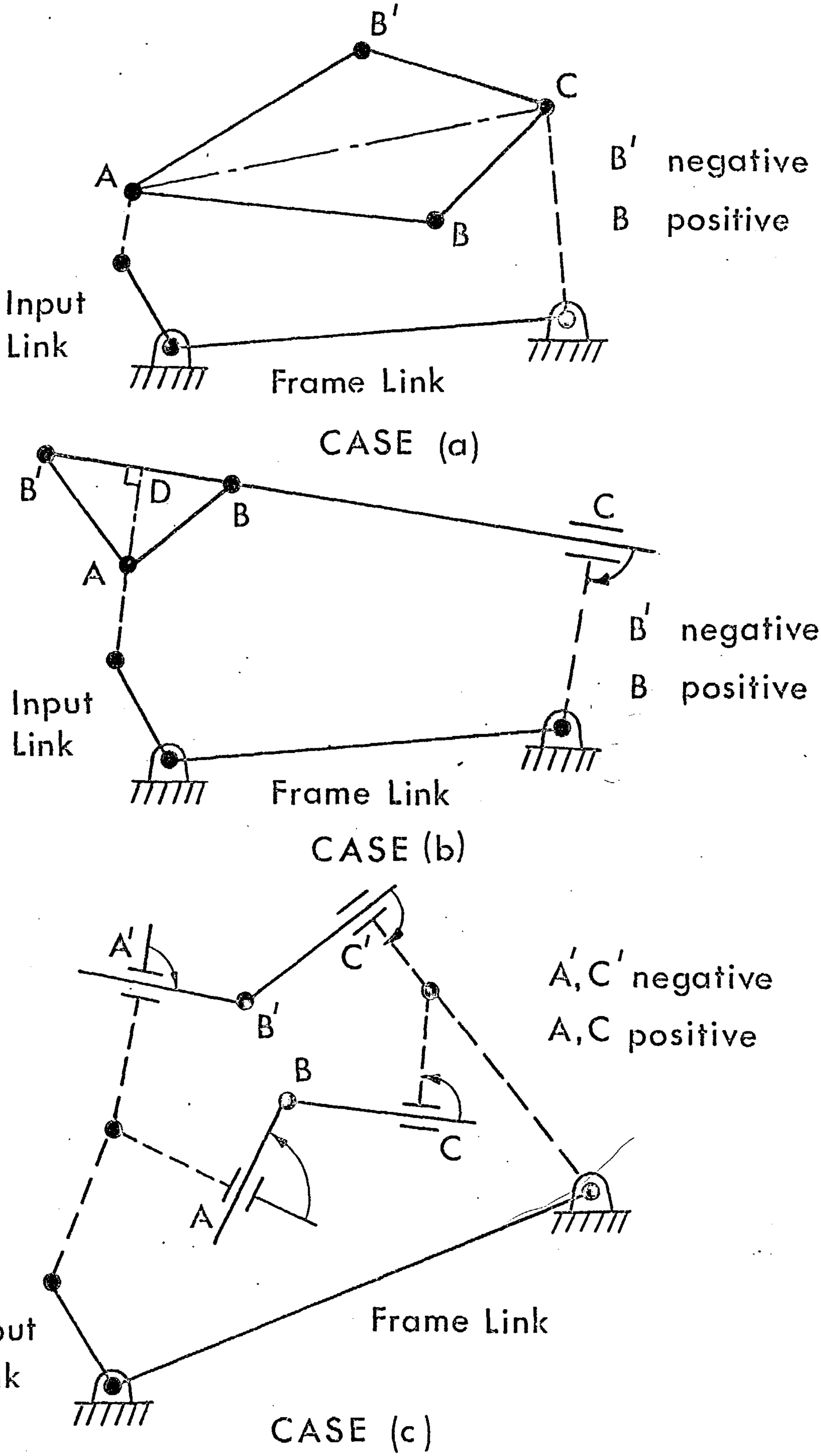

FIGURE B3. SIGNS FOR UNDETERMINED ARCS

The entry in ILINK is the arc number of the common arc (in the loop in which it first appears) that defines the orientation of the arc under consideration. The entry is :

(i) positive if the arcs in the two loops are coincident in length and angle, i.e. direction

(ii) negative if the arcs in the two loops are a fixed angle, γ, apart or the lengths are different.

The entry in ILOOP is the number of the loop containing the arc entered in ILINK and is positive. Thus for the determined arcs in Figure B1 :

$$\text{ILINK} = \begin{matrix} 1 & . & . & 4 & . & . \\ -4 & . & . & -3 & 4 & . \\ 1 & 2 & -2 & . & . & -4 \\ -6 & -5 & . & . & -1 & . \end{matrix}$$

$$\text{ILOOP} = \begin{matrix} 1 & . & . & 1 & . & . \\ 1 & . & . & 1 & 1 & . \\ 2 & 2 & 2 & . & . & 1 \\ 3 & 3 & . & . & 2 & . \end{matrix}$$

Note that for the first arc in the fourth loop, the minus sign in ILINK is due to the arc being traversed in the opposite direction.

B2.3 Numbers for Undetermined Arcs

An undetermined arc is one associated with a link whose orientation or length is neither known from a previous loop nor prescribed. Three cases must be considered.

(a) Both undetermined arcs are connected by revolute joints to determined arcs, Figure B2, groups (i) and (iia).

The entry in ILINK is the number of the arc in the current loop. The sign determines which of the two possible configurations is taken. The convention depends on the position of the revolute or prismatic joint joining the two undetermined arcs relative to the line joining the determined ends of the undetermined dyad when that line is traversed in the same direction as the loop i.e. input link pivot, ... frame. It is :

(i) positive if the common joint is on the right,

(ii) negative if the common joint is on the left.

Thus in Figure B3a, it depends on the position of B relative to AC as we travel from A to C. The joint in position B shows the positive case and that at B' the negative case.

The entry in ILOOP for :

a fixed length link is nought,
a sliding link is the number in the current loop of its guide link and is negative.

Thus for the undetermined arcs of this type in Figure B1, namely BC and CD in loop 1 and HI and IJ in loop 3 :

ILINK =	.	-2	-3	.	.	.
	.	.	.	.	.	.
	.	.	.	-4	-5	.
	.	.	.	.	.	.
ILOOP =	.	0	0	.	.	.
	.	.	.	.	.	.
	.	.	.	0	0	.
	.	.	.	.	.	.

(b) A fixed length undetermined link with two revolute joints in the current loop is connected to a sliding link which has a determined guide link, Figure B2, group (iib).

A positive direction must be defined for a sliding link since its length may change sign in some cases. It is taken as the loop direction for that link when the linkage is drawn with the input link in the reference position, CRNKI (see Section B3.2).

The entry in ILINK for the fixed length undetermined link is the number of the arc in the current loop. The sign is positive (negative) when the revolute joint connecting the two undetermined links is in the positive (negative) sliding link direction from the projection of the other revolute joint onto the sliding link.

The entry in ILOOP for the fixed length undetermined link is nought.

Thus in Figure B3b, D is the projection of A onto BC. If the positive direction for the sliding link is from B to C, the entries for AB as the third arc in the loop would be:

ILINK =	.	.	3	.	.
ILOOP =	.	.	0	.	.

The entries in ILINK and ILOOP for the sliding link are determined using the procedure in section c.

(c) Sliding links, Figure B2, groups (ii) and (iii).

The entry in ILINK is the number of the link in the current loop. Its sign depends on the sense of the right angle turned through as the prismatic joint is traversed in the same direction as the loop with the linkage in the reference position. It is :

(i) positive if the right angle is anticlockwise.

(ii) negative if the right angle is clockwise.

The two conditions are shown in Figure B3c. Joints A and C are positive; joints A' and C' are negative. If the guide link has zero length, the sign of the entry in ILINK is immaterial unless a later arc is common with it.

The entry in ILOOP is the arc number in the current loop of its guide link and is negative.

Thus for the undetermined arcs of this type in Figure B1, namely EF and FG in loop 2 and KL and LM in loop 4 :

```
ILINK =   .   .   .   .   .   .
          .  -2  -3   .   .   .
          .   .   .   .   .   .
          .   .  -3   4   .   .

ILOOP =   .   .   .   .   .   .
          .  -1  -2   .   .   .
          .   .   .   .   .   .
          .   .  -4  -5   .   .
```

B2.4 Numbers for Non-existent Arcs

Each row in the ILINK and ILOOP arrays must contain MAXARC entries. However, some loops may not contain that number of arcs. For instance, MAXARC is 6 for the linkage in Figure B1, but loop 1 consists of only four arcs and loops 2 and 4 contain only five arcs each. The entry in both ILINK and ILOOP for these non-existent arcs is nought.

Thus for the non-existent arcs in Figure B1 :

```
ILINK =   .   .   .   .   O   O
          .   .   .   .   .   O
          .   .   .   .   .   .
          .   .   .   .   .   O

ILOOP =   .   .   .   .   O   O
          .   .   .   .   .   O
          .   .   .   .   .   .
          .   .   .   .   .   O
```

B2.5 Complete Topological Arrays

The complete ILINK and ILOOP arrays for Figure B1 are :

```
ILINK =   1   -2   -3   4   O   O
         -4   -2   -3  -3   4   O
          1    2   -2  -4  -5  -4
         -6   -5   -3   4  -1   O

ILOOP =   1    O    O   1   O   O
          1   -1   -2   1   1   O
          2    2    2   O   O   1
          3    3   -4  -5   2   O
```

These may be entered row by row in 'linear form' on the data record e.g.

ILOOP=1,2*O,1,2*O,1,-1,-2,2*1,O,3*2, ...76*O,

The 76*O is appended to fill the remaining 76 (100- NLOOP*MAXARC) locations in the array with noughts.

B2.6 Arc Lengths and Angles

Any optimization routine requires an estimate of the values of the optimization variables from which to commence the search. PSALM is no exception. However, when PSALM is used for analysis, actual values must be supplied for these same quantities. For this reason, irrespective of which linkage parameters, if any, are variable and whether PSALM is to be used for synthesis or analysis, the dimensions of the linkage, whether estimates or actual values, are entered into two arrays, ARCL and GAMA, with 100 locations available for each. Again both arrays consist of NLOOP rows with MAXARC columns and the position of an entry defines for which arc that entry provides information.

ARCL contains the lengths of the arcs in consistent units e.g. all in mm or all in inches. The lengths of sliding links and non-existent arcs are entered as 0.0.

GAMA contains the angles, measured positive anticlockwise in degrees, between the directions in which common arcs are traversed in their respective loops. For this purpose, the frame arc in the first loop is regarded as being common with the x-axis which is any convenient reference direction in the machine of which the linkage forms part. The angles of arcs that are not common are entered as 0.0.

On the machine from which the linkage in Figure B1 is taken, the x-axis is horizontal, arcs AE and MA are vertical, joints C,G and D are collinear as are J,I and K. Also AJ lies above AD but is shown below in Figure B1 for clarity. For this linkage, these two arrays are of the following form but with actual values :

ARCL =	AB	BC	CD	DA	0.0	0.0
	AE	0.0	0.0	GD	DA	0.0
	AE	0.0	FH	HI	IJ	JA
	AJ	JK	0.0	0.0	MA	0.0
GAMA =	0.0	0.0	0.0	xDA	0.0	0.0
	D'AE	0.0	0.0	0.0	0.0	0.0
	0.0	0.0	0.0	0.0	0.0	DAJ
	180.0	180.0	0.0	0.0	180.0	0.0

Since the fifth arc in the second loop, DA, is identical to the fourth arc in the first loop and is traversed in the same direction, the corresponding entry in GAMA is 0.0. The same applies to the first arc in the third loop, AE, which is identical to the first arc in the second loop. On the other hand, the first arc in the last loop, AJ, is traversed in the opposite direction to the last arc in the third loop so that, although the entries in ARCL will be

the same, the entry in GAMA for AJ is 180.0. Similarly the entries in GAMA corresponding to FH, JK and MA in ARCL are 0.0, 180.0 and 180.0 respectively.

In the third loop, EF and FH are regarded as distinct arcs (rather than a single arc EH), so that the length of EF, which depends on the position of the input link and is calculated as part of the undetermined dyad in loop 2, is determined as far as loop 3 is concerned.

B2.7 Output Link

The output link is regarded as a ternary link and is specified using two identifiers, NOUTLK and NOUTLP, and two parameters, OUTLK and OUTANG.

NOUTLK — The number in its own loop of the arc common with the output arc. It is negative if the output arc length, OUTLK, and angle, OUTANG, are measured from the start of NOUTLK when the output loop, NOUTLP, is traversed in the order :

input link pivot,....,frame

It is positive if OUTLK and OUTANG are measured from the finish of NOUTLK. The nearer NOUTLK is to the finish of NOUTLP, the faster execution will be.

NOUTLP — The number of the loop containing NOUTLK.

OUTLK — The length of the output arc in the same units as the entries in ARCL. No value is required if the desired output quantity is the angular position of the output arc.
Default = 0.0.

OUTANG — The fixed angle in degrees which the output arc makes with NOUTLK. It is measured positive anticlockwise from the direction in which NOUTLK is traced to the direction in which OUTLK is traced.
Default = 0.0.

Thus if the output is taken from N in Figure B1 and since these are the last entries in the data set, the last record in the LINKS data set would end with :

NOUTLK=-4,NOUTLP=4,OUTLK=LN,OUTANG=0.0 &END

where the actual length of LN would be entered instead of the letters LN and OUTANG=0.0 may be omitted since the default value is zero.

B2.8 Complete Data Set, LINKS

The complete data set, LINKS, for the linkage in Figure B1 would be of the form :

```
&LINKS NLOOP=4,MAXARC=6,
ILINK=1,-2,-3,4,0,0,-4,-2,2*-3,4,0,
1,2,-2,-4,-5,-4,-6,-5,-3,4,-1,77*0,
ILOOP=1,0,0,1,0,0,1,-1,-2,1,1,0,
3*2,0,0,1,3,3,-4,-5,2,77*0,
ARCL=AB,BC,CD,DA,2*0.0,AE,2*0.0,GD,DA,0.0,
AE,0.0,FH,HI,IJ,JA,AJ,JK,2*0.0,MA,77*0.0,
GAMA=3*0.0,xDA,2*0.0,D'AE,5*0.0,
5*0.0,DAJ,2*180.0,2*0.0,180.0,77*0.0,
NOUTLK=-4,NOUTLP=4,OUTLK=LN &END
```

where the actual arc lengths and angles would be entered in the appropriate positions in ARCL, GAMA and OUTLK.

B3 OPTIMIZATION DATA SET - METHOD

The optimization data set, called METHOD, contains the information related to the optimization variables, the desired motion (i.e. objective function) and the Simplex algorithm.

B3.1 Identification of Optimization Variables

Which linkage parameters the optimization algorithm may alter is prescribed in two arrays and by several separate identifiers. The maximum permissible total number of optimization variables is 30.

The arrays, IVA and IVG, each contain locations for 100 entries. They are arranged in MAXARC columns of which the first NLOOP rows may be non-zero. The position of an entry in each array denotes whether the arc lengths and angles in the corresponding positions in the ARCL and GAMA arrays respectively may be altered.

In all cases, a nought is used to denote that the corresponding linkage parameter is to remain unaltered whilst a one denotes that it may be altered. The default value for all identifiers is nought. The correspondence between the identifiers and the parameters is given in Table B1.

Table B1. Correspondence between Identifiers and Linkage Parameters.

Optimization Variable Identifier	Linkage Parameter	Defined in Section
IVA	ARCL	B2.6
IVG	GAMA	B2.6
ILKOUT	OUTLK	B2.7
INGOUT	OUTANG	B2.7
ICRK	CRNKI	B3.2
IORIG	(ORIGLK	B3.2
	(ORIGNG	B3.2

For example, if the arc lengths AB, BC, CD, DA, HI, IJ and JK and the output arc length, LN, in Figure B1 are to be optimization variables, the identifiers would have the following values :

IVA = 1 1 1 1 0 0
0 0 0 0 0 0
0 0 0 1 1 0
0 1 0 0 0 0

ILKOUT = 1

The other identifiers would assume the default value of nought.

If an arc length or angle which is to be an optimization variable appears more than once in the ARCL or GAMA array, then a one should be entered into the IVA or IVG array only in the position corresponding to the first appearance. For example, the arc length DA appears in the fourth position in the first row and the fifth position in the second row of the ARCL array, but a one is entered into only the first of these positions in the IVA array. Otherwise a warning message that the lengths or angles cannot be varied independently of each other will be printed out.

If no linkage parameters are identified as optimization variables, it is assumed that the linkage defined by the parameters is to be analysed at the prescribed input link positions (see below).

Alternatively, all of the identifiers and the prescribed input link positions can be overridden by the data checking control :

IKIN data checking control, the linkage is analyzed at IKIN degree increments of input link rotation from the reference position (see below), minimum non-zero value equals ±1,
positive value = anticlockwise rotation,
negative value = clockwise rotation,
zero value = normal optimization.
Default = 0.

B3.2 Objective Function - Desired Motion

The positions of the input link at which the linkage is to be analyzed are prescribed as follows :

NDES number of positions, maximum value equals 181,

CRNKI reference position of the input link measured positive anticlockwise in degrees from the x-axis fixed in the machine frame. If it is to be an optimization variable, a non-zero value should be entered.
Default = 0.0

DELT array of incremental rotations of the input link measured positive anticlockwise in degrees from CRNKI.

The characteristic of the output link to be calculated at these positions is governed by :

MOTION = 0; x,y co-ordinates of the output point (defined by OUTLK and OUTANG) are required relative to Cartesian axes fixed in the machine frame,

1; angular positions of the output arc are required relative to the x-axis fixed in the machine frame,

2; distances of the output point from the origin of the cartesian axes fixed in the machine frame are required.

The parameters used to define the desired motion depend on the value of MOTION.

a) MOTION = 0

The relevant parameters in the same units as the entries in the ARCL array (apart from ORIGNG) are :

XADD
YADD the co-ordinate relative to the fixed Cartesian axes of the point relative to which the desired positions are defined.
Default XADD=0.0, YADD=0.0

DESX array containing the desired x co-ordinates of the output point relative to XADD

DESY array containing the desired y co-ordinates of the output point relative to YADD

ORIGLK the distance of the input link pivot from the origin of the fixed Cartesian axes. A non-zero value should be supplied if IORIG equals one.
Default = 0.0

ORIGNG the angular position in degrees of the input link pivot relative to the fixed x-axis. If it is to be an optimization variable, a non-zero value should be supplied.
Default = 0.0

b) MOTION = 1

In this case only one array is required, none of the other parameter being relevant.

DESANG array containing the desired angular positions in degrees of the output arc relative to the fixed x-axis.

c) MOTION = 2

The same array is used as for the previous case

DESANG array containing the desired distances of the output point from the fixed origin in the same units as the entries in the ARCL array.

ORIGLK
ORIGNG polar co-ordinates of the input link pivot (as for MOTION = 0).

The arrays containing the weighting factors corresponding to the desired motion values are given in Table B2. In each case the default equals 181*1.0.

Table B2 Correspondence between Weighting Factors and Desired Values

Weighting Factor Array	Desired Value Array
XMULT	DESX
YMULT	DESY
ANMULT	DESANG

Thus weighting factors for values in the DESANG array would appear in the ANMULT array.

B3.3 Initial Simplex

The initial simplex, as described in Section 6.4.2, is determined by the following parameters.

VAR variation in the interval (0.0, 1.0) of the values of the optimization variables in ARCL etc. within which the vertices are to be generated.

Upper limit, $u_i = (1.0+VAR)v_i$

Lower limit, $\ell_i = (1.0-VAR)v_i$

If VAR is zero and the program is being used for optimization, the program will use the values in OPHIGH and OPLOW (see Appendix B4.2) as the upper and lower limits respectively.
Default = 0.1

ISTART starting integer with nine or less digits for random number generation.
Default = 19

NGUESS number of sets of values of the optimization variables supplied by the user in (5X,5G15.7) format. NGUESS may be any positive number up to and including one more than the number of optimization variables. Each set corresponds to one vertex in the initial simplex and must start on a new record. These values are read in from input/output device 4 whereas all of the other input data is read in from input/output device 5. This facility is useful if results from previous runs are to be used as starting values for the current run. If the program has to calculate the objective function for a set of values while generating the initial simplex, it will write that set of values and the corresponding value of the objective function on input/output device 7 together with I (for initial) and the vertex number. At the end of a run, the program automatically writes one or more sets of values on device 7 together with F (for final), the associated vertex numbers and the values of the objective function. These values on device 7 are in the correct format for subsequent reading on device 4.
Default = 0.

B3.4 Simplex Coefficients

The coefficients used in the various operations described in Section 6.4.3 may be prescribed by the user as follows.

BOUNCE reflection coefficient, α in equation (6.18)
Default = 3.0

EXPAND expansion coefficient, β in equation (6.20)
Default = 2.0

SNAKE translation coefficient, γ
Default = 0.5

REDUCE contraction coefficient, δ in equations (6.21) and (6.22)
Default = 0.25

SHRINK shrinkage coefficient, ζ in equation (6.23)
Default = 0.5

B3.5 Convergence Parameters

The tests described in Section 6.4.4 are governed by the following parameters.

NITER the program will stop after NITER iterations if the following parameters have not been satisfied already.
Default = 2 to provide a check on the input data.

NCHECK the program will check for convergence every NCHECK iterations
Default = 1

FMIN acceptable value of the objective function which is defined in equation (6.1)

SMALL simplex is assumed to have converged if its 'size' falls below this value, ϵ in equation (6.24)
Default = 0.001

B3.6 Complete Data Set, METHOD

If the program is being used for optimization, a minimum set of data would be of the form :

```
&METHOD ICRK=1, CRNKI=350.0, NDES=3, FMIN=1.0,
DELT=1.0,2.0,3.0, MOTION=1, DESANG=25.0,30.0,40.0 &END
```

At least one of the identifiers in Table B1, e.g. ICRK, must be included and the parameters necessary to specify the desired output motion depend on the value assigned to MOTION.

B4 CONSTRAINT DATA SET - LIMITS

The constraint data set, called LIMITS, contains the parameters associated with loop closure, upper and lower limits for optimization variables and input to, and output from, the computer.

B4.1 Loop Closure and Transmission Angle

As explained in Section 6.3.1, a loop may change its closure if a pair of links within it assume a toggle position with two links

in line. However PSALM does not permit such a change in closure. Accordingly a four-bar linkage in the form of a parallelogram will change from that form to the anti-parallelogram form and vice versa as the input link rotates. The alternative action of maintaining the parallelogram form would require a change in closure of the undetermined dyad. Whether this will occur in practice depends on dynamic considerations, i.e. on the forces acting at the time, and not on kinematic considerations. To guard against this indeterminacy and to give acceptable transmission angles, the user may prescribe non-zero values for

TANGLE — permissible deviation in degrees from a right angle of the transmission angles for undetermined dyads with three revolute joints.
Default = 50.0

TOGGLE — link length additional to that required for loop closure for undetermined dyads with two revolute joints and one prismatic joint.
Default = 0.1

In both cases, if the criterion is not met and at least one of the undetermined arcs is an optimization variable, the program will change the value of the variable to satisfy the constraint. Otherwise the program will stop with a warning message.

B4.2 Limiting Values for Optimization Variables

If a limit is placed on the value that any of the optimization variables may take, then both upper and lower limits must be supplied for all of the optimization variables. This avoids the necessity for additional identifiers. The limiting values are provided in the order that corresponds to non-zero values of the following identifiers (see also Table B1).

IVA, arc lengths,

ILKOUT, output arc length,

IORIG, distance of input link pivot from the origin,

IVG, angles between arcs,

INGOUT, output arc angle,

IORIG, angular position of input link pivot,

ICRK, reference position of input link.

The parameters associated with the limiting values are given below.

LIMVAL = 0, no limits placed on the values of the optimization variables,

1, upper and lower limits are supplied for every optimization variable.
Default = 0.

OPLOW — array of lower limiting values (given in above order). Values are required if LIMVAL=1 or VAR=0.0 (see Appendix B3.3).

OPHIGH — array of upper limiting values in the same order as OPLOW. Values are required if values are entered in OPLOW.

Both arrays have 30 locations. An additional control parameter is required to determine the action to be taken if the constraints on the optimization variable values are violated.

STEPIN — If any values are generated that violate the constraint values prescribed in OPLOW and OPHIGH, they will be changed to STEPIN within the associated constraint boundary before any attempt is made to calculate the kinematics of the corresponding linkage.
Default = 0.001

B4.3 Optional Output Information

Additional information may be printed out at the discretion of the user. This is controlled by the following parameters.

KTHETA — This parameter may be used to check the loop closure prescribed in ILINK and ILOOP (see Appendix B2). If KTHETA equals one, the lengths and angular positions of each arc will be printed out on input/output device 8 for each position of the input link.
Default = 0

NVIOL — If the constraints on loop closure and transmission angle are violated more than NVIOL times within an iteration, details of the transgression will be printed out on input/output device 1 (see Appendix B4.4).
Default = 30

NPRINT — After each set of NPRINT iterations, the co-ordinates of the worst and best vertices, i.e. those having the highest and lowest values of the objective function respectively, are printed out on input/output device 1. This gives an indication of the size of the simplex and the rate of convergence.
Default = 100.

NPRT — After each set of NPRT iterations, the values of the objective function for the worst and best vertices are printed out on input/output device 1.
Default = 20

B4.4 Data Control

The two remaining parameters are used to indicate whether further information is to be produced by the computer or is being provided by the user.

IPLOT plotting parameter which takes effect after the results have been printed out. If IPLOT equals one, the (final) linkage is analysed at one degree increments of the input link position. The direction of rotation of the input link is assumed to be that indicated by the first two prescribed positions of the link. If the constraints of loop closure or transmission angle are violated, error messages will be written to input/output device 6 as for any analysis run and the position of the linkage output will be set to zero so that it will be obvious in any subsequent plot. The data for the plotting program will be written to input/output device 9.
Default = 0

LAST indicates whether another complete set of data, starting with a title (Appendix B1), follows and is to be used in the current run or not. Usually more than one set is provided only when a series of linkages is to be analysed.
= 0, this is not the last set, another follows,
1, this is the last set of data for this run.
Default = 1

B4.5 Complete Data Set, LIMITS

An 'empty' data set may be supplied if all of the default values are used. This implies that :

a) no limiting values are prescribed for the optimization variables,

b) the length and position of every arc at each prescribed position of the input link is not to be printed out,

c) no data is required for subsequent use in the plotting program.

Such a data set would be :

```
&LIMITS &END
```

with a space between the S and the second ampersand.

B5. COMPLETE SETS OF DATA

B5.1 Data for Analysis

A complete set of input data to analyse the linkage shown in Figure B1 is given below.

```
TEXTILE TEN-BAR LINKAGE SHOWN IN FIGURE B1
&LINKS NLOOP=4,MAXARC=6,ILINK=1,-2,-3,4,0,0,
-4,-2,-3,-3,4,0,1,2,-2,-4,-5,-4,-6,-5,-3,4,-1,77*0,
ILOOP=1,0,0,1,0,0,1,-1,-2,1,1,0,3*2,0,0,1,3,3,-4,-5,2,77*0,
ARCL=24.425,24.39,24.425,24.39,2*0.0,9.992,2*0.0,4.425,24.39,
0.0,9.992,0.0,3.75,13.29,15.0,2*41.383,42.0,2*0.0,27.0,77*0.0,
GAMA=3*0.0,172.62,2*0.0,-82.62,10*0.0,1.822,2*180.0,2*0.0,
180.0,77*0.0,NOUTLK=-4,NOUTLP=4,OUTLK=41.188 &END
&METHOD MOTION=0,IKIN=30 &END
&LIMITS TANGLE=90.0 &END
```

Since MOTION is set to zero, the Cartesian co-ordinates of the output point N on the sliding link LMN are printed out for 30 degree increments of the input link as set by IKIN.

If a check on the lengths of the sliding links is required for each position of the input link, KTHETA must be set to one in the constraint data set, LIMITS. The corresponding output for this set of data appears in Figure 7.4. This shows that, as the input link rotates, the input four-bar linkage ABCD changes from a parallelogram form to an anti-parallelogram form and vice versa to maintain joint C on the same side of BD throughout the motion. The limiting transmission angle, TANGLE, has been set to 90.0 to permit the linkage to rotate through the in-line positions.

B5.2 Data for Synthesis

The complete set of input data for the needle linkage depicted in Figure 8.4 as used for synthesis with the weighting factors shown in Figure 8.7 is listed below.

```
TEN-BAR NEEDLE LINKAGE SHOWN IN FIGURE 8.4
 &LINKS NLOOP=4,MAXARC=6,ILINK=1,2,3,4,0,0,1,2,3,-4,0,0,
 1,2,-3,-4,-3,4,1,2,3,-4,-5,-4,76*0.0,
 ILOOP=1,0,0,1,0,0,1,0,0,1,0,0,1,2,0,0,1,1,1,2,3,0,0,1,76*0,
 ARCL=19.,95.,104.5,112.4681,2*0.0,19.,105.0,31.0,110.0639,
 2*0.0,19.,105.0,61.0,12.5,24.0,112.4681,19.,105.0,61.0,
 245.5,85.0,352.7155,76*0.0,
 GAMA=3*0.0,238.3591,5*0.0,33.5934,6*0.0,47.3839,6*0.0,20.4425,
 76*0.0,NOUTLK=5,NOUTLP=4,OUTLK=121.6,OUTANG=131.6893 &END
 &METHOD INGOUT=1,ICRK=1,FMIN=0.1,NITER=2,MOTION=1,
 IVA=0,3*1,3*0,3*1,4*0,3*1,4*0,1,1,0,IVG=3*0,1,5*0,1,6*0,1,83*0,
 ANMULT=7*1.,10.,1.,10.,5*1.,2*5.,2*10.,162*1.0,
 DESANG=149.99,150.7,150.96,150.56,149.35,146.46,145.58,
 3*145.55,145.27,144.85,144.33,144.23,144.4,144.68,145.85,
 146.17,146.23,147.2,161*0.0,CRNKI=180.0,ISTART=789,SNAKE=0.1,
 DELT=0.,-15.,-30.,-45.,-60.,-90.,-120.,-135.,-150.,-165.,-195.,
 -210.,-225.,-231.,-240.,-255.,-270.,-285.,-300.,-330.,
 341*0.0,NDES=20 &END
 &LIMITS IPLOT=1 &END
```

The corresponding annotated print-out of the input data and the intermediate arrays is shown in Figures 7.3 and C1. The result of the run appears in Figure 7.2. The angular position of the input link is calculated since MOTION equals one. The linkage is unchanged during this run since the number of iterations has been limited to two by NITER and no linkage giving a lower value of the objective function was found during these iterations.

C. INTERMEDIATE ARRAYS

During execution of the program, several intermediate arrays are generated in subroutine SETUP from the topological arrays, ILINK and ILOOP. These arrays are written on input/output device 8, together with the title, to provide a check on the interpretation of the input topology. If device 8 is defaulted to the line printer, these arrays will appear with a print-out of the input data on a separate page from the results. Unless stated otherwise, these arrays each have NLOOP rows. Definitions of the arrays now follow in order of appearance in the print-out. In each case, the example is for the linkage in Figure B1.

LOOPL This single row array contains the number of arcs in each loop, e.g.

```
LOOPL =    4    5    6    5
```

LARCX This array with two columns contains the arc numbers of the undetermined arcs in each loop, e.g.

```
LARCX =    2    3
           2    3
           4    5
           3    4
```

The next three arrays each have MAXARC columns. As in ILINK and ILOOP, the position of an element defines the arc with which it is associated. Thus the second entry in the fourth row corresponds with the second arc in the fourth loop. In addition, however, each arc is assigned a sequential number, n_s, as determined by its position in the array. This is given by :

$$n_s = (r-1).MAXARC + c \qquad (C1)$$

where r = row or loop number,
c = column or arc number.

Thus for the linkage in Figure B1 where MAXARC equals six, the sequential number for the second arc in the fourth loop is {(4-1).6+2} i.e. 20. The values of the elements in these three arrays refer to these sequential numbers.

LARCD The value of an element is the sequential number of the common arc from which the angular position of the current arc can be determined directly, e.g.

```
LARCD =    1    0    0    4    0    0
           4    7    8    3    4    0
           7    8    8    0    0    4
          18   17   22   23    7    0
```

```
NUMBER OF ARCS IN EACH LOOP,LOOPL
   4   4   6   6
UNDETERMINED ARCS IN EACH LOOP,LARCX
   2   3
   2   3
   3   4
   4   5
INDICES OF ARCS THAT PROVIDE DATA FOR OTHER ARCS,LARCD
   1   0   0   4   0   0
   1   0   0   4   0   0
   1   8   0   0   3   4
   1   8  15   0   0   4
INDICES OF FRAME ARCS CORRESPONDING TO LARCD,LARCF
   4   0   0   4   0   0
   4   0   0   4   0   0
   4  10   0   0   4   4
   4  10  18   0   0   4
ARRAY OF IDENTICAL ARCS,IDENTA
   1   0   0   4   0   0
   1   8   0   0   0   0
   1   8  15   0   0   4
   1   8  15   0   0   0
ARRAY OF VARIABLES CORRESPONDING TO ARCS
   0   1   2   3   0   0
   0   4   5   6   0   0
   0   4   7   8   9   3
   0   4   7  10  11   0
ARRAY OF VARIABLES CORRESPONDING TO ANGLES
   0   0   0  12   0   0
   0   0   0  13   0   0
   0   0   0   0  14  12
   0   0   0   0   0   0
NUMBER OF OPTIMIZATION VARIABLES,MARBLE =  16
ARRAYS "JOINT","SLIDE","CONFIG"
    1         1         1         1
 -1.00     -1.00      1.00      1.00
 -1.00     -1.00      1.00      1.00
     FMIN      SMALL       VAR     TANGLE    TOGGLE    STEPIN
   0.1000    0.0010    0.1000   50.0000    0.1000    0.0010
   BOUNCE    EXPAND    SNAKE     REDUCE    SHRINK
   3.0000    2.0000    0.1000    0.2500    0.5000
  NGUESS  IKIN  LIMVAL  NVIOL NITER  NCHECK NPRINT  NPRT
     0       0       0      30       2       1     100      20
```

FIGURE C·I INTERMEDIATE ARRAYS FOR NEEDLE LINKAGE

LARCF The value of an element is the sequential number of the frame arc in the loop of which the common arc given in the corresponding position in LARCD is a member, e.g.

LARCF =

4	0	0	4	0	0
4	11	11	4	4	0
11	11	11	0	0	4
18	18	23	23	11	0

If there is more than one frame arc in the loop concerned, the last one in the loop is the one which is used as the reference frame arc (see page 5-6).

IDENTA This array lists arcs that are identical irrespective of the direction of tracing. The value of an element is the lowest sequential number assigned to that identical arc, e.g.

IDENTA=

0	0	0	4	0	0
7	8	0	0	4	0
7	8	0	0	0	18
18	0	0	0	0	0

These three arrays are followed by the number of optimization variables, MARBLE. If MARBLE is not zero, it is followed by two arrays that give the numbers in order of appearance of the optimization variables corresponding to the arc lengths and angles. The position of the elements in these two arrays corresponds to that in the ARCL and GAMA arrays respectively.

Finally three single row arrays are printed out.

JOINT This array gives the type of the undetermined dyad in each loop. The value of an entry corresponds to that given in Figure B2 for the various dyads, e.g.

JOINT= 1 7 1 6

The two remaining arrays, SLIDE and CONFIG, are connected with the closure of the undetermined dyad and form a double-row array. A value of 1.57 or -1.57, i.e. the value of a right angle in radians, appears for each prismatic joint connected with that dyad. The sign is governed by the direction of the right angle turned through as the prismatic joint is traversed within the loop. If there are two or three revolute joints connected with the dyad, a value of 1.00 or -1.00 appears for the remaining entry or entries for that loop. In these cases, the sign corresponds to that used in equation (5.14), (5.19) or (5.22), whichever is appropriate. For example,

SLIDE	=	1.00	1.57	1.00	1.57
CONFIG	=	1.00	1.57	1.00	-1.57

A complete set of intermediate arrays and the final part of the input data check for the set of data for synthesis listed in Section B5.2 is given in Figure C1. It corresponds to the needle linkage depicted in Figure 8.4.

COMPUTER-AIDED SYNTHESIS OF LINKAGES —A MOTORCYCLE DESIGN STUDY

K. OLDHAM, MA, CEng, MIMechE
J.N. FAWCETT, BSc, PhD, CEng, MIMechE
Department of Mechanical Engineering, University of Newcastle-upon-Tyne

SYNOPSIS The geometry of current motorcycle rear suspension systems is such that the centre distance between the gearbox output sprocket and the rear wheel sprocket varies as the suspension deflects.

This paper describes the application of a computer program for the synthesis of linkages to the design of a six-bar linkage arrangement. The design was carried out in three stages. Firstly, a four-bar linkage was obtained whereby a constant sprocket centre distance is maintained at all times. In the second stage, the program was used to determine the method of adjusting this linkage to allow for chain wear. Lastly, two further links were added to provide a brake reaction link that does not rotate relative to the frame as the suspension deflects. The effect of increasing the number of iterations is considered and the advantage of using the program interactively is demonstrated.

1. INTRODUCTION

Current practice in the design of motor cycle rear suspensions is to mount the wheel on a single link which can swing about a pivot on the frame of the machine. The angular movement of the link is controlled by a spring and damper arrangement. A typical configuration is shown diagrammatically in Figure 1.

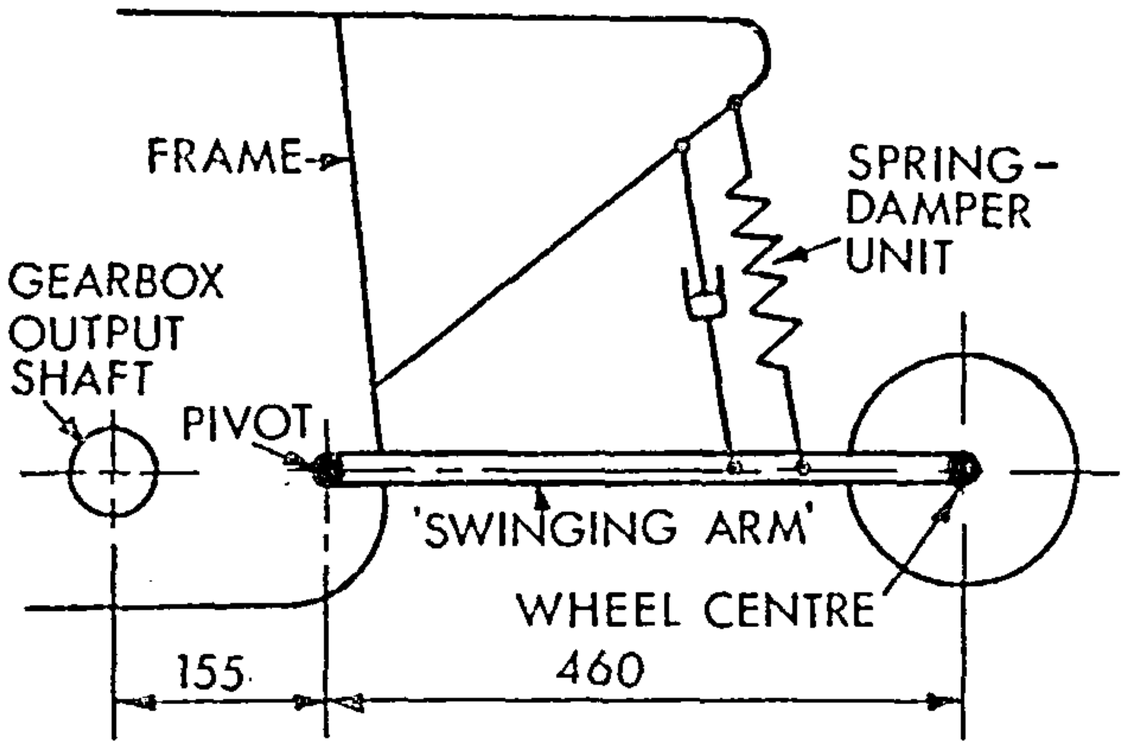

Fig. 1: Typical rear suspension. Chain and road wheel not shown

In this 'swinging arm' configuration the wheel moves in a circular arc with centre at the swinging arm pivot. Since the pivot is separated by a considerable distance from the gearbox output shaft, the distance between the centres of the wheel and gearbox output shaft changes as the suspension moves.

Thus, if a chain drive is used between the engine and wheel, the sprocket centre distance will be constantly changing causing increased chain wear and, at maximum wheel deflection, excessive slack in the chain. If the slack in the chain is ±6 mm at mid-span when the swinging arm is horizontal, it will increase to ±40 mm as the wheel is moved vertically through 140 mm. There is a danger that the chain will leave the sprocket under these conditions, particularly if the load in the chain is reversed by closing the throttle to slow down, or vice versa.

If the swinging arm were pivoted on the output shaft of the gearbox, there would be no variation in the sprocket centre distance. This arrangement has been tried, but it is difficult to achieve a compact and stiff layout since the arm itself becomes very long.

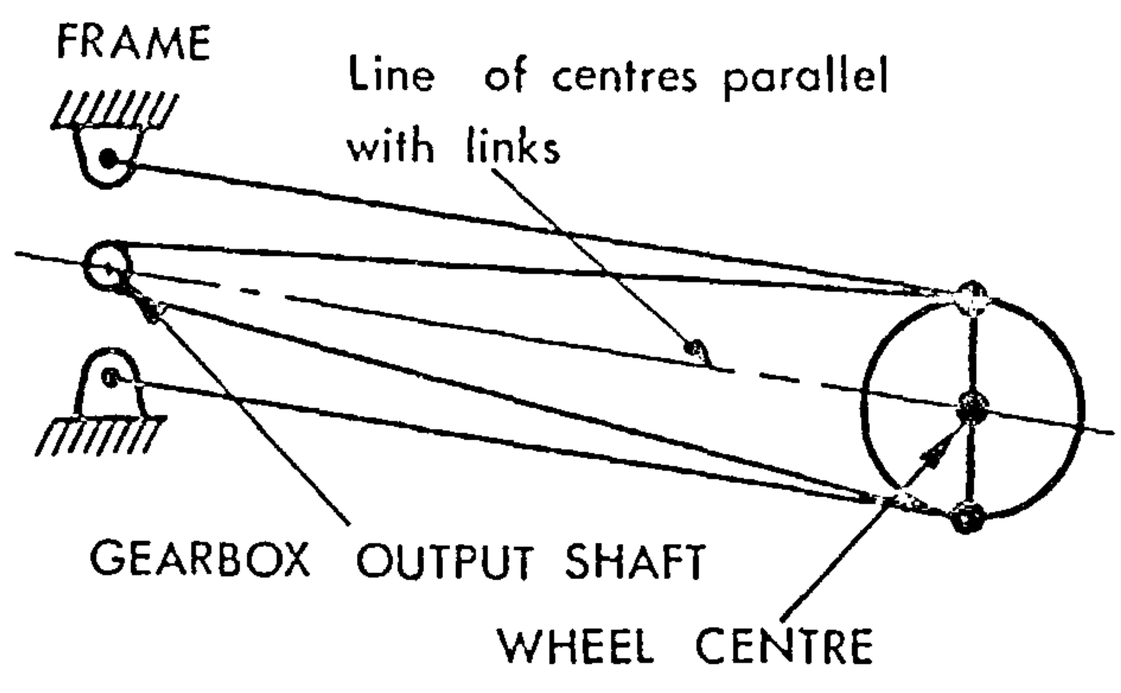

Fig. 2: Parallelogram linkage, constant centre distance

Alternatively the parallelogram layout of Figure 2 with two arms pivoted on a line passing through the gearbox output shaft, could be used. This again requires long links and imposes strict limits on the pivot positions. Both of these layouts are difficult to incorporate into a practical design.

2. NOTATION

T Vertical travel of wheel centre,

WS Sprocket centre distance,

Δ Variation in sprocket centre distance,

δ Variation in angular position of brake reaction link, degrees.

All of the other symbols and letters used are illustrated in Figures 3 and 8. All linear dimensions are in mm.

3. USE OF NON PARALLEL LINKS

A more convenient design can be achieved by using a linkage in which the links are not parallel throughout the motion. By choosing suitable dimensions for the links it is possible to design a four-bar linkage in which a point on the coupler moves on a circular path about a desired centre. The general layout is shown in Figure 3 with the frame as the fixed link AB, a lower link BC, the coupler CDW on which the wheel is carried and an upper link DA. The design requirement is that the wheel centre W should move on a circular arc of given radius about the gearbox output sprocket S.

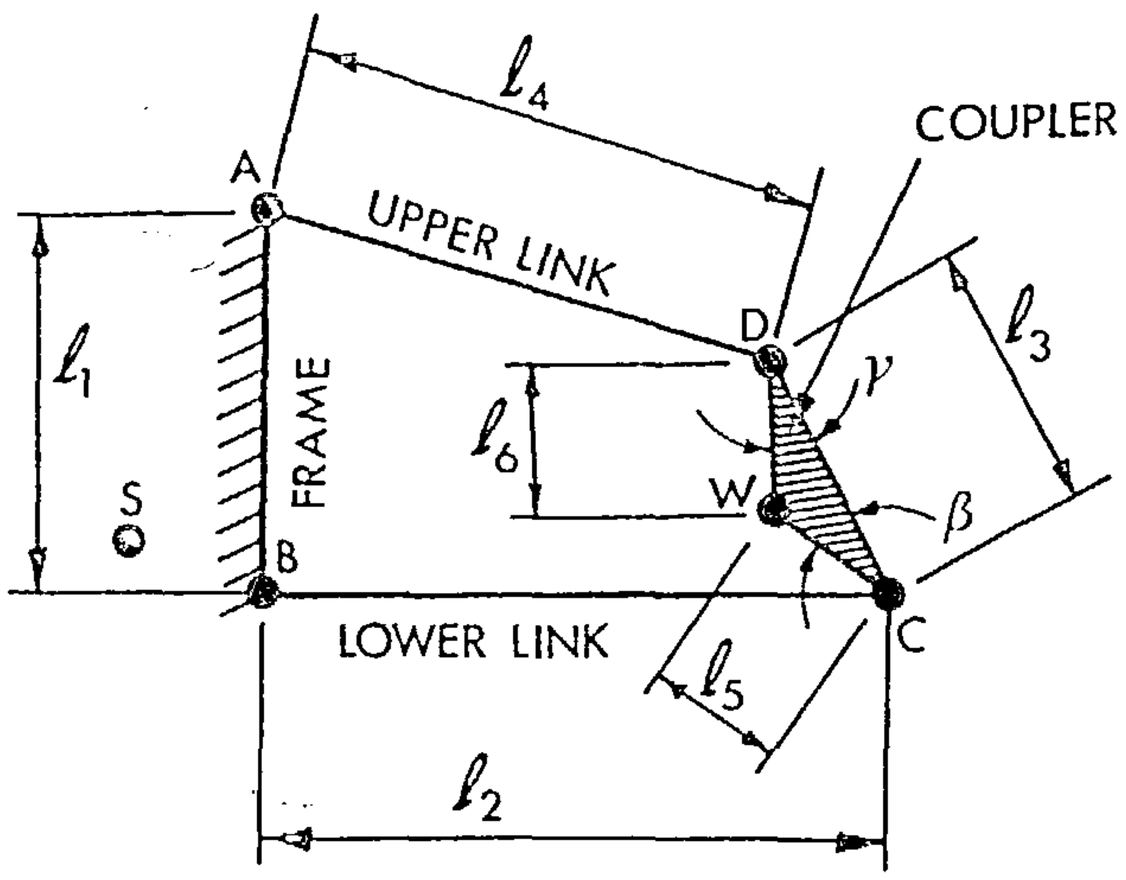

Fig. 3: General layout of four-bar linkage

4. USE OF COMPUTER PROGRAM FOR MECHANISM SYNTHESIS

The problem is basically one of mechanism synthesis for path generation. A variety of solutions to the link lengths is possible in achieving the required path but many of these will be impractical.

A computer program called PSALM - Program for the Synthesis and Analysis of Linkage Mechanisms - has been developed by Oldham from the concepts given by Youssef et al. (1). Given an initial linkage and required output motion the program will change the link lengths using a Simplex optimisation routine until a close approximation to the desired motion is obtained. The user is free to specify which link lengths may be varied and may also place limits on these lengths to take account of practical space considerations.

To define the required motion, an existing arrangement, with the dimensions shown in Figure 1, was taken. The requirement was therefore that the wheel centre W should travel on a circular arc of radius 615 mm with centre at S and allow a movement, T, of 100 mm above and below the position shown. Referring again to Figure 3, the lower link BC was regarded as the input link and the required motion of W specified as a set of 21 pairs of x,y co-ordinates corresponding to specified positions of the input link. This correspondence between the positions of W and the input link was required by the program for linkages where the input link rotates through only a limited angle. It is not a requirement of the example and so the specification of the motion was overconstrained. In addition, the position of the lower frame pivot was fixed relative to S and the upper frame pivot constrained to lie vertically above the lower pivot. These restrictions were applied to achieve a practical solution at this stage.

This left seven variable parameters. The initial guess for these was :

(a) frame link, AB : ℓ_1 = 250 mm

(b) lower link, BC : ℓ_2 = 460 mm
reference angle = 10 degrees below the horizontal

(c) coupler, CDW : ℓ_3 = 150 mm
ℓ_5 = 50 mm
β = 10 degrees clockwise

(d) upper link, DA : ℓ_4 = 460 mm

Using a power residue random number generator, the program generated seven other linkages with dimensions lying within ±50% of the initial guess. If any of the generated linkages do not form a closed loop, the program automatically adjusts the link lengths until closure is achieved.

For each of these linkages, the program calculated the error. This is defined as the sum of the squares of the distance between the desired output position and the actual output position for each of the input link positions. The resultant errors lay between 4000 mm^2 and 1050000 mm^2. After 124 iterations the program had reduced the error to 820 mm^2 but converged to a local minimum. The biggest change was in the frame link which had been shortened to 125 mm.

The program was started again from the same initial guess but with β specified as 350 degrees anticlockwise (rather than 10 degrees clockwise). The initial errors lay between 4000 mm^2 and 1030000 mm^2. After 238 iterations, the program had reduced the error to 1.5 mm^2. The difference in the two runs is that in the first set of linkages the generated values of β were between 5 and 15 degrees, whereas in the second set the values were between 175 and 525 degrees. The larger range allowed W to move to the other side of the coupler to a final position of 423.2 degrees, i.e. 63.2 degrees, anticlockwise compared with 9.9 degrees clockwise for the first run. This shows that the initial guess and the way in which it is specified can have a significant effect on the result.

The linkage resulting from the second run is shown in Figure 4a. The diameter of the wheel shown is 640 mm. Over the required suspension movement, the sprocket centre distance varies from the desired 615 mm by +0.20 mm in the bottom position, to -0.07 mm about halfway up and then to +0.01 mm in the top position. This variation, Δ, is less than the errors due to manufacturing tolerances but could be reduced to

+0.06 mm and -0.07 mm by limiting the movement in the downward direction to 70 mm below the horizontal and increasing the upward travel to 130 mm. A full-size model has demonstrated the

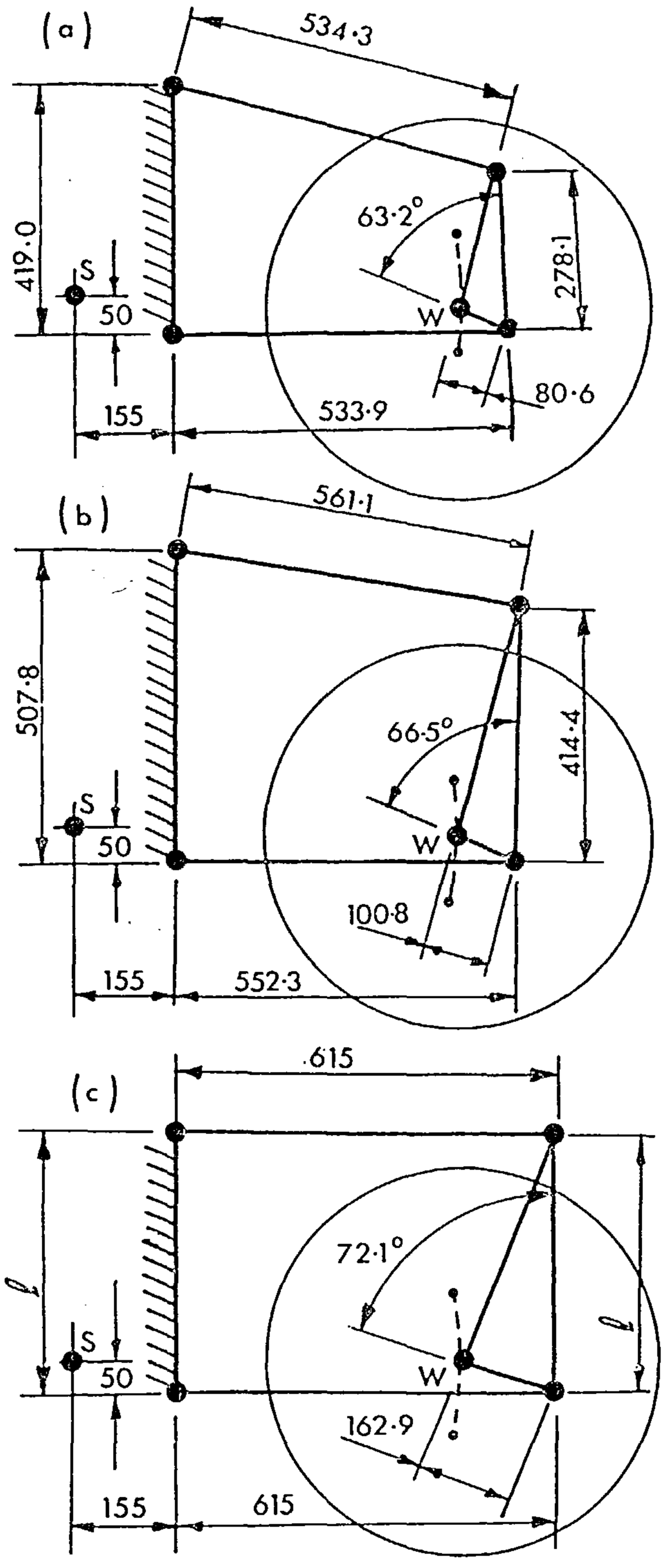

Fig. 4. Four-bar linkages, original specification
Centre distance, WS = 615
(a) Second run, Δ = 0.13, T = 200
(b) Third run, Δ = 0.23, T = 200
(c) Parallelogram linkage,
Δ = 0, T = 1230

extent of the circular arc. The pivot positions on the frame have been moved apart from the initial guess value to 419 mm. They are well spaced but still convenient. A practical design could be achieved using the dimensions given. The spring damper units could be attached to any of the moving links to suit the frame layout.

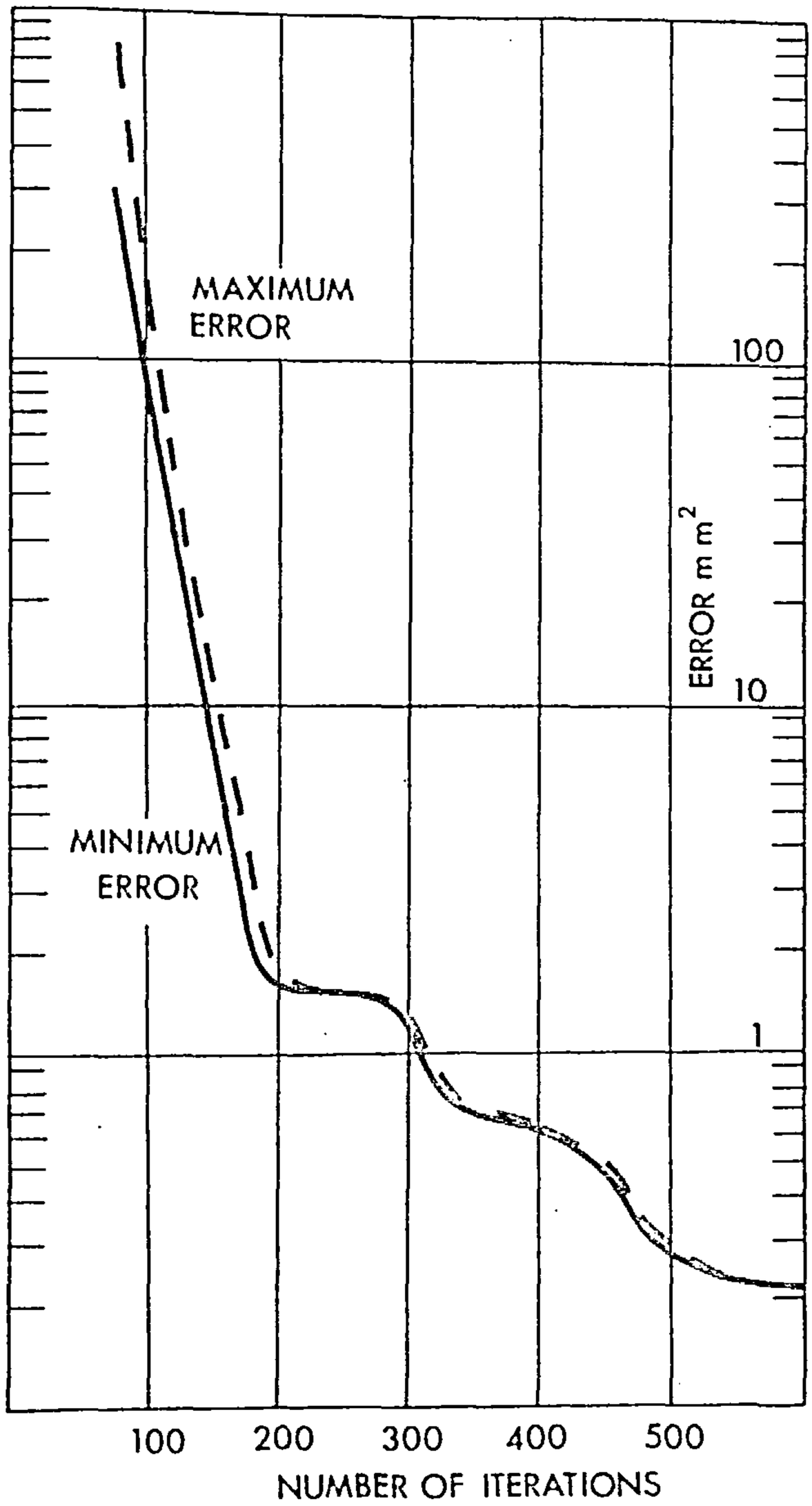

Fig. 5: Progress of optimisation
Simplex algorithm
Seven parameters

The program was run for a third time using the same starting values as the second run. This time the program did not converge to the local minimum with an error of 1.5 mm^2 but, as shown in Figure 5, skirted it and reduced the error to 0.225 mm^2 after a total of 586 iterations. In the neighbourhood of the local minimum, the maximum and minimum errors are very close together. This means that the Simplex polyhedron is small and changes slowly as is shown by the errors hardly decreasing between iterations 220 and 270. The difference in the two runs is that the earlier (second) run was carried out in two stages. Intermediate values were written to a file after 200 iterations and read in again to complete the run. This transcription altered the values sufficiently, by rounding off, to cause the program to converge to a different minimum. Interrupting a run in this way is not necessarily detrimental as it has the effect of starting the program from slightly different initial values.

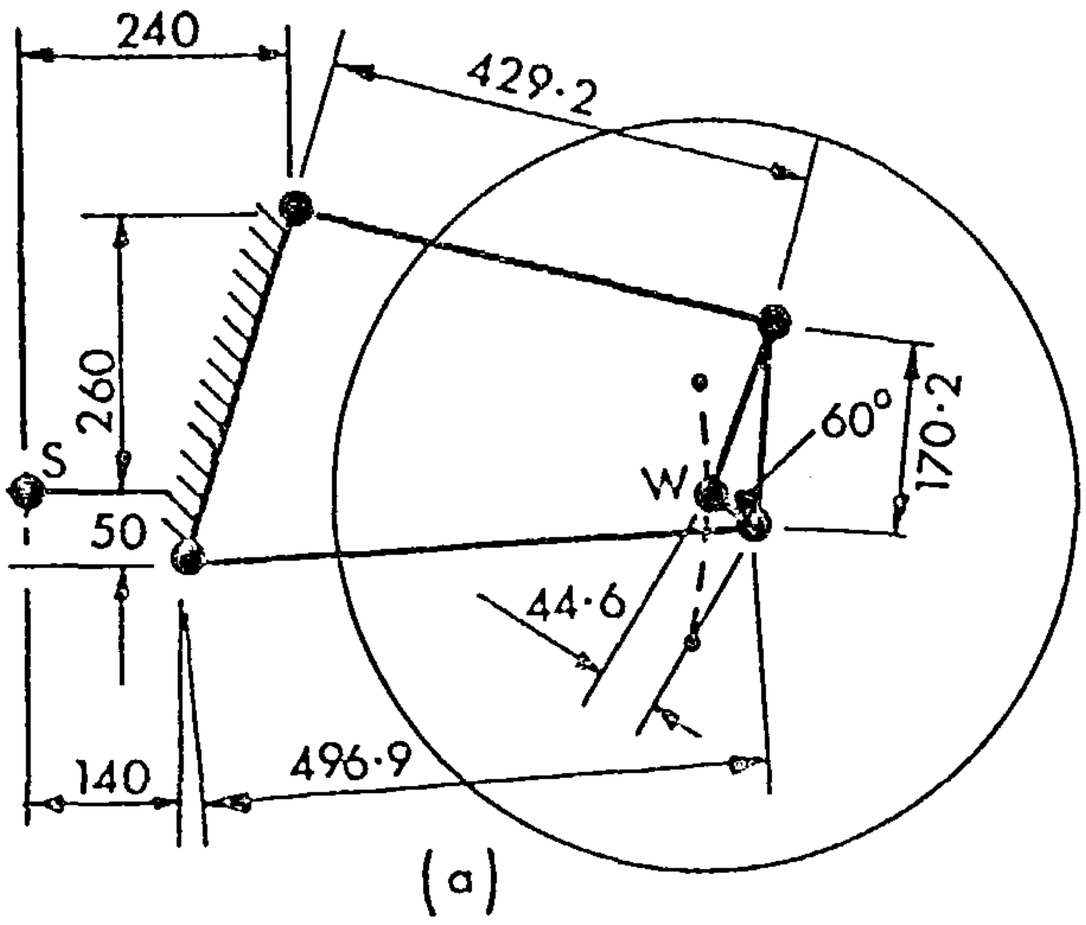

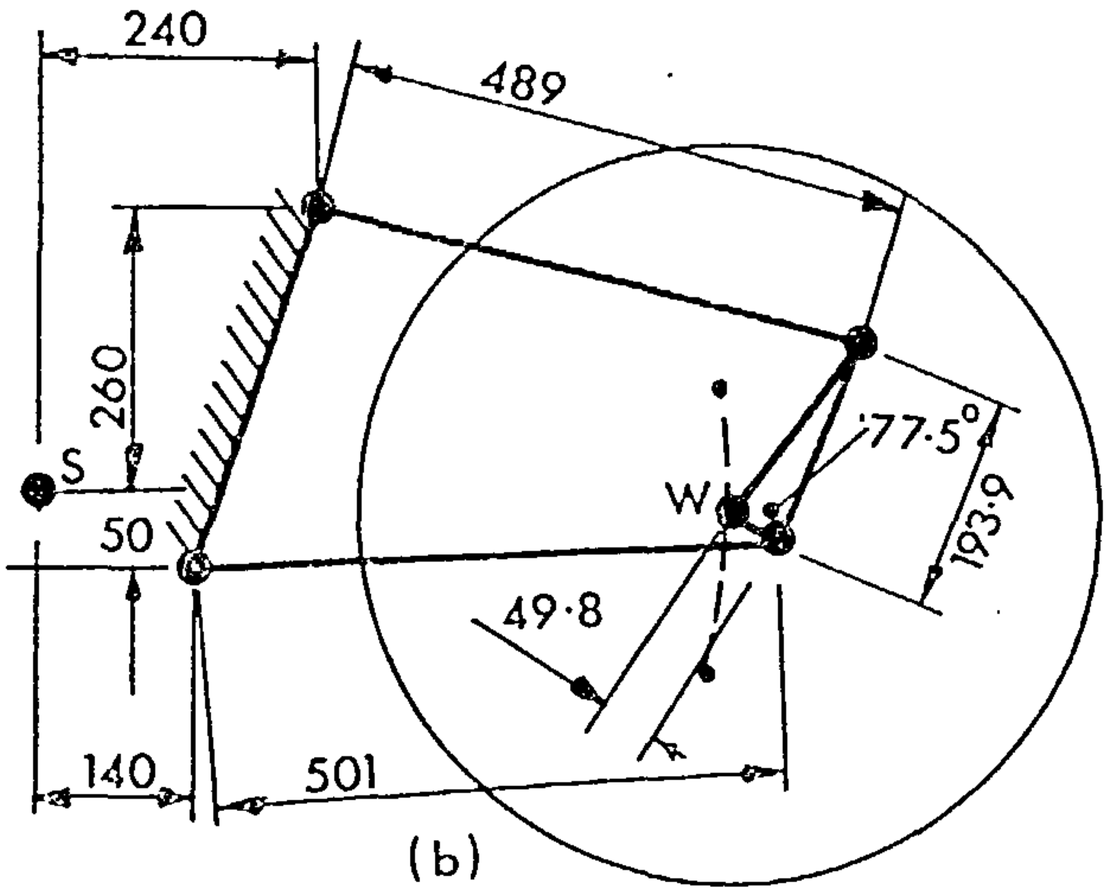

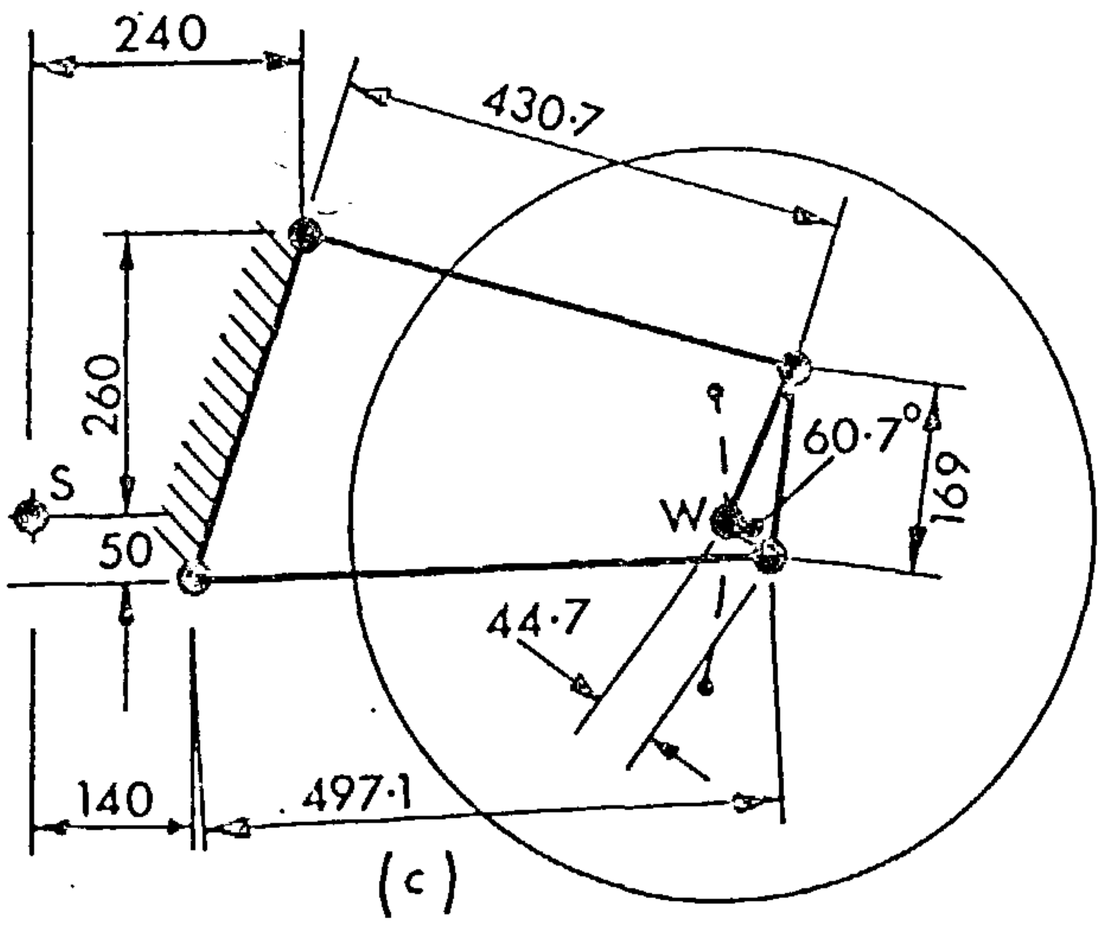

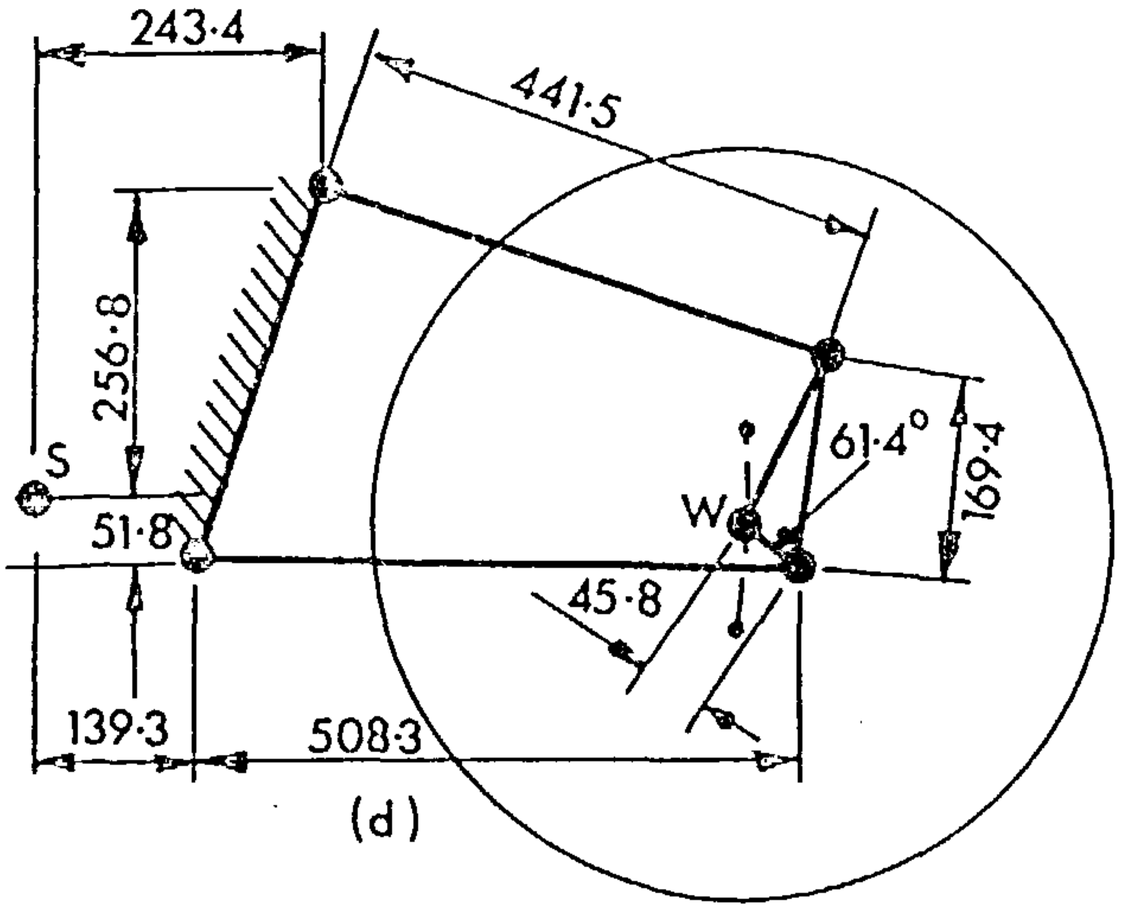

Fig. 6: Four-bar linkages, revised specification

Linkage	(a)	(b)	(c)	(d)
Variation, Δ	0.3	0.16	0.33	0.26
Travel, T	227	248	251	250
Centre distance, WS	600	600	600	610

The linkage resulting from the third run is shown in Figure 4b. Over the specified suspension travel of 200 mm, the sprocket centre distance varies from the desired 615 mm by -0.15 mm at the bottom, +0.06 mm in the horizontal position and -0.17 mm at the top. The improvement in centre distance variation is negligible but the centre of the travel is now the horizontal position. Thus the reduction in the error is associated with an improvement in the position, rather than the quality, of the circular arc. As the suspension deflects, the chain will slacken slightly whereas the chain tightens with the linkage in Figure 4a.

The links in Figure 4b are all longer than the corresponding links in Figure 4a. Thus the program has moved towards the parallelogram linkage shown in Figure 4c where the triangular coupler is congruent with the triangular frame link and the upper and lower links are equal in length. The length ℓ may be any convenient value. This linkage will trace a perfect circle around S but is not very suitable for a rear suspension as the links are too long.

The dimensions shown however represent only some of many possible solutions and it is a fairly simple matter, using these as a new first guess, to obtain another solution in which other practical limitations on pivot positions, link lengths etc. have been imposed. Thus for best results the program should be used interactively as a design aid with the designer ensuring that it converges to a convenient solution. By observing the progress of the output the designer can decide when and how to intervene if the solution is converging towards an impractical mechanism.

5. REVISED SPECIFICATION

Following discussions with CCM Ltd., Bolton, who manufacture moto-cross machines, it was decided to re-run the program with revised frame pivot positions to suit an existing frame design. The upper pivot, A, was fixed at (240, 260) mm and the lower pivot, B, at (140, -50) mm relative to S. The number of Cartesian co-ordinates specifying the motion of W was increased to 26 pairs to give a larger wheel movement. The initial values were ℓ_2 = 530 mm, ℓ_3 = 125 mm, ℓ_4 = 425 mm, ℓ_5 = 60 mm, β = 400 degrees anticlockwise (using the notation

in Figure 3) and the reference angle for the input link = 10 degrees below the horizontal. After 159 iterations, the program converged to a local minimum with an error of 63 mm^2.

It was felt that this poor result was due to over-constraining the program by specifying the desired motion of W as pairs of x,y co-ordinates for given positions of the lower link, BC. Since the motion of the lower link relative to that of W is not important as long as W moves on the required arc, the program was changed to provide the additional option of defining the position of W in terms of its distance from S.

The input data was altered accordingly but was otherwise unchanged. The 26 positions of W were prescribed as 600 mm from S and the reference angle of the lower link was fixed at seven degrees below the horizontal because varying it would no longer have any effect on the error. After 165 iterations, the revised program converged to a minimum with an error of 0.196 mm^2. This corresponds to a variation, Δ, in the centre distance of 0.3 mm over a vertical travel, T, of 227 mm. The resulting linkage is shown in Figure 6a.

To accommodate a revised specification calling for a wheel movement of 250 mm (110 mm above the horizontal and 140 mm below), two more positions were prescribed for the lower link since this, indirectly, controls the travel. The program was re-run with the same initial data and converged to the linkage shown in Figure 6b after 238 iterations. This gives an error of 0.136 mm^2 corresponding to a Δ of 0.16 mm over a T of 248 mm. Although Δ is nearly half, the upper link and the coupler link are considerably longer than their counterparts in Figure 6a.

The program was re-run therefore using the linkage in Figure 6a as the initial guess. After 69 iterations, the program converged to the linkage shown in Figure 6c. This gives an error of 0.159 mm^2 (Δ = 0.33 mm for T = 251 mm). Although the centre distance variation is greater than that produced by the linkage in Figure 6b, it is still within acceptable limits and the link lengths offer a better mechanical layout.

Thus changing the frame pivot positions and altering the program slightly has resulted in a smaller, and hence lighter, linkage. Over a vertical travel of 200 mm, the linkage in Figure 6c gives a slightly smaller Δ than that in Figure 4b. The result, to some extent, is still a matter of trial and error as it depends on the initial guess. Thus the program should be used interactively with the designer using his skill to guide it towards a suitable solution.

6. CHAIN WEAR

During use, a motor-cycle chain wears. When the linkage shown in Figure 6c was discussed with CCM Ltd., it was pointed out that it was essential to provide a means for adjusting the sprocket centre distance, WS, by one chain pitch. A final specification calling for WS to be 610±6.5 mm was therefore agreed. The adjustment could be provided by making the length of the upper or lower links adjustable or by varying the pivot positions. An ideal method would act simultaneously on the linkages on either side of the rear wheel to avoid misalignment. It was decided therefore to make the position of the lower pivot, B, adjustable since a given movement of this pivot will have more effect on the centre distance than the same movement of the upper pivot, A.

The basic linkage of Figure 6c had first to be revised to increase the centre distance from 600 mm to the 610 mm mean value of the final specification. The initial values were ℓ_2 = 506.9 mm, ℓ_3 = 170.25 mm, ℓ_4 = 439.2 mm, ℓ_5 = 44.6 mm and β = 420 degrees anticlockwise. After 67 iterations, the program converged to a minimum with an error of 0.167 mm^2 (Δ = 0.27 mm). Rounding the link lengths to the nearest half millimetre such that ℓ_2 = 507 mm, ℓ_3 = 169.5 mm, ℓ_4 = 441 mm and ℓ_5 = 45 mm, changed the mean centre distance to 609.73 mm but reduced the variation about that to 0.23 mm.

In the standard single link suspension, the adjustment for chain wear is obtained by mounting the frame pivot on an eccentric. This method was investigated by using the program in an analysis mode. The program automatically operates in this mode if there are no variable parameters. Mounting the lower pivot on an eccentric with an eccentricity of 6.5 mm would provide the desired adjustment. To decide whether the point about which the eccentric should be rotated should be above or below the pivot, an analysis of the centre distance variation at the extreme positions of the eccentric was carried out for both cases. The resulting values are shown in Figure 7a. Since all of these values are unacceptable, it was decided to use the program again in the synthesis mode to determine how the pivot should be adjusted.

To allow the position of the lower pivot to vary, the linkage had to be specified 'the other way round' i.e. with the upper link as the input link. Since the upper link moves through a larger angle than the lower link, the number of prescribed input link angles was increased from 28 to 33. The program was re-run to check whether these angles gave the required travel. Starting with the results of the earlier synthesis run, the program gave a linkage appropriate for an upward movement of 150 mm and a downward movement of 110 mm. The prescribed input link angles were altered to account for this and the program re-run starting with the results of the last run. After 80 iterations, the program gave a linkage with an error of 0.14 mm^2 (Δ = 0.19 mm). When the link lengths were rounded to the nearest 0.1 mm, Δ increased to 0.3 mm. However, the maximum error occurred at the bottom end of the travel, so the linkage was rotated slightly about S by moving the frame pivots to utilise a more accurate part of the curve. This reduced Δ to 0.26 mm. The corresponding linkage is shown in Figure 6d.

Having re-established the basic linkage, the program was re-run keeping all of the moving link lengths constant but allowing the lower frame pivot position to vary to give centre distances of 603.5 mm and 616.5 mm. After 40 and 31 iterations respectively, the program gave the results shown in Figure 7b. These correspond very closely to moving the pivot along a straight line rather than along a circular arc provided by

an eccentric, and so offer a convenient mechanical solution.

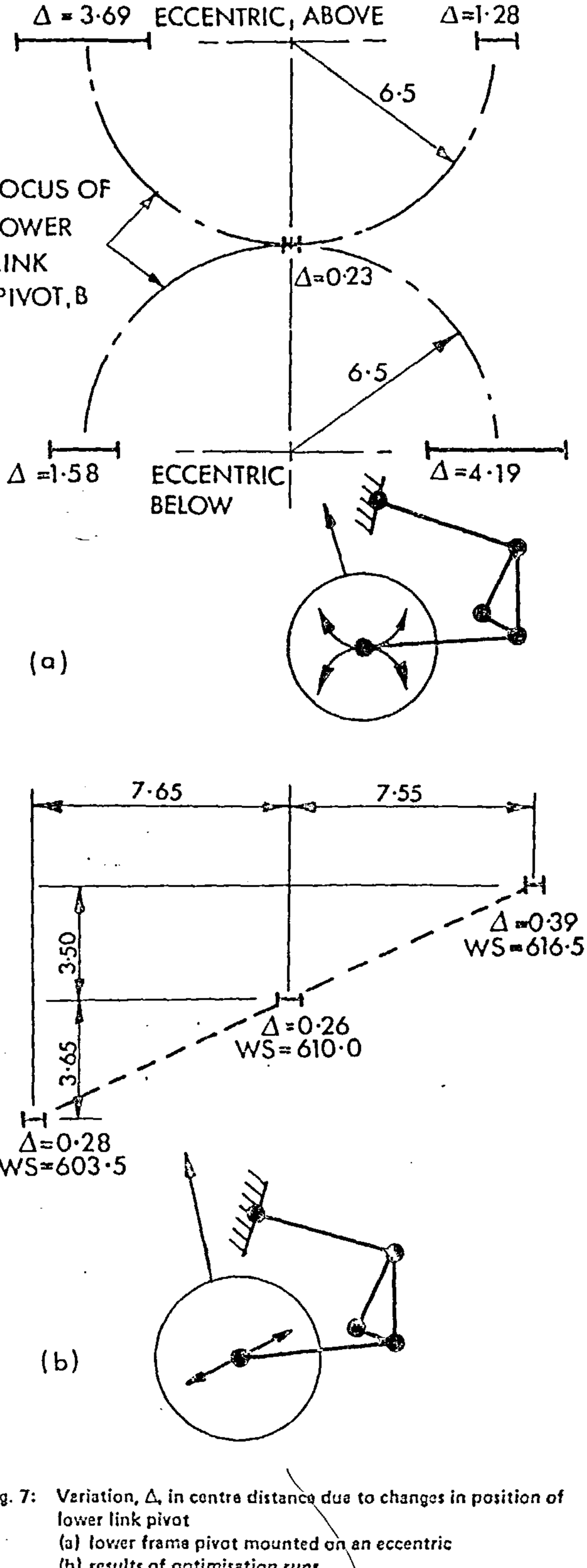

Fig. 7: Variation, Δ, in centre distance due to changes in position of lower link pivot
(a) lower frame pivot mounted on an eccentric
(b) results of optimisation runs

7. BRAKE REACTION LINK

With the current CCM single link suspension, the brake reaction is taken by a plate fixed directly to the 'swinging arm'. As the suspension deflects, the plate rotates relative to the frame. If the plate were attached to the coupler of Figure 6d it would rotate in the opposite direction and through a much larger angle, under the same conditions. It was felt that this might cause a significant difference in handling characteristics during braking.

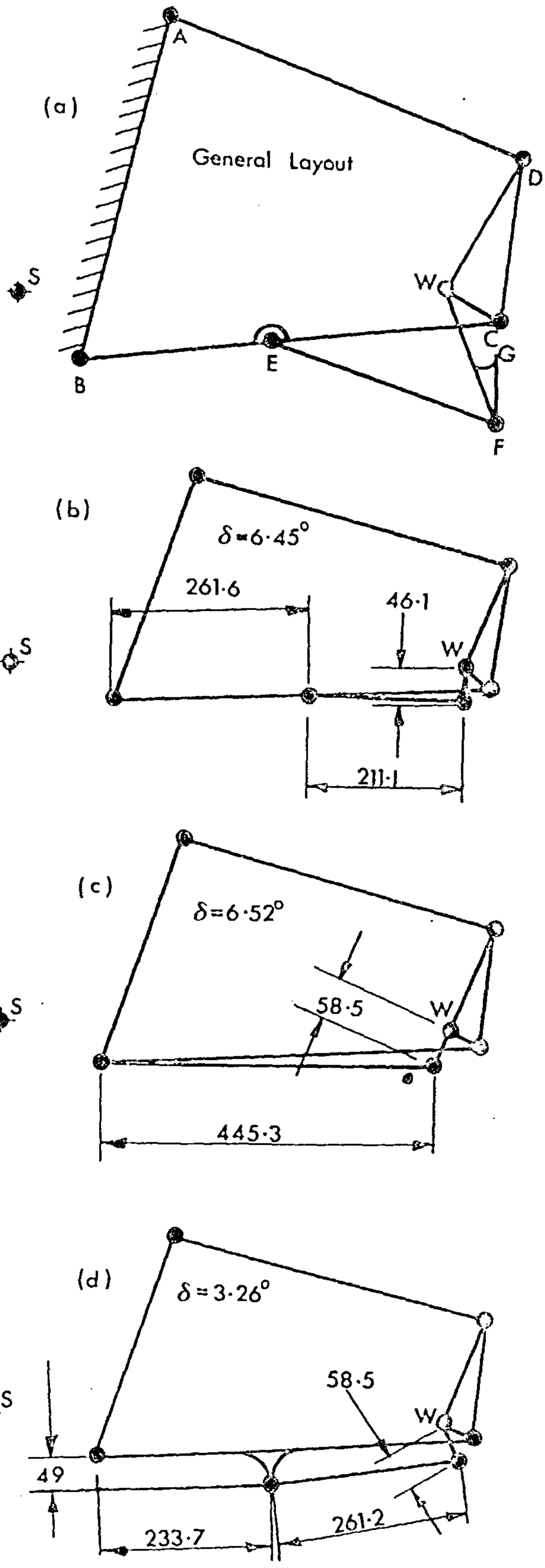

Fig. 8. Linkages with brake reaction link

described in this paper, involving 1400 iterations, had been performed on the IBM370 computer, the total central processor time would have been about 45 seconds.

It would have been difficult to design a linkage to give the required accuracy of output i.e. a circular arc of radius 610 mm±0.3 mm, without using a digital computer since both analogue computers and skilled draughtsmen could only determine the wheel centre position to within ±1 mm for this size of linkage. On the other hand, by using this synthesis program, it has been possible to design a practical linkage with the desired characteristics. The amount of computer time used was small, costing about £25 for the whole project.

10. CONCLUSIONS

The limitations of the current 'swinging arm' design of rear suspension may be overcome by using a four-bar linkage to ensure that the distance between the centres of the gearbox output shaft and the rear wheel remains constant throughout the suspension movement. This should result in a smoother transmission and increased chain life. A linkage in which the links do not remain parallel over the suspension travel offers a much more convenient arrangement than the parallelogram type as it allows much greater flexibility in the choice of link dimensions and pivot positions, without any additional complication.

The application of the mechanism synthesis program to a practical path and motion generation problem has demonstrated its usefulness in design particularly where high accuracy is required. The program leaves the designer free to use his creative skill in choosing the most appropriate type of linkage and its configuration whilst relieving him of the task of finding the best link lengths. As more experience is gained with the program, the best method of selecting and specifying the initial guess will become clearer.

11. ACKNOWLEDGEMENTS

The authors acknowledge with thanks the interest and co-operation of Mr. A. Clews, CCM Ltd., the help of the Computing Laboratory of the University of Newcastle upon Tyne and the support of the Science Research Council (grant B/RG 1285).

REFERENCES

(1) Youssef, A.H., Oldham, K. and Maunder, L. 'Optimal Kinematic Synthesis of Planar Linkage Mechanisms', Proc. Fourth World Congress on the Theory of Machines and Mechanisms, I.Mech.E., 1975, 393-398.

(2) Oldham, K. and Youssef, A.H., 'Kinematic Analysis of Planar Linkages', Department of Mechanical Engineering, University of Newcastle upon Tyne, Internal Report Ta 29, May 1975.

This paper is presented for written discussion. The MS was received on 17th March 1976 and was accepted for publication on 30th September 1976. 22.